Immiscible displacement of trapped oil through experimental and data mining techniques.

ABUNUMAH, O.

2021

IMMISCIBLE DISPLACEMENT OF TRAPPED OIL THROUGH EXPERIMENTAL AND DATA MINING TECHNIQUES

OFASA ABUNUMAH

PhD   2021

IMMISCIBLE DISPLACEMENT OF TRAPPED OIL THROUGH EXPERIMENTAL AND DATA MINING TECHNIQUES

OFASA ABUNUMAH

A thesis submitted in partial fulfilment
of the requirements of the
Robert Gordon University
for the degree of Doctor of Philosophy

This research programme was carried out in collaboration
with the

Centre for Process Integration and Membrane Technology

October 2021

DEDICATION

I dedicate this work to all the men and women who have believed and supported me in my life's journey, including my awesome father, Mr. Ohwojenene Augustine Erharhe, Mrs. Queenie Iwheta and family, Mr. Otaigbe and family, Mr. Peter A, and my loving mother of blessed memories.

I also dedicate this to the Abunumah and Imonisan families. I hope it inspires every member to get to the top of their chosen path.

ACKNOWLEDGEMENT

ABSTRACT

Extensive experimental and data mining techniques have been applied to investigate the potential and competitiveness of gases used in immiscible gas enhanced oil recovery (EOR) processes. Methane (CH_4), Nitrogen (N_2), Air ($21\%O_2/N_2$) and Carbon Dioxide (CO_2) are some of the gases injected in reservoirs to displace trapped oil from reservoir pores. The EOR screening process has been well documented in the literature. However, for immiscible gas EOR technology, very few resources are available for evaluating the selection and performance criteria for commonly injected EOR gases; immiscible EOR gases are usually lumped up in published screening models; and the gases are reportedly selected based on availability and accessibility, rather than on technical criteria, such as displacement efficiency. Furthermore, available experimental studies have only investigated EOR gases separately. This research has been able to fill these gaps and more through rigorous data mining and gas experiments processes.

The methodology utilised empirical approaches set in three phases. Phase I applied data mining techniques to 10,850 data from 484 EOR field projects to identify twenty-four EOR geological and engineering quantities, and objective functions. Phase II utilised Phase I outcomes to design and execute a set of rigorous gas experiments, involving 1,920 experimental runs comprising five reservoir analogous core samples, eight gases, eight isobars, and six isotherms, to generate and analyse 15,360 experimental data points. Several established and modified constitutive equations were used to model gas responses to EOR geological and engineering quantities. In Phase III, Phase I and Phase II results were coupled for the purpose of knowledge validation and application.

This research's outcomes have contributed to reservoir engineering practice and knowledge in providing useful information on EOR gases' competitiveness. Results from Phase I indicates that immiscible gas EOR can be unbundled through data mining and clustering techniques. A novel Screening Model has been developed for immiscible gas EOR that

incorporates sensitivity and criticality markers for each petrophysical quantity investigated. It has been demonstrated in Phase II that in a heterogeneous system, CH_4 is the most competitive gas for ten geological and engineering quantities and objective functions, such as Volumetric Rate, Interstitial Velocity, and Well Density. Similarly, CO_2 is most competitive for ten other quantities investigated, such as Mobility and Interstitial Momentum. N_2 is the most competitive for the cost of injected gas per area coverage. Air is second-best for several objective functions. Suffice to state that at some structural settings and operational conditions, such as porosity, pore size, surface area, and temperature, the competitiveness ranking of the gases switches position. Such was observed between N_2 and CO_2 in low porosity (4% and 3%) core samples. EOR gas mixtures and non EOR gases, such as 20% CH_4/N_2, He, and Ar, were added to the experiments to investigate the relationship between gas flow and gas properties. It was observed that the structural variability (heterogeneity) of the system distorts the correlation between gas properties, such as molecular weight, and the performance criteria of the respective gases. The results from Phase I and II couple significantly in Phase III. Based on well number and placement, it has been demonstrated that the well placement of CH_4, CO_2, and Air favours a negative pore size gradient, while N_2 favours a positive gradient. The economic analysis demonstrates that CO_2 incurs the least cumulative injectant cost and the highest capital expenditure cost (CAPAX). The three Phases validate the field and laboratory well density profile. CH_4 requires the least well density (0.2 well/acre, 1.0 well/cm^2) compared to CO_2 (0.7 well/acre, 2.0 well/cm^2). In some analyses, it was discovered that gas mixture, such as 20%CH_4/N_2, performs better than when the individual component gas acted alone. Single-phase and two-phase relationships have been analytically and experimentally coupled. The experimental findings at low pressure could also lend utility to the gas separation, fluidised bed, and catalytic reaction processes and industry.

Key Words: Enhanced Oil Recovery, EOR Screening, Mobility ratio, Permeability, Well Density, Pore Gradient CO_2, N_2, CH_4, Air, Capillary Number, Gas Experiment, Porous Media.

TABLE OF CONTENTS

LIST OF TABLES

LIST OF FIGURES

NOMENCLATURE

Symbol	Description	Units
$\dot{V}$	Gas volumetric rate	$cm^3.s^{-1}$
C_p	Specific heat capacity at constant pressure	$J/K.g$
L	Length of the material	cm
l	Length of the contrast, in the direction of flow	cm
M	Relative mobility	dimensionless
$\dot{m}$	Mass flow rate	$g.s^{-1}$
M_g	Mobility of the displacing fluid (gas)	$mD.cp^{-1}$
M_i	Mobility of the displacing fluid, such as water	$mD.cp^{-1}$
M_o	Mobility of the displaced fluid (oil)	$mD.cp^{-1}$
MW	Molar/Molecular weight	g/mole
MW_{og}	Mean molecular weight of the oil and gas mixture in the oil phase	g/mole
MW_{go}	Mean molecular weight of the oil and gas mixture in the gas phase	g/mole
n	Numbers of moles	Mole
N_c	Capillary number	dimensionless

P	Pressure	atm
P_{atm}	Atmospheric pressure	atm
Pchg	Parachor of component gas	$(J.cm^{-2})^{1/4}.$ $cm^3.mol^{-1}$
Pch_i	Parachor of component "i"	$(J.cm^{-2})^{1/4}.$ $cm^3.mol^{-1}$
Pch_o	Parachor of component oil	$(J.cm^{-2})^{1/4}.$ $cm^3.mol^{-1}$
P_f	Final pressure at the inlet and outlet	atm
P_i	Initial pressure at the inlet and outlet	atm
P_m	Mean pressure	atm
P_o	Pressure oil exerts on the surface	atm
P_w	Pressure of the displacing fluid exerts on the surface	atm
P_p	Well pattern predictor	dimensionless
Q	Total discharge or volumetric flow rate	$cm^3.sec^{-1}$
Q_g	Gas flow rate	$cm^3.sec^{-1}$
R	Gas constant	$J.mol^{-1}.k^{-1}$
r	Effective radius of the interface or the radius of the pore or capillaries	cm

r_i	Radii of the pores at the inflow side	cm
r_o	Radii of the pores at the outflow side	cm
s_{oi}	Initial oil saturation at discovery or the start of EOR implementation	dimensionless
s_{oir}	Irreducible oil saturation	dimensionless
s_{or}	Residual oil saturation at the end of the EOR application	dimensionless
T	Temperature	K
V	Volume of gas	cm^3
v	Interstitial velocity of the fluid	ms^{-1}
W_{Den}	Well density	well.$acre^{-1}$
W_I	Number of injection wells	dimensionless
W_P	Number of production wells	dimensionless
x_i	Mole fraction of component "i" in liquid phase	dimensionless
y_i	Mole fraction of component "i" in the gas phase	dimensionless
x_g	Mole fraction of oil in the gas phase	dimensionless
x_o	Mole fraction of oil in the oil phases	dimensionless

y_g	Mole fraction of gas in the gas phase	dimensionless
y_0	Mole fraction of gas in the oil phase	dimensionless
z	Dimensionless compressibility factor of gas	dimensionless

Greek Letters

γ_o	The specific gravity of oil	dimensionless
λ_p	The parameter that is related to the distribution of pore sizes	dimensionless
σ_{ITF}	Interfacial tension (IFT)	dynes.cm^{-1}
σ	Surface tension between fluids	dynes.cm^{-1}
$\sigma_{og-Immisc}$	Surface tension between immiscible displaced and displacing fluid	dynes.cm^{-1}
ϕ_E	Fraction of energy loss	dimensionless
λ	Mean free path of gas	cm
μ	Viscosity of fluid	cp
μ_g	Viscosity of gas phase	cp
σ	Surface tension	dynes.cm^{-1}
φ	Porosity	%
η	Kinematic viscosity	m^2.s^{-1}

Abbreviations

ABEX	Abandonment Expenditure
boe	Barrel of oil equivalent
CAPEX	Capital cost
cgs	Centimetre-gram-seconds unit system
EOR	Enhanced Oil Recovery
EOS	Equation of State
FEED	Front End Engineering and Design
OPEX	Operating cost
PVT	Pressure, Volume and Temperature
SOP	Sweep Optimisation Parameter

Chapter One

1 INTRODUCTION

1.1 Overview

Most oilfields are ageing, and the primary and secondary recovery methods used to produce them leave about 70% of the oil originally in place (OOIP) trapped in reservoir pores across the world (Babadagli 2020, IEA 2014, Sivasankar and Kumar 2017, and Vladimir and Eduardo 2010). Enhanced Oil Recovery (EOR) technologies offer established techniques to recover some of this trapped oil in reservoirs (Gbadamosi 2018). EOR is any tertiary reservoir engineering mechanism and method applied to recover trapped oil. According to Babadagli (2020) and Li (2011), there are over 50,000 active oilfields worldwide. Therefore, there would be a continued utility for EOR in the oil industry as long as oil remains the primary global energy source. However, there are more than four EOR technologies, and over ten EOR processes to choose from as depicted in Table 1-1. Consequently, the first step to applying EOR technology is to evaluate and identify the EOR process that is technically and economically applicable and competitive for the reservoir of interest. These steps involve a series of rigorous activities that are together referred to as EOR screening and selection.

Table 1-1 Showing major EOR technologies and some of the recovery processes.

Technology	Method	Processes/Variants
Gas	Gas Injection (Miscible/Immiscible)	Carbon Dioxide, CO_2
		Hydrocarbon gas, e.g., CH_4
		Nitrogen, N_2
		Air
Thermal	Heat Injection	Cyclic Steam Injection,
		Steam Flooding,
		Steam-Assisted Gravity Drainage
Chemical	Chemical Injection	Polymer Flooding
		Alkali
		Surfactant
		Alkali-Surfactant-Polymer (ASP)
Microbial EOR	Microbial Injection	Microbes

According to the study of Babadagli (2020), Lee (2010), and Rotondi *et al.* (2015), the event phases in EOR implementation can be described as shown in Figure 1-1. It takes about three to eight years to implement an EOR project, and the screening phase takes about 15% of that time. It is evident in Figure 1-1 that the phases are sequential. Without the screening phase, it is impracticable to proceed to the subsequent phases (Delamaide *et al.*, 2014a, 2014b, and Wilson 2015).
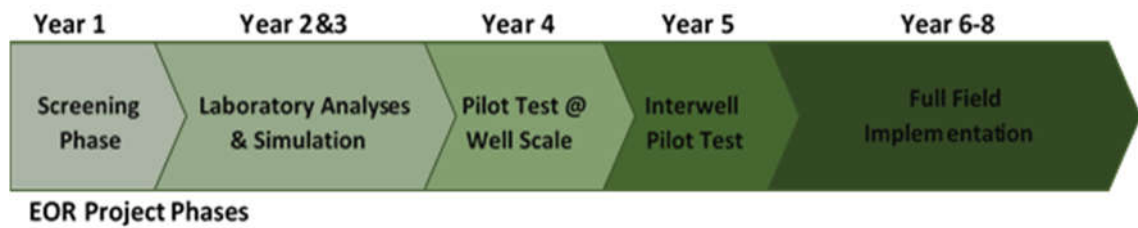
Figure 1-1 The main Phases in EOR project development (reproduced from Rotondi et al. 2015).

The figure also implies that an unreliable screening phase could significantly impact the subsequent development phases adversely, thereby causing loss of time, money and leading to project failures in some cases (Delamaide *et al.*, 2014a, Delamaide *et al.*, 2014b, Lee 2010, and Wilson 2015). Consequently, a suitable selection or screening process should reliably and critically evaluate important factors, such as oilfield conditions, parameters, and properties against known technologies and processes. This would result in a significantly reduced implementation cost, time, and technological complexity.

Current screening and selection methods suggested by authors, such as Guerillot (1988), Surguchev and Li (2000), Saleh *et al.* (2014), Nageh *et al.* (2015) Kang *et al.,* (2014) Taber *et al.* (1997), and Trujillo *et al.* (2010) have been observed to only consider limited subsurface conditions of oilfields at the screening phase. These methods have often led to integration problems with other surface conditions and EOR development phases, thereby leading to project failures and lack of EOR confidence (Delamaide *et al.*, 2014a, Delamaide *et al.*, 2014b, Lee 2010, and Wilson 2015). Consequently, some experts have called for a more integrated approach to EOR screening and application (Al-Mayan *et al.* 2016, Ghoodjani and Bolouri 2015, and Kang *et al.,* 2014). Furthermore, it would be considered best practice if technology users had a holistic overview of the technological and operational implications of the respective EOR alternatives at the earliest possible time in the EOR project design.

It has also been noted by several authors that without EOR, brownfields that are being farmed out to indigenous operators in countries, such as the United

States, Nigeria, Trinidad, and Tobago would not be economically viable to the local operators (DPR 2014, George 2014, and Sinanan and Budri 2010). Therefore, the prospective users of an integrated EOR screening model proposed in this research would include brownfield operators, marginal field operators, and small and medium scale operators. This research was set to treat the first two essential phases in Figure 1-1, which comprise the activities in the first three years, that is, the EOR Screening and Laboratory analyses phases.

1.2 Gas EOR

Gas EOR is an established technology that involves injecting gas into the reservoir for an areal sweep and displacement of trapped oil droplets in the reservoir pores and towards production wells. Gases such as Carbon Dioxide, CO_2, Hydrocarbon gas, CH_4, Nitrogen, N_2, and Air, $70\%N_2/O_2$, have been reportedly injected in these processes (Abunumah, Ogunlude, and Gobina 2021a, 2021b, 2021c, Dellinger, Patton and Holbrook 1984, and Godec *et al.* 2011). These types of displacement processes have been applied across the world in oilfields, such as the Permian Basin in Texas and New Mexico, Williston Basin in North and South Dakota, the North Sea continental shelf in Europe, Daqing oil fields, and Zhong Yuan oilfields in China (Alvarado and Manrique, 2010, Jia *et al.* 2012, Gui *et al.* 2010, Hoffman 2012, and Yu *et al.* 2008,). In gas EOR technology, gas is injected to displace trapped oil through two primary mechanisms, miscible and immiscible mechanisms (Marcel 1980). Highlights of various Gas EOR processes are mentioned below.

1.2.1 CO_2-EOR

This process involves injecting CO_2 into the reservoir to enhance oil recovery (Alvarado and Manrique 2010a, 2010b). The common displacement configurations are miscible and immiscible CO_2 injection (Bank, Riestenberg and Koperna 2007, Dellinger, Patton and Holbrook 1984, Meyer 2007, and Sweatman, Crookshank and Edman 2011). In immiscible CO_2, a direct displacement takes place between the gas or gas slug and oil droplets. Bank,

Riestenberg and Koperna (2007) indicated that immiscible displacement occurs when there is insufficient pressure from the injected gas to cause miscibility between CO_2 and reservoir oil or where the reservoir composition is less favourable (such as heavy oil). This research has identified 236 CO_2 EOR projects published in journals papers. The majority of these projects are located in the United States. The other locations include China, Trinidad and Tobago, Turkey, and Norway. Of the 236 CO_2 projects identified, 21 of them are implemented as immiscible gas EOR.

Alvarado and Manrique (2010) have extensively reported on CO_2 gas EOR projects. Generally, this EOR process is most suitable for light API gravity oil. One of the main challenges in implementing CO_2 EOR is the guarantee of CO_2 supply. Where there are CO_2 generations, such as China, but no existing supporting infrastructures, such as a CO_2 pipeline grid, the gas would have to be conveyed to the field by other means such as tankers and marine barges. This could present technical and economic challenges to the operators. This could significantly account for China's oil industry's inability to harness CO_2 EOR, even though China produces the highest CO_2 (10 gigatons) in the world (IEA 2020). Natural sources of CO_2 have been reported close to oil play in the United States (NPC 2011). The natural availability of CO_2 makes project development more economically viable than oilfields elsewhere, where CO_2 can only be obtained from anthropogenic sources. Examples of the latter are Canadian Weyburn and Midale fields. Here, CO_2 is transported 205 miles via pipelines from Great Plain Synfuels Plant, North Dakota (Kokal and Al-Kaabi 2010, and NPC 2011).

Furthermore, CO_2 contact with connate water forms a weak acid, as shown in the chemical reaction equation:

$$CO_2 + H_2O \rightarrow H_2CO_3$$

This reaction (H_2CO_3) product is a weak but corrosive acid that could cause corrosion problems to the facility, well management, and maintenance. These issues can be overcome by using corrosion-resistant materials. For new reservoirs, corrosion resistance can be easily implemented in the planning

and installation stages. However, for old fields with already installed facilities, this can be a daunting task that attracts material replacement costs and potential operational shutdown of some reservoir sections. Nevertheless, the past 58 years have seen the growing development of CO_2 gas EOR worldwide (Sweatman, Crookshank and Edman 2011), prompting David and Robert (1996) and Godec *et al.* (2011) to regard CO_2 injection as one of the most promising gas EOR processes.

Furthermore, CO_2 provides an environmental solution to the problem of greenhouse gases through carbon capture and sequestration (CCS). Anthropogenic CO_2 can be used to replace displaced oil droplets in reservoir pores at a rate of 20-50% (Lorsong 2013, Neele *et al.*, 2014, Saini 2019, and Zhang *et al.*, 2020). CCS is capable of mitigating greenhouse CO_2 by 14% (IEA 2013).

1.2.2 Hydrocarbon EOR

Hydrocarbon EOR is associated with hydrocarbon gas (usually natural gas, CH_4) injection into a reservoir to enhance oil recovery. Gbadamosi (2018) has reported some hydrocarbon gas projects in the North Sea. In most cases, the gases are forced to form miscible fluid when in contact with reservoir oil. However, there are also immiscible hydrocarbon gas EOR where the gas does not enter a miscible phase with the oil. According to David and Robert (1996), the performance of hydrocarbon EOR is related to the injected pore volume of the gas. This can range from 5 to 20% pore volume.

Most hydrocarbon EOR projects are in the United States. Some other locations include Canada, Brazil, China, Norway, and the United Kingdom. Of the 61 projects investigated in journals, 14 of them are implemented as immiscible hydrocarbon gas EOR. Taber *et al.* (1999) have outlined the screening criteria for hydrocarbon gas EOR selection. However, the criteria provided by these authors fell short of screening for immiscible hydrocarbon gas EOR.

Furthermore, hydrocarbon gas EOR can be used to re-store produced and unneeded natural gas in a reservoir for future use; this can reduce gas flaring,

which is an environmental hazard, significantly in some climes. Therefore, places with high gas flaring problems, such as Nigeria and Russia, should be suitable for hydrocarbon gas EOR. This action would give economic value to the supposed flared gas. Alvarado and Manrique (2010) and NPC (2011) highlighted this further in Alaska, where the option to inject hydrocarbon is driven by the lack of a gas pipeline to convey the gas to markets in Canada and the United States.

1.2.3 Nitrogen EOR

Nitrogen (N_2) EOR is the injection of Nitrogen gas into a reservoir to displace the trapped oil. Nitrogen was identified as the third most implemented gas in immiscible gas EOR. The projects spread across fields in the United States, Trinidad and Tobago, Canada, and Brazil. Forty-one N_2 EOR projects were reported by authors, such as Alvarado and Manrique (2010) and Clancy *et al.* (1985). Twenty-four of these projects are immiscible gas EOR implementation. An advantage of N_2 over CO_2 and CH_4 is injectant availability. Nitrogen as an injection gas has been explored due to its high compressible nature, inert chemical properties, and relatively low generation cost, considering that one of the main raw materials is atmospheric Air. Thus, the N_2 gas injected can be generated on-site from Air.

1.2.4 Air EOR

The application of Air EOR is not yet as popular as the other immiscible gas EOR processes according to the number of reports in published journals. Thirty projects were identified in the database. Findings in journals and texts indicate that the majority of such projects are located in China. Rodríguez and Christopher (2004), Surguchev (2009), and Surguchev, Koundin, and Yannimaras (1999) have extensively investigated Air EOR. Alvarado and Manrique (2010) stated that there is an increasing prospect for Air injection. One of the advantages of Air EOR is the availability of injectant. The mechanism of Air EOR is a bit different from the other gas mechanism, in that part of the process involves oxidation reaction that produces flue gas that in

turn contributes to the drive and oil recovery (Fink 2015, Ezekiel *et al.*, 2014, Surguchev 2009, Jia and Sheng 2017, Rodríguez and Christopher 2004, and Surguchev, Koundin and Yannimaras 1999). Understandably, the presence of oxygen in Air makes this EOR method susceptible to corrosion and explosion. Chen, Song and Zhang (2012) and Jia, Yin and Ma (2018) reported improved recovery from Air EOR. Although, Jia, Yin, and Ma (2018) have noticed and cautioned on the hazard of oxygen breakthrough at the production well during their reservoir simulation of Air injection. They were able to experiment with the displacement efficiency of low-oxygen Air as a function of permeability. The result shows that as the injection pore volume increases, so does the displacement efficiency in the different permeabilities sampled. It further confirms that the recovery efficiency is a function of the injection rate. This information contributes to the engineering framework for the optimisation of immiscible gas EOR in this research.

1.3 State of the art EOR Screening Methods

1.3.1 EOR Screening Criteria

One of the main aims of reservoir engineering is to identify which EOR technology can produce the most oil after primary and secondary oil recoveries have become ineffective. One of the technologies screened for in the industry is Gas EOR. As previously stated, CO_2, CH_4, N_2, and Air are the leading gases injected in gas EOR technology.

However, different gases may exhibit certain flow regimes that could improve or inhibit their EOR potential and efficiency. Abunumah, Ogunlude, and Gobina (2021) stated that understanding the pressure, volume, temperature (PVT) flow behaviour of gases with respect to EOR technology would enable engineers to quickly relate flow regimes of each gas to its oil displacement potential, hence its competitiveness, given a set of reservoir conditions or constraints.

Some approaches could be used to evaluate gas applicability and competitiveness. They include numerical, analytical, and experimental methods (Chen 2007). Authors, such as Guerillot (1988), Kang *et al.* (2014), Mahdavi and Zebarjad (2018), Nageh *et al.* (2015), Surguchev and Li (2000), Taber *et al.* (1997), Trujillo *et al.* (2010), and Saleh *et al.* (2014) have used various types of numerical methods to evaluate and develop screening criteria for selecting suitable EOR processes and injectants for reservoirs of interest.

Taber *et al.* (1997) EOR Screening model is the most applied and cited EOR criteria in the industry. Their model is based on statistical analysis using data from successful EOR projects to create analogues for screening new EOR projects. Before Taber *et al.* (1997), Guerillot (1988) had developed a screening software called SARAH (Systeme d' Aide en Recuperation Assisree d'Hydrocarbures). He used Expert System and Fuzzy Logic on reservoir data to build an EOR screening model. Similarly, Surguchev and Li (2000) applied Artificial Neural Networks (ANN) on EOR data to produce a set of criteria for EOR screening. On the other hand, Trujillo *et al.* (2010) used analogies and benchmarking to develop a model for EOR Screening. Other authors who have developed EOR screening models in a similar vein include Nageh *et al.* (2015), Kang *et al.* (2014), and Saleh *et al.* (2014).

Furthermore, Zhuravljov and Lanetc (2019) have used numerical simulation to study CO_2, CH_4, and N_2. However, they focused their evaluation on the effect of gas compressibility and incompressibility on oil displacement performances in immiscible gas EOR. Yin and Ma (2018) did an Air EOR experiment that suggests that low-oxygen Air injection can improve oil recovery in high permeability than low permeability reservoirs. Their results contrast those of Buckley and Leverett (1942), Muggeridge *et al.* (2014), and Thomas (2001), which reported that injectant permeability is inversely proportional to the favourable mobility ratio that is required to improve oil recovery.

Some other authors have carried out experimental investigations based on the potential of gas EOR performance. Such authors include Dellinger and

Holbrook (1984), Gui *et al.* (2010), Jia *et al.* (2012), Khodaei Booran *et al.* (2016), Li and Horne (2001a), and Masalmeh *et al.* (2011). However, their studies were conducted on a single or two gases basis (usually CH_4 or CO_2), thereby missing the opportunity to compare the broad spectrum of EOR gases and the effects of the gas properties, such as viscosity and molecular weight, and reservoir parameters, such as pore size and heterogeneity (permeability contrast) on the respective gas performance.

1.3.2 EOR Screening Software:

Existing screening software implement authored EOR screening model to rank EOR technology according to their suitability to the reservoir of interest. Table 1-2 is a compilation of software used for EOR Screening based on a literature survey carried out in this study.

Some software are found to implement the screening model developed by Taber, Martin, and Seright in 1997. For example, EORGui (the most cited EOR screening software in petroleum journals) and Screening 2.0 both used Taber *et al.* (1997) screening criteria. El Ela and Sayyouh (2014) had categorised Egyptian oilfields into various EOR methods using EORGui. One of the benefits of this software is that it is concise and offers quick screening for reservoirs. Nevertheless, it also lumps up immiscible gas EOR.

Table 1-2 Shows state of the art EOR screening software and the EOR criteria implemented.

Screening Software	Promoting Company	No. of EOR Methods	Used Criteria	Graphical User Interface	Authors Citing
SWORD	IRIS	11	Database	Yes	Surguchev *et al.* 2010
EORgui	Petroleum Solutions	9	Taber, Martin, and Seright	Yes	Trujillo *et al*, 2010, Shuker Talib *et al.* 2012, and Sinanan and Budri 2010
SelectEOR (PRIze)	Alberta Research Centre	17	Database and authors	Yes	Alvarado *et al.* 2002, Sinanan and Budri 2010, and Trujillo *et al.* 2010
Screening 2.0	I.C.P. ECOPETROL	19	Lewin, Farouq, Taber	-	Trujillo *et al.*, 2010
Expert System	Cairo University	>10	Database	-	Shindy *et al.*, 1997, Gharbi, 2000, and Abbas and Song 2011
Expert analytical system	TatNIPIneft	-	Database	-	Ibatullin *et al.*, 2002
Expert system	King Saud University	-	Database	-	Shokir *et al.*, 2002

There are about nine subsurface properties in existing screening models. Nevertheless, some reservoir properties that have been identified as critical in recent EOR studies and field experience, such as reservoir salinity that

causes scaling in some EOR projects, are not included in these models. There is also the absence of porosity and pore size in the criteria.

Furthermore, in the screening model of Taber *et al.* (1997) and the GuiEOR software, the criteria for immiscible gas EOR processes are lumped up as 'immiscible EOR'. While miscible gas EOR processes are segregated and treated as individual processes with the corresponding criteria. The lumped-up representation of immiscible gas EOR wrongly suggests that the screening requirements and the displacement performance of the various gases injected in immiscible gas EOR are all the same. This is quite misleading and a recognisable shortfall in existing screening models.

Furthermore, experimental assessment of the screening process for immiscible EOR gases has not been extensively investigated in light of essential engineering quantities, such as momentum, kinetic energy, and well density. Although there are many studies on gas flow in porous media (Castricum *et al.*, 2015, Robinson *et al*., 2004, Ogunlude, Abunumah and Gobina 2020, Huang *et al.*, 2019, Wu *et al.,* 2020, and Jia 2018). However, many of these studies are not discussed in the context of EOR. The ones that did focus on EOR considered only a limited number of quantities.

1.4 Short Fall of Current EOR Screening methods and Studies

A review of EOR articles and journals reveal some shortfalls in existing EOR screening models, as highlighted below:

I. Models are passive and static.
II. Little or no emphasis on immiscible gas EOR processes.
III. The limited scope of operational parameters, such as the non-inclusion of well density.
IV. They are not optimised for the life cycle events in EOR projects.
V. Lack of objective functions for evaluating EOR performances and competitiveness.

VI.   They have not been extensively validated experimentally.

VII.   Available experimental works are limited to very few engineering quantities.

Examples of the limitation of existing EOR screening have been reported by Delamaide *et al.* (2014a) and Thornton, Hassan, and Eubank (1996). The Oil and Gas Journal 2014 EOR survey database reported that eleven projects had been evaluated as discouraging, while eight EOR projects are planned to be discontinued. These failures could be, among other odds, the consequence of the selection and application of ineffective EOR process implementation in these reservoirs (Lee 2010, Delamaide *et al*., 2014a, 2014b, and Wilson 2015).

1.5 Rationale for Study

It has been more than two decades since the popular Taber *et al.* (1997) EOR screening criteria were developed. Over these years, there have been engineering and operational evolutions in EOR applications that requires investigation and coupling with existing criteria. There have been reported failures and successes that have impacted EOR decision-making that could be traced to EOR selection (Lee 2010). Few authors, such as Saleh *et al.* (2014) and Siena (2016), have attempted to update the Taber screening criteria model to reflect contemporary EOR developments. Saleh *et al.* (2014) criteria model expanded the API gravity range for some EOR processes. However, as Delamaide *et al*. (2014a) stated, these authors are still used to approaching screening criteria through the legacy guide of Taber *et al.* (1997). Thereby repeating some of the Taber model's limitations, such as the omission of porosity, pore sizes, salinity, and the bundling of immiscible gas EOR mentioned previously. Consequently, a revisit to EOR screening criteria should not only update the data for setting EOR criteria but should also seek to:

I.   Identify mission-critical parameters in the life of EOR projects that investigators have not hitherto considered.

II.   Identify and retire, where necessary, parameters that have lost their functionality or have become redundant due to the current technological evolution of engineering processes.

III.   Unbundle the screening criteria for immiscible gas EOR such that the respective gas performances can be evaluated, compared, and contrasted using data mining and experimental methods.

IV.   Ultimately develop a screening model based on the five-event phases earlier identified in Figure 1-1 as necessary for optimising EOR projects, with emphasis on the experimental laboratory phase.

These updates would require significant resources to achieve with respect to data processing, fund, workforce, simulation, field, and laboratory experiments. Therefore, this research has elected to focus on the most unattended EOR screening sector, which is the immiscible Gas EOR.

1.6 Aims and objectives

1.6.1 Aim:

Evaluate the selection criteria and competitiveness of gases that are injected during immiscible gas EOR projects using data mining and experimental approaches.

1.6.2 Objective:

The aim of this research was aptly achieved through the following set objectives:

1. Identify geological and engineering quantities and objective functions critical for characterising and selecting EOR processes through data mining techniques.

2. Design and conduct pressure, volume, and temperature (PVT) gas experiments based on quantities and functions identified in objective one.

3. Determine the potential performance and competitiveness of the respective immiscible EOR gases through experimental data analyses.
4. Propose optimisation solutions for selecting gases in EOR projects based on the coupling and validation of experimental and data mining results.

1.7 Scope of Research

Although this research has generally investigated common EOR technologies in the industry, the focus was centred on immiscible gas EOR. Therefore, the experiments carried out were concerned with immiscible gas EOR. An empirical analogy was drawn between gas EOR and other EOR technology where practicable. Nevertheless, no experiments were carried out for these other EOR technologies, such as Thermal and Chemical EOR. The data used are from global oilfields deposited in industry journals and from gas flow experiments conducted at the Centre for Process Integration and Membrane Technology, Aberdeen. There may be other EOR projects that were not captured in the database used for this study. The report did not consider EOR application in unconventional oil fields like shale oil, although some core petrophysical properties investigated here have similar qualities as those found in shale oil reservoirs.

1.8 Structure of Research

The rest of this research contains the objectives and methods used to develop a robust screening model for immiscible gas EOR. It also contains a rigorous investigation of existing screening models and EOR quantities. It ended with a series of results and discussions from extensive analyses of field data from global EOR projects and laboratory experiments. The research has been structured according to the following subject matter:

S/N	Structure	Achievement
I.	**Chapter One**	Overview of EOR State of the Art, Research Gap, Aim and Objectives.

II.	**Chapter Two**	Theoretical and analytical review, and characterisation of EOR enabling factors.
III.	**Chapter Three**	Design and defence of Research Methodology: Phases I, II, and III.
IV.	**Chapter Four**	**Phase I:** Design of procedure for Data mining and characterisation of EOR process screening and performance factors.
V.	**Chapter Five**	Results, analyses and discussions of identified critical EOR process screening and performance factors.
VI.	**Chapter Six**	**Phase II**: Design of procedure for the experimental evaluation of select EOR screening and performance factors.
VII.	**Chapter Seven**	Results, analyses and discussions of gas screening and performance factors.
/III.	**Chapter Eight**	**Phase III**: Coupling of Phase I and II results for competitive evaluation.
IX.	**Chapter Nine**	Conclusions and Recommendations.

At the end of the research, the first two phases involved in a typical EOR project were completed, as shown in Figure 1-2.
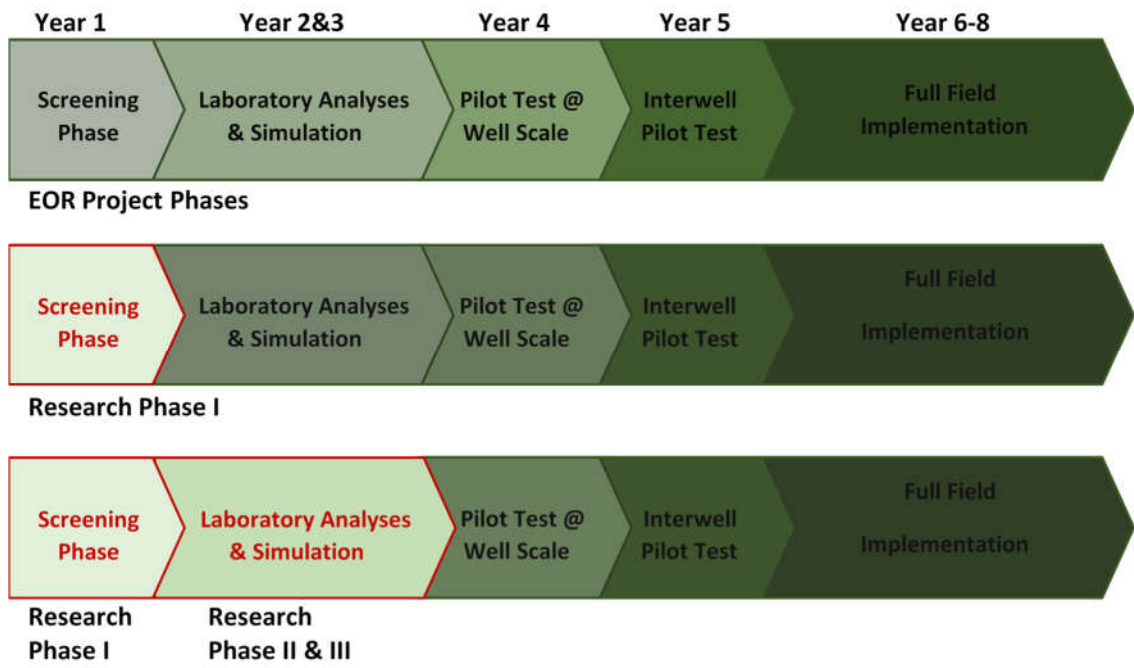
Figure 1-2 Showing the tasks in the three phases of the research, designed to reveal and complete the first two phases of an EOR project.

Chapter Two

2 LITERATURE REVIEW

2.1 Overview

A thorough investigation of over 500 relevant journals, reports and texts related to EOR technology has been conducted. Simple dimensional and dimensionless quantities are applied in the industry to relate EOR production response to injected fluids. In the review of relevant literature materials, essential geological and engineering factors involved in the proper engineering of successful EOR processes were identified and documented. The aim was to gather industry understanding of the relationship between the oil recovery determining factors, such as petrophysical parameters and properties, and their selective coupling to enhance recovery of trapped oil. The preceding paragraphs detailed various geological and engineering theories that govern the relationship among EOR factors, and between EOR factors and oil recovery. Simple mathematical equations have been used to express and understand these engineering theories and relationships. A set of combinatorial quantities have been suggested and tested in the course of the research. Additional efforts were made to identify industry requirements for a robust EOR screening model that would optimise activities and events involved in the life cycle of EOR applications and projects.

2.2 Fluid Flow through Porous Media

For oil, like many other fluids, to flow from point A to point B of a porous media, certain flow governing rules centred around the full spectrum of continuum mechanics must be satisfied. Once these rules are understood, it becomes easier to adjust them in unfavourable conditions to fit individual cases and circumstances. The main focus of EOR is to improve oil recovery

on a microscopic or pore scale (displacement efficiency) and macroscopic scale (sweep efficiency) typically through the agency of other fluids such as gas. The most used governing theories for characterising fluid (liquid and gas) flow through porous media are derived from constitutive equations and engineering principles which are in turn hedged on thermodynamic laws, equations of state such Boyle's and Charles's laws, conservation laws such as conservation of momentum, mass-energy, process laws and principles laws such as Darcy's, Material Balance, Hagen–Poiseuille, Buckley–Leverett's, Welge's, and Fick's laws and principles. These laws, theories and principles are also appropriately designed to characterise immiscible flows. Hence, they very well lend themselves to the investigation of immiscible gas EOR in this research. The mechanisms for immiscible flow include slug displacement. In this work gas and oil are the fluids of interest. Figure 2-1a shows an oil-wet capillary with trapped oil. Gas is injected as a slug to displace the oil (Figure 2-1b). The displacement process is considered immiscible and piston-like. Furthermore, a clear-cut boundary is considered to exist between the gas and oil at the point of contact.
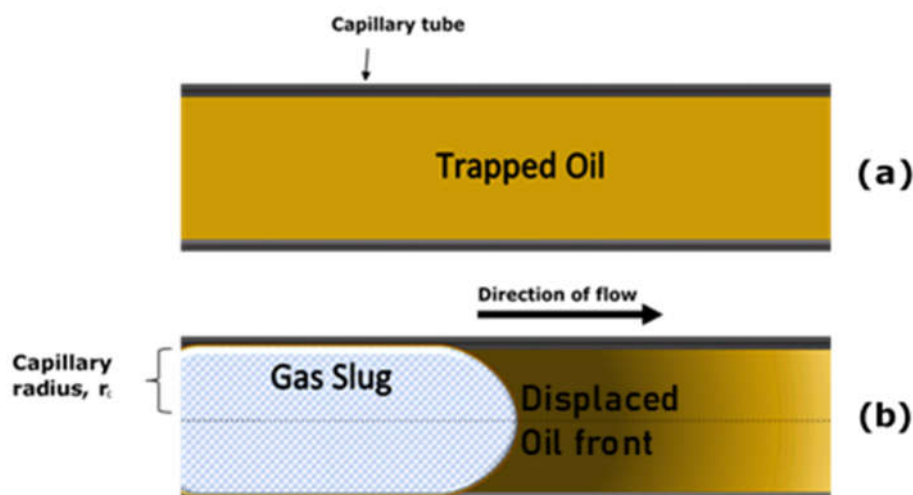
Figure 2-1 Capillary system (a) containing trapped oil and (b) gas-oil displacement by slug flow with a displaced oil front visible.

The study of this type of displacement is necessary to evaluate the competitiveness of the EOR injectants. An extensive journal review of authors, such as Thomas (2001), Warner and Holstein (2007), Yu *et al.*

(2011) and Muggeridge *et al.* (2014), reveals common factors held by the oil industry as affecting microscopic and macroscopic gas/oil recovery efficiency of immiscible gas EOR processes. These are (1) initial saturation conditions, (2) fluid viscosity ratios, (3) relative permeability ratios, (4) mobility ratios, (5) formation dip, (6) capillary and gravitational forces, (7) interstitial velocity, (8) other factors include diffusion, permeability, density difference, rate of injection, permeability contrast and the cross-section open to flow. This research extensively explored some of these factors as reliable criteria to evaluate immiscible EOR gases' respective performances. In this study, the relative ability of each EOR gas to meet the optimisation requirement of these factors is considered a measure of their respective competitiveness.

2.3 Characterisation of EOR Quantities

Reservoir characterisation is a well developed concept in reservoir study. Geological and engineering quantities, such as porosity and mobility, are often used to characterise and group reservoirs (Abunumah, Ogunlude, and Gobina 2021a, Curtis *et al.,* 2002, Desbarats and Dimitrakopoulos, 1990). The process generates valuable information that universally appeals to engineers' understanding of reservoir behaviour, recovery approach and analogues. According to Civan (2015), Aminzadeh and Dasgupta (2013), Slatt (2013a, 2013b), Yu *et al.* (2011), Buynevich *et al.* (2009), Fanchi (2002), and Schatzinger (1999), a robust characterisation process should integrate geological and engineering data to provide both qualitative and quantitative measures of reservoir description (behaviour) and production (performance).

Consequently, to set the research in an industry-inclined path, a characterisation process was conducted, and the outcome was further utilised to design an experimental process. Reservoir and EOR information were ingeniously grouped into two reservoir and performance factors. The reservoir factors include rock parameters and fluid properties. These have significant utility because they remain practically constant for chemically similar hydrocarbons (Robert 2007, Curtis *et al.,* 2002). Therefore, they

facilitate the characterisation of reservoirs and the setting of universal criteria or benchmarks for EOR screening, selection and applicability.

In contrast, the performance factors are objective functions applied to optimise and compare the relative potential of the respective EOR processes. The significant difference between the two groups is that the former describes the reservoirs' intrinsic petrophysical characteristics, such as permeability and viscosity. While the latter are usually combinatorial concepts, such as mobility and momentum, that describe the engineering characteristics for evaluating EOR processes prospects and potential performances. Also, combinatorial quantities enable investigators to study individual EOR process competitiveness from a multi-mechanism coupling. Authors have generally not considered these functions as a useful characterising concept except for Müller-Petke and Yaramanci (2015), who considered transmissibility as an important characterisation quantity. These reservoir quantities and concepts have been described in the following sub-sections strictly in the context of gas EOR technology. Furthermore, several engineering principles, such as first principles and continuum mechanics, were applied to measure quantities' values directly or analytically through equations of state in their explicit forms or modified forms. All these processes are presented in the subsequent sections.

2.3.1 Reservoir Parameters and Fluid Properties:

These are geological, often structural parameters and engineering quantities that industry experts consider as factors that inform the selection and applicability of EOR processes.

2.3.1.1   Porosity

The porosity in reservoir rock is the space or pores available in the rock matrix (Lim and Kim 2004, Klobes and Munro 2006). It could be referred to as the volume or void fraction of the reservoir rock (Kennedy 2015, Cone and Kersey 1992). It is a scalar quantity, usually represented by φ (phi). Geologically, it measures a rock's storage and transport capacity (Sheng *et al*., 2020).

Mathematically, it is expressed in Eq. 2-1 as the ratio of pore volume, V_p, to the total rock (matrix) volume V_t (Klobes and Munro 2006):

$$\varphi = \frac{V_p}{V_t} \qquad \text{2-1}$$

According to Rick and Diana (1993) and Satter and Iqbal (2016), this ratio is usually less than 1 or 100%. The rule porosity adds to oil recovery is its capacity to hold or store fluid and, at the same time, act as a passage or conduit for moving fluids, oil, water, and gas (Sheng 2020). Factors that determine the type, quality, and extent of porosity, such as rock types, depth, grain size, pore size, and throat diameter, have been well documented in detail by Henry and David (1993), Hartmann and Beaumont (1999), and Philip (1994). Several methods are available for determining the porosity of a reservoir or porous media. These methods include Boyle's law, Scanning Electron Microscope (SEM), density differential, and Archimedes principles. In this work, the density differential and Archimedes method were applied to estimate the analogous core samples' porosity, as suggested in Cone and Kersey (1992) and Kennedy (2015).

Figure 2-2 shows three different types of pore sizes identified in Cone and Kersey (1992) and Hartmann and Beaumont (1999). Although they are packed in the same cubic dimension, their grain sizes, hence the number of pores and pore sizes, are different. This type of matrix could lead to different porosities. The concept of pore size gradient λ can be applied to Figure 2-2 with respect to flow direction.

The pore size gradient is given as (Rabbani *et al*. 2018):

$$\lambda = \left(\frac{ro - ri}{l} \right) \qquad \text{2-2}$$

Where:

r_o and r_i are the radii of the pores at the outflow and inflow side, in cm.

l is the length of the contrast, in the direction of flow, in cm.

λ can assume values of zero, positive and negative numbers. For the sample stack of pore sizes in Figure 2-2, where flow is from top to bottom, the pore size gradient is calculated as a negative gradient ($[2nm-200nm]/3x10^7] = -66x10^{-7}$). Rabbani *et al*. (2018) and Ko *et al.* (2018) experimentally demonstrated that the pore size gradient significantly influences gas diffusion, viscous fingering and recovery efficiency of a displacement process. The authors favoured a negative pore size gradient over a positive one in managing viscous fingering. It is speculated that the pore gradient could provide useful information for EOR well number, type, and placement. This research, therefore, investigated gas EOR performance using a pore gradient system.
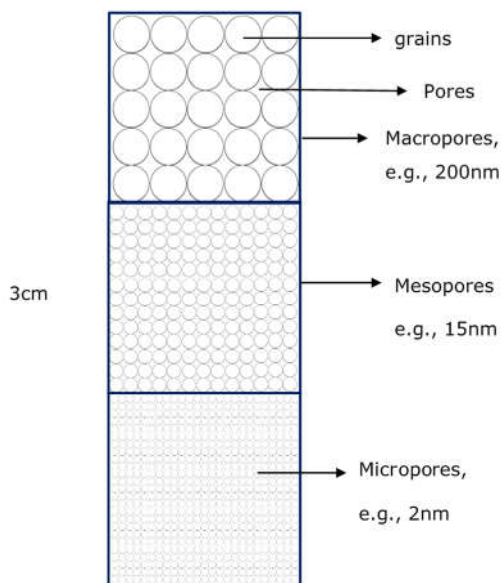
Figure 2-2 Schematic of 3 equal layers of different pore sizes.

At discovery, fluids in reservoir pores try to maintain some forms of dynamic equilibrium with each other's surface and with the surface of the rock material in which they are contained through certain governing rules, such as pressure, surface tension and wettability. These dynamics determine which phase or fluid would be preferentially or selectively allowed to flow through the pores the most when production starts. Although Ohen and (2015), Skerlec (1999), Beaumont *et al.* (1999), Kersey (1992) and Schowalter (1979) highlighted that pore geometry is essential for fluid flow because it

affects permeability, capillary, displacement and buoyance pressure. Nevertheless, many authors have not included it in their EOR screening criteria (Alvarado and Manrique 2010a, 2010b, Bachu 2016, Brashear and Kuuskraa 1978, Goodlett *et al.* 1986, Karović-Maričić, Leković, Danilović 2014, Kuuskraa and Godec 1987, Taber *et al.* 1997, and Zerafat *et al.* 2011). For authors that included this parameter, some stated that it is not a critical criterion. Thus, the importance attached to porosity as a parameter for predicting EOR performances varied from author to author (Guerillot 1988, Surguchev and Li 2000, Trujillo *et al.* 2010, Saleh *et al.* 2014, Kang *et al.* 2014 and Nageh *et al.* 2015, Gbadamosi 2018). In this study, the field data underwent a characterisation analysis to determine whether EOR reservoirs are discriminated by porosity profile and whether porosity is a reliable or critical parameter for EOR screening and process selection. It also investigated the relationship between porosity and other petrophysical parameters within the scope of EOR operations. In the experimental analysis, the pore sizes were investigated to determine comparative potential performances of the respective gases injected during immiscible gas EOR and how the results compare to the data mining analyses. Furthermore, porosity and pore size gradient profilings were carried out for the respective EOR gases.

Data Acquisition

The porosities were collated from EOR field data published in journals, texts and reports. Where reservoir porosity values are not available, established structural correlations such as permeability-porosity correlations were used to estimate values for porosity.

In the experimental phase, the Archimedes principle and the density differential ratio methods were used to estimate analogous core samples' porosity.

2.3.1.2 Permeability

Permeability is the rock property that qualifies and quantifies a rock's ability and performance to allow flow or flowability (Merlet *et al.*, 2020, Ohen and Kersey 1992 and Morton-Thompson, and Woods 1993, and Hartmann, Beaumont and Coalson 2000). While porosity reflects fluid storage and flow, permeability reflects flow (Ayan *et al.,* 1994). In a multiphase system, common in reservoirs, where water, oil, and gas are together in the pore space, flowability is not the same for all components (Breit 1993). There is a preferential flow regime for each phase referred to as the effective and relative permeability of each fluid. The phases' relative permeability is an essential factor in EOR evaluation (Muggeridge *et al.,* 2014).

The bulk permeability of porous media to a fluid is obtainable through different routes. These include experimental, analytical and pseud-empirical routes. The most common method of estimating permeability is by the Darcy equation. Darcy (1856) experimentally determined that permeability, K, of fluid flow between two points in a porous media is proportional to flow rate, Q , and viscosity, μ, of the fluid and the apparent length, l, travelled by the fluid; and inversely related to the fluid entering area, A, and the diminishing pressure difference, $\Delta\mathrm{P}$, across the travelled length between the two points. The theory is represented in Eq. 2-3 (Atangana 2018):

$$Q = \frac{-KA}{\mu}\frac{\Delta\mathrm{P}}{l} \hspace{4cm} \text{2-3}$$

Collecting Eq. 2-3 with respect to K transforms the equation to:

$$\mathrm{K} = \frac{-Q\mu}{A\left(\frac{\Delta\mathrm{P}}{l}\right)} \hspace{4cm} \text{2-4}$$

The factor, $\frac{\Delta\mathrm{P}}{l}$, represent the pressure gradient for the pair of the pressure and porous media apparent length (Prada and Civan 1999, and Tiab and Donaldson 2015). The negative sign indicates the pressure diminishes towards the direction of flow.

Some authors have derived correlations between permeability and other petrophysical quantities so that when those quantities are available, permeability can be estimated (Moura and Toralles 2019, Nelson, Batzle, and Fanchi 2006, Buryakovsky, Chilingar and Aminzadeh 2001 and Nagel and Byerley 1992). Models based on the Kozeny-Carman equation, grain size, mineralogical factors, capillary pressure, surface area, and water saturation exist for this purpose (Nelson, Batzle, and Fanchi 2006). Analytical operations on the Darcy and Hagen-Poiseuille equations also lead to a reduced form of the Kozeny-Carman equation for estimating permeability from porosity, capillary pore radius, r_c as in Eq. 2-5 (Buryakovsky 2001 and Tiab and Donaldson 2015):

$$r_c{}^2 = \frac{8K}{\varphi}$$
2-5

Reservoir rock permeability ranges from 0.1mD to 10,000mD (Gluyas and Swarbrick 2004 and Glover 2000). The quality of reservoir rock permeability can be classified thus:

Fair, < 10mD
High, 10 – 100mD
Very high, 100 – 1,000mD
Exceptional, >1,000mD

Authors such as Guerillot (1988), Taber *et al.* (1997), Surguchev and Li (2000), Trujillo *et al.* (2010), Saleh *et al.* (2014), Nageh *et al.* (2015) and Kang *et al.* (2014), have consistently promoted permeability as an essential reservoir parameter for EOR process screening and selection. In this study, permeability has been extensively examined both in data mining of field data and experimental data procedures. The investigation was carried out on permeability as a stand-alone variable for enhanced oil recovery and also as a function of combinatorial quantities such as mobility.

How permeability affects recovery depends on the fluid and porous media characteristics being treated. Wang *et al.* (2019b) indicate that permeability could be influenced by pore size.   From the relative permeability curve and

the Darcy equation (Ahmed 2018, Wheaton 2016, and Ahmed 2010a), it is demonstrated that increasing permeability increases oil recovery, that is, where oil is the fluid of interest. However, if the displacing fluid (e.g., gas) is the fluid of interest, then the relative mobility ratio and the Buckley-Leverett equation suggest that low permeability is most desirable (Ahmed and Meehan 2012, Donaldson, and Alam 2008, Fanchi 2010a, 2010b, Fanchi 2002b, Lyons 2010, Satter and Iqbal 2016, Sheng 2011 and Richard 2007). Yu and Sepehrnoori (2018) found CO_2 EOR to perform better at lower permeability reservoirs (0.001mD) than higher permeability ones (0.1mD). Amirkhani, Harami and Asghari (2020) experimentally demonstrated that CO_2 has a higher permeability than CH_4 and N_2. This study is more interested in understanding the displacing fluid (gas) permeability profiles while using the displaced fluid (oil) as a coupling fluid. Consequently, the EOR reservoirs were characterised through a data mining procedure to investigate whether the respective gas EOR processes are discriminated by permeability. Where that is the case, then EOR gas permeability experiments are consequently designed and conducted for the gases to evaluate their competitive potential and to test the quality of the experimental results coupling with the data mining results.

Data Acquisition

The bulk permeability values for reservoirs were obtained from field data that were provided in journals and industry reports. Where permeability is not available in the records, established correlational equations between permeability and other petrophysical quantities, such as saturation and porosity, were used to obtain permeability. A typical example of such correlation is Eq. 2-5.

For the EOR gas experiments, Eq. 2-3 was used to obtain the bulk permeability of the gases.

2.3.1.3 Areal extent

Investigators have not extensively studied the EOR characterisation of reservoir areal extent and the possible effect on EOR process screening, selection, applicability and potential. The areal geometry of reservoir perimeter is usually described as circular, and sometimes rectangular. However, wellbores are strictly circular. A well placed at the centre of a reservoir would enforce a radial flow between the boundaries of the wellbore and the circular or rectangular reservoir perimeters. The radial flow between these boundaries can be described by an effective flow radius. Thus, the areal extent of a reservoir, by the nature of the radial flow, can be reduced to a radial extent.

The existing screening models reviewed indicate no author has included areal or radial extent it as a relevant screening parameter. Authors may have found no reliable correlation between EOR applicability and the areal extent; therefore, they did not include it in their EOR screening models. This study found the need to revisit the areal extent, especially considering that Hagen-Poiseuille and Darcy's laws for radial flow have an element of the areal extent. The function of the radial extent is often discussed in the context of the pressure gradient. The pressure gradient is demonstrably correlated with volume rate and permeability (Boukadi et al. 1998, Ding et al. 2014, Hao et al. 2008, Prada and Civan 1999, Song et al., 2010, Wang et al. 2021, and Wei et al., 2009). Furthermore, permeability is an important parameter in all authored screening criteria (Taber *et al.* 1997, Guerillot 198, Surguchev and Li 2000, Trujillo *et al.* 2010, Saleh *et al.* 2014, Nageh *et al.* 2015 and Kang *et al.* 2014). It is, therefore, expected that areal or radial extent could have its unique impact on EOR process selection and performances, including other EOR activities such as infill well drilling and spacing.

In reservoir terms, the radial thickness can be defined as half of the difference between the outer reservoir boundaries and the well bore's inner diameter (Davim 2012). Consequently, the fluid flow profile is usually represented as a radial flow instead of the typical Darcy linear flow. Therefore, the travelled length, l, in the linear Darcy equation (Eq. 2-3) is substituted with a radial

extent parameter, $\ln(r_1/r_2)$, that is, the natural log ratio of the reservoir radius (r_1) and internal wellbore radius (r_2), assuming a single well reservoir. According to Kuuskraa (1982), the $\ln(r_1/r_2)$ is relatively a vital denominator. It is stated that, in theory and practice, increasing r_2 by a factor of 200 would effectively increase fluid flow by two to four-fold, thereby making this factor relevant for consideration in well density evaluation. Consequently, the radial thickness parameter was considered in the data mining and experimental design for this study.

Data Acquisition

Values for the radial extent or flow radius, r_i for EOR fields is derived from the reported reservoir area, A_i, by applying the simple geometry equation (Weisstein 1999). The subscript, i can be a reservoir or wellbore.

$$r_i = \sqrt{\frac{A_i}{\pi}} \qquad\qquad \text{2-6}$$

Where the reservoir area is not supplied or absent in the global EOR data set, the r_i is subsequently estimated from Darcy and Hagen-Poiseuille equation using other available petrophysical data.

For the gas experiments, the radial extent of the core samples can be measured accurately using a calliper.

2.3.1.4 *Pay Zone or Reservoir Thickness*

The reservoir pay zone is a quantitative measure of the vertical extent or thickness of a reservoir. Like the areal extent, the pay zone thickness also describes useful gradients such as pressure, temperature and vertical permeability gradients. It offers utility in several state equations that describe reservoirs, such as the Darcy and Hagen-Poiseuille equations. It also couples with other engineering quantities such as transmissibility to facilitate knowledge in reservoir fluid transmitting capacity. Ran *et al.* (2019) and Wu and Liu (2019) mentioned that oil reserve and recovery are sensitive to pay zone thickness. Ado (2020) mentioned that when Air was injected at a constant rate into three reservoir models with different pay zone thicknesses (24m, 16m, and 8m), oil recovery was slightly affected by the thickness. Wu and Liu (2019) showed a more dramatic and positive influence of thickness on fluid flow. However, their study was for steam EOR process. Existing EOR screening models included this geological parameter as a criterion for selecting EOR processes (Alvarado and Manrique 2010a, 2010b, Bachu 2016, Brashear and Kuuskraa 1978, Goodlett *et al.* 1986, Karović-Maričić, Leković, Danilović 2014, Kuuskraa and Godec 1987, Taber *et al.* 1997, and Zerafat *et*

al. 2011). Considering the reservoir simulation study of Ado (2020) and Wu and Liu (2019) on reservoir thickness and its persistence in equations of fluid dynamic and screening models, the reservoir thickness is intuitively expected to be a potentially reliable factor for the gas EOR process characterisation, selection, and performance. Therefore, coupling data mining of field and experimental data is expected to reveal some uncharted information.

Data Acquisition

Reservoir pay zone values were obtained from global EOR field data. Where it was not provided in the EOR database, a combined analytical method involving the Kantzas, Bryan, and Taheri (2012), Wu (2005), Poiseuille (1940), the Kozeny-Carman and Darcy (1856) equations were used to derive an apparent pay zone or vertical thickness, h, with respect to permeability, K, as:

$$h = 2\sqrt{2K} \qquad\qquad\qquad 2\text{-}7$$

The analytical operation that derived Eq 2-13 was not necessary for the experiments since the vertical thickness, *h*, of the analogous core samples is directly measurable by a metre rule.

2.3.1.5 *Capillary, Displacement and Buoyancy Pressures*

These engineering quantities describe the pressure relationship between the phases in a multiphase porous network system and their gas-oil displacement performance. Fluid permeation through pores can only occur when there is sufficient pressure to overcome surface energy differences (Robinson *et al.*, 2004). Kennedy (2015) and Skerlec (1999) submitted that capillary pressure curves describe how much non-wetting fluid can be forced into a plug or pore by an externally applied pressure. Kantzas, Bryan, and Taheri (2012) further stated that permeability depends on the type of gas, applied pressure, and media. It is further deduced that each gas would form a continuum, similar to a liquid filament, in the connected matrix at different minimum pressure. For a two-phase system (water or gas and oil), capillary pressure, P_c can be represented as (Germic *et al.,* 1997):

$$P_c = P_o - P_i \qquad\qquad\qquad 2\text{-}8$$

Where:

P_c = Capillary pressure

P_o = the pressure oil exerts on the surface,

P_i = the pressure the displacing fluid (water or gas) exerts on the surface.

Another type of pressure encountered is fluid displacement in the porous networks is the displacement pressure, P_d. This is the minimum pressure required by a fluid to enter a pore network and form a continuous fluid filament (Skerlec, 1999). Displacement pressure (in, dynes/cm^2) and the capillary pressure theoretically share the same formula, and both can be written with respect to the surface tension between the two immiscible fluids using the Young-Laplace equation in Eq. 2-9 (Vavra, Kaldi, and Sneider 1992). However, the study deduced that the displacement pressure magnitude needs to be just about sufficient to overcome the capillary pressure for gas-oil displacement to happen.

$$P_c = P_o - P_i = \frac{2\sigma cos\theta}{r} = P_d \qquad\qquad 2\text{-}9$$

Where:

r = is the effective radius of the interface or the pore's radius,

σ = the surface tension,

and cosθ = is the wetting angle of the liquid on the surface of the capillary.

In an immiscible system, the buoyancy pressure quantifies the tendency for a displacing fluid to float or rise when it enters a porous network with existing wetting fluid (Skerlec 1999, Beaumont *et al.,* 1999, Chowalter, 1979, and Germic *et al.,*1997). Lucia (2007), Ruikang *et al*. (2010), Skerlec (1999), and Hubbert (1953) indicated that the reservoir fluid potential, which is a measure of the capacity for fluids to migrate from one point to another, can be reduced

to a buoyancy factor. According to these authors, the buoyancy pressure, P_b is a function of the density differential between the pore's original fluid ρ_o, the displacing fluid ρ_g and the height, h_o of the less dense fluid column as shown in Eq. 2-10

$$P_b = (\rho_o - \rho_g)gh_o \qquad\qquad\qquad 2\text{-}10$$

Therefore, based on the works of previous authors (Skerlec 1999, Beaumont et al. 1999, Chowalter, 1979, Germic et al. 1997, Lucia 2007, Ruikang et al. 2010, Skerlec 1999, and Hubbert 1953), for gas to displace oil through the contribution of a buoyancy mechanism in a porous network, the buoyancy pressure's driving force has to overcome the capillary forces between the existing fluids and the displacing fluid. This leads to the deduction in Eq. 2-11.

$$P_b = (P_o - P_g)gh_o > \left(\frac{2\sigma cos\theta}{r}\right)_o + \left(\frac{2\sigma cos\theta}{r}\right)_g > \frac{2(\sigma cos\theta)_o + (\sigma cos\theta)_g}{r} \qquad 2\text{-}11$$

On a microscopic level, with a single capillary, it is understood from these equations that the capillary, displacement, and buoyancy pressures are inversely proportional to the pore radius. In contrast, only the buoyancy pressure is proportional to the oil column's height in the pore of radius, r, such that h_o is analogically approximated to $2r$. Eq 2-10 is a theoretical supposition that gas EOR displacement performance can be stacked according to the displacing fluid densities. This could amount to a hasty conclusion since there are other forces and mechanisms involved in fluid migration and displacement at the microscopic level. The capillary pressure function is a critical parameter for fluid flow and displacement mechanism because it relates a vital fluid property, surface energy, with the rock property, pore size (Vavra, Kaldi and Sneider 1992). The relationship between capillary pressure, displacement efficiency, saturation, injected pore volume and PVT properties, such as density, has been well documented by several authors (Hugill, and Van Welsenes 1986, Fanchi 2007, McCaughan 2012, McCaughan, Iglauer and Bresme 2013, Vega and Kovscek 2010, and Nielsen, Bourg and Sposito, 2012). Vega and Kovscek (2010), Espinoza and Santamarina (2010), and Tunio *et al.* (2011) suggested that the interfacial interaction between rock

surfaces, the immiscible oil and gas determines enhanced oil recovery efficiency.

Investigators have used statistical, experimental, analytical, and numerical simulation methods to investigate surface tension in two-phase flow. Some of these investigations involve PVT analysis of the fluid properties. Fanchi (2007) compared different correlations used for estimating surface tension. Nielsen, Bourg and Sposito (2012) and Firoozabadi and Ramey (1988) critiqued different methods for estimating surface tension and proposed a modified method. Based on the number of citations in journals, commonly applied correlations are Ramey (1973) Weinaug and Katz (1943) Robert (2007), Beggs (1987), and Macleod-Sudgen equations in Eq. 2-12, which relates surface tension, σ_{og}, to the respective oil and gas Parochor parameters, Pch_o and Pch_g, oil and gas densities, ρ_o and ρ_g, the mean molecular weight of the oil and gas mixture in the oil phase, MW_{og}, the mean molecular weight of the oil and gas mixture in the gas phase, MW_{go}, the mole fractions of the oil and gas in the oil phase x_o, and y_o, and the mole fractions of the oil and gas in the gas phase, x_g, and y_g.

$$\sigma_{og}{}^{1/4} = Pch_o \left[\frac{\rho_o}{MW_{og}} x_o - \frac{\rho_g}{MW_{go}} y_o \right] - Pch_g \left[\frac{\rho_o}{MW_{og}} x_g - \frac{\rho_g}{MW_{go}} y_g \right] \qquad \text{2-12}$$

Pch_o and Pch_g are the characteristic Parachor parameters developed by Sugden (1924), ρ_o and ρ_g are the oil and gas density, respectively. They are used to estimate surface tension (Van Krevelen and Te Nijenhuis, 2009). Some of the fluids identified in reservoir fluids and EOR gases and their Parachors have been listed in Table 2-1.

Table 2-1 The Parachors for pure substances encountered in EOR processes (Weinaug and Katz, 1943 and Adewumi 2009)

S/N	Component	Parachor	Component	Parachor
1.	CO_2	78	nC_4	189.9
2.	N_2	41	iC_5	225
3.	C_1	77	nC_5	231.5
4.	C_2	108	nC_6	271
5.	C_3	150.3	nC_7	312.5
6.	iC_4	181.5	nC_8	351.5

Robert (2007), Whitson and Brulé (2000), Weinaug and Katz (1943), and Adewumi (2009) have suggested equations for estimating the Parachor of oil, Pch_o, and gas, Pch_g, which reproduces outcomes similar to the graphical solution previously published by Ramey (1973). Eq. 2-13 and 2-14 are found to be the most portable ones, and they relate the Parachor of oil to their API gravity and molecular weights of oil, MW_o, and gas MW_g (Robert 2007).

$$Pch_o = (2.376 + 0.0102 API^0) MW_o \qquad \text{2-13}$$

$$Pch_g = (25.2 + 2.86 MW_g) \qquad \text{2-14}$$

Eq 2-13 and 2-14 can be applied to estimate the Parachor of other substances and mixtures not shown in Table 2-1, such as Air.

For an oil gas system, combining Eq. 2-9 and 2-12 yields:

$$P_c = \frac{2\left(Pch_o\left[\frac{\rho_o}{MW_{og}}x_o - \frac{\rho_g}{MW_{go}}y_o\right] - Pch_g\left[\frac{\rho_o}{MW_{og}}x_g - \frac{\rho_g}{MW_{go}}y_g\right]\right)^4 \cos\theta}{r} \qquad \text{2-15}$$

The theoretical implication of Eq. 2-12, 2-13, 2-14, and 2-15 is significant because:

I. It physically relates surface tension to fluid properties that can be quantitatively and explicitly determined during PVT analysis.

II. It creates a theoretical basis for the analogues between single-phase and multi-phase systems through intrinsic and intensive properties, such as molecular weight and density.

III. It offers both analytical and theoretical basis for coupling molecular weight and density with effective saturation, hence the relative permeability and displacement efficiency of an injectant or EOR gas.

Therefore, for a comparative gas investigation, such as the one presented in this research, the qualitative and quantitative implication of injection pressure could be considered independent of the flow model (i.e., single or two-phase). This suggests that the pressure effect in a single-phase model would be a multiple factor of its effect in a two-phase model. Some authors have validated this relation (Fanchi 2007), although some have also criticised its accuracy in principle (Nielsen, Bourg, and Sposito, 2012).

With the preceding equations, it could be deduced that for a comparative two-phases study involving different displacing injectants (CH_4, N_2, Air and CO_2) but one displaced fluid (oil) in a capillary system, the comparative single-phase analysis of the gases in the capillary system could be considered, in principle, to approximate the two-phase analysis of the gases (Abou-Kassem, Islam, and Farouq Ali 2020). Yu-shu and Karsten (1996) had earlier stated that single-phase systems could be considered a special case of a two-phase system. Abou-Kassem, Islam, and Farouq Ali (2020) stated that the volumetric and viscosity properties of water and gas in a multiphase system are no different from those in a single-phase. It is therefore not uncommon to find single-phase imposition on complex reservoir characterisation. For example, given a hypothetical oil-wet capillary system, saturated with oil of molecular weight, MW_o and density, ρ_o, when a second fluid is injected into the capillary such that an immiscible isothermal flow with negligible

compositional effect is achieved, the MW_o and ρ_o of the oil would remain relatively constant throughout the flow process. Therefore, the injected fluid can form a surface tension inertia with the *in-situ* oil. Eq.2-18 suggests that for any other non-wetting fluid (gas) imposed into the capillary, the oil's surface tension should respond to the invading fluid based on the molecular weight and density of the invading fluids. Considering the dimensions of surface tension (force/unit area), this could further be stretched to imply that the capillary *in-situ* oil responds to the invading gases' momentum (Adewumi 2009). Suppose this is correct, as it should by virtue of the theories above, it can therefore be suggested that the potential performance of the respective EOR gases injected in an immiscible two-phase flow system, involving oil and gas, can be significantly characterised and compared based on their individual physical property's behaviour to PVT events in the capillary or porous media. Several other theoretical bases for using single-phase and two-phase analogy have been provided in the experimental phase to validate this work's single-phase model.

Capillary pressure and surface tension have not been included in the screening criteria for EOR selection by authors. In this research, capillary pressure was considered in the data mining and experimental approaches. By the nature of Eq. 2-16, the desirable conditions for the reservoir oil are low capillary pressure and high surface tension. Similarly, the optimisation goals for the gas are low capillary pressure and high surface tension. Consequently, the reservoir and gas that meet these optimisation conditions would be considered the most competitive.

Data Acquisition

Mercury invasion experiments can acquire pressure types, such as capillary pressure, from reservoir core samples. However, when such data are not supplied, an analytical method such as Eq. 2-12, 2-13 2-14, and 2-15 can be coupled to estimate the reservoir system's surface tension and capillary pressure for an idealised two-phase immiscible and piston-like displacement of oil by gas, $\sigma_{og-immisc}$ as in Eq. 2-16 and Eq. 2-17. The conditions are that

there is negligible or no oil fraction dissolved in the displacing gas phase (front), and there is negligible or no dissolved displacing gas in the oil phase at the boundary of contact, suggestive of a negligible compositional effect.

$$\sigma_{og-immisc} = \left(Pch_o \left[\frac{\rho_o}{MW_o} \right] - Pch_g \left[\frac{\rho_g}{MW_g} \right] \right)^4 \qquad \text{2-16}$$

$$P_c = \frac{2 \left(Pch_o \left[\frac{\rho_o}{MW_o} \right] - Pch_g \left[\frac{\rho_g}{MW_g} \right] \right)^4 cos\theta}{r} \qquad \text{2-17}$$

For the EOR gases, the surface tension was acquired using Eq. 2-17. The oil component in the equation is hypothetically assumed to be negligible or zero since the gas is only in phase with the media's saturation. This assumption has been validly used for mercury capillary pressure measurements. The displacement pressure was considered equivalent to capillary pressure by way of Eq. 2-9, and it was experimentally determined for each gas. The displacement pressure was obtained by extrapolating the experimental pressure data backward to the pressure point where the exit gas flow rate is just about approaching zero. The capillary pressure of EOR reservoirs and the displacement pressure data were then used to characterised reservoir oil and EOR gases, respectively. The buoyancy pressure in Eq. 2-10 contrast the densities of oil and the displacing gas; therefore, it was used to couple gas-oil displacement potential for the respective EOR gases.

2.3.1.6   *Capillary Number*

The capillary number is a dimensionless quantity that is extremely critical for recovering trapped oil (Ahmed and Meehan, 2012). Muggeridge *et al.* (2014) identified the capillary number as the factor that influences microscopic displacement efficiency. Eq. 2-18 is a mathematical representation of capillary number, N_c, as a function of interstitial velocity, *v*, viscosity, *μ*, and surface tension, *σ* (Ahmed and Meehan, 2012 and Qi *et al*., 2021):

$$N_c = \frac{v\mu}{\sigma} \qquad \text{2-18}$$

Investigation of experimental and analytical study of capillary number theories by authors, such as Muggeridge *et al.* (2014), Apostolos *et al.* (2016), and Guo *et al.* (2015) indicated that for trapped oil to be reasonably mobilised by a displacing fluid, such as CO_2 and N_2, N_c needs to assume values above 10^{-5}. Capillary trapping is likely to occur when $N_c < 10^{-5}$ (Muggeridge *et al.* 2014, Apostolos *et al.,* 2016). An analytical review of the Eq. 2-18 shows that the N_c can be controlled by increasing the *v* (interstitial velocity). However, it is often impracticable to achieve a high injection pressure in the reservoir pore interstices that is sufficient and safe to cause a reasonable increase in interstitial velocity, especially for reservoirs with poor permeability and where the displacing fluid viscosity is high, such as polymer injectant. Such a situation would run into injectivity issues. However, this is not a gas injection problem. Although care must be taken to avoid viscous fingering reservoir structural damage in the case of gas injection. Muggeridge *et al.* (2014) and Ahmed and Meehan (2012) suggested that reducing σ can favourably influence N_c. Fluids, such as surfactants, alkalines are examples of fluids that can reduce σ. Although the capillary number is an essential indicator of fluid flow, it did not make it to published EOR screening criteria. Consequently, it is expedient to investigate how EOR gases respond to capillary number.

Data Acquisition

As highlighted earlier, the system is an immiscible gas-oil displacement. Therefore, the capillary number can be approximated by combining Eq. 2-16 and 2-18 to yield Eq. 2-19.

$$N_c = \frac{v\mu}{\left(Pch_o\left[\frac{\rho_o}{MW_o}\right] - Pch_g\left[\frac{\rho_g}{MW_g}\right]\right)^4}$$

2-19

Eq. 2-19 was applied to field and experimental data to obtain values for N_c for the reservoirs and the respective gases.

2.3.1.7   *Permeability Contrast*

Besides injection pressure, temperature and surface area, Fanchi (2000), Masoudi, Karkooti and Othman (2013) Masoudi, (2012), Gbadamosi (2018), Vega and Kovscek (2010) identified permeability, permeability variation, mobility, number and type of wells, well rates, and well locations or placement as some of the parameters affecting oil recovery. Bagheri and Beiranvand (2006) stated that reservoir rock types and their structural vertical and horizontal heterogeneities are important components of the reservoir characterisation process. The impact of this heterogeneity on recovery could be significant if not adequately accounted for in the field development plan (Wu and Liu, 2019 and Koneshloo, 2018). Therefore, a good development plan should involve characterising and comparing the economics of alternative processes suitable to optimise the reservoir structural heterogeneity. Consequently, the study of injected gas's effectiveness in creating the desired microscopic displacement efficiency, areal sweep efficiency and vertical sweep efficiency for heterogeneous reservoirs is imperative (Tungdumrongsub and Muggeridge 2010). There are several studies in this area, but few or none have simultaneously compared or characterised the four EOR gases based on their respective responses to permeability contrasts. Wu and Liu (2019) found that oil recovery decrease with reservoir heterogeneity for steams EOR process. Wu *et al.* (2020) simulation experiment found that CO_2/N_2 mixture injection performed better in heterogeneous reservoirs than the individual gases. Jia (2018) has compared Air and N_2 performance using simulation. Recovery was said to decrease with increased heterogeneity generally. However, Jia (2018) found that Air performed better than N_2 quantitatively. Jia (2018) has used two wells in his investigation, one up-dip and the second down-dip. He also simulated both vertical and horizontal wells. Although Fanchi (2000) had earlier stated that the type of well is significant to sweep efficiency in heterogeneous reservoirs, Jia (2018) maintained that the type of well did not record a significant effect on the performances of the gases used. It was not clear what the wells' topology was with respect to the permeability contrast direction. Castricum *et al.* (2015) carried out some gas experiments in porous

media for CH_4, N_2, and CO_2. They found useful permeance segregation or permselectivity for the three gases, however, the discussion of their results was not in the context of gas EOR processes.

It is important to understand the permeability variation gradient of the reservoir and what grade of permeability the wells are interfacing with. Dykstra and Parsons (1950) have created a correlation for vertical sweep efficiency of waterflooding with reservoir parameters, such as permeability variation and mobility ratio (Ahmed 2018). Dykstra and Parsons (1950) described a dimensionless measure of characterising reservoir heterogeneity. This measure is termed the Dykstra–Parsons Coefficient, V_K. Several authors have extended the Dykstra and Parsons method from waterflooding to different EOR processes, such as polymer and surfactant flooding. However, unlike this research, none of the other studies has simultaneously compared the four EOR gases' full spectrum using the same method.

The V_K is observed to lend itself to well-pattern planning in oil recovery strategy for reservoirs with permeability contrast (Fanchi and Batzle 2000 and Lyons 2009). With a better understanding of how the objective functions (volumetric flow rate, mobility, velocity, and momentum) interact with V_K, it would be possible to make the optimal decision in well placement and patterns. A good well strategy should take advantage of the V_K to place injection well in locations and directions to favour and optimise oil displacement to the producer well.

According to Lyons (2009) and Fanchi (2010) correlation, increasing permeability contrast is averse to volumetric sweep efficiency. This assertion corroborates the numerical simulation study of immiscible displacement by Khataniar and Peters (1992). Understandably, the irregularity in the permeability profile of a porous media is expected to dampen the momentum of both the injected volume rate and mobility of the displacing fluid, hence the need to return to V_K study.

The Dykstra-Parsons coefficient is estimated as the ratio of the standard deviation to the mean of the samples permeability variation. This can be

applied to other properties, such as pore size and porosity (Tiab and Donaldson 2016). V_K is often derived using values read off from a log-normal distribution graph (Lyons 2009). It is the equivalence of the coefficient of variance (CV) in statistics. Although the research discovered a weighing caveat to V_K estimation process when the dimensional extent of the respective permeabilities differs. This weighing effect is not accounted for in the coefficient of variance. However, this study had some core samples with remarkably similar dimensions, hence without loss of generalisation, the statistical coefficient of variation method suffices for estimating core samples heterogeneity, which is, in turn, a measure of the permeability variation or contrast, V_K (Hou *et al*., 2016). Since it has been established that volumetric flow rate and mobility ratio are affected by V_K, this research has to determine which gas would perform the most given a V_K.

Reservoir permeability rhythm, which describes the arrangements of different blocks of permeabilities in the reservoir, is also an essential factor to couple with reservoir heterogeneity. Wu and Liu (2019), Hou *et al.* (2016), Jiaona, Pengsong, and Di (2012), and Baojun, Xingjia and Cai (1997) discovered that permeability rhythm significantly affects oil recovery in the steam EOR process. This study experimentally expanded on Wu and Liu (2019) and Hou *et al.* (2016) with respect to well placement and economics in evaluating permeability rhythm for gas EOR processes.

Consider a hypothetical reservoir having two horizontal wells: an injection well and a producer well located above and below a reservoir with vertical permeability contrast and rhythm in Figure 2-3. It is assumed that the effective displacement mechanism is an immiscible displacement, and the conservation of momentum or momentum transfer is valid. The gravity effect is assumed as negligible. The favourable gas shall be the one whose objective functions: that is, volumetric flow rate and mobility both suggest the same well placement configuration. Where this coupling condition is met, the two parameters are therefore considered to be mutually inclusive. A gas whose objective functions suggest different configurations of well placement is considered to be mutually exclusive. Thereby implying that an operator

cannot secure the favourable and desired objective of high injected PV and low mobility ratio simultaneously. Consequently, the operator is forced to decide which optimisation objective to prioritise between Injected PV and Mobility ratio in order to enhance recovery efficiency.
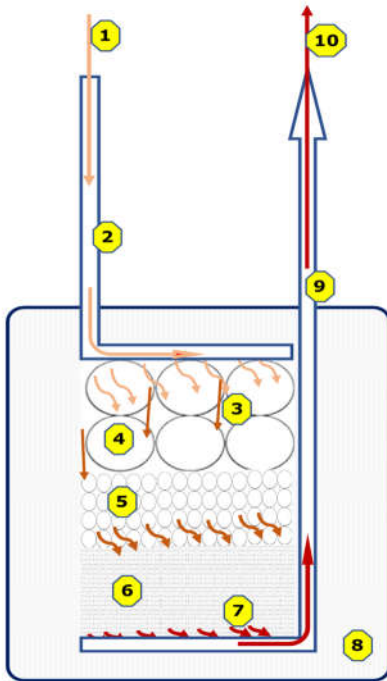
Figure 2-3 Schematic of a simple hypothetical gas EOR reservoir with permeability contrast showing three layers of reservoir rock with similar porosity but different pore sizes : (1) Injected EOR gas, (2) Injection Well (3) Permeating gas (4) 6000nm pore size layer (5) 200nm pore size layer (6) 15nm pore size layer (7) displaced EOR oil and gas (8) impermeable area of reservoir (9) horizontal producer well (10) produced EOR oil and gas.

Given a porous system with three blocks of equal thickness but different pores sizes (such as $d_1=15nm$ and $d_2=200nm$, and $d_3=6000nm$) that can be hypothetically moved around, the maximum number of combinations or topologies available to optimise EOR quantities such as flow rate, permeability, mobility ratio, gas cost, recovery factor is 6. The 6 combinations are shown in Figure 2-4. Each of the topologies represents a structural rhythm. The evaluation is to experimentally identify the gas and rhythm coupling that would optimise EOR quantities, and reduce operational complexity and technicality. Since the flow in porous media depends on the direction of flow, it is expected that the respective EOR gases and quantities

would respond differently to structural and geometrical gradients, such as the 6 compound pore gradients in Figure 2-4.
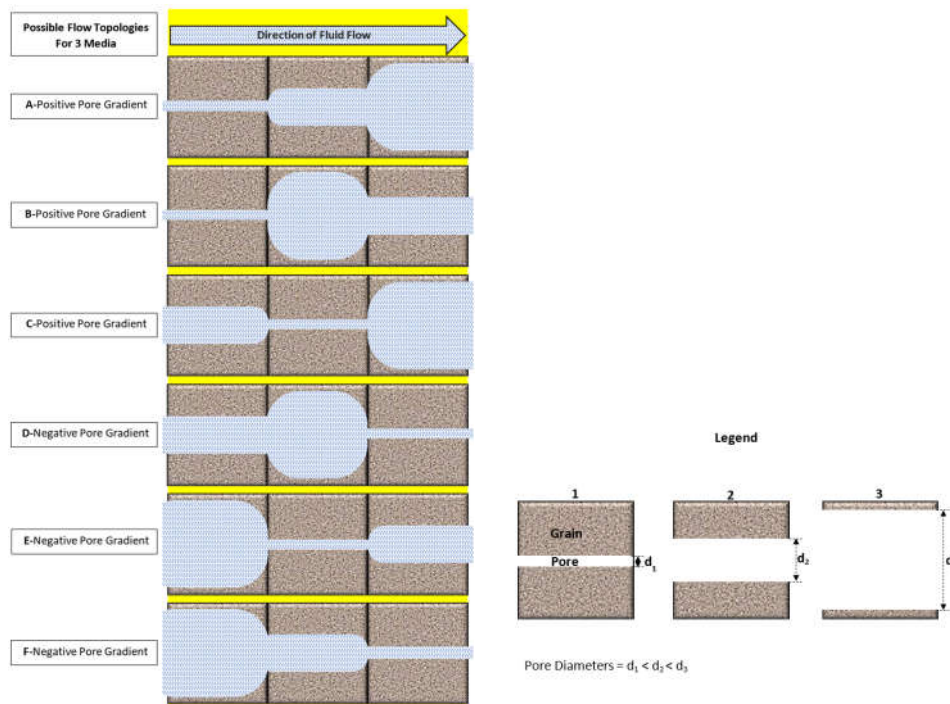
Figure 2-4 Shows 3 different media, the fluid flow profile through them and the potential topologies for optimising EOR gases and quantities.

2.3.1.8   Viscosity

Viscosity is a measure of the fluid resistance to flow when a shearing force is applied to the fluid (Beggs 1987, Yu-shu and Karsten 1996, DOE 2010). Transport theory states that viscosity is caused by the transfer of momentum between two parallel planes (Mason 2020, Chapman and Cowling 1990). The fluid resistance can also be considered as a measure of fluid friction. Therefore, it is expected that the more viscous a fluid is, the more difficult it is to flow through a channel or capillary. Viscosity is an important fluid property utilised in many industries where fluids are applied, such as oil and gas, pharmaceuticals, and construction industries. In the oil industry, viscosity is the single most important fluid property for estimating pressure drop and flowrate in reservoirs (Wang *et al.*, 2020, Hemmati-Sarapardeh *et al.*, 2014, Hemmati-Sarapardeh *et al.*, 2013, Ikiensikimama and Ogboja, 2009, Bergman and Sutton 2007, Al-Marhoun 2004, Naseri, Nikazar and

Dehghani 2005, Elsharkawy and Alikhan 1999). Nazari *et al.* (2015) and Curtis *et al.* (2002) further emphasised that although porosity, permeability, and pressure may determine how a reservoir would behave, density and viscosity are the factors that detect the oil recovery approach operators would apply in a reservoir and the potential oil recovery.

The appraisal of viscosity in characterising immiscible oil displacement during EOR is commonly expressed as viscosity and mobility ratios. These ratios are fundamental dimensionless quantities used to estimate the applicability and quality of the displacement process of oil by another fluid, such as water and gas (Nazari *et al.*, 2015, Buckley and Leverett, 1942). The viscosity ratio, $\lambda_{oil-gas}$, is the dimensionless ratio of the displaced fluid, μ_o, (e.g. Oil) phase viscosity to the displacing fluid (water, gas, polymer or combined fluids) phase viscosity. For gas-oil immiscible displacement system viscosity ratio, $\lambda_{oil-gas}$ (Apostolos, Jonathan, and Saeed, 2016):

$$\lambda_{oil-gas} = \left(\frac{\mu_o}{\mu_g}\right) \qquad\qquad 2\text{-}20$$

Where μ_g, is the dynamic viscosity of the gas.

Similarly, the mobility ratio is the ratio of the displacing fluid's mobility to the displaced fluid mobility (Ahmed and Meehan 2012, Donaldson and Alam 2008, Fanchi 2002a, 2010a, 2010b, Lake and Carroll 2016, Lyons 2010, Satter and Iqbal 2016, Sheng 2011b, 2011a).

Mamudu, Olalekan, and Uyi, (2015) analytical investigation of water-oil displacement indicates that recovery increases when viscosity ratios decrease. Such immiscible displacement of oil by water at a pore-scale could be considered to resemble the piston and cylinder type of displacement. However, when Nazari *et al*. (2015) investigated relative permeability and viscosity ratio for immiscible water-oil displacement, they concluded that viscosity ratio is more significant than relative permeability change. This finding invariably makes it possible to reduce the mobility ratio to viscosity ratio in certain circumstances. Thereby re-echoing other author's statements

on the influence of viscosity on oil recovery (Wang *et al.*, 2020, Hemmati-Sarapardeh *et al.*, 2014, Hemmati-Sarapardeh *et al.*, 2013, Ikiensikimama and Ogboja, 2009, Bergman and Sutton 2007, Al-Marhoun 2004, Naseri, Nikazar and Dehghani 2005, Elsharkawy and Alikhan 1999, Nazari *et al.*, 2015 and Curtis *et al.*, 2002). Furthermore, the preceding discussion indicates there is a knowledge opportunity in this area of fluid mechanics.

Some of the factors that affect gas viscosity have been well documented by Pruess (1991), Yu-shu, Karsten (1996), Towler (2007), and Cerpa *et al.* (2019). These include temperature, pressure, fluid composition, and density. Authors such as Mason (2020) and Al-Dahhan *et al.* (1997) have argued that gas kinetic theory does not suggest that a change in pressure or density effectively affects gas viscosity. However, Wang *et al.* (2020) identified in their work that viscosity is affected by pressure change around a certain minimum pressure. When this happens, the relationship is directly proportional.

Nevertheless, hardly any experimental study has investigated whether the porosity, pore size and aspect ratio of the porous media affects EOR gas viscosity when coupled with pressure (Abunumah, Ogunlude, and Gobina 2021c). Wang *et al.* (2019a) show that viscosity could be influenced by pore size. Starov and Zhdanov (2001) analytical study submitted that porosity is inversely proportional to viscosity on a log-log graph. Sheng *et al.* (2020) used an analytical method to identify positive log-log relations between aspect ratio and apparent permeability. They observed that the effectiveness of the relationship is not diminished when the aspect ratio is above 10. Since permeability is analytically proportional to viscosity by way of the Darcy equation of flow, it can be deduced from Sheng *et al.* (2020) that the relationship between aspect ratio and viscosity may also exist. This type of information is required to enable the proper engineering of mobility and viscosity ratios for enhanced oil recovery.

In EOR technologies, fluids such as gas, steam, and polymers are injected into oil reservoirs to displace and produce oil droplets trapped in reservoir

pores. It has been suggested in Muggeridge *et al.* (2014) that it would be difficult to displace a viscous fluid with one of lesser viscosity. Typical gases used to achieve oil displacement are CO_2, N_2, CH_4, and Air (Jia *et al.,* 2012, Hoffman 2012, Yu *et al.,* 2008, Alvarado and Manrique 2010a, 2010b, Gui *et al.,* 2010, Muggeridge *et al.,* 2014). Unfortunately, oil is about 100 times more viscous than these gases (Mason 2020, Warner and Holstein 2007 and Lake *et al*., 2007).

Authors such as Taber *et al.* (1997), Guerillot (1988), Surguchev and Li (2000), Trujillo *et al.* (2010), Saleh *et al.* (2014), Kang *et al.* (2014), and Nageh *et al.* (2015), have included viscosity as a screening criterion for gas EOR application. Furthermore, the Darcy, Hegen-Pousillie, and Buckley-Leverett equations of flow incorporate viscosity as a variable for measuring fluid flow and immiscible displacement performance. However, these authors have not characterised the viscosity of gases injected in EOR projects. Therefore, this study offers an opportunity to investigate the coupling effect of reservoir oil and displacement gas viscosities.

Data Acquisition

Reservoir fluid viscosity data are generally acquired from laboratory experiments at reservoir temperature. However, where laboratory data are unavailable, empirical correlations can be applied to individual or combined field data to predict an estimate of the oil viscosity. These field data include reservoir temperature, pressure, oil API gravity, solution gas-oil ratio, saturation pressure, reservoir fluid composition, mixture molecular weight, normal boiling point, and critical temperature (Naseri, Nikazar and Dehghani, 2005). To make a robust database, this study was desirous of estimating the reservoir's viscosity whose oil viscosity data was not supplied. After a review of oil field data available to the study and their boundary conditions, a thorough review of twenty published and established correlations was conducted (Naseri, Nikazar and Dehghani, 2005, Al-Marhoun, 1988, Al-Shammasi, 2001, Dindoruk and Christman, 2001, Hanafy *et al., 1*997, Beal, 1946, Connally, 1959, Labedi, 1992, Frashad, *et al.*, 1996, Lasater, 1958,

Velarde, Blasingame, and McCain, 1997, Standing, 1947). It was concluded that Naseri, Nikazar and Dehghani (2005) viscosity correlation model is the best fit for this study because it covers a wide range of dead oil viscosity, μ_{od} (cp). Furthermore, their correlation is a function of API gravity and reservoir temperature, T (^{o}F), which are common parameters in the field database and can be easily obtained from the oil density and reservoir temperature gradient. The Naseri, Nikazar and Dehghani (2005) correlation is presented in Eq.2-21.

$$\mu_{od} = \text{anti } \log_{10} (11.2699 - 4.2699 \log_{10} (API) - 2.052 \log_{10} (T))$$ 2-21

For EOR gas viscosity acquisition, the study discovered several empirical and analytical routes to acquire the EOR gas viscosity data from experimental data. Worthy of note are Darcy, Hegen-Pousillie, and Kinetic energy equations of states. A reservoir or porous media, such as the core samples used in the experiments, can be considered as a bundle of microcapillary tubes (Buryakovsky *et al.*, 2001). The capillary tube system can also be applied experimentally as a simple viscometer for measuring and studying the viscous behaviour of fluids (Zhang and Hoshino 2018). Consequently, the samples used in this research also acted as a viscometer tool to generate data that could be plugged into the Hagen-Poiseuille and Darcy equation of state. The equations of state were analytically modified to account for compressible isothermal radial gas transport in porous media.

The traditional Hagen-Poiseuille equation is expressed in Eq. 2-22 in a linear flow form through a straight pipe of capillary, where Q_c is the capillary volumetric flowrate, in $cm^3.s^{-1}$; r_c is the capillary radius, in cm; dP is the differential pressure across the capillary, in $dyne.cm^{-2}$; μ is the fluid viscosity, in poises, and l_c is the length of capillary, in cm. The equation is represented thus (Loudon and McCulloh 1999):

$$Q_c = -\frac{\pi r_c^4}{8\mu} \left(\frac{dP}{dl_c}\right)$$ 2-22

The negative coefficient is due to the flow being in the direction of diminishing pressure.

For a flow through a circular capillary with a radius, r_c, the fluid entrant area is (Weisstein 2003):

$$A = \pi r^2 \qquad\qquad 2\text{-}23$$

Substituting the entrant area in 2-23 into Eq. 2-22 gives:

$$Q = \frac{A^2}{8\pi\mu}\left(\frac{dP}{dr}\right) \qquad\qquad 2\text{-}24$$

For a configuration with stacks of capillaries forming a radial geometry, the surface area, A, available for fluid entrance can be related to an effective height, h, and the geometric radius, r of the stack:

$$A = 2\pi rh \qquad\qquad 2\text{-}25$$

The radial surface area in 2-25 can substitute the linear area in Eq. 2-24 to give:

$$Q = -\frac{\pi h^2 r^2}{2\mu}\left(\frac{dP}{dr}\right) \qquad\qquad 2\text{-}26$$

For an isothermal flow where the quantities are measured at the output Q_2, the outlet flow rate to atmospheric pressure, P_2, the following gas equation holds:

$$QP = Q_1 P_1 = Q_2 P_2 \qquad\qquad 2\text{-}27$$

Substituting for Q in relation to the output:

$$Q_2 P_2 = -\frac{\pi h^2 r^2}{2\mu}\frac{P dP}{dr} \qquad\qquad 2\text{-}28$$

Rearrange and integrate with respect to pressure and flow path:

$$\int Q_2 \frac{dr}{r^2} = -\int \frac{\pi h^2}{2\mu} \frac{PdP}{P_2}$$

2-29

Integrating both sides of the equation and applying the boundary conditions of pressure and radial length in the direction of flow resolve the negative coefficient on the right side and generate a new negative coefficient on the left side due to the direction of flow towards diminishing radial boundaries. It would cancel out when $\left(\frac{1}{r_1} - \frac{1}{r_2}\right)$ is operated on because the outer radius, r_1, is larger than the inner radius r_2.

$$-Q_2 \left(\frac{1}{r_1} - \frac{1}{r_2}\right) = \frac{\pi h^2}{4\mu} \frac{({P_1}^2 - {P_2}^2)}{P_2}$$

2-30

Make viscosity the subject of the formula in Eq.2-30:

$$\mu = -\frac{\pi h}{4Q_2 P_2} \left(\frac{{P_1}^2 - {P_2}^2}{\left(\frac{1}{r_1} - \frac{1}{r_2}\right)}\right)$$

2-31

All the quantities on the right side of Eq. 2-31 can be explicitly measured in the experiment to significant accuracy. Consequently, with the oil and gas viscosity data acquired, the study was set to characterise and couple this quantity with the petrophysical structural parameters of interest: porosity, pore size, and aspect ratio. Consequently, it is useful to describe the selection criteria for these parameters in the context of reservoir realities. Suffice to state that the viscosity measured here is an intrinsic viscosity. The viscosity profile for a single-phase model such as this experiment can be imposed on a multiphase reservoir model. Abou-Kassem, Islam, and Farouq Ali (2020) stated that there is no difference in viscosity for single and multiphase.

2.3.1.9   API Gravity

The API gravity is a measure of the reservoir's oil density. It is an established reservoir characterisation parameter in the petroleum industry (Curtis *et al.,* 2002, Robert, 2007). Its characterisation capabilities have been extended to EOR applicability and selection models by authors such as Taber *et al.* (1997),

Guerillot (1988), Surguchev and Li (2000), Trujillo *et al.* (2010), Saleh *et al.* (2014), Kang *et al.* (2014) and Nageh *et al.* (2015).

The API gravity is the mathematical inverse of the reservoir fluid specific gravity, γ_o, represented in Eq 2-32 :

$$API = \frac{141.5}{\gamma_o} - 131.5 \qquad\qquad 2\text{-}32$$

From a global reservoir perspective, API values range from 4 to 70 (Curry and Kacewicz 2012, Curtis *et al.*, 2002). This parameter has been used to classify oil into three main groups.

  I.   Ultraheavy to Heavy oil <20

 II.   Intermediate oil >20<45

III.   Light to condensate oil >45<70

Curtis *et al*. (2002) emphasised that oil density knowledge is instrumental in selecting a recovery approach than factors such as porosity and permeability. In Taber *et al.* (1997) EOR screening model, API gravity was set as a criterion for evaluating EOR technologies' applicability. In light of recent technologies, this study has offered to use the most recent global EOR dataset to investigate the current reality of API gravity for EOR classification and selection. Furthermore, previous studies did not couple the field data with gas data for specific gravities or densities.

Data Acquisition

To couple the gas experiments with oil property characterisation, the API was reduced to specific gravity because gases are not quantified in API standard but rather specific gravities. The starting point is to calculate the respective densities of the EOR oils and gases. The API supplied in the database with Eq 2-32 was used to acquire field oil specific gravity. For the EOR gases, the Newton Second law was applied in the form of Eq 2-33. to estimate the apparent specific gravity of the EOR gases from experimental data with

pressure P, volumetric rate $\dot{v}$, mass rate, $\dot{m}$, root mean square velocity v_{rms} and amount of moles, n.

$$P\,\dot{V} = \frac{1}{3}\dot{m}n v_{rms}^2$$

2-33

The density of the gas molecules can be obtained thus:

$$\rho_g = \frac{\dot{m}n}{\dot{V}} = \frac{3P}{v_{rms}^2}$$

2-34

The root means squared velocity quantifies the algebraic sum of the x, y and z components of the molecules' velocities. This is equivalent to about three times the average velocity in the centre of mass for directional flow. Where applicable for validation and ease of usage, the ideal gas law equation solution was also used to obtain density (Eq. 2-23). Where the pressure P, volume v, Temperature T, and moles n, of the gases together with the gas constant R, are represented as (Laugier and Garai 2007):

$$PV = nRT$$

2-35

Consequently, in a steady-state flow, with volumetric rate, $\dot{v}$, and where n can be written in terms of t*he mass flow rate, $\dot{m}$,* and molecular mass M, Eq. 2-36 can thus be rewritten as:

$$P\,\dot{V} = \frac{\dot{m}}{M}RT$$

2-36

It can be further reduced to:

$$P = \frac{\dot{m}}{\dot{V}}\frac{RT}{M} = \rho_g\frac{RT}{M}$$

2-37

$$\rho_g = \frac{PM}{RT}$$

2-38

The specific gravities of the EOR oils γ_o, and gases γ_g, were obtained by normalizing their densities with air ρ_{air} (12.93×10^{-4} g.cm^{-3}) and water ρ_w (0.997 g.cm^{-3}) densities, respectively, which are the industry reference

densities (Standard, A.S.T.M., 2017, Towler, 2007, Tat and Van Gerpen, 2000, and Peramanu, Pruden, and Rahimi, 1999)

$$\gamma_o = \frac{\rho_o}{\rho_w}$$

2-39

$$\gamma_g = \frac{\rho_g}{\rho_{air}}$$

2-40

2.3.2 Performance Description

These are engineering quantities used to evaluate the performances and competitiveness of the EOR gases. They are also used to couple the data mining and experimental phases of this research.

2.3.2.1 Recovery Factor (% EOR production)

Since the ultimate aim for field development is to maximise oil recovery, it is expected that in selecting an EOR method to apply in a field, reservoir engineers would appreciate information indicating the historical recovery performance of EOR application in fields analogous to theirs. Vega and Kovscek (2010) tied the recovery factor of an immiscible gas EOR to factors that have been discussed in the previous session, such as the volumetric flow rate, surface tension, and structural heterogeneity. Sakthikumar, Madaoui, and Chastang (1995) experimentally determined that Air-oil EOR recovery (46%) is slightly greater than N_2-oil recovery (43%). Kantzas, Chatzis, and Dullien (1988) found that N_2 and Air can potentially recover up to 99% of trapped oil. Fassihi, Yannimaras, and Kumar (1997) Babadagli *et al*. (2001), Teigland and Kleppe (2006) deposited different values for immiscible EOR recovery. Nevertheless, the literature review shows that immiscible gas EOR is generally above 5%. Figure 2-5 gives the recovery performance of various gas EOR methods as investigated by Al Adasani and Bai (2011). It is shown that CO_2 has a higher recovery factor than the other gases. This result can only be taken at face value as this research has discovered the probable reason for the difference in recovery factor.
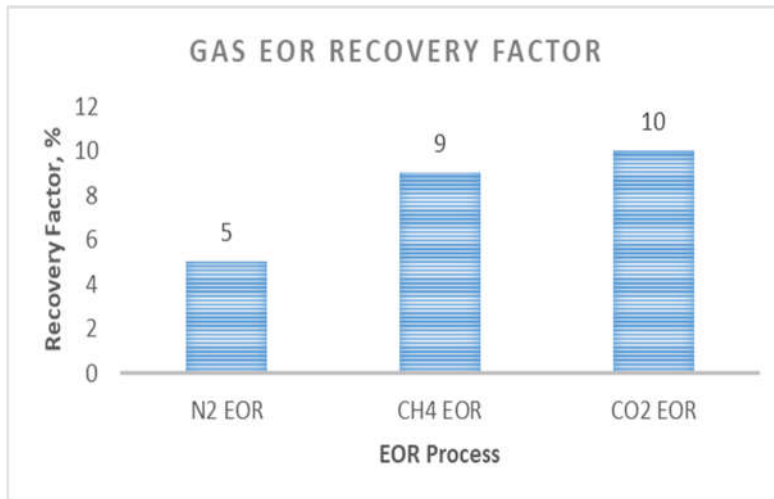
Figure 2-5 Recovery Factor for EOR various Methods (Al Adasani and Bai 2011)

The mechanism for the immiscible displacement of liquid by gas in porous media has been extensively studied and validated. The most common mechanism is slug flow, as shown in Figure 2-6, where a slug of gas displaces the in-situ liquid in a capillary tube (Figure 2-6a) in a piston-like fashion (Figure 2-6b). However, the slug and the wall of the capillary do not form a perfect piston system.

Authors such as Taylor (1960), Fairbrother and Stubbs (1935), and Davies and Taylor (1950) pioneered the subject. They determined a layer of the liquid film adjacent to the capillary wall that is not displaced by the slug. The liquid film thickness, δ of the immobile layer is the difference between the radius of the capillary, r_c, and the slug, r_c ($\delta = r_c - r_d$). This immobile layer, δ, has been found to depend on the characteristics and nature of the slug (displacing fluid), such as its velocity, viscosity, and radius relative to those of the capillary and displaced fluid (Rochinha 2011 and Soares, Mendes and Carvalho 2008).
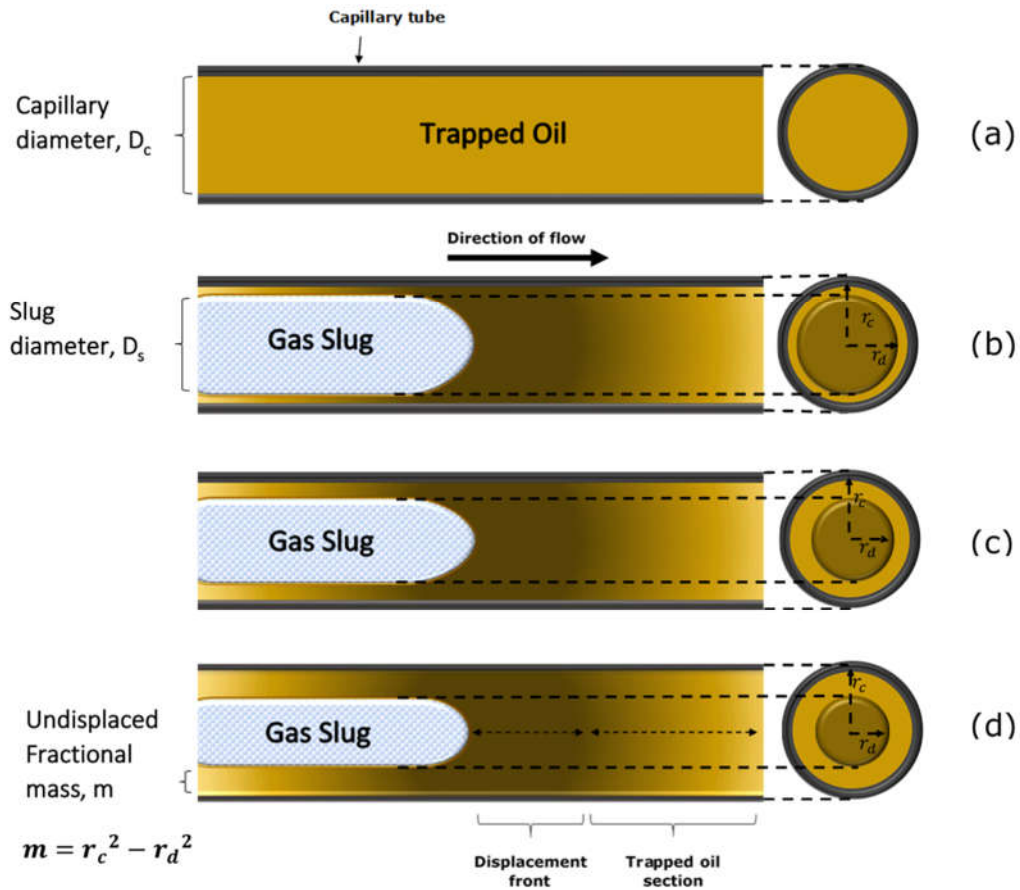
Figure 2-6 Gas-oil displacement process in porous media showing different potential residual saturation as a function of slug radius.

The δ layer as a fraction of the reference total capillary liquid thickness can be considered as a measure of the fraction of un-displaced mass, m, or volume, left after the displacement process is completed. This quantity is used to measure the effectiveness of a gas-liquid or liquid-liquid displacement process. Soares, Mendes, and Carvalho (2008) described m, as a function of the slug head displacement velocity, U_d, to the average velocity, u, of the displaced fluid front ahead of the slug and represented it as:

$$m = \frac{U_d - u}{U_d} = 1 - \left(\frac{r_d}{r_c}\right)^2 \qquad\qquad 2\text{-}41$$

Several authors have extensively used experimental, analytical and numerical methods to validate the concept of m, (Peng *et al.,* 2021, de Sousa *et al.,* 2007, Cheng Hills and Azzorpardi 1998, Olbricht 1996). An extensive review

of the several methods and correlations for m can be found in Soares, Mendes and Carvalho (2006).

Furthermore, Bretherton (1960) described a power correlation between m and capillary number that is of significant utility to this study. The m was found to be proportional to the capillary number. Majumder, Mehta and Khandekar, (2013), Miao *et al.* (2017), and Eain, Egan and Punch, J., (2013) confirmed that m is empirically related to the square root of capillary number, for N_c value ranging from 10^{-5} to 10^{-1} and their mathematical representation for m is thus:

$$m = N_c^{1/2}$$
2-42

It was further confirmed that gas-liquid experiments that bear the relationship in Eq. 2-42 were conducted in laminar flow Reynolds number (Magnini *et al.*, 2017, and Soares, Mendes and Carvalho 2008), which makes their assertion applicable to this work. Recall that (Muggeridge *et al.* (2014), Apostolos *et al.* (2016), and Guo *et al.,* 2015) stated that for EOR displacement to take place, N_c *must be above* 10^{-4}, therefore these boundary conditions mention in Majumder, Mehta and Khandekar, (2013) and Miao *et al.* (2017) apply to EOR application and this study.

In reservoir engineering, the displacement potential of an EOR technology, process, and injectant is based on their ability to reduce residual oil saturation at the pore scale. The m in Eq. 2-42 is analogically equivalent to the residual oil saturation s_{or} at the end of the EOR displacement in Eq. 2-43. Li *et al.* (2017) represented displacement efficiency, E_d as a function of residual oil saturation, s_{or}, due to a given displacement mechanism (in this case, immiscible gas-oil displacement) and the initial oil saturation, s_{oi} at the start of EOR implementation in Eq. 2-43.

$$E_d = \frac{s_{oi} - s_{or}}{s_{oi}}$$
2-43

Coupling equation Eq. 2-42 and 2-43 yields:

$$E_d = \frac{s_{oi} - N_c^{1/2}}{s_{oi}} \qquad \text{2-44}$$

This can be further factorised to:

$$E_d = 1 - \frac{(N_c)^{\frac{1}{2}}}{s_{oi}} \qquad \text{2-45}$$

Eq.2-41, 2-49, and Figure 2-6a-d indicate that the un-displaced oil fraction for different displacing fluids differs. Injectant that produces slugs with a larger radius is expected to perform better than the one with a slimmer slug. Meaning injectants or displacing fluid performance can be characterised by this quantity.

Consequently, Eq. 2-45 is a useful analytical solution for evaluating displacing gas potential to reduce oil saturation and improve the displacement of trapped oil. Although existing screening methods do not integrate the recovery performance index, it is expected that a proper knowledge of this factor based on a fair comparison among EOR processes could change the EOR selection decision process. In this research, the optimisation goal is to identify the EOR process and EOR gas that maximises the displacement efficiency, E_d.

Data Acquisition

The recovery factor as a function of the displacement efficiency was acquired from reported field data. For the EOR gases, the potential displacement efficiency was acquired by applying Eq. 2-49 to experimental data.

2.3.2.2   Mobility Ratio

In this study, a relative mobility ratio measure was considered a potential criterion for evaluating gas EOR performance based on the literature review (Ahmed and Meehan 2012, Donaldson, and Alam 2008, Fanchi 2010a, 2010b, Fanchi 2002a, Lyons 2010, Satter and Iqbal 2016, Sheng 2011). Baker (1998) and Muggeridge *et al.* (2014) have explained the general concept of

fluid mobility in reservoir terms. Effective mobility describes the fluid flow through porous media in relation to its resistance and saturation. In a multiphase flow, mobility is defined as the effective permeability divided by the dynamic fluid viscosity (Tiab and Donaldson 2016, Sydansk, 2007, Lyons and Plisga, 2011). A reduced form of effective mobility is intrinsic mobility which is the fluid mobility for a single-phase flow. Intrinsic mobility is a valuable quantity because, by this definition, intrinsic mobility combines a rock parameter, permeability, and fluid property, viscosity (Abunumah, Ogunlude, and Gobina 2021a). The combinatorial relationship of this quantity is expressed in Eq. 2-46 (Abunumah, Ogunlude, and Gobina 2021a).

$$ M_i = \frac{K_i}{\mu_i} = \left(\frac{K}{\mu} \right)_i $$ 2-46

Where:

M_i = intrinsic mobility of fluid i in mD.cp^{-1},

K_i = intrinsic or absolute permeability of the fluid i in mD,

μ_i = is the dynamic viscosity of the fluid i in cp,

The subscript i = could be gas or water or oil.

Lohman (1988) and Widmoser (1983) and Heath (1980) suggest that mobility varies from reservoir to reservoir, from fluid to fluid, from direction to direction, and from temperature to temperature. Argawal (2012) stated that mobility is extensively affected by pore size and configuration. These authors' conclusions suggest the variability of this quantity along with other reservoir parameters. Therefore, in selecting a gas for EOR application in a reservoir with varying porosity, pore size, and aspect ratio, the gas with the most potential to attain the ratio of unity can be considered the most competitive with respect to viscosity. In EOR processes, fluids are usually injected into the reservoir to displace oil. The dimensionless quantity that relates the displacing fluid mobility and the displaced fluid effective mobility is referred to as the relative mobility ratio (Fanchi 2010a, 2010b, Abdus and Ghulam

2016, and Sheng 2011). Mobility ratio is also a measure of the displacing fluid's effectiveness in displacing trapped oil from reservoir pores in an immiscible piston-like displacement (Muggeridge *et al.,* 2014, Ahmed and Meehan, 2012, Lyons and Plisga, 2011, Lyons, 2009 and Sydansk, 2007). Eq. 2-47 is a mathematical representation of M (Muggeridge *et al.,* 2014).

$$M = \frac{M_{displacing}}{M_{displaced}} = \frac{M_i}{M_o}$$

2-47

M = relative mobility, dimensionless quantity,

M_i = mobility of the displacing fluid, such as water, steam, gas in mD.cp^{-1},

M_o = mobility of the displaced fluid, that is, oil in mD.cp^{-1}.

Eq. 2-47 can be rewritten in terms of the effective permeability and phase viscosity of the respective fluids by substituting Eq. 2-46 in Eq. 2-47. Reservoir engineers must have sufficient control over this dimensionless quantity.

$$M = \frac{\left(\frac{K}{\mu}\right)_i}{\left(\frac{K}{\mu}\right)_o}$$

2-48

According to Lyon (2009) and Dellinger, Patton and Holbrook (1984), a high mobility ratio causes reduced displacement and low sweep efficiency. Mobility control is the method applied by reservoir engineers to ensure that mobility of the injectant/displacing fluid is lower than the mobility of the fluid that is being displaced in order to achieve a stable displacement process across the porous media (Dellinger, Patton and Holbrook 1984). Regardless of the EOR method used and fluid injected (steam or polymer or gas), Abunumah, Ogunlude, and Gobina (2021), Muggeridge *et al.* (2014), Hamid and Muggeridge (2018a, 2018b), and Holstein (2007) highlighted that to achieve favourable displacement, the mobility ratio must be such that the value approaches unity or less (i.e., M≤1).

Figure 2-7 is a schematic of the typical mobility regime in Eq. 2-47. As the displacing fluid mobility decreases relative to oil mobility, M tends towards M<1 (desirable condition). Conversely, when the displacing fluid mobility increases, M tends towards M>1. This is an undesirable condition in reservoir engineering as it means the displacing fluid is more mobile than the displaced fluid or oil. Mobility control aims to bring the M to the shaded (lemon green) area of the curve.
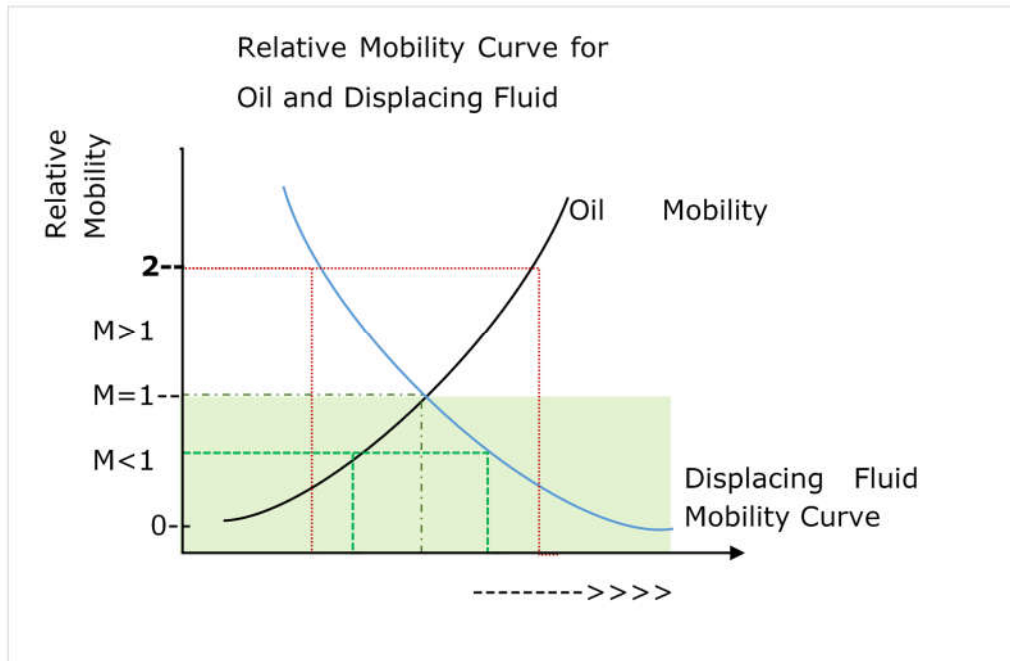
Figure 2-7 Relative Mobility Curve for Oil and displacing system.

Figure 2-8 shows how the gas/oil displacement process responds to the relative mobility ratio. Here gas is the displacing fluid, while oil is the displaced fluid. Six cases with varying mobility were investigated for a five-spot well pattern. It is observed that in cases A and B, where mobility ratios, M is 0.151 and 1, respectively, the oil displacement process is very stable. However, in cases D, E and F, where the relative mobility ratios are 4.58, 17.3 and 71.5, respectively, it would be observed that the displacement process increasingly becomes unstable (Lyons and Plisga 2011). Thereby it causes viscous fingering or channelling of the displacing gas, and consequently, an early breakthrough of gas at the production well, as shown in cases D, E and F (Dellinger, Patton and Holbrook 1984).

EOR Technologies, such as thermal and chemical methods, could be applied to achieve a lower M value by applying thermal energy to the oil to reduce the oil viscosity. Such action invariably increases the oil mobility in contrast to the displacing fluid mobility. Conversely, chemicals, such as a polymer, could be applied to reduce the displacing fluid's mobility compared to oil mobility.

However, in this work, the focus is to investigate the Mobility control for gases applied in EOR projects. In the Mobility equation, fluid viscosity is an important parameter. Ordinarily, gas seems to be at a disadvantage in displacing oil, considering that gas's viscosity at reservoir conditions is usually about 0.02cp while that of oil is between one and two orders of magnitude higher (Mason 2020). Although in an EOR practice, water is usually combined with the gas in a process called Water Alternate Gas (WAG), thereby reducing the gas mobility.
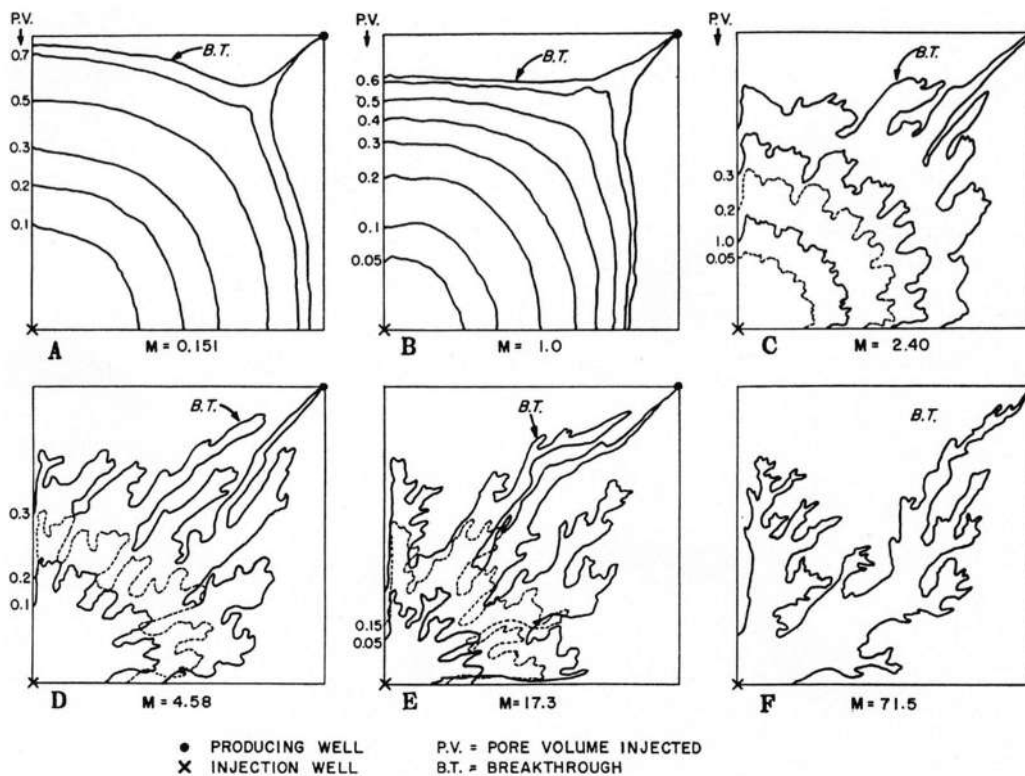
Figure 2-8 Areal view of the effect of mobility ratio on gas/oil displacement process (Warner and Holstein, 2007)

Considering how gas mobility significantly affects EOR performance as explained in the Mobility equation and demonstrated in Figure 2-8, experiments have been designed to investigate the relative performance of EOR gases using mobility as the assessment criteria. These experiments not only investigated the mobility status of gases, but they also investigated the mobility regimes of the gases vis-à-vis properties and parameters, such as mean pressure, operating temperature, molecular weight, and kinetic diameter, and mean free path. Such information gathered would support engineers in mobility control processes. For instance, if there is a change in pressure as commonly encountered in oil production, to what extent would it affect the mobility equilibrium of the respective gases applied in the immiscible gas EOR process.

In this study, intrinsic mobility was investigated as an objective function. The first objective is to identify whether global EOR reservoirs can be characterised by this mobility using data mining techniques. Where this is true, then experiments are conducted to investigate how the respective EOR gases optimise this objective function's requirement. None of the EOR screen models has mobility as a screening criterion. Furthermore, none of the literature has characterised EOR reservoirs and gases by their mobility description. Therefore, adopting this quantity has significant utility.

Data Acquisition

This study used apparent intrinsic mobilities. This quantity was obtained by applying field permeability and viscosity data to Eq. 2-46. For EOR gases, intrinsic mobility, $\frac{K}{\mu}$, was acquired by applying experimental data to a modified Darcy (1856) flow equation as seen in Eq. 2-75, where Q_{std} is the gas flow rate that has been normalised to standard condition, $\frac{(P_1{}^2 - P_2{}^2)}{\ln\frac{r_1}{r_2}}$ is the radial pressure gradient and h is the height of the sample, and T is the average temperature of the existing gas.

$$Q_{std} = 858 \frac{K\,h}{\mu\,T} \frac{(P_1{}^2 - P_2{}^2)}{\ln\frac{r_1}{r_2}}$$

<div align="right">2-49</div>

Eq. 2-75 is in the centimetre-gram-seconds (cgs) unit system, and the full derivation of the equation is detailed in the experimental phase in subsections 6.1.5.1., 6.1.5.2, and 6.1.5.3.

2.3.2.3   Velocity

The interstitial velocity, which is the true velocity of the fluids in reservoir pores interstices, has been investigated to identify which of the EOR gases offer the most favourable oil displacement velocity. According to Muggeridge *et al.* (2014), microscopic displacement is a significant factor in the general improvement of reservoir sweep efficiency, and it is related to velocity by way of the capillary number. Futhermore, Holdich (2002) suggested that velocity is a measure of resistance to flow. In an attempt to find a criterion for stable displacement, Hill (1952), Chuoke, Van der Poel and Killian (1957), Van Meurs and Van der Poel (1959), Dumore (1964) were able to experimentally describe the concept of critical velocity for a two-phase immiscible displacement system. The critical velocity is the interstitial velocity at which the injected displacing fluid forms a stable displacement interface with the displaced fluid. Significantly above this rate, the system could go into viscous fingering.

These velocity descriptions, coupled with the consistent featuring of velocity in fluid flow equations, consequently informed the study to select it as a potential critical criterion for characterising gas immiscible EOR processes. Although the interstitial velocity is a variable determining capillary number in Eq. 2-18, it is, however, the critical velocity that explicitly describes the stability between the displacing and displaced fluids flow. The velocity is adopted both as a factor to characterise EOR reservoirs and as an objective function to evaluate gas performance. This type of analysis is not present in previous studies.

Data Acquisition

The route to acquire this data would depend on the EOS's practicability and validity for the set conditions and available data. Interstitial velocity can be determined experimentally. However, where that is not possible, the interstitial velocity is analytically derived from the established equation of states such as Darcy's, Hagen-Poiseuille, Bernoulli's and Kinetic Energy EOS (Holdich, 2002, Atkins and Escudier, 2013, and Darcy, 1856 and Poiseuille, 1940). In this study, the interstitial gas velocity was obtained by applying the Darcy law to experimented data. The experimental gas volumetric rate, Q_{std}, core sample area, A and porosity, φ, data were fed into Eq. 2-50 to obtain the interstitial velocity.

$$v = \frac{Q_{std}}{A\varphi} \qquad \qquad 2\text{-}50$$

In contrast, the oil apparent interstitial velocity was measured as a potential velocity. It derived from the analytical manipulation of Darcy and Poiseuille laws coupled with the reservoir porosity.

2.3.2.4 *Momentum*

The flow of fluids through porous media should typically conform to mass, linear momentum, and energy conservation. Several authors have charted this area with respect to momentum in open channels and jets (Sundén and Fu, 2016, Henrie, Carpenter and Nicholas, 2016, Chanson, 2012, Faghri and Zhang, 2020). But there is hardly literature that has described momentum in gas EOR processes (Colin, 2006). Gas injected into reservoir pores involves coupling interactions of velocities and masses that can be described by momentum. When this momentum interacts with in situ fluids and pore matrix momentum, the quality of the interactions can be further characterised by momentum transferability or flux. Accounting for momentum and momentum flux has a major utility in understanding gas-oil displacement. A displacing particle may have a large momentum but a low capacity to diffuse the momentum onto the displaced particle. Therefore, the coupling effect of momentum and momentum flux potential is essential in

evaluating displacing fluids' competitiveness. As an objective function, the research's optimisation goal is to evaluate and identify the gas that offers the most competitive coupling of these quantities.

Momentum, P, is a combinatorial engineering quantity, and it is directly proportional to the component mass, m_i and velocity, v_i. Therefore, the relative momentum capacity for the respective gas-oil system would be:

$$P = \sum_{i=1}^{n} m_i v_i \qquad \text{2-51}$$

And the kinetic energy, KE, possessed by the system is:

$$KE = \frac{1}{2} \sum_{i=1}^{n} (m_i v_i^2)_2 \qquad \text{2-52}$$

When two bodies with respective velocities in an initial state (1) experience collision, they would possess a new final state (2). By way of the conservation of momentum, the initial (1) and final (2) momentum balance should be:

$$P_1 - P_2 = \sum_{i=1}^{n} (m_i v_i)_1 - \sum_{i=1}^{n} (m_i v_i)_2 = 0 \qquad \text{2-53}$$

In a perfectly inelastic collision between two bodies, where one body was relatively at rest before the collision, the constituent bodies after collision would possess a common velocity, v_2. The velocity balance:

$$\sum_{i=1}^{n} (m_i v_i)_1 = v_2 \sum_{i=1}^{n} (m_i)_2 \qquad \text{2-54}$$

$$v_2 = \frac{\sum_{i=1}^{n} (m_i v_i)_1}{\sum_{i=1}^{n} (m_i)_2} \qquad \text{2-55}$$

For this system, the initial and final Kinetic Energy KE$_1$ and KE$_2$ becomes

$$KE_1 = \frac{1}{2}\sum_{i=1}^{n}(m_i v_i{}^2)_1 \qquad\qquad 2\text{-}56$$

$$KE_2 = \frac{1}{2}v_2{}^2\sum_{i=1}^{n}(m_i)_2 \qquad\qquad 2\text{-}57$$

Substituting for v_2 2-55 into Eq. 2-57 and collecting like terms gives:

$$KE_2 = \frac{1}{2}\left(\frac{\sum_{i=1}^{n}(m_i v_i)_1}{\sum_{i=1}^{n}(m_i)_2}\right)^2\sum_{i=1}^{n}(m_i)_2 = \frac{1}{2}\frac{(\sum_{i=1}^{n}(m_i v_i)_1)^2}{\sum_{i=1}^{n}(m_i)_2} \qquad\qquad 2\text{-}58$$

The fraction of energy lost, ϕ_E, between the bodies due to factors such as friction can be estimated as

$$\phi_E = \frac{KE_1 - KE_2}{KE_1} = \frac{\sum_{i=1}^{n}(m_i v_i{}^2)_1 - \frac{(\sum_{i=1}^{n}(m_i v_i)_1)^2}{\sum_{i=1}^{n}(m_i)_2}}{\sum_{i=1}^{n}(m_i v_i{}^2)_1} \qquad\qquad 2\text{-}59$$

Fluid displacement of trapped oil particles can be idealised as perfect inelastic collision, whereby the displacement fluid and the relatively stationary residual oil assume a new velocity at the point of contact in a piston-like shape.

Applying Eq. 2-54 for gas-oil displacement with the mass of gas and oil particles represented as m_g and m_o respectively, and their respective initial velocity of v_{g1} and v_{o1}, the initial and final momentum conservative balance would be:

$$m_g v_{g1} + m_0 v_{o1} = (m_g + m_0)v_2 \qquad\qquad 2\text{-}60$$

The trapped oil particles are considered to be at rest ($v_{o1} = 0$) relative to the invading gas, therefore the equation reduces to:

$$m_g v_{g1} = (m_g + m_0)v_2$$

2-61

The final assumed displacing velocity, v_2 is

$$v_2 = \frac{m_g v_{g1}}{m_g + m_0}$$

2-62

For this system, the initial and final Kinetic Energy KE$_1$ and KE$_2$ becomes

$$KE_1 = \frac{1}{2} m_g v_{g1}{}^2$$

2-63

$$KE_2 = \frac{1}{2}(m_g + m_0)\left(\left(\frac{m_g}{m_g + m_0}\right)v_{g1}\right)^2 = \frac{1}{2}\left(\frac{(m_g v_{g1})^2}{m_g + m_0}\right)$$

2-64

The fraction of energy loss, ϕ_E, between the bodies can be estimated as:

$$\phi_E = \frac{KE_1 - KE_2}{KE_1} = \frac{(m_g v_{g1}{}^2) - \left(\frac{(m_g v_{g1})^2}{m_g + m_0}\right)}{(m_g v_{g1}{}^2)} = \left(1 - \frac{m_g}{m_g + m_0}\right)$$

2-65

This can be further reduced to Eq. 2-66:

$$\phi_E = \left(\frac{m_0}{m_g + m_0}\right)$$

2-66

Data Acquisition

The linear momentum and energy loss data for gas-oil displacement were acquired from Eq. 2-61, 2-62 and 2-66. The momentum flux was measured by the fluid's momentum diffusivity parameter, v, which relates dynamic viscosity, μ, and density, ρ,:

$$\eta = \frac{\mu}{\rho}$$

2-67

2.3.2.5 Transmissibility

Transmissibility is a quantitative measure of the capacity or rate at which a reservoir pay zone transmits reservoir fluids (Agarwal 2012, Satter 2008, Dielman 2005, Heath 1980 and Widmoser 1983). The Transmissibility, T_i, of a fluid reservoir system is represented mathematically as the integral of permeability over the reservoir thickness, h, divided by viscosity, μ. A steady-state form of T_i can be seen in Eq. 2-68 (Harrison and Chauvel 2007):

$$T_i = \frac{K_i}{\mu_i}h = M_i h \qquad\qquad 2\text{-}68$$

Some authors have de-emphasised the utility of dynamic viscosity in the transmissibility equation. Desbarats and Dimitrakopoulos (1990) rationalised it as unity. In contrast, Lohman (1988) and Widmoser (1983) introduced kinematic viscosity and specific weight respectively of the fluid of interest. However, in this study, dynamic viscosity was used in obtaining transmissibility. Therefore, the transmissibility equation is an analytic product of mobility, M_i, and pay zone thickness, h.

$$T_i = M_i h \qquad\qquad 2\text{-}69$$

It has been stated by Müller-Petke and Yaramanci (2015) and Desbarats and Dimitrakopoulos (1990) that this engineering quantity is important in estimating the overall fluid transport capacity of the reservoir grid. Transmissibility models are often used in reservoir simulations to investigate flow between reservoir grids (Panteha 2018 and Wang and Gupta 1999). This suggests that reservoirs could be characterised by transmissibility, therefore, this might impact the selection of EOR gases to displace trapped oil. Transmissibility is a combinatorial objective function. For gas EOR, the optimisation criterion involves identifying the gas that offers the desired transmissibility potential, therefore, improving the gas selection process. However, authors such as Taber *et al.* (1997), Guerillot (1988), Surguchev and Li (2000), Trujillo *et al.* (2010), Saleh *et al.* (2014), Kang *et al.* (2014) and Nageh *et al.* (2015) have not included transmissibility in their EOR

screening model. This study provided an EOR solution for this engineering quantity.

Data Acquisition

The transmissibility of the oil and gas are obtainable from the application of Eq. 2-68. The variables are either supplied or derived in previous subsections and from experiments in the gas of gases.

2.3.2.6   Sweep Optimisation Curve and Parameter

One of the most important experimental study findings is developing an optimisation curve that can be used to evaluate gas reservoir sweep competitiveness and estimate a desirable balance between injection volume rate and mobility. In previous subsections, the experimental data confirmed that the injection volume rate and mobility are inversely related. This result is in line with other gas investigations, such as Dyes, Caudle and Erickson (1954).

In previous studies by investigators, such as Dyes, Caudle and Erickson (1954), Caudle and Dyes (1958), Bagci (2007), and Lyons and Plisga (2011), it has been confirmed that the recovery factor, R_f, is based on the quality of the vertical and areal sweep, and the displacement efficiencies, which are functions of injection/production well pattern topography, mobility ratio, the volume of displacing phase injected and relative permeability ratio. It is been established that the R_f increases with gas volume injected and decreases with mobility ratio (Holstein 2007 and Caudle and Erickson 1954). Consequently, a proportionality equation can be drawn as shown in 2-70 …

$$R_f = k_{gi}\ \frac{V_{gas}}{\lambda_{gas}}$$
$$\text{2-70}$$

Where k_{gi} is the proportionality constants peculiar to the displacing fluid i. Eq. 2-70 can be rearranged thus:

$$\frac{R_f}{k_{gi}} = \frac{V_{gas}}{\lambda_{gas}}$$

<div align="right">2-71</div>

The term $\frac{R_f}{k_{gi}}$, on the right had side of Eq 2-71 can be considered a measure of the micro (pore level displacement) and macro (areal reach or spread) recovery. The measures reflect the extent or quality of the overall recovery process. The term is notionally described as the Sweep Optimisation Parameter, SOP. Therefore Eq 2-71 can be rewritten as:

$$\frac{R_f}{k_{v-\lambda}} = \text{SOP} = \frac{V_{gas}}{\lambda_{gas}}$$

<div align="right">2-72</div>

V_{gas} and λ_{gas} assumes different values at different pressure and temperature, therefore:

$$\text{SOP}\,(P,T) = \frac{V_{gas}}{\lambda_{gas}}$$

<div align="right">2-73</div>

Eq. 2-73 shows that SOP values are dependent on the injection Pressure, P of the gas and the porous media. For every P, above a certain pressure threshold for a pair of porous media and gas, there is a unique SOP value. The SOP was further used to evaluate the competitiveness of EOR gases in immiscible gas EOR. The optimisation goal is to identify the gas with the highest SOP.

Data Acquisition

In this study, graphical method was adopted to estimate the value of SOP from the pressure graph of V_{gas} and λ_{gas}. The graphical method was appropriate because of the power-equation relationship of V_{gas} and λ_{gas} with injection pressure. V_{gas} and λ_{gas} values were read off from the graph and applied to Eq. 2-74 to obtain estimates for SOP at different pressure and temperature.

2.3.3 Infrastructure Description

2.3.3.1   Well density

Well Density is a combinatory engineering quantity derived from the numbers of wells and reservoir areal extent. As used in this research, well density is a measure of the well requirement for an EOR method to perform optimally with respect to the size of the field, oil recovery, and well cost. Performance, in this case, should be described as a minimum well requirement without compromising oil recovery (Slatt 2013a, and Shepherd 2009). The Well Density (W_{Den}), as derived in Eq. 2-74, represents the estimated number of wells, required to drain one acre of reservoir undergoing a particular EOR technology. The well density is calculated as (Shepherd 2009):

$$W_{Den} = \frac{W_P + W_I}{A}$$ 2-74

Where:

W_{Den} = the well density (Well/Acre),

W_P = the number of production wells,

W_I = the number of injection wells.

The impact of well density on EOR has not been well studied. The expectation is that some EOR processes may generally display a profile that is consistent with high well density than others. The well-density profile could even be significant when the EOR processes are coupled with reservoir geometrical, geological and fluids realities. If a predictive model can be generated from this analysis for W_{Den}, then reservoir engineers and management personnel can have a broader technological and economic scope for comparing EOR methods at the screening stage. A typical well cost $10-$40 million and 30 to 50 days to drill (Matthew 2017, PSAC 2015, Zhang *et al*., 2015 and Pershad *et al.*, 2012). However, if one has two EOR technologies options with different W_{Den} (every other thing being equal), optimization requires that the EOR process with the lowest W_{Den} should be selected. This would save drilling cost

and time and reduce application. Well density and its impact on various EOR performances is an area that has not been investigated in detail. There was hardly any direct or recent journal article found on this subject matter with respect to EOR methods. Holm (1980) compared infill wells and EOR implementation as two competing oil recovery strategies that could also be combined for synergetic oil recovery. The author, however, submitted that well spacing is critical to chemical EOR than to gas EOR. The author further reported that short-circuiting of displacing fluids, such as CO_2, could be reduced by maintaining the often applied well spacing of 40 acres in reservoirs with high permeability. Using numerical data analysis in the US oilfields, Cutler (1924) and Keller and Callaway (1950) agreed that increased well density improves the ultimate recovery factor. However, the two authors disagreed on the mechanism, conditions and extent of such improvement. Kern (1981) did a data analysis of 48 reserves in the Permian Basin and concluded that in water flooded reservoirs with lower permeability (<1.2mD), there is a significant correlation between well spacing and recovery efficiency. However, at higher permeability (>1.2dm), no correlation was observed. On the contrary, Suman (1934) rejected the previous authors' claims of the relationship between well spacing and recovery efficiency, insisting that the most significant recovery is achieved from relatively sparse well density. It would be observed that not only are these authored works old, but they are also not much agreement in their respective positions. Li *et al*. (2015) investigation shows that well density improves oil recovery efficiency; however, beyond 3 well/km^2, the oil recovery efficiency graph plateau or flattens out, but their study did not include an EOR situation that involves a fluid injection process.

Furthermore, there has been a grave concern about how these authors used the concept of well density and well spacing interchangeably. After a rigorous study and modelling of the two concepts using spatial analysis, it was concluded that the authors might have been mistaken. Two or more reservoirs may have the same well spacing but different well density. This is especially observable in well patterns that are of direct line topology, such as the nine-spot pattern. To prove the practicality of this, the study used spatial modelling and analysis. The highlight of the analysis could be seen in Figure 2-9.

Field	Reservoir Area	No. of Wells	Spacing	Density, well/acre
A	1 acre (43,560ft2)	22	66ft	22.00
B	2 acres (87,120ft2)	33	66ft	16.50
C	3 acres (130,680ft2)	44	66ft	14.66
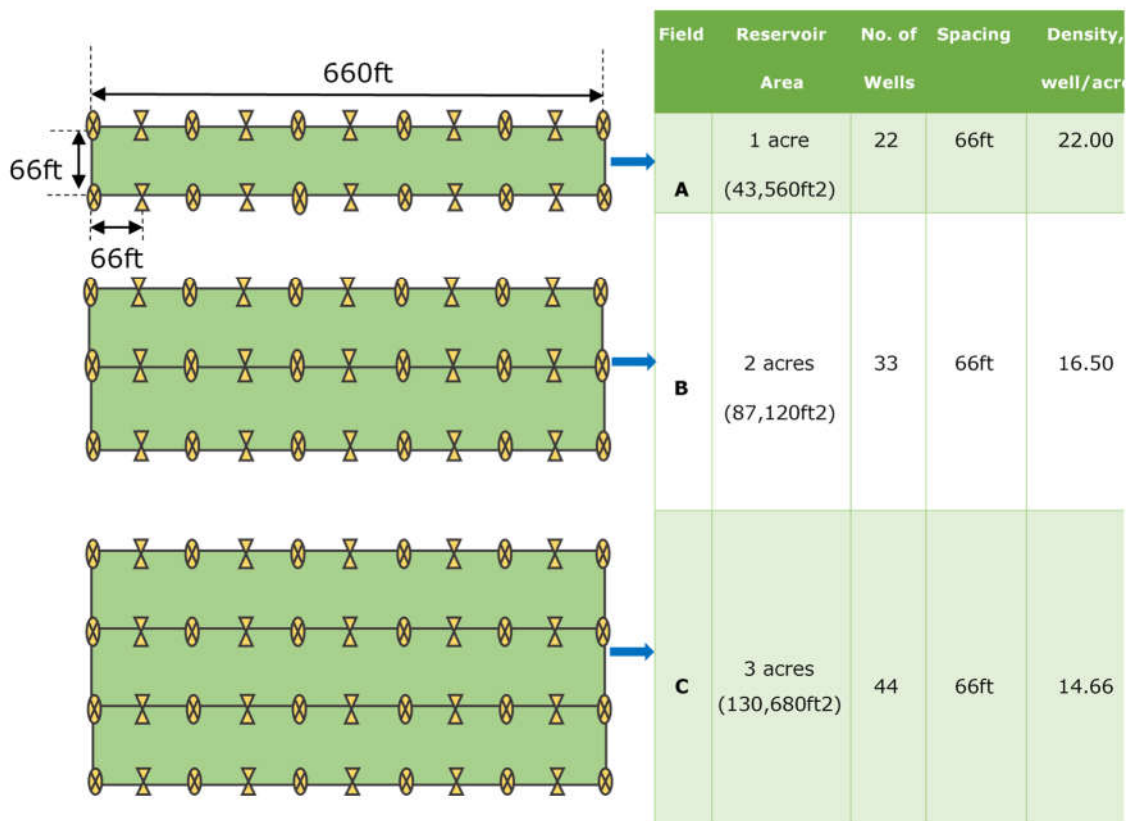
Figure 2-9 Three hypothetical reservoirs with the same well spacing but different well density.

Figure 2-9 shows three hypothetical reservoirs (A, B and C) of different sizes but with their wells equally spaced yet, they have different Well densities. For B and C to have the same density as A (22wells/acre), one would need to add 11 and 22 more wells to B and C, respectively. This would, however, now change the well spacing and architecture for B and C. Meanwhile, Kern (1981)

compared the correlation between recovery efficiency and reservoir size for 25 reservoirs with the same well spacing (40acres); the author observed that for a constant well spacing, recovery efficiency is correlated with reservoir size. Applying Kern (1981) findings on the hypothetical reservoirs in Figure 2-9 implies that by the sheer sizes of the respective fields, the recovery efficiency of Field C would be higher than Field B, and that of B would be higher than A. Even though they all have the same well spatial architecture, the two concepts might not be the same. Hence, they should be investigated separately. Therefore, using well spacing to make a case for well density or using them interchangeably could be misleading as the former undermines the synergetic impact of well topology and reservoir size.

Suffice to note that these authors were considering well density in the light of primary and secondary recovery. In the EOR application context, it is not easy to fully appreciate how much analogy could be drawn from their studies, as the primary recovery mechanism operates quite differently from the EOR mechanism. In this research, the well density parameter was adopted and investigated to establish the characterisation of EOR processes based on their well requirement in the data mining stage. The knowledge was used to design the experiments to investigate the well density parameter for EOR gases.

Data Acquisition

The well density was obtained by plugging oilfield data of wells and reservoir area into Eq. 2-74. Where the well records are not available, the well density was ignored. For the gas experiment, an empirical-analytical approach was used to predict the respective gases' potential well density. The volume rate (cm^3) is normalised by the equivalent pay zone (cm) of the core samples, and a single well model was assumed. In this way the normalised volume (now the gas sweep area, cm^2) coupled with the single well model gives a measure of the well density.

2.3.3.2   *EOR Well Patterns and Placement*

An attempt has been made to investigate how well patterns could affect EOR projects' performance. Well pattern or topology could be considered the distinct spatial arrangement of wells in a field as a single system. According to Duda and Il (2010), Zhang *et al.* (2015), Shepherd (2009), Slatt (2013a) and Zou *et al.* (2011) well patterns bear useful information regarding the locations, spacing, density and ratio of the producer to injection wells. The common normal and inverted well patterns are shown in Figure 2-10 as 5-spot, 7-sport and 9-spot. Each pattern was created with a similar scale. The visual intensity of the injected fluid indicates that the normal patterns propagate the injected fluid more effectively, and the normal 9-spot pattern is relatively better. Holm (1980) had earlier posited that well patterns could be tailored to optimise EOR application efficiency. Ahmed (2006) further suggested that well patterns can be tailored around directional permeability trends to improve sweep efficiency. Since permeability variation or heterogeneity could be a significant factor for EOR performance, it, therefore, follows that EOR methods could respond differently to the respective well pattern. For gas EOR, this research was designed to identify the respective gas performance in scenarios that range from pore size variability, porosity and permeability contrast. The knowledge from the experiments and data mining was coupled to explain how well pattern could affect gas EOR process.

El Ela and Sayyouh (2014), Holm (1980) and Duda and Il (2010) had claimed that well pattern modelling could be used to optimise EOR methods in general, but the authors fell short of describing the details. For example, whether EOR methods can be uniquely associated with well patterns. The effect of well patterns was also reported with respect to a CO_2 EOR implementation at the SACROC field in the Permian Basin, United States. Walzel (2017) emphatically stated that by targeting the well patterns production in the SACROC field, oil recovery was tripled.

A mathematical analysis of the well compositions in regular well patterns shown in Figure 2-10 reveals that the ratio between the injection wells (W_i) and production wells (W_p) are usually within a certain range for different well

patterns, regardless of the number of repetition (reoccurring unit cells) within the pattern block. This preliminary analysis reveals the possibility for each category of well pattern to be uniquely expressed by arithmetic or geometric series.
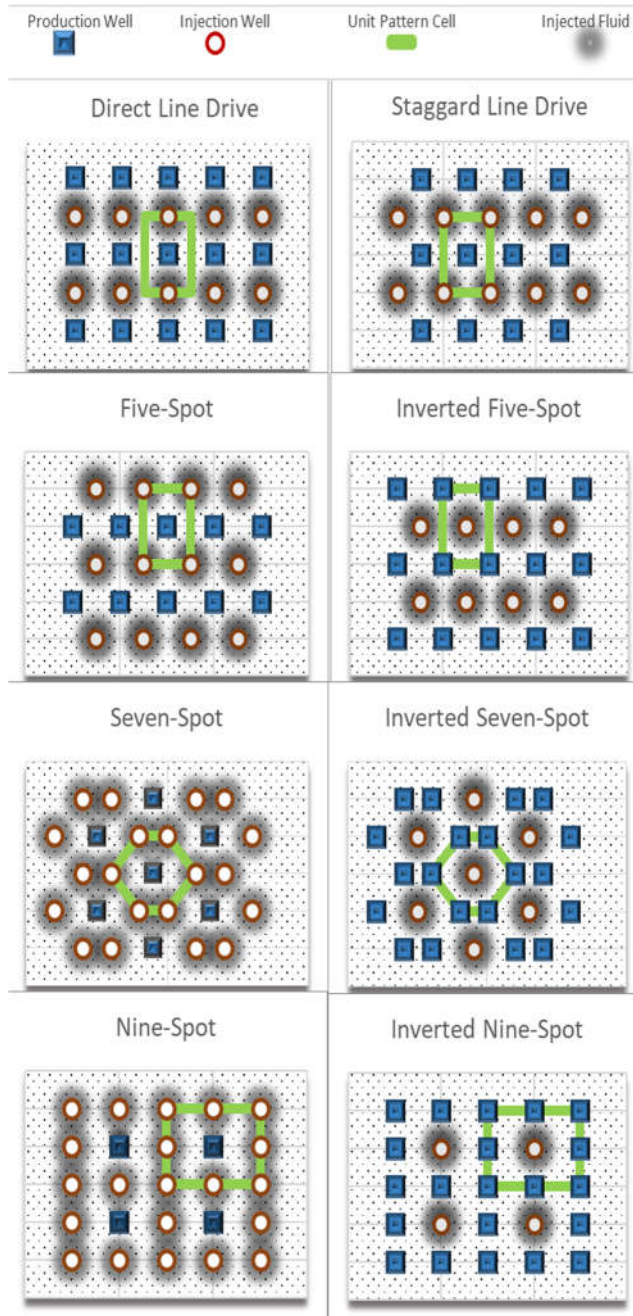
Figure 2-10 Regular Well Pattern showing a different arrangement of production and injection.

Such understanding could be implemented in screening models to:

I.   Identify and categorise well patterns that are often implemented for certain EOR processes.

II. Pre-empt the selection of EOR methods that would be most agreeable to the existing well pattern.

Such knowledge is expected to facilitate the association of well patterns to EOR processes and the manoeuvrability or convertibility of one well pattern to fit prospective EOR processes. In Figure 2-10, a 9-spot unit can be converted to 4 sets of 5-spot units by changing the existing centre production well to an injection well and then drilling four infill wells inside the 9-spot unit.

Consequent to the possible effect of well pattern on EOR methods performance, a simple dimensionless quantity called Pattern Predictor (P_P) has been presented in in Eq. 2-75. It relates the number of injection well, W_I, required to service a production well, W_P in the pattern matrix.

$$P_P = \frac{\sum_{i=1}^{n} W_{Ii}}{\sum_{i=1}^{n} W_{Pi}} \qquad\qquad 2\text{-}75$$

Eq. 2-75 can also be considered a measure of the Well Ratio Index. It is expected that if the investigation of P_P shows clustering behaviour in an EOR database and if it further correlates significantly with other reservoir parameters and properties, then an engineering case could be made to consider well pattern in EOR screening criteria.

Before now, the general practice is to determine the well requirements for a selected EOR method at the Reservoir Simulation Phase (Rotondi *et al.,* 2015). However, this research attempts to make it possible for engineers to estimate the most optimised patterns for each EOR method, given a reservoir with known conditions. A rigorous attempt was made to develop a mathematical series or sequence from the various well patterns in Figure 2-10 (using oil field data of EOR projects and experimental data), which could then be used to confidently predict well patterns of an unknown field, given the well data of the field. 1st, $2^{nd,}$ and 3rd order mathematical sequence approaches have been tried, but these have not yielded useful results.

It is assumed that a predictive sequence could be achievable through appropriate mathematical operations or programming. Duda and Il (2010) buttress this possibility when they stated that the ratio of injectors to producers and their relative position to one another indicates the type of well pattern formed. In the meantime, combining the Eq. 2-75 and Figure 2-10 suggest that an EOR process that has $P_P < 1$ indicates an inverted well pattern or topology is implemented or favourable to that process (i.e., more producer wells than injection wells). Where $P_P > 1$, it means the well pattern is a normal one. Where $P_P < 1$, it implies an inverted (i.e., less producer wells than injection wells). The well pattern characterisation has both economic and technical implications.

By the recovery factor and injected volume principle, normal pattern could engender higher micro and macro sweep efficiency of the reservoir at a shorter time frame than the inverted pattern. It is also instructive to note that the normal well pattern implies relatively high injectant cost as can be visually and qualitatively observed when the intensities of the injected fluid of the normal and inverted cases in the seven-spot pattern are compared (Figure 2-10). Furthermore, producer well encounter more operational problems and undergo more workover (i.e., maintenance) than injector wells (Holditch, 1992, Gidley 1992, Osborne 1992, and Robinson 1992), therefore, EOR technology and process that favour inverted well pattern would invariably incur higher cost and technical burden than EOR technology and process that use normal well pattern.

Consequently, the optimisation goal, therefore, is to minimise the technical and cost impact of P_P during the screening and selection of EOR process.

Data Acquisition

The data for this analysis was obtained by plugging field data of injection and production wells into Eq. 2-75. For the EOR gases, a qualitative approach was used to predict the potential well pattern.

2.3.3.3   EOR Cost and Facility Description

It is expected that different EOR methods would share similar and also peculiar cost and facilities requirements (Abunumah, Ogunlude, and Gobina 2021b). This section is to study the relative facility needs unique to gas EOR methods. The utility of this analysis is both technical and economical (Babadagli 2020, 2007). It would allow decision-makers to compare, in advance, their asset capacity to withstand the facility incidental to a proposed gas EOR method and the attended economic feasibility. CO_2 EOR, for instance, would require a separate pipeline grid to network CO_2 gas between anthropogenic sources and reservoirs implementing CO_2 EOR (Spinelli *et al.* 2012), especially for fields outside the US Permian basin or where there are no existing or pool-able infrastructure.

In contrast, CH_4 can use the existing natural gas grid to get the injectant to reservoirs implementing CH_4 EOR. These are some of the operational, logistic and cost discriminations among CH_4, N_2, Air and CO_2 implementation. Some of the identified facility needs of EOR in general are: power, space, pumps, compressor unit, and separation units (Putnam 2013). Suffice to state that offshore and onshore oil fields' facility requirements would differ significantly due to peculiar constraints in an offshore environment, such as space and isolation.

Economic optimisation is the definitive aim of EOR engineering management. EOR projects are found to be sensitive to the oil price, fiscal incentives and complex oil recovery cost (Babadagli, 2020, 2007, El Ela and Sayyouh 2014 Compernolle *et al.,* 2017, Welkenhuysen *et al.,* 2018, Kemp and Stephen 2014, and Zekri and Jerbi 2002). A qualitative inspection of Figure 2-11 shows a time lag correlation between the number of new EOR project execution and oil price stability and security. Oil price and EOR project cost are essential variables for evaluating profitability optimisation. Therefore, the competitive cost of a gas EOR process can be an incentive when juxtaposed with the oil price reality in Figure 2-11.
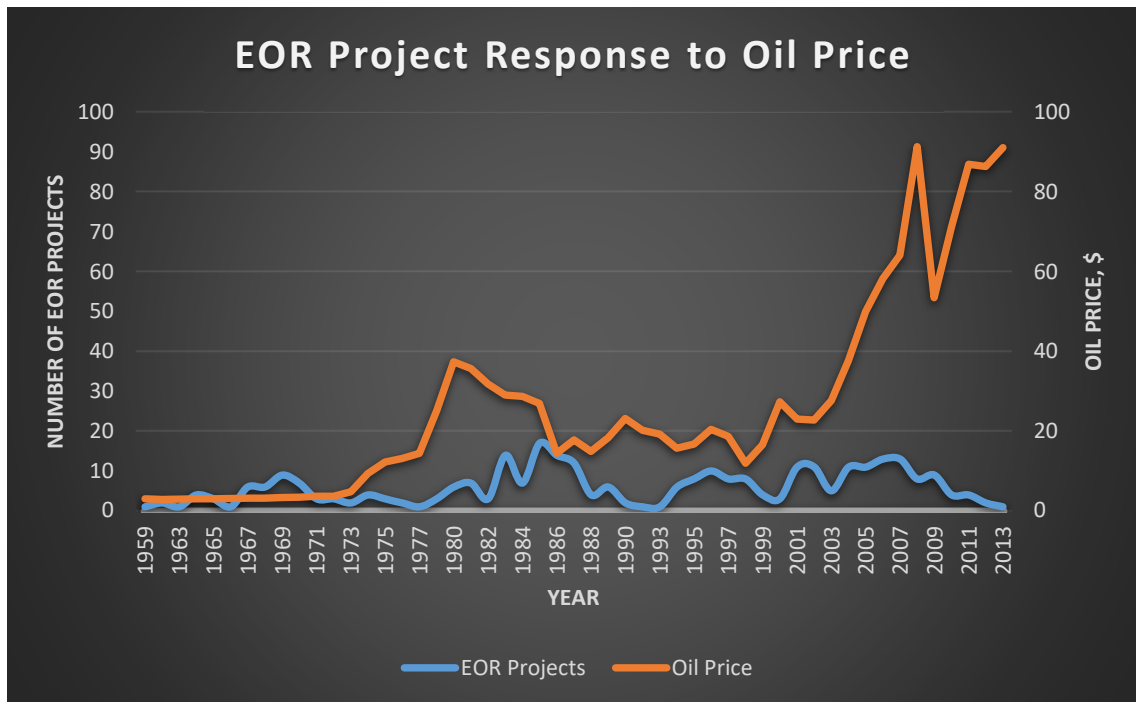
Figure 2-11 Showing historic EOR project response to the oil price.

Pershad *et al.* (2012) made comprehensive cost modelling for CO_2 EOR in the North Sea. Zekri and Jerbi (2002) presented an economic evaluation for CO_2 and CH_4. It is found that the EOR cost is categorised into CAPEX and OPEX. The injectant cost is often treated as a major cost element separate from the OPEX by some authors (Zekri and Jerbi 2002, Pershad *et al.,* 2012 Babadagli, 2020). In Zekri and Jerbi (2002) economic evaluation of CO_2 and CH_4, CO_2 CAPEX was three times more than CH_4 CAPEX. In contrast, CH_4 ($5.41/bbl) cost per barrel of oil produced was two times higher than for CO_2 ($11.59/bbl). The OPEX was approximately the same ($1.40/bbl). Bahadori (2018) has a higher value for CO_2 EOR oil at $20/bbl. Roefs *et al.* (2019), in their analysis, mentioned the threshold cost of CO_2 that would make the project economical. Beyond this cost, CO_2 becomes unprofitable. The cost of infill wells would be significant, but the injectant cost might be sovereign to it (Zekri and Jerbi 2002, Putnam 2013). Meyer (2007) stated that the injected CO_2 gas cost can account for up to 68% of total implementation cost. Gas EOR comparison investigation is very scanty in published literature. This research offers a cost comparison for the four EOR gases from the field and experimental data. A cost model has been proposed in Table 2-2 based on

Zekri and Jerbi (2002), Pershad *et al.* (2012). The cost model was used to evaluate the gas EOR competitiveness.

Table 2-2 Cost Model for the competitive analysis of immiscible gas EOR execution.

S/N	Cost/Revenue Centre	Cost/Revenue Element	Base Value	Link	Description and Remark
1	CAPEX	New Well CAPEX	27	$million/ well	New infill wells are required to match up well pattern and density for gas injection and oil production. It depends on the gas EOR process.
		Existing Well conversion CAPEX	40%	of New Well CAPEX	Conversion/upgrade of existing wells either for gas injection or oil production due to well pattern reassignment.
		Injection/Recycling Unit Capex	27	$million per Mt of peak gas recycling	Injection/recycling system such as compressor, separator and storage.
2	OPEX	Platform OPEX	5%	of platform CAPEX	It depends on injected gas
		Well OPEX	4%	of well CAPEX	Include maintenance of well; depends on well density demand of EOR process.
		Fresh gas purchase cost	Depends on EOR gas	$/tonne of gas	Cost of getting a fresh supply of gas to the EOR fields.
3	Planning Cost	Planning Cost	5%	of total CAPEX	Including planning, and Front-End Engineering and Design (FEED) study
4	ABEX	Decommissioning Unit Cost	0.6	$/bbl. Of OOIP	Pershad *et al.* (2012) suggested a decommissioning cost of 0.6 $/bbl. of OOIP based on the empirical data from Miller oil field decommissioning costs. It depends on the gas EOR process.
		Incremental decommissioning cost of gas EOR	15%	of total CAPEX	Due to the additional platform, wells and other infrastructure
5	Revenue	Oil Price	$47	Per bbl.	Brent @ 01/01/2021

Data acquisition

Oil price information of January 1st, 2021 for Brent crude was obtained online from msn.com (https://www.msn.com/en-gb/money/stockdetails/fi-auvwzr). Brent crude was selected as the base oil because it is a light oil with an API gravity (39) value that is fairly close to the average API value in the field database (36) used in this study.

The research used BOC (https://www.boconline.co.uk/en/index.html) gas pricing quotation of January 1st, 2021. The price of the four EOR gases present in Table 2-3 has been normalised to the United States dollars as of January 1st, 2021. BOC is a UK company that supplies industrial-grade gas at industry prices.

Table 2-3 Price of EOR gases used in the experiment and EOR economic evaluation.

Gas	CH$_4$	N$_2$	Air	CO$_2$
Unit price, ($/cm^3)	4.5E-05	5.7E-06	6.1E-06	3.4E-06

Potential injected gas volume was obtained explicitly from experiment data. Potential oil production volume was acquired by coupling experimental displacement efficiency, sweep optimisation parameter, and gas flow rate. This approach is based on previous investigators' conclusion that produced oil rate is proportional to EOR injectant volume rate and inversely related to mobility (Ahmed 2010a, Holstein 2007, Wang 2013, and Zou *et al.*, 2011).

2.4 Contribution to Knowledge and Practice

This research was designed in response to the shortcoming identified in existing EOR technology selection approaches as highlighted by authors, such as Lee (2010) and Delamaide *et al*. (2014a) and further emphasised by Ghoodjani and Bolouri (2015), Kang *et al.* (2014) and Al-Mayan *et al.* (2016). It was also designed to expand the experimental perspective of the gas EOR study. A special focus and detailed consideration were apportioned to

immiscible gas EOR. One of the reasons for this focus is because immiscible gas EOR is the least reported and represented in EOR in screening models and software that have been inspired by the works of authors, such as Taber *et al.* (1997), Guerillot (1988), Surguchev and Li (2000), Trujillo *et al.* (2010), Saleh *et al.* (2014), Nageh *et al.* (2015) and Kang *et al.* (2014). Therefore, in satisfying the research aim and objectives, the following contributions to knowledge and practice have been made.

2.4.1 Contribution to Knowledge

I.   This research has provided useful insight into EOR gases' competitiveness with an extensive validation of observations in EOR applications.

II.   The research was able to identify additional parameters and quantities that have both economic and engineering utility, and that should be considered when selecting EOR technology and gases. Parameters, such as well density, have not been previously considered by other authors in EOR screening criteria.

III. The relationship between single-phase and multi-phase flows that could be useful for comparing fluid flow has been derived through the analytical method. Future researchers can apply this knowledge beyond the reservoir engineering field to fields such as Trickle-Bed Reactor, Catalytic Membrane Reactor, and Industrial Gas Separation process.

IV.   The work has derived some useful equations for gas flow studies, some of which are shown in Table A 1, APPENDIX A.

V.   The effect of the mixture on the mobility of injectant gases has been presented. The function of this knowledge is that it provides an understanding of how injectant's performance, such as N_2, can be affected when in contact with *in-situ* reservoir gases, such as CH_4, during oil immiscible gas EOR.

VI.   The research has provided a solution for the effect of temperature, molecular weight and other gas thermodynamic properties on intrinsic gas mobility and EOR performance.

VII. The research has proposed a Sweep Optimisation Parameter (SOP) for evaluating the oil recovery competitiveness of Immiscible Gas EOR.

VIII. Before now, EOR reservoirs have not been simultaneously characterised for velocity, momentum, Well density and mobility for all EOR gases. This research offers these characterisations.

2.4.2 Contribution to Industry Practice

I.   Before now, EOR gases have been lumped up together as 'immiscible' in EOR screening criteria by authors. There is a general lack of screening criteria that compares the gases. For immiscible gas EOR, unlike other EOR processes, engineers cannot promptly identify what gas to select amongst the four EOR gases based on their respective potential performance. However, this research has contributed and provided a screening model that segregates the individual gases (CO_2, N_2, and CH_4, Air) in immiscible gas EOR. As suggested by this study, engineers can now select a gas for further investigation based on the reservoir suitability and potential to perform.

II.   The sensitivity and criticality markers added to the newly developed screening criteria would help reservoir engineers appreciate their circle of influence and control with respect to important EOR performance parameters.

III.   Furthermore, it has been able to use experimental methods to provide a performance matrix for engineers to evaluate potential oil recovery and control performance.

IV.   With the well density criteria introduced, engineers would now be able to make informed decisions on which EOR process can optimise already insisting well assets in a field. This application is important because it would significantly save the cost of drilling new infill wells that would not have been necessary had the well density optimising EOR process been selected.

V.   The findings from this research lend themselves to applications in analogues industries such as the petrochemical industry.

2.4.3 Contribution to Journal Publication and Conference Proceedings

1. Abunumah, O., Ogunlude, P., Gobina, E., 2021. Experimental Evaluation of the Mobility Profile of Enhanced Oil Recovery Gases. *Advances in Chemical Engineering and Science,* 11(02), p.155. https://doi.org/10.4236/aces.2021.112010

2. Ogunlude, P., Abunumah, O. and Gobina, E., 2020. A Study of Gas Diffusion Characteristics on Nano-Structured Ceramic Membranes. *European Journal of Engineering and Formal Sciences*, *4*(1), pp.21-23. https://doi.org/10.26417/ejef.v4i1.p21-23

3. Abunumah, O., Ogunlude, P. and Gobina, E. 2021. The effect of pressure and porous media structural parameters coupling on gas apparent viscosity. In Proceedings of the ICANM 2021: 8th International conference and exhibition on advanced and nanomaterials 2021 (ICANM 2021), 9-11 August 2021, [virtual conference]. Ontario: ICANM, pages 42-46. Available from: https://rgu-repository.worktribe.com/output/1427964.

4. Abunumah, O., Ogunlude, P. and Gobina, E. 2021. Cost description and characterisation of gas enhanced oil recovery processes. In 2021 TUBA (Turkish Academy of Science) World conference on energy science and technology (TUBA WCEST-2021) book of abstracts, 8-12 August 2021, [virtual conference]. Ankara: Turkish Academy of Sciences https://doi.org/10.53478/TUBA.2021.017.

2.4.4 Contribution at International Conferences

1. Ofasa Abunumah, Priscilla Ogunlude, Edward Gobina. *Determination of the effect of system temperature on the sweep quality of gases.* 8thInternational Conference on Analytical Chemistry and Chromatographic Methods, September 06-07, 2021, Webinar CONFERENCE

2. Ofasa Abunumah, Priscilla Ogunlude, Edward Gobina. *Experimental characterisation of energy possession and losses of industrial gases.* 8thInternational Conference on Analytical Chemistry and Chromatographic Methods, September 06-07, 2021, Webinar CONFERENCE

3. Abunumah, O., Ogunlude, P. and Gobina, E. 2021. *Cost description and characterisation of gas enhanced oil recovery processes.* In 2021 TUBA (Turkish Academy of Science) World conference on energy science and technology (TUBA WCEST-2021) 8-12 August 2021, [virtual conference], Ankara: Turkish Academy of Sciences

4. Abunumah, O., Ogunlude, P. and Gobina, E. 2021. *The effect of pressure and porous media structural parameters coupling on gas apparent viscosity.* In 2021 TUBA (Turkish Academy of Science) World conference on energy science and technology (TUBA WCEST-2021) 8-12 August 2021, [virtual conference], Ankara: Turkish Academy of Sciences

5. Abunumah, O., Ogunlude, P. and Gobina, E. 2021. *The effect of pressure and porous media structural parameters coupling on gas apparent viscosity. In Proceedings of the ICANM 2021:* 8th International conference and exhibition on advanced and nanomaterials 2021 (ICANM 2021), 9-11 August 2021, [virtual conference].

6. Ofasa Abunumah, Priscilla Ogunlude, Edward Gobina. *Mathematical modelling and experimental investigation of the gas flow in porous media for enhanced oil recovery processes.* 2nd International Conference on Analytical Chemistry and Chromatography Methods to be held November 20-21, 2019, in Berlin, Germany.

7. Ofasa Abunumah, Priscilla Ogunlude, Edward Gobina. *The Experimental Investigation of the Effect of Operating Temperature on Gas Flow Mobility in Ceramic Membrane.* 36th Global Conference on Smart Materials and Nanotechnology to be held November 18-19, 2019, in Rome, Italy.

2.4.5 Accepted Paper

1. Ofasa Abunumah, Priscilla Ogunlude, Edward Gobina. *The Interstitial Energy of Immiscible Gas Enhanced Oil Recovery (IGEOR) Gases in Porous Media.* Journal of Chemical Engineering and Process Technology.
2. Ofasa Abunumah, Priscilla Ogunlude, Edward Gobina. *Experimental Validation of The Well Density Profile for Immiscible Gas Enhanced Oil Recovery Projects.* Journal of Chemical Engineering and Process Technology.

2.4.6 Accepted Abstracts

3. Ofasa Abunumah, Priscilla Ogunlude, Idris Hashim, Florence Aisueni, Evans Ogoun, Samuel Antwi, Muktar Ramala and Edward Gobina. *Effect Of Reservoir Temperature On Carbon Capture And Sequestration (Ccs) Characterisation.* International Conference on Studies in Engineering, Science, and Technology (ICSEST) is scheduled for November 11-14, 2021 in Antalya, Turkey.
4. Ofasa Abunumah, Priscilla Ogunlude, Idris Hashim, Florence Aisueni, Evans Ogoun, Samuel Antwi, Muktar Ramala and Edward Gobina. *Effect Of Reservoir Structural Rhythm On Carbon Capture And Sequestration (Ccs) Performance*. International Conference on Studies in Engineering, Science, and Technology (ICSEST) is scheduled for November 11-14, 2021 in Antalya, Turkey.
5. Abunumah Ofasa, Ogunlude Priscilla, Gobina Edward. *A Novel Experimental Method for Characterising Nano Insulating Materials (NIM) And Infill Gases*. AVS 67th International Symposium & Exhibition (AVS 67), is scheduled for October 24-29, 2021, in Charlotte, North Carolina.
6. Abunumah Ofasa, Ogunlude Priscilla, Gobina Edward. *Cost Description and Characterisation of Gases used in immiscible gas Enhanced Oil Recovery processes (IGEOR)*. AVS 67th

International Symposium & Exhibition (AVS 67), is scheduled for October 24-29, 2021, in Charlotte, North Carolina

7. Abunumah Ofasa, Ogunlude Priscilla, Gobina Edward. *Experimental Characterisation of Kinetic Temperature Acquisition of Common Industry Gases in Nano Spaces (<100nm)*. Sixth International Conference on Fossil and Renewable Energy" (F&R Energy-2022) is scheduled for February 15-17, 2022 in Houston, TX, USA.

8. Abunumah Ofasa, Ogunlude Priscilla, Gobina Edward. *Well Density Characterisation of Enhanced Oil Recovery Technologies and Reservoirs,* Sixth International Conference on Fossil and Renewable Energy. (F&R Energy-2022) is scheduled for February 15-17, 2022 in Houston, TX, USA.

Chapter Three

3 METHODOLOGY

3.1 Approach

The methodology used to achieve the aim and objectives set in this research invokes synergy from two broad engineering investigation areas. Four approaches have been identified for investigating engineering processes. These are empirical, analytical, numerical simulation, and laboratory experiments. Chen (2007) has written extensively on each approach's merits and suitability.

After an extensive review of methods applied in various research and reservoir studies, two empirical approaches were selected: a data mining approach comprising analogical and mathematical analysis of empirical field data from global EOR projects and a laboratory experimental approach comprising PVT analysis of EOR gases' physical and thermodynamic properties in conditions analogous to reservoir conditions.

Consequently, the research was designed and carried out in two phases. The first phase saw the identification and characterisation of parameters for immiscible gas EOR using data mining techniques. The second phase involved the characterisation of EOR gases and validating the data mining results for immiscible gas EOR, using experimental techniques. The third phase, which is mostly intertwined in the second phase, entails analogical validation techniques. In this phase, the results from the two previous phases were coupled and extensively discussed to extrapolate key findings to reservoir scale and demonstrate how the findings explain the phenomena behind EOR theories and practices.

3.1.1 Analogical Method:

Here, the reservoir's petrophysical properties under investigation are compared to the properties of an analogous EOR reservoir to predict the suitability and performance of the EOR process (Chen 2007). This method could also be applied to scale up laboratory findings and properties to reservoir environment just as much as it could be used to scale up findings from data mining (Wheaton 2016, Jordan 2015 and Abu-Elbashar *et al.* 1990). In this study, the analogical method has been extensively applied. It was applied to create a benchmark for EOR screening criteria, validate and couple data mining and experimental results for the respective engineering quantities, parameters, and properties investigated. It was also used to compare EOR screening models

3.1.2 Mathematical Method:

Chen (2007) identified the mathematical model as the most used classical reservoir engineering method for predicting a wide variety of reservoir applications. The techniques under this method include material balance, decline curve, analytical and statistical processes. Since the research involve a significant amount of data to develop a representative EOR screening model, the statistical technique was adopted in phase one. The adoption of this technique is due to its compatibility with the data analysis of databases and experimental results. Some authors have applied this method to evaluate and characterise reservoir processes, such as EOR recovery and viscous fingering (Pruess 1991).

3.1.2.1 Analytical

The analytical process makes it possible for engineers to apply theoretical and empirical equations to solve real problems. One can combine several equations of state to derive new engineering quantities using techniques such as dimensional analysis. The principles are quite familiar and straightforward. Analytical processes are fundamentally based on continuum mechanics, a subject that aptly unifies solid and fluid mechanics, thermodynamics, and

heat transfer, all of which are a material consideration in this study. It is used to validate principal engineering laws of conservation of mass, the balance of linear momentum, the balance of angular momentum, and balance of energy (Pilvin 2019, Andri *et al*., 2017, Sadd 2018, Bergstrom 2015, Chandrasekharaiah and Debnath 2014, Malkin 2012, Risby and Hamouda 2011, Berker 2002, and Coratekin, *et al*., 1999) This study extensively utilised these processes in deriving missing data and quantities that are impractical to measure physically.

3.1.2.2   *Statistical and Machine Learning*

Although statistical and machine learning are both data mining techniques, the former has the advantage of being interpretative while the latter has its strength in being predictive, such as neural networks and fuzzy logic (James *et al., 2013*, Chen 2007, Hastie, Tibshirani, and Friedman 2009). However, unlike other fields where output is the most important outcome, in engineering, understanding processes, associations, correlations, and structure of the data are as important as predicting the outcomes. Such understanding often leads to better control and engineering of processes for optimisation. To this end, unsupervised statistical learning has been suggested by James *et al.* (2013) and Hastie, Tibshirani, and Friedman (2009). Their suggestion was applied to the database to identify the critical relationship and correlations that affect the performance of EOR. Chen (2007) stated that to improve confidence, reservoir properties must be within the regression database limit used to develop the empirical correlation model. Consequently, the objective here is to develop an empirical correlation model with data from implemented EOR projects across the globe and then apply a generalised analogical method to screen other reservoirs with analogous properties. Manrique, Kitchen and Alvarado (2009) referred to this type of exercise as experience-based guidance for EOR screening.

3.1.3 Experimental Method:

Gerbe and Green (2008) identified three types of experiments as-field, laboratory and natural experiments. Laboratory experimental investigations in reservoir engineering offer the opportunity to discover the existing relationship between rheological properties and flow conditions for fluids within a porous media (Yu-shu and Karsten 1996).

After identifying an engineering problem, it is often required to find solutions within a deductive domain. This could be achieved by firstly identifying the qualities and properties of the engineering problem. Consequently, the specific instrumentation and operations required to control, measure and predict the cause and effect of the qualities and properties can then be set up within the confine of available technology (Nesselroade and Cattell 2013, and Ghani 2014). Experiments are usually accompanied by data analysis. It involves examining the raw data, applying appropriate statistical and mathematical techniques to identify the existence of significant relations among the properties in the problem domain, and translating these relations to the solutions domain.

According to Thorbes (2008), unlike field experiments or empirical methods, the laboratory experiment is a cost-effective approach to quantify processes and examine the boundary application of existing analytical theories and numerical simulation solutions. Furthermore, the experimental model allows a wide range of parameters to be varied and investigated (Lane-Serff 2001), unlike the empirical method. Therefore, the laboratory experiment could be a valuable method for testing and validating predictions in reservoir engineering. The process often leads to discovering new phenomena that require theoretical explanation or the updates of existing models through constants of proportionality (coefficients). Therefore, fluid dynamics need to relate theory to reliable application (Thorbes 2008). In this study, the experimental results were extensively used to couple gas PVT behaviour to enhanced oil recovery in the reservoir. Although the full similarity between laboratory experiments could be difficult to achieve due to real systems'

complexity nevertheless, in this study, care was taken to conduct the experiments with reservoir conditions as the motive. Where required, sound engineering assumptions were made.

A significant number of authors have used this method for PVT analysis of gases and reservoir systems. Amirkhani, Harami, and Asghari (2020), Ogunlude *et al.* (2019), and Ogunlude, Abunumah, and Gobina (2020) have used experimental methods to characterise gas separation in porous media. Rashidi and Nasirian (2019) experimented with the transport properties of CH_4, N_2, and CO_2 in composite membranes with temperature variation. In the literature review of authors such as Nesselroade and Cattell (2013), and Ghani (2014), and Cash, Stanković, and Štorga (2016), it was discovered that there are certain milestones an experimental engineering approach should fulfil. Consequently, this experiment was designed to fit into these requirements, as shown in Table 3-1.

Table 3-1 Essential phases of engineering experiment applied in this research.

S/N	Experimental Phases	Research Remark
I.	Problem Domain Definition	Immiscible Gas EOR Screening Criteria and Gas Competitiveness Evaluation.
II.	Parameter description and Properties functions	Criteria development, petrophysical properties relevant to the problem domain and equation of state- Darcy, Buckley-Leverett and Welge equations.
III.	Design and Instrumentation	Planning, Apparatus layout, Materials, Equipment, and Quality Control.
IV.	Conditions and Control definitions, and Operations initiation	Laboratory conditions, parameters boundary, assumptions, and limitations based on milestones I, II, and III.
V.	Data generation and records	Numerical and qualitative observations.
VI.	Analysis and validation	Statistical and mathematical techniques, cause and effect mapping, the existence of significant relations, errors, assumptions.
VII.	Solution Domain	Functional Screening Criteria, EOR Gas Performance Characterisation.

3.1.4 Study Area and Scope:

The study area comprises global EOR fields, as reported in oil and gas industry documents. The experiment is limited to gases used in immiscible gas EOR.

3.1.5 Data Type:

The data used for this study are both primary and secondary. The data sets were mostly reservoir petrophysical parameters and properties, such as permeability, oil viscosity, saturation and API gravity, as well as physical and thermodynamic properties of gases. Yongxiang (2014) stated that data preparation is an important foundation for data mining. Accordingly, care was taken to prepare the data involved in this study properly. One of the challenges from the available data was that they were from different sources, thus were presented in different unit systems, such as the volume of oil being computed as barrels of oil equivalent (boe), metric ton, and Cubic metre (m^3). These unit systems were resolved to a standard unit using conversion factors. Also, there were some missing data in some records. Where missing data includes critical parameters, and no reliable correlation is available for estimating the unknown data from the known parameters, such records were discarded from the analysis.

Chapter Four

4 PHASE I: DATA MINING EVALUATION OF EOR GASES

4.1 Overview

Parameter and property categorisation is essential to design an appropriate engineering experiment. The importance is reflected in Table 3-1 as one of the phases for this research. Since the problem statement is industry-based, it was important to elicit the required parameters from the empirical industry database. This is the primary purpose of the data mining phase. At the end of this phase, this study was able to apply statistical tools to identify key parameters that determine the selection and performs of EOR processes in a reservoir. These parameters were then characterised and applied to develop two set screening criteria: one for gas EOR selection and the other for further experimental investigation.

4.1.1 Procedure for Data mining

It is noted that database comprehensiveness and integrity are essential for developing an extensive and reliable data mining model (Rostami *et al*., 2019, 2020). Therefore, cautious attempts were made to fulfil these criteria in the data collection and processing exercise.

4.1.1.1 STEP 1: Data collection

I.   EOR projects data were collated from various surveys and journals, such as the Oil and Gas Journal's Global EOR Survey, Canadian journals, and EOR Survey conducts in places like the North Sea, China and Brazil.

II.   A total of 484 EOR projects were collated, 354 were used for various analyses. While 30 were assigned for validation of the screening model.

III.   Some data were reported in different units and formats. These were reformatted and unified by applying the appropriate conversion factor.

IV.   Where parameters were reported as a range, such as permeability, the range's simple arithmetic average was computed. Saleh *et al.* (2014) has also used this method in a similar reservoir data study.

V.   A visual and software inspection of data was conducted to eliminate data inconsistency and errors. Two types of errors that were mostly identified were: Data field with a bogus or impracticable value, such as a reservoir porosity being reported as 300%. However, porosity is never up to 100% (Rick and Diana 1993); and data field with a wrong data type, such as having a string value in an integer data field.

VI.   A Global EOR Database (GED) was then produced.

VII.   Using Conditional Functions in Microsoft Excel, the data were checked and cleaned for duplicity and redundancy. This way, statistical bias from repeated data would be eliminated.

VIII.   An excel algorithm was run to document the data count for each reported quantity.

IX.   Another database was created called the Global EOR Database by EOR technologies and process categories (GEDT). The database was divided into nine EOR, four EOR technologies, and four immiscible gas processes.

4.1.1.2   STEP 2: Handling of Missing Data

The EOR project records collated were observed to have some missing data (mostly petrophysical parameters) necessary for a balanced and robust analysis. Imputation and correlational functions, as suggested in Olinsky, Chen, and Harlow (2003), Jerez *et al.* (2010), Sánchez-Minero *et al.* (2014), and Will (2019), were the two main methods used to overcome the missing data challenge significantly. Where practicable, missing petrophysical parameters were estimated from established industry correlations. For instance, reservoir records with missing viscosity were estimated using Naseri, Nikazar, and Dehghani (2005) API-Viscosity correlation. Missing

reservoir temperatures were estimated using reservoir depth and temperature gradient (Forrest, Marcucci and Scott 2005, Harrison and Chauvel 2007).

4.1.1.3   STEP 3: Parameters and Derivations

As discussed in this report's preceding subsections, previous studies (Saleh *et al.* 2014, Kang 2014) only investigated certain reservoir petrophysical parameters. It ranges from 6-9 parameters. However, in this research, the parameter domain was expanded to include some combinatorial quantities such as intrinsic mobility and well density.

4.1.1.4   STEP 4: Statistical Operation

Statistical operations were carried out on the database to discover essential patterns, trends, relationships, and references. Such operations would identify the mean values of reservoir parameters that are useful as a benchmark for making analogical references between established EOR reservoir projects and a prospective one. Where applicable, coefficient of variance (CV) was applied to determine and compare the criticality and sensitivity of parameters in the data distribution (Hou *et al*., 2016), thereby enabling the streamlining of the EOR selection process to suit the reservoir of interest closely. Furthermore, the statistical operations were applied to explain and update EOR theories; and, most importantly, improve the engineering of EOR processes. The following statistical tools and data mining techniques have been extensively applied in this study.

I.   Mean
II.   Standard Deviation
III.   Coefficient of Variation
IV.   Coefficient of determination
V.   Maximum and Minimum
VI.   Scaling and Normalisation
VII.   Interquartile Range (IQR)
VIII.   Clustering and Classification

4.1.1.5 STEP 5: Data Presentation and Visualisation

According to Lindsay (2016), data visualisation offers unique access to data analysis. It facilitates the sharing of insights among data users and understanding the information in a data set. In visualizing their results, some authors, such as Saleh *et al.* (2014), have used a histogram to investigate patterns and trends in the EOR database, while others have used data clustering, or a mix of both, such as Taber *et al.* (1997) and Siena *et al.* (2016). Data clustering was the main data visualisation approach used in this research because the study was interested in capturing trends, range-bounds, absolute limits, and technological evolution.

4.1.1.6 STEP 6: Criticality and Sensitivity Tests

These tests aim to discover parameters critical to various EOR processes and those with high tolerance or variance. The Coefficient of Variation (CV) was significantly applied here because it can be used to measure sensitivity (Hou *et al.*, 2016). A parameter could be considered high tolerance if the observation points are scattered enough to represent the database's universal dataset significantly. For instance, the permeability range for the immiscible gas EOR process can be compared against the universal set of permeability distribution. If a particular parameter is tightly clustered for a particular EOR process, it could be satisfactory to argue that such parameter is critical to the EOR method, and therefore, the process performance is sensitive to deviation from the cluster centre. For instance, Taber *et al.* (1997) stated that depth is critical for miscible gas EOR; however, depth is not considered critical for immiscible gas EOR.

Consequently, it is expected that depth should be tightly clustered around a certain range-bound for most miscible gas EOR implementation than for immiscible gas EOR. However, where an observation does not match the previous author's screening model, theory, or claim, other journals and engineering investigations were conducted to reconcile or explain the disparity. This technique was also employed in assessing the experimental phase results.

4.1.1.7 STEP 7: Correlations and Coefficient of Determination Tests

These tests are conducted to identify the relations between petrophysical parameters and discover pairs of critical-critical parameters, critical-non-critical parameters relationships. These relationships aided in reducing the dimensionality of the screening criteria and parametric redundancy. If two parameters, A and B, have significant covariation, then A could represent B in the screening process (instead of using both A and B), that is, if certain conditions are met. Such conditions would include whether B is a determinant of a third parameter C, then C interaction with B must be analogical to C interaction with A; otherwise, A cannot be considered to universally representing B. Lindsay (2016) called this the rule of causality.

4.1.2 Limitations, Constraints, and Scope of Data mining Approach

Concerning, data imbalance, some EOR methods have more data points than others which might influence or tilt the balance of comparison between EOR methods. Some parameters which may be important, such as reservoir thickness, were not available in a great proportion of the data set. Other statistical problems include the management of outliers in the dataset. Where applicable, percentiles were applied to mitigate the problem of outliers.

4.1.3 Accuracy and Errors

A rigorous effort was made to scrutinise data during collation and processing. It should be noted that the data used in this phase are secondary data from third-party published and publicly available datasets. Correlations used to mathematically estimate values are well known and cited correlations. Overall, the accuracy and integrity of these data and correlations are to the extent that they were peer-reviewed before publication. Furthermore, the researcher extensively compared several engineering principles and EOR before settling for the ones that sufficiently describe the study's context.

4.1.4 Engineering Assumptions

Engineering assumptions were taken seriously. The work of other authors set the tune for the engineering assumptions considered. It is assumed that data derived from reservoir engineering correlations, such as the Pay zone of some reservoirs, are significantly correct in the real term. It is expected that the reservoir systems significantly obey continuum mechanics. It is assumed that the principles applied best fit the context of the application. A rigorous validity test was made before any equation of state or principle is applied. For example, the condition for Hagen-Poiseuille EOS to be valid, according to Zhang and Kazunori (2018), is laminar flow, that is, Reynold number, Re, value under 2000. Tecs (2020) mention that this condition is such that the ratio of the length, L, to diameter, $2r$, of the capillary should be greater than $1/48$th of Re as shown in Eq 4-1:

$$\frac{\Delta L}{r} > \frac{Re}{48}$$

4-1

Furthermore, the study assumes immiscible gas displacement of oil by gas.

Chapter Five

5 DATA MINING RESULTS AND DISCUSSION

5.1 Overview

In this chapter, results and engineering understanding of findings were depicted after a series of critical analyses of the EOR database, using engineering and data mining methods. Some of the EOR parameters reviewed in the literature review chapter have been investigated and reported in detail. In contrast, some other parameters have been lightly discussed or put aside for further in-depth discussion in the experimental phase. This section begins with a general outlook of EOR technology, then was subsequently narrowed down to principal factors for immiscible gas EOR and how to advance the selection of EOR methods.

5.2 Objectives Achieved

The following objectives have been achieved in the proceeding section:

I. EOR parameters have been characterised as required in Objective I.
II. Existing EOR Screening Models have been revisited, and a new set of criteria and screening models produced.
III. EOR performance parameters and properties have been empirically determined and selected for the experimental phase as required in Objective I.

At the end of this chapter, it is expected that the 'Screening Phase' of Rotondi *et al.* (2015) flowchart would have been revealed.

Research Phase I

5.3 Data Summary of Phase One

In this phase, 10,850 reservoir petrophysical data from 485 EOR projects across the world have been collated and extensively investigated in the following sections. The data are publicly available secondary data.

5.4 EOR Projects overview

The EOR Survey generated records for 485 EOR projects globally, of which 347 are Gas EOR, 68 of which are immiscible gas EOR projects. The United States has the highest EOR projects at 65%. CO_2 EOR is the most implemented gas EOR method, while N_2 is the most implemented immiscible gas EOR method.

Figure 5-1 has been used to describe EOR parameter variabilities (variances) on a semi-log graph. This mean weighed variances measured here indicate a domain for each EOR parameter. The graph is important because it could be regarded as a measure of the probabilistic discrimination or convergence that exists within the respective parameter dataset. In the graph, parameters that are <1, such as reservoir temperature, are considered low-variance parameters; therefore, the probability of the EOR process being discriminated against with respect to this particular parameter in the dataset distribution is low. While those parameters that are >1, such as viscosity, are high-variance, implying that the chances of discrimination are high. Viscosity and oil mobility have relatively high variation index; therefore, the likelihood of these quantities being segregated according to EOR processes is high. If there is no significant dispersion in a distribution, it means all members (EOR Processes) in that distribution share similar features. Therefore, they cannot be a

discrimination measure to question or uphold. Figure 5-1 was instrumental in preparing the expectation from subsequent data analyses.
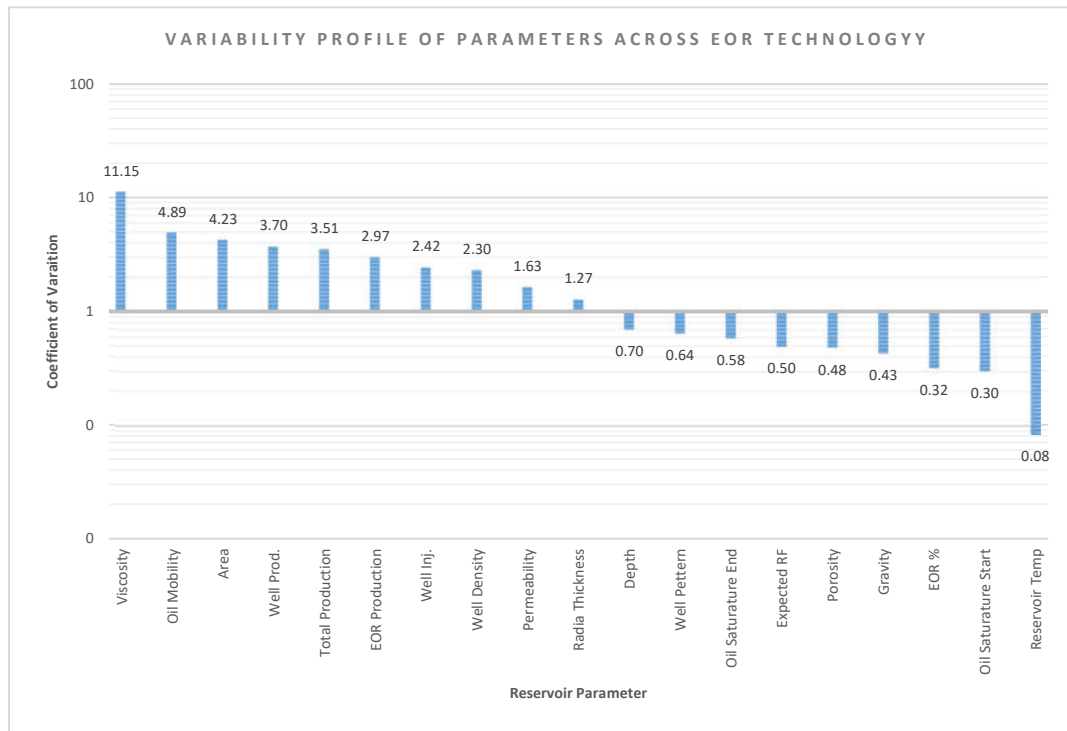
Figure 5-1 Graph showing the dispersion of EOR parameters as a predictor for the probability of parameter segregation and discrimination across and within EOR technologies.

5.5 EOR Parameters Clustering

The field data have been presented in a cluster format. There are 4 cluster demarcations in each graph. Each cluster represents an EOR technology or a process. Each data point on the graph cluster represents a field data value for a reservoir quantity, such as reservoir permeability. The y-axis bears the numerical value range for the quantity. While the x-axis does not bear any numerical values, it is just a holder for reservoir frequency. Consequently, values are read off the y-axis.

5.5.1 Reservoir Rock Parameters

The permeability distribution of EOR projects implemented from 1960 to 2013 reveals interesting clusters and permeability evolution over time for certain EOR applications.

5.5.1.1   *Permeability*

Figure 5-2 a and b show that few EOR technologies and processes are relatively segregated along with the reservoir permeability. In Figure 5-2a, Chemical, MEOR, and Thermal all occupy different sections of the permeability spectrum. Thermal occupies the higher end of the spectrum. In comparison, Gas EOR have the widest spread or range of permeability. The quality of the spread suggests that Gas technology can be implemented in all Chemical and MEOR reservoirs, but not all reservoirs that implement Gas technology are suitable for Chemical and MEOR. Overall, Figure 5-2a indicate that EOR technologies can be characterised by permeability. The CV analysis shows that the technologies most and least sensitive to permeability are MEOR and Gas technologies, respectively.

a.   b.
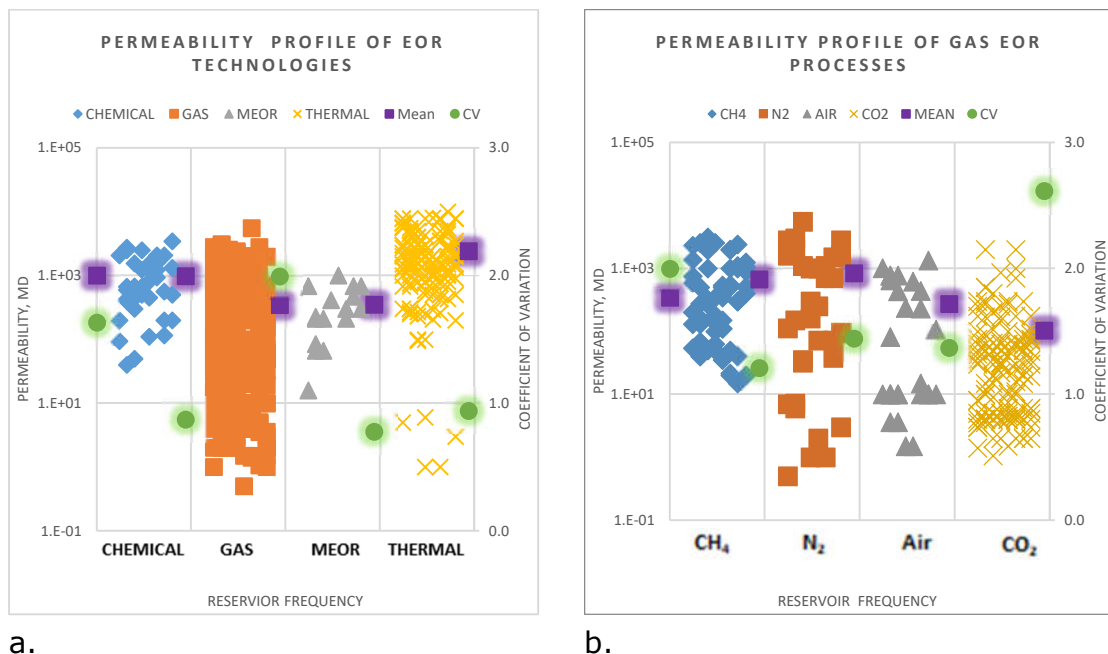
Figure 5-2 Permeability clustering for various (a) EOR technologies and (b) gas EOR processes.

Figure 5-2b isolated Gas technology to investigate whether processes in this technology can be categorised by permeability and thus be used as a suitable criterion for selecting EOR gases within gas EOR technology. Here, three distinct clusters were identified (CH_4, N_2 and Air/CO_2). CH_4 was the most restrictive cluster. CH_4 injection was often implemented in reservoirs with permeability between 15mD and 2,500mD. N_2 process possesses the widest permeability range (5999mD). According to the time stamp on the database used in this study, in the last decade, the implementation of N_2 EOR was found to be mostly in relatively high permeability reservoirs. Air and CO_2 share similar clusters. They both favour reservoirs with lower permeability, even though both gases have higher molecular weights than CH_4 and N_2. By way of the respective CVs in Figure 5-2b, it was identified that the gas process that is most and least sensitive to permeability are respectively CH_4 and CO_2.

A closer observation of Figure 5-2b reveals sub-clusters for N_2 (3 clusters), Air (2 clusters), and CO_2 (2 clusters). These sub-clusters may hold vital information about other combinatorial factors, such as transmissibility and mobility, that need to be at play for these gases to be suitable for certain reservoirs permeability. Subsequent consideration of other reservoir parameters is expected to reveal this further. Taber *et al.* (1997) criteria stated that permeability is not a critical parameter for CH_4 EOR. Taber's criteria could be misleading in this respect, especially if the cluster plot patterns here are not by coincidence but by deliberate reservoir engineering decisions. Considering the nature of these graphs, permeability could be classified as a parameter for screening and selecting the EOR process in Gas Technology.

5.5.1.2   Reservoir Porosity

In the data presented in Figure 5-3a, porosity clearly shows distinct clustering behaviour in the global dataset. Thermal technology requires relatively higher porosity reservoirs (20% to 40%). While Gas technology (CH_4, N_2, Air and CO_2) have significantly evolved within the range of 5% - 33%. It should be noted that, with respect to porosity, CH_4 and N_2 and CO_2 share fairly the same

porosity profile in Figure 5-3b. The porosity profile for Air EOR is tightly clustered at the centre of the graph in Figure 5-3b, and it is a subset of the CH_4 and CO_2 porosity range. All CH_4 and CO_2 reservoirs would accept Air process, but not all Air reservoirs would accept CH_4 and CO_2 processes. The Taber *et al*. (1997) screening criteria did not consider porosity as a parameter in general. However, a visual investigation of the clusters in Figure 5-3a indicates a meaningful and implicating pattern across EOR technologies. That is, as observed, thermal technology (steam) is quite segregated from gas technology. Air is discriminated against within gas technology.

a.   b.
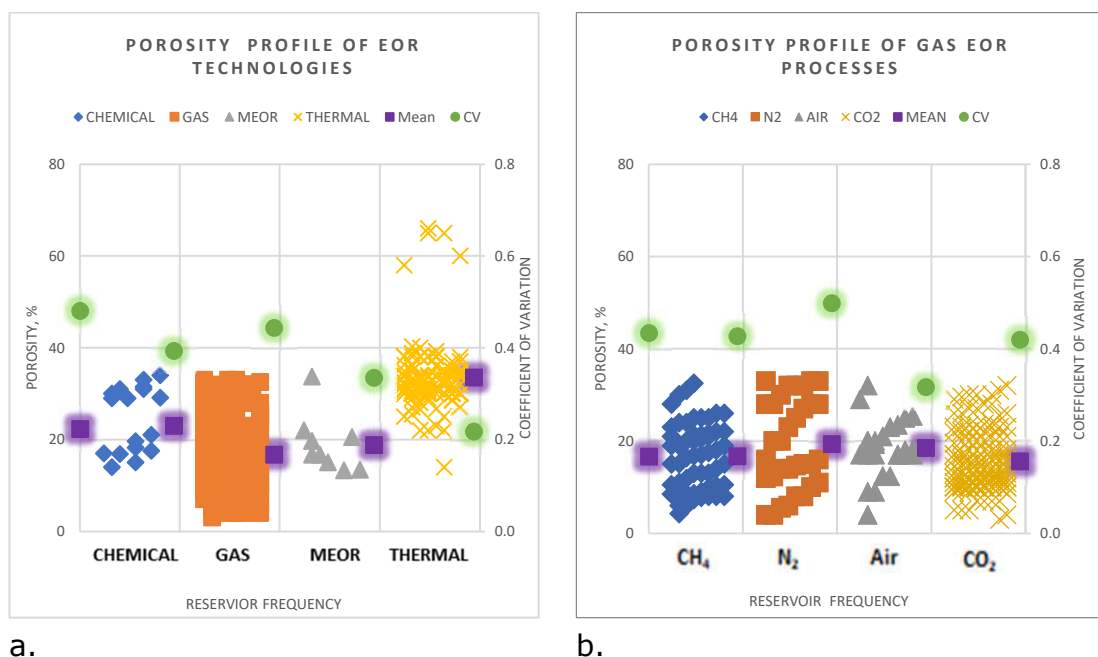
Figure 5-3 Porosity clustering for various (a) EOR technologies and (b) gas EOR processes.

Porosity has not also been included as a parameter by other authors such as Kang *et al*. (2014), Saleh *et al*. (2014). Perhaps, as Delamaide *et al*. (2014a) earlier stated, this could be because these authors used the parametric framework already set by Taber *et al*. (1997). Al Adasani and Bai (2011) proposed an update for the Taber *et al*. (1997) screening criteria. In their screening criteria model, they included screening for porosity. The result in this cluster compares well with the Al Adasani and Bai (2011) model, except for the minimum porosity limit suggested by them for steam and CO_2 flooding. The difference between this research and Al Adasani and Bai (2001) is that their CO_2 EOR lower limit for porosity is 17% which is higher than the

5% presented in this study. The disparity could be due to the effect of outliers or technology enhancements. It could also be that Al Adasani and Bai (2011) did not have access to the field data that implemented such low porosity at the time of their study. Al Adasani and Bai (2011) had used 2010 EOR survey data. Using a 2010 EOR survey data has enabled them to update the Taber *et al*. (1997) criteria that had earlier used a 1996 survey data (Al Adasani and Bai 2011, Taber *et al*. 1997). Therefore, this study updates the studies of both authors by way of using the most recent EOR global survey data, 2014. Consequent to the analysis in Figure 5-3, porosity was selected for experimental investigation.

5.5.1.3   *Depth*

The clusters in Figure 5-4a are well segregated across EOR technologies and could be used to characterise EOR depth requirements. Major EOR methods, such as steam, Air, CH_4 and CO_2, show distinct clusters. The database time stamp and the cluster profiles of CO_2 and CH_4 EOR indicate there are increasing projects in deeper reservoirs in recent years. These reservoirs are mostly beyond 3,300ft depth (Bahadori 2018). This depth could be explained by the Minimum Miscible Pressure (MMP) requirement of miscible gas EOR, that is, the pressure required to achieve miscibility between the injected gas and oil (Vega and Kovscek 2010, Bahadori 2018, DOE 2010).

Understandably, the reservoir pressure is usually proportional to the reservoir depth. Therefore, the deeper the reservoir, the more suitable it is for miscible gas EOR. All the gas EOR technology processes are shown to be implemented in deeper reservoirs than other EOR technologies, such as Thermal and Chemical.
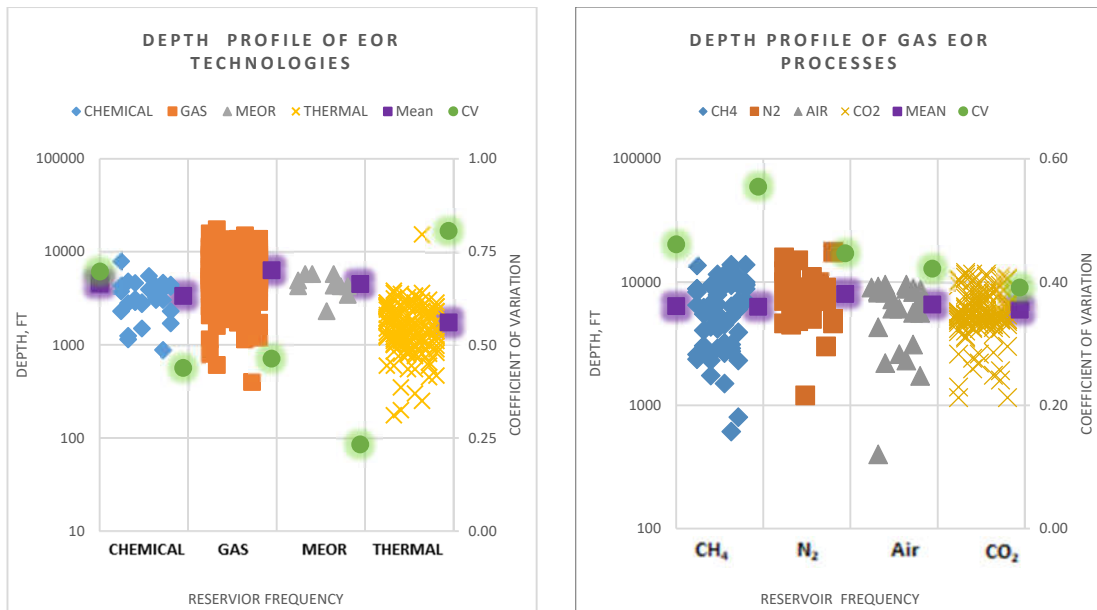
Figure 5-4 Reservoir depth clustering for various (a) EOR technologies and (b) gas EOR processes.

There is no mark cluster segregation within Gas EOR technology, as shown from the mean depth distribution in Figure 5-4b. Therefore, depth cannot be considered as a criterion for classifying gas EOR processes and does not satisfy objective one. Nevertheless, it is a valid criterion for screening across EOR technologies. The clusters in the graph correspond well with Taber *et al.* (1997) screening criteria.

5.5.1.4   *Temperature*

According to Taber *et al.* (1997) and Khojastehmehr, Madani and Daryasafar (2019), Temperature is not a critical property for EOR screening except for Air and Chemical EOR processes. The clusters in Figure 5-5b indicate that CH_4 has been applied in reservoirs with a wide range of temperature value between 300K and 420K. From the cluster patterns, it was observed that other EOR processes are subsets within the CH_4 temperature range. However, some clusters are more cohesive than others. For instance, for Thermal (Steam) and Air EOR, their clusters are relatively closely packed or cohesive than others.
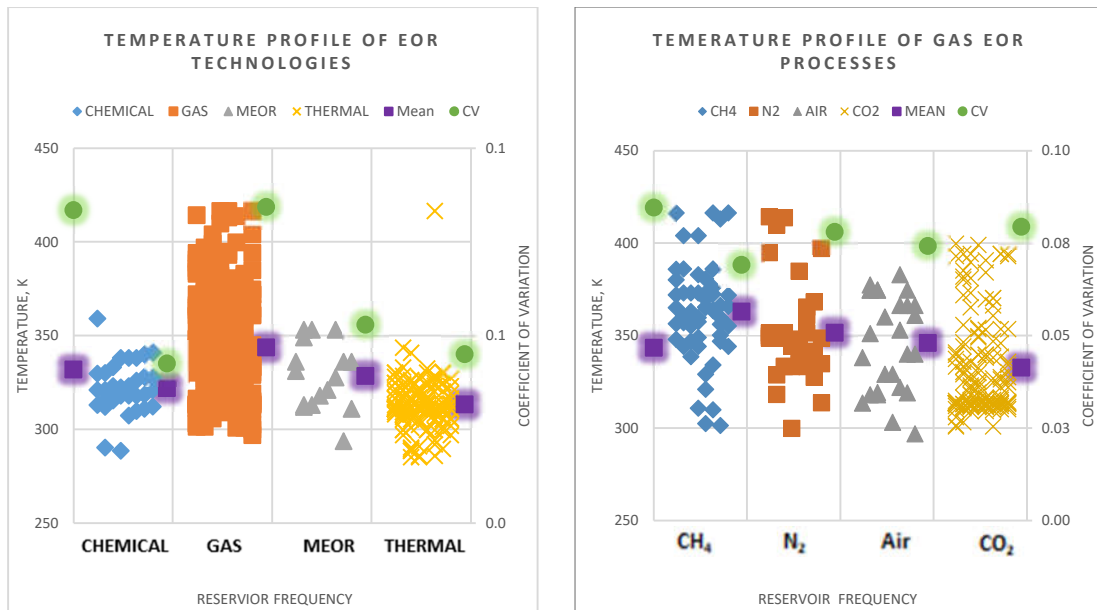
Figure 5-5 Reservoir temperature clustering for various (a) EOR technologies and (b) gas EOR processes.

The study further discovered the relationship between depth and temperature in reservoir engineering. Reservoirs that cluster around the high depth region in Figure 5-4a are mostly gas EOR reservoirs clustered around the high-temperature region in Figure 5-5a. Similarly, the shallow depth region clusters, such as the Thermal cluster, are in the lower temperature region in Figure 5-5a. The possible engineering explanation for this would be that temperature gradient, like pressure, is directly related to reservoir depth (Pedersen and Lindeloff 2003, Harrison and Chauvel 2007, Satter, Iqbal and Buchwalter 2008, Satter and Iqbal 2015 and Kargarpour 2017). From the CVs in Figure 5-5b, it can be stated that CH_4 is the most sensitive to temperature variation, while CO_2 is the least sensitive.

Although the temperature cannot be used for EOR screening, it is a reservoir property that can be used to evaluate the performance of gases within Gas EOR technology to determine the effect of temperature on the performance of the individual gases used in immiscible gas EOR. Therefore, this parameter would be evaluated in the experimental phase. The traditional Darcy equation used in reservoir evaluation does not include Temperature (Golan 1992,

Hartmann and Beaumont 1999, Matthews 1999 and Holstein 2007). However, it could be modified to include this property using the ideal gas and combined gas law equations and other thermodynamic properties of gases, such as specific heat capacity and thermal conductivity.

5.5.1.5   *Area and Radial Extent*

Figure 5-6a and b represent the area and notional radial thickness distribution of EOR projects in the global database of EOR. This radial thickness assumes that a reservoir has a hypothetical single well, and the radial thickness of the reservoir is in reference to the single well's radius. The observed segregation and clear-cut clusters indicate that the reservoirs' radial extent can be utilised to characterise EOR Technologies. Chemical and MEOR technologies are observed to be restrictive and implemented in smaller reservoirs than gas and Thermal technologies in Figure 5-6a. The radial extent of the reservoirs was derived from the reported area of the respective reservoirs. This radial extent reflects the horizontal extent of the reservoir. The area used to arrive at this parameter is different from the surface area in the Darcy equation. The radius here is equivalent to the external radius found in the denominator of the Darcy equation. The radial extent has not been considered in any available screening model, including Taber *et al.* (1997). However, the clusters in Figure 5-6a demonstrate that EOR applications can be characterised by radial extent across EOR technologies. In Figure 5-6b, the gas technology was clusterised by gas processes. The gas processes cluster segregation is not as marked as in Figure 5-6a. Nevertheless, the CVs in Figure 5-6b indicate the sensitivity to radial extent differs for the respective gases. Therefore, this property has been identified and selected as an EOR screening and performance property.
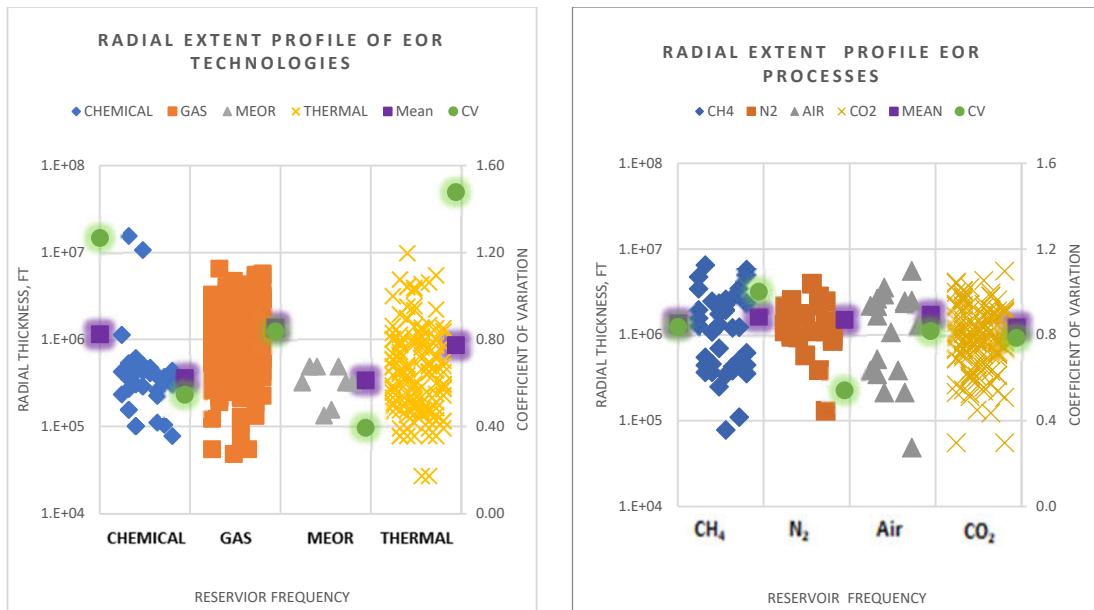
a.

b.

Figure 5-6. Reservoir radial extent clusters for various (a) EOR technologies and (b) gas EOR processes.

Consequently, it was adopted for evaluation in the experimental phase. Furthermore, this property fits nicely into the Darcy equation. Therefore, it is practicable to experimentally investigate its relationship with the respective gas performance and other petrophysical properties. It is therefore concluded that radial extent has satisfied objective one of this study.

5.5.1.6   *Pay Zone Thickness*

Figure 5-7a indicates that EOR technologies can be characterised by pay zone thickness. It is shown that gas technology has the widest range of pay zone acceptance, and MEOR has the least range. This is reflected both in the shape of the clusters and their respective CVs. It can be stated further that MEOR is the most sensitive to pay zone thickness. Pay zone thickness above 200ft typically demands Thermal technology. In contrast, a reservoir pay zone below 20ft is mostly suitable for Gas technology.

Having established the segregation across technologies, Figure 5-7b was plotted to investigate the internal segregation that might exist within Gas technology. It is observed that N_2 is applied in the widest pay zone range.

This ranges from a 3ft reservoir to as high as a 274ft reservoir. The higher pay zone reservoirs favour the lighter gases such as CH_4 and N_2, while the shorter pay zone reservoirs favour the heavier CO_2 gas. This segregation may be connected with the effect of gravity and buoyancy on the injected EOR gases. As gas migrates through reservoir pores from injection to producer wells, both linear and vertical migration components must be accounted for (Shepherd 2009 and Beaumont and Fiedler 1999). For a reservoir with no overburden pressure or gas gap, the displacing gases could acquire buoyancy sovereignty and escape the pay zone. The lighter gases would tend to have more upward migration capacity than the heavier gases due to the relative difference in densities. Therefore, a shorter pay zone would effectively allow the escape of a lighter gas faster than a higher pay zone. It is suggested that to overcome this challenge, shorter well spacing should be implemented between the injection and producer wells sufficient enough to neutralise the vertical upward migration of the gas molecules. Nevertheless, this would cause costly additional infill wells.

a.   **b.**
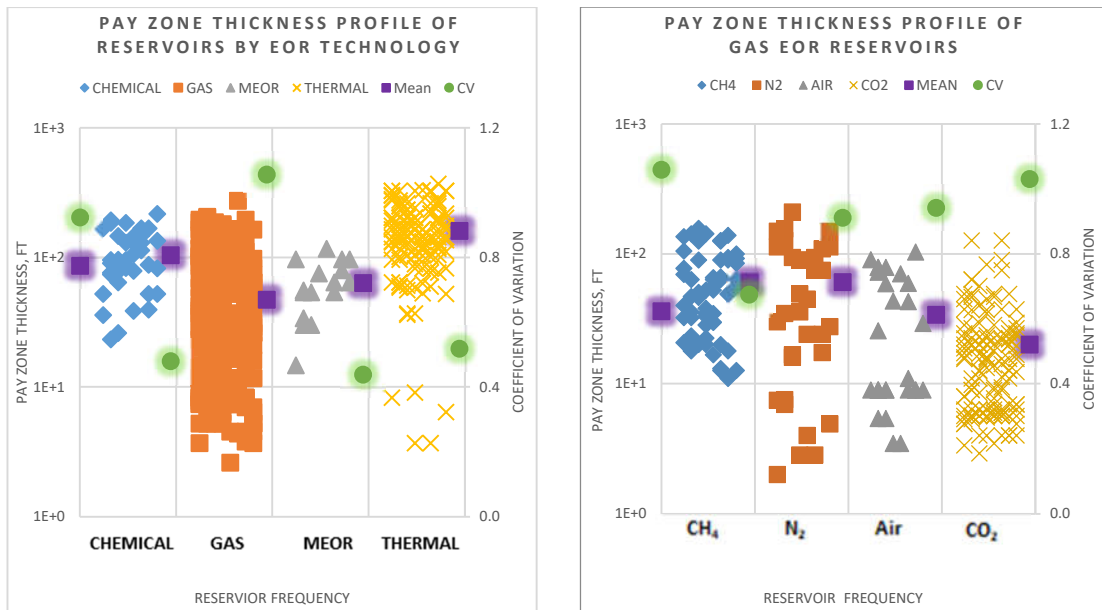
Figure 5-7 Reservoir Pay zone thickness clusters for various (a) EOR technologies and (b) gas EOR processes.

Reservoir thickness or pay zone is an evaluated parameter in the screening criteria of Taber *et al.* (1997), Saleh *et al.* (2014), Kang (2014) and, Al Adasani and Bai (2011). However, the understanding from this study conflicts with some of these authors. Taber *et al.* (1997) and Al Adasani and Bai (2011) did not recognise that Chemical technology and CH_4 are generally sensitive to higher reservoir pay zone. Their models did not provide for MEOR. Furthermore, they also overlooked the effect of buoyancy and gravity in the displacement process. This study has attempted to offer an established theoretical basis for the observation in the gas clusters.

Similarly, in the Darcy and Hagen-Poiseuille equations of state, the reservoir vertical extent or pay zone is represented as part of the surface area variable. Based on these clusters and equations, reservoir thickness was adopted into the experimental phase to investigate the competitiveness of the gases.

5.5.2 Reservoir Fluid Properties

5.5.2.1 Displacement Efficiency

There are patterns formed by the clusters presented in Figure 5-8a. The displacement efficiency, which is the ratio of the difference between the start and expected end oil saturation to the start saturation (abandonment saturation) (Eq. 2-43), reflects the extent to which an EOR method can effectively recover trapped oil.

From the mean distribution of the clusters in Figure 5-8a, it is indicated that gas technology (66%) performs relatively better in displacing residual oil than the other technologies, Chemical (51%) and Thermal (61%). While steam, Air and CO_2 EOR can achieve 40%-50% on a historical average. If EOR recovery is considered to come from mostly displacement efficiency (as opposed to sweep efficiency), there would seem to be a conflict between the findings here and Al Adasani and Bai's (2011) earlier mentioned in Section 2.3.2.1. Whereby the average recovery efficiency from hydrocarbon (CH_4) EOR could be considered underestimated by Al Adasani and Bai's (2011).
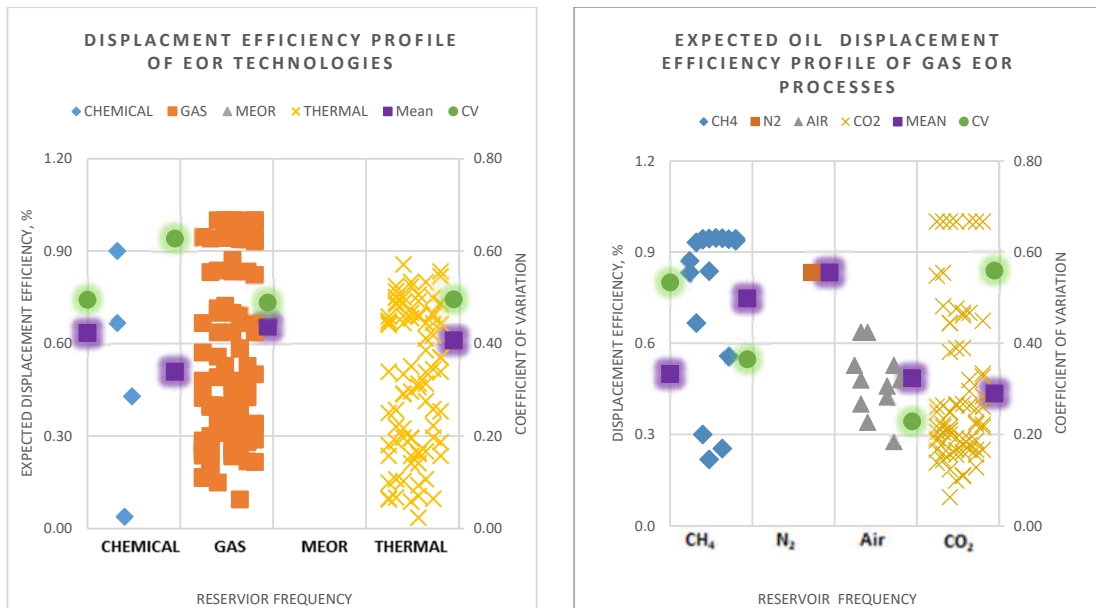
Figure 5-8 Displacement efficiency clustering for various (a) EOR technologies and (b) gas EOR processes.

According to the global EOR data used in this study, the estimated oil displacement performance in decreasing order, based on historical average (Figure 5-8b), is CH_4 > Air > CO_2 (Note: there was insufficient data to evaluate N_2 performance). CO_2 is relatively poor in displacing oil at the pore level, according to the plot in Figure 5-8b. This is understandable, considering the engineering mechanism involved in gas EOR. The absence of minimum miscible pressure (MMP) in immiscible CO_2 significantly draws down its performance. As highlighted here, the positive prospect of CH_4 EOR is encouraging to the proposed strategy for the North Sea EOR assets. CH_4 has been reported by OGA (2014) to be one of the core options planned to recover trapped oil in the North Sea basin. This performance profile would also facilitate CH_4 EOR programmes in countries where there is access to relatively cheap or free hydrocarbon gases, such as flared hydrocarbon gases in Nigeria and Canada.

5.5.2.2   Oil Saturation

Figures 5-9a and c show that EOR technologies are characterised by saturation. Furthermore, Figure 5-9a shows that Chemical technology has the

most restrictive start saturation range. It is followed by Thermal technology. Gas Technology has a broader spread at 20-92%. It suggests that Gas technology can be implemented earlier or later than other technologies. Figure 5-9c highlighted that, on average, the end saturation or residual saturation is the highest for Thermal technology (38%), compared to Chemical (30%) and Gas (27%). Data were not available for MEOR analysis.
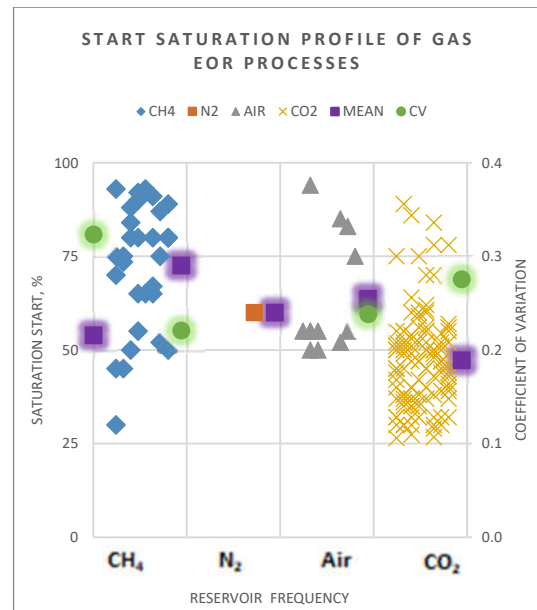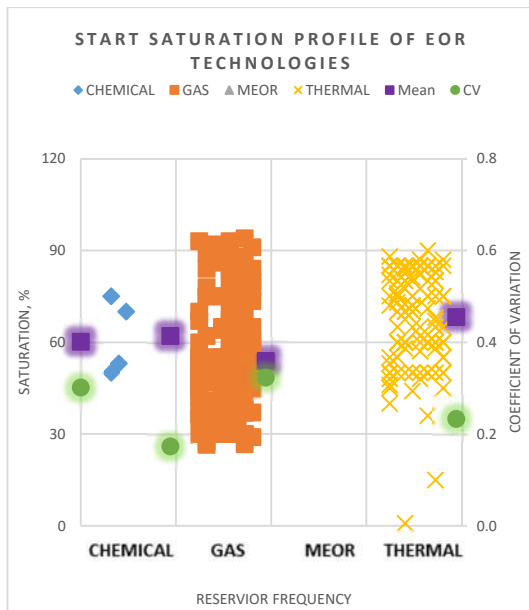
a.

b.
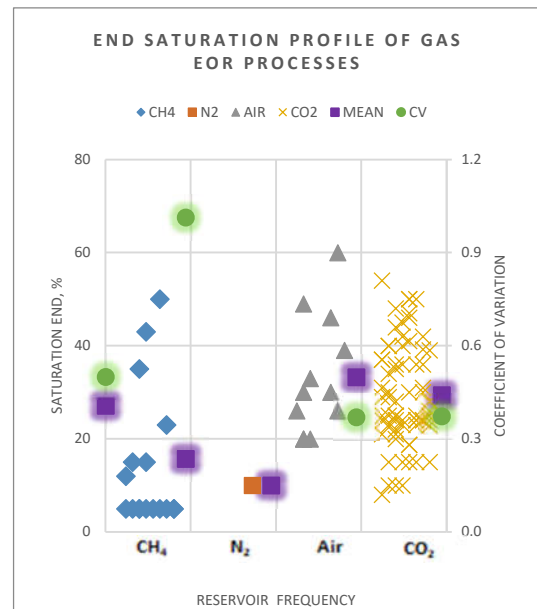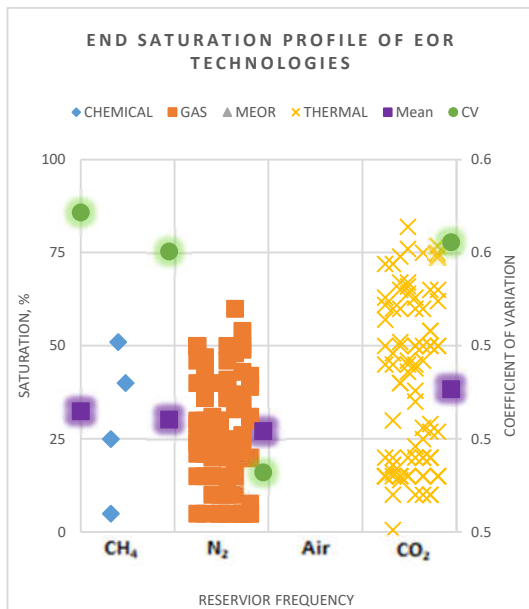
c.

d.

Figure 5-9 Oil saturation clustering for various (a) EOR technologies and (b) gas EOR processes.

Similarly, when Gas technology was investigated in Figure 5-9b and d, it was observed that CO_2 has the highest number of projects in low oil start saturation reservoirs compared to other EOR processes, such as Air and CH_4 EOR. CH_4 is mostly implemented in higher saturation reservoirs. Figure 5-9d profiles the residual or end saturation of the respective gas EOR processes. Since the aim of implementing EOR is to reduce residual oil saturation to the barest minimum, it, therefore, follows that by the cluster segregation and average values in Figure 5-8d, CH_4 displaces the most oil because it has the least end saturation than Air and CO_2 (there was no sufficient data for N_2 evaluation).

The clustering fits well with Taber *et al*. (1997) criteria. Although there was sufficient segregation within gas EOR that warrants the selection of oil saturation for the experimental phase, this could not be achieved due to experimental laboratory constraints at the time.

5.5.2.3   API Gravity

According to the clusters in Figure 5-10a, most thermal projects are implemented in heavy oil reservoirs around 14°API. In contrast, Gas technology has been extensively implemented in the light oil reservoirs around 35°API. The CVs in Figure 5-10a indicate that Gas technology is most sensitive to API Gravity properties. Similarly, within gas EOR technology in Figure 5-10b, it is observed that the oil API Gravity discriminates gas processes. The tightest cluster is Air EOR, with a CV of 0.15. They are implying that Air process is very sensitive to API Gravity. It is further revealed from the nature of their clusters that CH_4 and CO_2 share similar API gravity profiles. N_2 has the most extended API Gravity range of 16-60 API. Although Figure 5-10b is well clustered, it is understood that reservoirs suitable for Air would also be suitable for other gases.
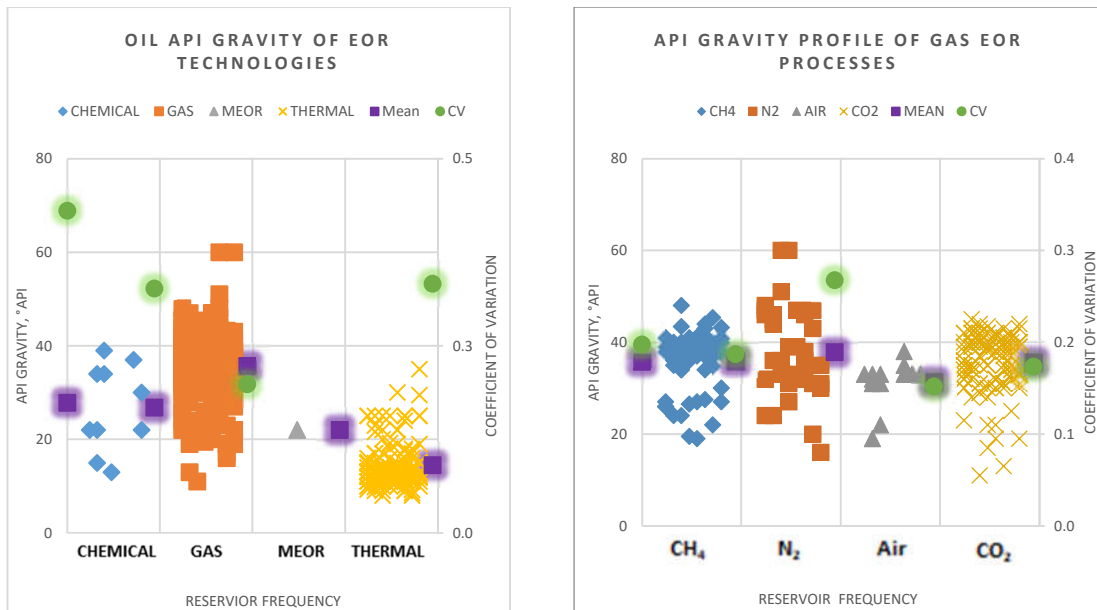
a.   b.

Figure 5-10 Oil API Gravity clustering for various (a) EOR technologies and (b) gas EOR processes.

Nevertheless, not all reservoirs suitable for other gas would be suitable for Air. The cluster analysis compares well with the Taber *et al*. (1997) screening model. API gravity is not represented in the Darcy equation; however, it is observed to be a valid property for EOR characterisation. Furthermore, the following section indicates that there could be a deductive relationship between API gravity and the viscosity of the oil. This property was adopted in the experiments as density.

5.5.2.4   *Viscosity*

The viscosity profiles of EOR technologies are presented in Figure 5-11a. The clusters indicate that EOR technologies can be discriminated by viscosity. The EOR technology most sensitive to viscosity is MEOR. In Figure 5-11a and b, the relative rankings of the average viscosities of the respective technologies (Figure 5-11a) and processes (Figure 5-11b) resemble the opposite or reverse of the ranking of API gravity in Figure 5-10a and b, respectively. Thereby suggesting a corresponding relationship between the two reservoir fluid properties.

Thermal technology viscosity distribution is quite distinct from the other EOR methods, suggesting that Thermal technology is mostly applied in reservoirs with higher viscosity. The cluster distinction in Figure 5-11b within Gas technology is not very pronounced compared to EOR technologies clusters in Figure 5-11a. It is observed that the cluster for Air is higher than other gases. Taber *et al.* (1997) criteria are similar to the results found in this research (Figure 5-11a). Therefore, viscosity could be considered as a critical property for EOR selection across EOR technologies. Furthermore, viscosity is also considered as a property for performance investigation within gas EOR technology. This fluid property was therefore selected for investigation in the gas experiment.

a.   b.
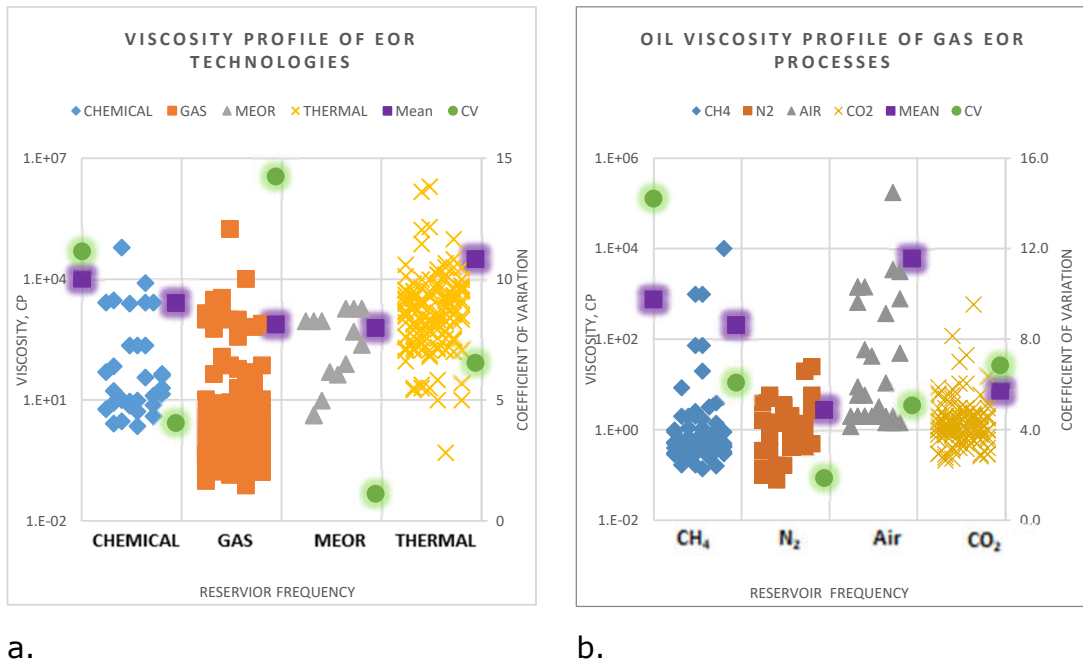
Figure 5-11 Oil viscosity clustering for various (a) EOR technologies and (b) gas EOR processes.

5.5.3 Performance Parameters

5.5.3.1 Incremental Oil Production

This parameter in Figures 5.17a and b aims to identify segregation across EOR technologies and within Gas technology and determine the gas process that is likely to produce the highest incremental oil, everything being equal. Because many of these field productions are solely from EOR, it was difficult

to evaluate the EOR method using this property explicitly. Nevertheless, if fields whose oil production is 100% from EOR are ignored in Figure 5.17a, then a statement could be drawn by taking a historical average of each EOR performance. In which case, EOR Technologies could be ranked in decreasing order of incremental oil production as Gas, Thermal and Chemical. Similarly, within Gas technology (Figure 5-12b), it could be ranked as CO_2, CH_4, N_2 and Air processes. The order is somewhat in line with Al Adasani and Bai (2011) study, as summarised in Figure 2-5. Al Adasani and Bai (2011) investigated EOR performance based on oil recovery.

a.   b.
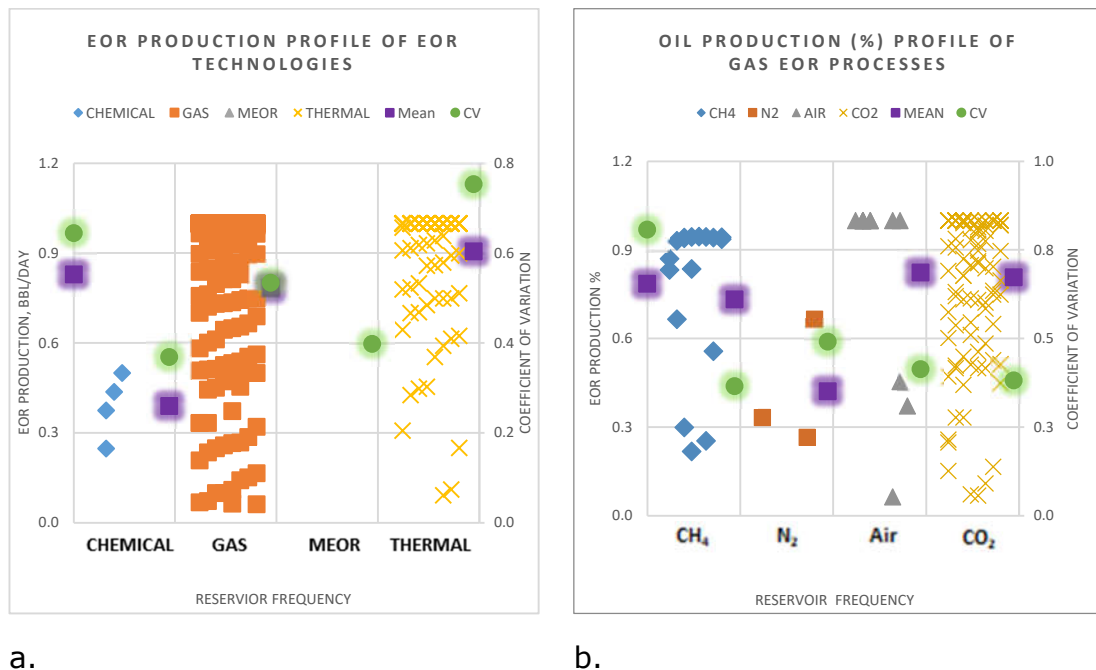
Figure 5-12. Incremental oil production clustering for various (a) EOR technologies and (b) gas EOR processes.

However, this study investigated performance based on incremental oil production in Figure 5-12a and b. The segregation within and across EOR technology was difficult to establish here. Consequently, it was not explicitly considered in the experimental stage.

5.5.3.2   *Oil Mobility*

The intrinsic mobility profile of EOR projects investigated is represented in Figure 5-13a and b. 'Intrinsic mobility' was aptly used here because the

mobility of EOR gases presented in Figure 5-13a and b were derived from the ratio of the intrinsic (single-phase) permeabilities and viscosity of the respective reservoir oil. The clusters are quite distinct across EOR technologies in Figure 5-13a. It is shown that gas technology is generally implemented in reservoirs with higher intrinsic mobility oil than other EOR technologies. Similarly, Figure 5-13b shows the segregation of gas processes by intrinsic mobility. It would be observed in the clusters and in Abunumah, Ogunlude, and Gobina (2021) that most of the CH_4 and N_2 projects are implemented in reservoirs with relatively high intrinsic mobility. There reverse is the case with Air and CO_2. This suggests a qualitative association between intrinsic mobility segregation and gases' molecular weights. Mobility is not a petrophysical quantity considered in EOR screening criteria and has not been represented in existing EOR selection models.
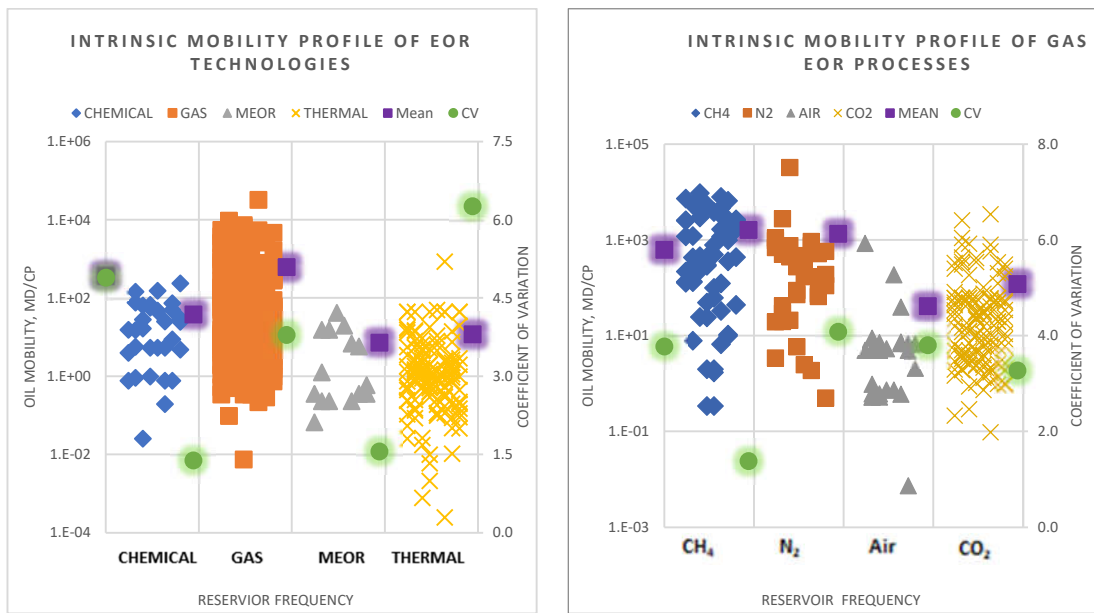
a.   b.

Figure 5-13. Oil intrinsic mobility distribution of EOR reservoirs for (a) EOR technologies and (b) gas EOR processes.

However, it is an important function in Darcy and Buckley-Leverett flow equations. It is, therefore, interesting to notice that EOR technology can be characterised by it. Consequently, this quantity was adopted for experimental investigation.

5.5.3.3　Intrinsic Oil Velocity

Velocity has been selected as an objective function for evaluating EOR gases. It is demonstrated in Figure 5-14 that CH_4 reservoir intrinsic velocity is significantly segregated from those of N_2, Air, and CO_2 reservoirs. Nevertheless, it is seen that the different gas EOR implementations in these reservoirs are sensitive to velocity to varying degrees. The Air EOR process is the most clustered, thus the most sensitive. CH_4 reservoirs have the least velocity. Implying that these reservoirs may have relative disadvantages in momentum, capillary number, and energy, as these engineering quantities are a function of velocity. The Phase II and III experiments would establish if the gas velocity informs the application of the gases in the respective reservoirs.
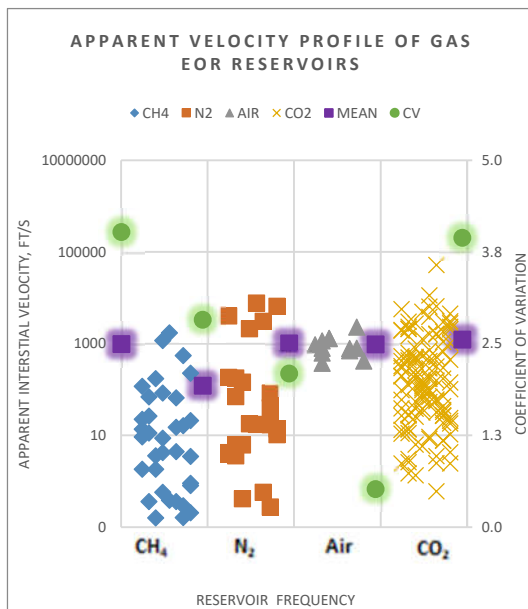
Figure 5-14. Oil interstitial velocity distribution of gas EOR processes reservoirs.

5.5.3.4　Intrinsic Oil Momentum

Figure 5-15 shows the intrinsic interstitial momentum distribution of gas EOR reservoirs. It can be stated that the reservoirs are significantly segregated by momentum. The mean Air momentum value may have been affected by the two reservoirs with high momentum ratings, which could be considered superficial. CO_2 EOR reservoirs have a higher momentum than CH_4 and N_2.

The importance of momentum has been stated in the literature review. High potential momentum, such as the one exhibited by CO_2 reservoirs, would be useful if it is in the same direction of the injectant flow, that is, towards the nearest producer well; otherwise, it would be averse to the energy or momentum transfer of the injected gas. The experimental p hase would be used to couple Figure 5-15 to evaluate how the EOR reservoirs and gases stack in performance.
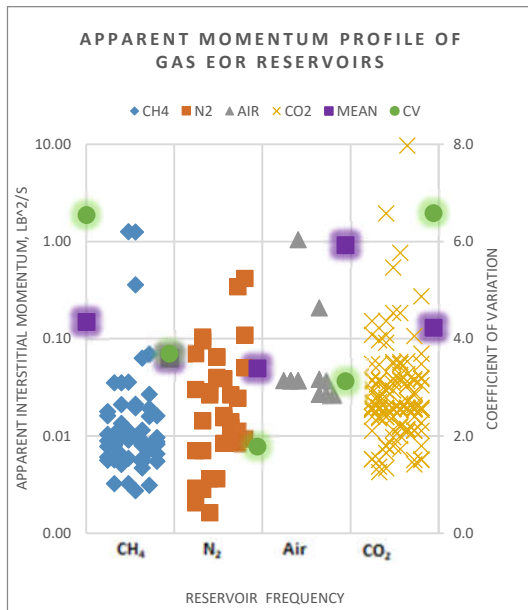
Figure 5-15. Oil Momentum distribution of gas EOR processes reservoirs.

5.5.3.5   *Intrinsic Oil Transmissibility*

Transmissibility is a measure of the oil to transmits to the nearest producer well. Figure 5-16 indicates that CH_4 has the highest capacity to transmit through the reservoirs' pores, and at the same time, it is the most sensitive to this quantity. Air reservoir offers the least transmissibility opportunity. It has been demonstrated that gas EOR reservoirs are characterised by transmissibility. The gas experiments would further advance the importance of this quantity.
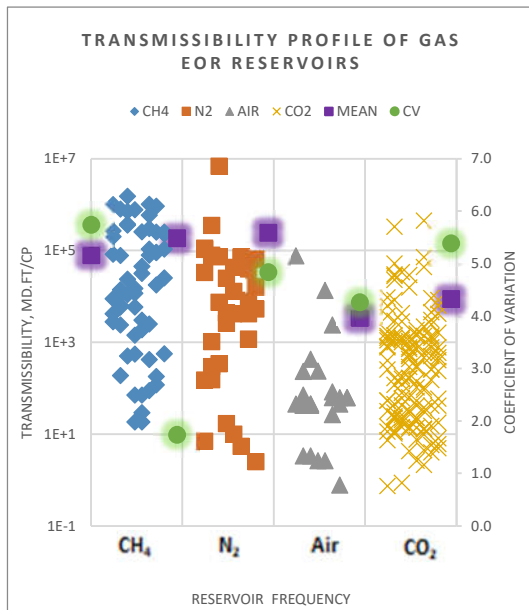
Figure 5-16. Oil transmissibility distribution of gas EOR processes reservoirs.

5.5.3.6 Well Density

The well density is a combinatorial quantity introduced in the screening criteria proposal to investigate the existence of well profiling for the respective EOR methods. This enabled the study to identify if EOR technologies and gas processes can be characterised based on their respective well requirements. Surprisingly, the clusters presented in Figure 5-17a and b show interesting patterns. From the clusters in Figure 5-17a, it would be observed that Thermal technology has the highest well density requirement with an average of 0.52well/acre and as high as 3.84well/acre. This is followed by Chemical technology at an average well requirement of 0.20 well/acre. The Chemical EOR is shown to be very clustered, therefore, implying it is the most sensitive to well density. The sensitivity is quantitatively described by the CV of 0.72. In Figure 5-17b, gas processes were compared. Clusters reveals that CH_4 requires the least well density (0.02well/acre) followed by N_2 (0.05well/acre) and (1.86well/acre). Furthermore, it was observed that N_2 is the most sensitive to well density, while Air is the least sensitive. The significance of these findings is that it would cost more wells to implement Thermal and Chemical technologies than Gas and MEOR technologies. Furthermore, in the Gas technology domain, it

can be seen that it would cost more wells to implement CO_2 processes than to implement CH_4 and N_2.
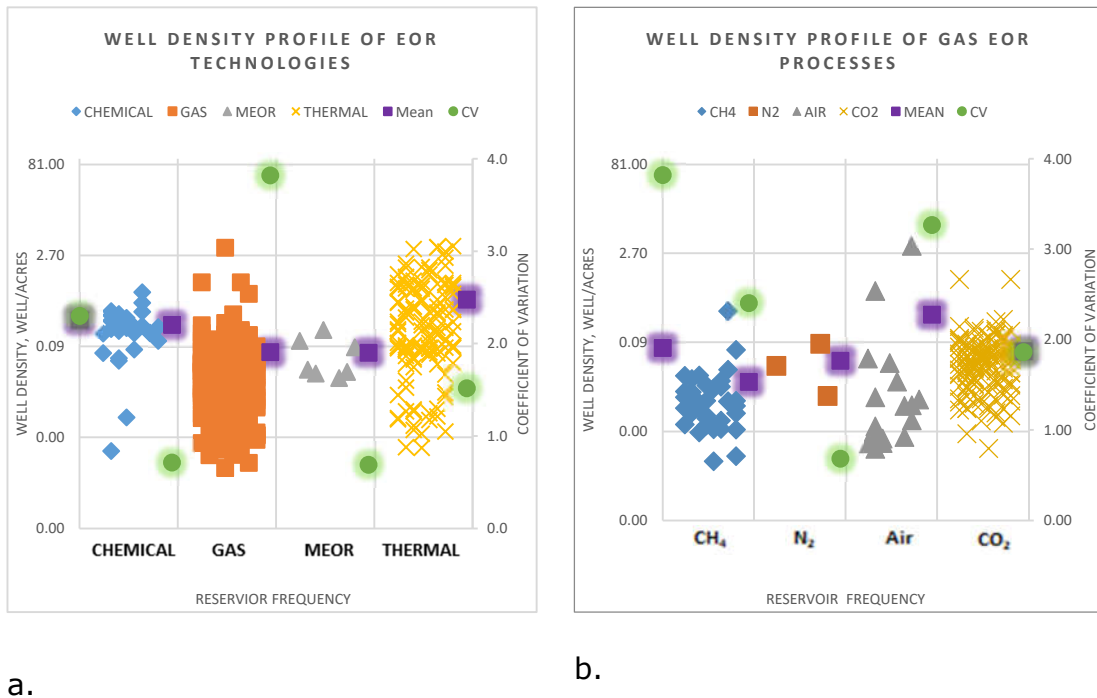
a.

b.

Figure 5-17 Well density clustering for various (a) EOR technologies and (b) gas EOR processes.

Holm (1980) and Zhenxue (2014) investigations significantly validate the findings in Figure 5-17a and b, which suggest larger well spacing for CO_2 EOR (7 acres) compared to Chemical Technology (5 acres). The claim of validation by Holm (1980) cannot be fully established until further engineering interpretation of this observation is made per the segregated conditions and parameters analysed in his studies, such as permeability. As earlier mentioned in the literature review, there are hardly detailed contemporary journal references to well spacing or density in EOR operation. It is not easy to properly verify or compare the results here thoroughly. However, this quantity is not included in the previous screening model, nor is it present in the Darcy and Buckley-Leverett equations. It is, however, possible to explain this quantity using these equations. This quantity has been implicitly investigated in the course of the experimental phase.

5.5.3.7   Well Pattern

The Well pattern predictor (P_P) for each EOR technology is presented in Figure 5-18a. This quantity is derived as the injection to production well ratio. It is a measure of a well ratio index. Although predicting this quantity from field data is not well understood or reported in journals, the clusters in Figure 5.19a show some well pattern discrimination across technologies. Well pattern predictor (P_P) values less than one ($P_P < 1$) indicate an inverted well pattern. P_P values above one ($P_P > 1$) indicate a normal well pattern as illustrated in Figure 2-10. Gas and Thermal technologies seem to include all types of well patterns (i.e., normal and inverted). The lowest value set (0.1-0.002) of P_P is found in Thermal Technology. Signifying relatively high production wells than injection wells. This is suggestive of the proposition that Thermal Technology is a favourable candidate for seven and nine spot inverted patterns.

Chemical and MEOR are generally restricted to inverted well patterns. Their low CV values suggest Chemical and MEOR are the most sensitive to well patterns. In Figure 5-18b, the respective well patterns within Gas technology are not significantly distinguished. However, CO_2 is shown to be the most sensitive to this quantity. Therefore, Air is seen to be popular with the inverted well pattern. The normal well patterns ($P_P > 1$) are mostly utilised in CO_2 projects.

WELL PATTERN PROFILE OF EOR TECHNOLOGIES

WELL PATTERN PROFILE OF GAS EOR RESERVOIRS
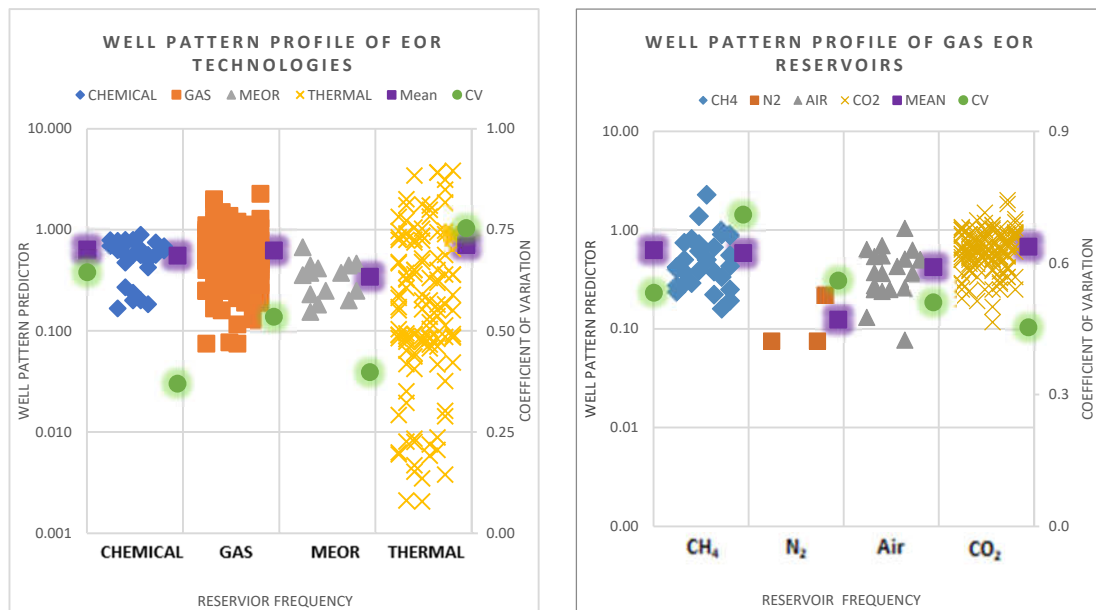
a.

b.

Figure 5-18 Well pattern clustering for various (a) EOR technologies and (b) gas EOR processes.

Duda and Il (2010), El Ela and Sayyouh (2014), Holm (1980) had claimed that well pattern modelling could be used to optimise EOR methods in general but fell short of describing the details, for example, whether EOR methods can be uniquely associated with different well patterns. The effect of well patterns was also reported with respect to CO_2 EOR implementation at SACROC field in the Permian Basin, US. Walzel (2017) emphatically stated that production was tripled within a couple of years by targeting the well patterns. This research has also demonstrated that more than 80% of gas EOR projects are implemented in an inverted well pattern (Well Pattern Predictor<1) as against normal well patterns (Well Pattern Predictor>1).

5.6 New Immiscible Gas EOR Screening Model

Table 5-1 shows a new screening model for immiscible gas EOR. This is the outcome of rigorous exercises involving data mining of collated EOR field data using different statistical techniques and codes in R and Microsoft Excel. A qualitative and quantitative evaluation has been applied to observations and

relationships across (Thermal, Gas and Chemical) technologies and within Gas EOR technology.

Al Adasani and Bai (2011) (in Table 5-2), and Taber *et al.* (1997) screening models were used to compare and contrast the new criteria in the new screening model. The parameter values in the new screening criteria compare well with the two authored EOR screening criteria for most parameters and properties. However, in some other respects, such as porosity and viscosity, the proposed criteria are more up-to-date with events in global EOR implementations. The proposed criteria also accounted for recent evolutions in EOR applications as reported in journals, technical reports, and field surveys that were not captured in previous EOR studies.

This screening model's key feature focuses on immiscible EOR for the four commonly applied EOR gases, unlike previous models that lumped the four gases as one. Authors such as Clancy *et al*. (1985) have developed screening criteria for N_2 immiscible EOR. The data used were nevertheless quite limited. Furthermore, they did not offer a robust means to compare N_2 with other EOR gases. This screening model is formulated based on some assumptions:

I.   That immiscible gas EOR projects data reported in surveys and journals are significantly correct and reported in good faith.
II. That successful projects are successful enough for them to be replicated in analogical reservoirs.
III. For successful projects, engineering methods and decisions made by engineers were significantly the best among the alternatives and are mostly valid to date.

The investigation applied due engineering diligence to mitigate deviations from these assumptions. For instance, the interquartile range was used to spot outliers; however, care was taken not to dismiss the potential implication of outliers that are markers for technological evolution. Some reservoirs in China that implemented EOR CH_4 appear to have reported extremely high viscosity compared to other CH_4 global reservoir records. A polymer EOR project in Taber South, Canada, was seen to be operated in a traditionally

thermal EOR reservoir candidate (800–80,000cp). By existing screening standards, this characterisation popped up as an outlier.

However, an independent investigation into the field suggested that the operators have used technology, such as horizontal wells to overcome the challenge of polymer injectivity in the reservoir. Taber *et al.* (1997) screening criteria would screen a reservoir as a candidate for Polymer flooding only if the viscosity is between 10cp to 150cp. While for immiscible gases, Taber *et al.* (1997) suggested a viscosity of <600cp. This new screening criteria, however, raised the bar to 9600cp. These are some of the criticisms of existing EOR screening criteria held by Lee (2010), Delamaide *et al*. (2014a, 2014b), and Wilson (2015). Although, the process of balancing the data to generate these new screening criteria was rigorous and taunting. However, the outcome was worth it.

Table 5-1 Proposed Screening Criteria developed from the most recent global EOR database to reflect operational and technological evolution in the EOR industry, with parameter sensitivity marker.

New Immiscible Gas Screening Criteria with Sensitivity Markers										
		Viscosity	Oil Mobility	Permeability	Oil Saturation, Start	Radial Thickness	Depth	Porosity	API Gravity	Temp
CH_4	Mean	210	1,650	668	73	1.62E+6	6,285	17	36	363
	Value Range	>0.14 <10201	>0.35 <9.6+3	>15 <3.1E+3	>30	>0.07E+6	>610	>4	19 – 48	
	Sensitivity	NS	NS	NS	S	MS	MS	S	S	NS
N_2	Mean	3	1,329	841	#N/A	1.49E+6	8,003	19	38	352
	Value Range	<25	<0.51 <3.3E+4	<5.5E+3	#N/A	>1.3E+4	>1,200	>4	>16	
	Sensitivity	NS	NS	NS	#N/A	MS	S	MS	S	NS
AIR	Mean	6,182	42	271	64	1.71E+6	6,572	18	31	346
	Value Range	>1.19 <1.7E+5	<854	>1.5 <1.3E0+3	>50	>6.0E+4	>400	4>	19-38	
	Sensitivity	NS	NS	NS	S	MS	S	S	S	NS
CO_2	Mean	7	121	103	47	1.23E+06	5,986	16	36	333
	Value Range	>0.2 <592	>0.1 <3.5E3	>1.06 <2.0E3	>26	>5.0E+04	>1,150	>3	11-45	
	Sensitivity	NS	NS	NS	S	MS	S	S	S	NS
DISCRIMINATORY PARAMETER WITHIN GAS TECHNOLOGY		C	C	C	C	MC	MC	NC	NC	NC
DISCRIMINATORY PARAMETER ACROSS EOR TECHNOLOGY		VC	VC	C	MC	C	MC	MC	MC	NC
Key:		S=Sensitive		C=Critical		V=Very		M=Moderate		N=Not

Table 5-2 Al Adasani and Bai (2011) Screening Criteria for Gas EOR as compared to proposed screening criteria in this study.

EOR method	Gravity (°API)	Viscosity (cp)	Porosity (%)	Oil saturation (% PV)	Permeability (mD)	Net thickness	Depth (ft)	Temperature (°F)
Reservoir criteria for EOR gas processes								
Miscible gas EOR								
CO_2	22-45 Avg. 37	0-35 Avg. 2	3–37 Avg. 15	15-89 Avg. 46	1.5-4500 Avg. 209	Wide Range	1500-13365 Avg. 6230	82-257 Avg. 138
Hydrocarbon	23–57 Avg. 38	0.04-18000 Avg. 286	4.25–45 Avg. 4.5	30–98 Avg. 71	0.1–5000 Avg. 726	Thin, unless dipping	4000–15900 Avg. 8343	85–329 Avg. 202
WAG	33–39 Avg.35	0.3–0.9 Avg. 0.6	11–24 Avg.18.3		130–1000 Avg. 1043	NC	7545–8887 Avg. 8216	194–253 Avg. 229
Nitrogen	38–54 Avg. 47	0-0.2 Avg. 0.07	7.5–14 Avg.11	0.76–0.8 Avg. 0.78	0.2–35 Avg. 15	Thin, unless dipping	10000-18500 Avg. 14633	190–325 Avg. 266
Immiscible Gas EOR								
Nitrogen	16–54 Avg.34.6	0-18000 Avg. 2256	11–28 Avg. 19	47–98.5 Avg. 71	3–2800 Avg. 1041		1700–18500 Avg. 7914	82–325 Avg. 173
CO_2	11–35 Avg.22	0.6-592 Avg. 65	17–32 Avg. 26	42–78 Avg. 56	30–1000 Avg. 217		1150–8500 Avg. 3385	82–198 Avg. 124
Hydrocarbon	22–48 Avg.35	0.25-4 Avg. 2.1	5–22 Avg.13.5	75–83 Avg. 79	40–1000 Avg. 520		6000–7000 Avg. 6500	170–180 Avg. 175
Hydrocarbon + WAG	9.3–41 Avg.31	0.17-16000 Avg.3948	18–31.9 Avg. 25	Avg. 88	100–6600 Avg. 2393			

Although, Al Adasani and Bai (2011) supplied more updated screening criteria that unbundled immiscible gas in Taber *et al*. (1997). However, the new screening criteria model developed in the study offers an advantage that would be of significant utility to users, such as the inclusion of a probabilistic sensitivity and criticality marker. The sensitivity marker is a statistical measure of how sensitive or reactive the applicability and performance of an EOR process is impacted when a parameter of interest is varied. For instance, in Table 5-1, the gases, N_2, Air and CO_2 are quite sensitive to variation from the mean depth. However, CH_4 has a low sensitivity to depth. The 'range' as included in most published EOR screening models is not sufficient to describe the risk or loss of effectiveness of a process when a petrophysical parameter deviates from the measure of central tendency, which in most cases is the mean. With the sensitivity and discriminatory marker included in this new

screening criteria, a simple program can be developed to succinctly screen reservoirs for immiscible EOR gases.

5.7 DISCUSSION OF RESULTS

An EOR screening model has been developed from this study with an emphasis on gas EOR. The proposed screening criteria reflects recent EOR process evolution in the EOR industry. Eleven EOR parameters, including some derived combinatorial parameters, have been thoroughly investigated using data mining techniques and a literature review. While these proposed criteria compare well with some parameters and properties in Al Adasani and Bai (2011), Saleh *et al.* (2014), and Taber *et al.* (1997), screening criteria, there are, however, some instances where the values for some parameters and properties do not compare.

Forty-one EOR quantities were categorised into Reservoir Rock, Fluid and Performance parameters. The properties relationship between EOR processes and selection have been extensively investigated using a global EOR database and mathematical techniques. The results indicate that all the reservoir properties under the reservoir rock parameter category form well-defined clusters. For the Reservoir Fluid category, not all properties responded with distinct clusters, such as Displacement Efficiency. Similarly, in the EOR Performance category, Incremental Oil Production and Well Patterns could not be characterised.

The general assessment of the quantities investigated was carried out in such a way that:

I. Quantities that do not form distinct and segregated clusters within the universal data set are considered ineffective in characterising EOR Technologies. This suggests that the property may not be critical in screening reservoirs for EOR Technologies or EOR processes.

II. Quantities that have defined and segregated clusters within the universal data set are considered suitable for characterising EOR Technologies.

III. Quantities that are well defined and segregated within a particular EOR Technology are considered suitable for characterising EOR processes within that EOR Technology.

Although the clusters' quality varies from quantity to quantity and from process to process. A tightly clustered quantity is considered to imply reduced dispersion of the property around the mean value (Stephanie 2014). Thereby suggesting the property is critical, and the EOR process may be sensitive to it. It was observed in all categories that a property whose cluster is widely dispersed is likely to overlap with other clusters. This is observed as the oil intrinsic mobility cluster in CO_2 gas EOR overlaps with the oil intrinsic mobility cluster in Steam EOR even though they are entirely different technologies. This suggests that CO_2 and Steam EOR can be applied to the same reservoir with respect to intrinsic mobility. Although CO_2 gas and CH_4 gas are both gas EOR technology, their intrinsic mobility clusters are separated, as revealed in Figure 5-13b. This suggests that intrinsic mobility is a distinguishing factor between CO_2 gas and CH_4 gas EOR. Therefore, these reservoir properties could be used as a criterion to characterise Gas EOR processes and consequently applied to evaluate gas performance in experimental studies.

5.7.1 Method for Identifying and Selecting Criteria for Immiscible Gas Experiments

The two categories of criteria considered for this evaluation are selection criteria and performance criteria—the criteria aid in selecting gas technology, while performance criteria aid in identifying the most competitive gas.

An assessment method to identify which reservoir engineering quantities to adopt for the next phase of the study (that is, the experimental phase for immiscible gas EOR) was set as follows:

I. Quantity clusters are evaluated across EOR technologies and within Gas EOR technology. Across technologies means clusters that can be categorised based on their spread and relevance across the broad spectrum of EOR technologies (i.e., Thermal, Chemical and Gas EOR technologies).

Within Gas EOR technology, means finding segregated clusters within Gas EOR Technology processes such as CO_2 and N_2 EOR processes. The former would identify whether a quantity is discriminated by EOR technology, while the latter would determine whether a quantity is discriminated based on gas EOR processes.

II.   Where clusters of different gas EOR processes overlap with each other (regardless of whether they also overlap with processes in other EOR technology, such as Thermal and Chemical EOR), the quantity represented in the clusters would be selected as fit for performance evaluation in the gas experiment.

III.   Where clusters of gas EOR processes do not overlap with each other or any other EOR technology, the quantity represented in the clusters should be selected as fit for EOR selection evaluation in the gas experiment.

IV.   Where an EOR quantity is tightly clustered, that is, implying strong cohesion than separation, it is considered that this quantity is potentially a critical and sensitive quantity to the gas EOR process (Stephanie 2014). The quantity represented in such clusters is selected as fit for sensitivity evaluation in the immiscible gas experiments.

Based on these criteria, as imposed on the results from the data mining in Section 5.5, and the Darcy and Buckley-Leverett equation for immiscible flow through porous media, the study was able to fulfil the objective one of the researches, which is to identify EOR parameters that are necessary and critical for selecting and determining the performance of gas EOR processes. Table 5-3 shows the quantities identified in the data mining evaluation for gas EOR. The third column indicates quantities that could be used to screen for gas EOR. A 'Yes' implies that the quantity can be used as a criterion for screening and selecting gas processes within gas EOR Technology. A 'No' indicates that all gas EOR processes share a similar value range for that property; therefore, the property cannot be used as a selection criterion forthwith. However, it could be qualitatively considered for performance evaluation. For example, from the viscosity graph (Figure 5-11b), it would be observed that different gas EOR processes (clusters) significantly share a similar viscosity range.

Table 5-3. Petrophysical Parameters and Properties identified for immiscible gas EOR experiments.

			Screening Evaluation	Experimental Evaluation		
S/N	Category	Quantity	Selection Criteria	Performance	Present in Darcy/Hagen-Poiseuille/ Buckley Leverett Equations	Remark
1	Reservoir Rock Parameters	Permeability	Yes	Yes	Yes	Intrinsic property
		Porosity	No	Yes	No	Intrinsic property
		Depth	No	Yes	No	
		Temperature	Yes	Yes	Yes	Intensive Property
		Area/Radius	Yes	Yes	Yes	Extensive Property
2	Reservoir Fluid Properties	Oil Saturation	Yes	Yes	Yes	
		API Gravity	Yes	Yes	No	
		Viscosity	No	Yes	Yes	
		Oil Mobility	Yes	Yes	Yes	Derived
3	EOR Performance Parameters	Incremental Oil Production	Yes	Yes	Yes	
		Displacement Efficiency	Yes	Yes	No	
		Well Density	Yes	Yes	Yes	Derived
		Well Pattern Index	No	Yes	No	

However, for the oil intrinsic mobility graph (Figure 5-13b), various gas EOR processes (clusters) assumed a different intrinsic mobility range. This

suggests, therefore, that viscosity is not an essential criterion for selecting the gas EOR process since all reservoirs that implemented gas EOR technology have similar viscosity. However, oil intrinsic mobility is important for selecting the gas EOR process since all gas EOR Technology formed different clusters. Consequently, in Table 5-3, in the 'Selection Criteria' column, Viscosity is registered as 'No', while Oil intrinsic mobility is registered as 'Yes'.

In summary, some thirteen quantities were registered as 'Yes' (Performance Column) for experimental evaluation. Eight of these quantities are represented in the Darcy and Buckley-Leverett equation for immiscible flow. These properties representations in these equations are classified as:

I.   Direct representation, such as reservoir radius or permeability being a tensor in the Darcy equation.
II.   Deduced representation, such as intrinsic mobility.
III.   Correlational representation, such as Well density.
        Consequently, the experiment was set to determine how the relationship among these properties could be used to evaluate and improve the respective gases' competitive performance in immiscible gas EOR (Nesselroade and Cattell 2013, and Ghani 2014).

Chapter Six

6 PHASE II: EXPERIMENTAL EVALUATION OF EOR GASES

6.1 Engineering Basis for Experimental Evaluation

Most of the experimental techniques applied in this phase are fairly standard to the industry. Where new procedures and assumptions are used, the bases for making such decisions are subsequently described in detail. Several analytical frameworks were used to validate the use of theoretical concepts of fluid and solid mechanics and balances, as promoted in Andri *et al.* (2017), Bergstrom (2015), Berker (2002), Coratekin, *et al*., (1999), Chandrasekharaiah and Debnath (2014), Sadd (2018), Malkin (2012), and Risby and Hamouda (2011).

6.1.1 Adoption of Intrinsic Mobility

From the data mining of the global EOR database consisting of 484 EOR projects, it was identified that the ratio between oil intrinsic permeability in reservoir rock and oil viscosity indicates a distinct cluster pattern for each EOR process in the database. The distinction signifies that this ratio could be used as a criterion for characterising reservoirs and EOR processes. The ratio was referred to in the research as the intrinsic mobility of oil because it was derived from the reservoir oil's intrinsic permeability and the dynamic viscosity. It is represented as $M_{o\infty}$. Where the subscript 'o' and '∞' represent oil and intrinsicality, respectively. However, intrinsic mobility is different from the conventional mobility encountered in multiphase reservoir engineering calculations, which is the ratio of effective permeability to phase viscosity (Sam 1993), however, intrinsic mobility offers a useful analytical basis for

experiments because it combines rock (permeability, k) and fluid (viscosity, μ) properties.

Gas is a displacing fluid for oil in immiscible gas EOR; therefore, the intrinsic mobility analogy of the oil can be extended to gases. Consequently, in this research, intrinsic mobility $M_{i\infty}$ (where the subscript 'i' is any EOR gas) of the gases was confidently adopted as the engineering basis and a critical criterion for evaluating the respective gases' selection and performance competitiveness in displacing trapped oil. The benefit of adopting gas Intrinsic Mobility $M_{i\infty}$, which is the ratio of intrinsic gas permeability to its viscosity ($M_{i\infty} = k_i/\mu_i$), as a cardinal parameter is that it allows the evaluation of other petrophysical properties and parameters, such as PVT, pore size and molecular weight in the experiments. The effect of these properties and parameters on $M_{i\infty}$ can thus be measured in an experiment for further analyses. The individual intrinsic mobility of oil and gas can therefore be directly compared.

6.1.2 Intrinsic Mobility Vs Relative Mobility

The relative mobility, as expressed in Eq. 2-48, is made of four variables. The variables in the denominator are those of oil. The variables in the numerator are those of the gas under investigation. Since it is a comparative study among gases, unlike miscible gas EOR, where the gas dissolves in the oil to reduce the oil's viscosity (Breit 1992 and Gbadamosi *et al.* 2018), here, these gases do not attain miscibility with the oil. Therefore, it is assumed that at the point of displacement, certain properties of the denominator (that is, oil), such as density and viscosity, would remain significantly the same and would therefore be a common factor for all gases investigated within the experimental condition. This assumption is consistent with the Buckley-Leverett condition for immiscible fluid displacement.

Another study that was used to validate the experimental approach in this research is based on the outcome of Deb, Chayantrakom and Lenbury (2012), where they compared single-phase (SPM) flow of microalgae and two-phase

(TPM) flow dynamics of microalgae injected with CO_2 gas. It could be derived from their results that there is a steady-state relationship between single-phase microalgae flow and the two-phase microalgae/CO_2 as represented in Figure 6-1a-b and Figure 6-2a-d:
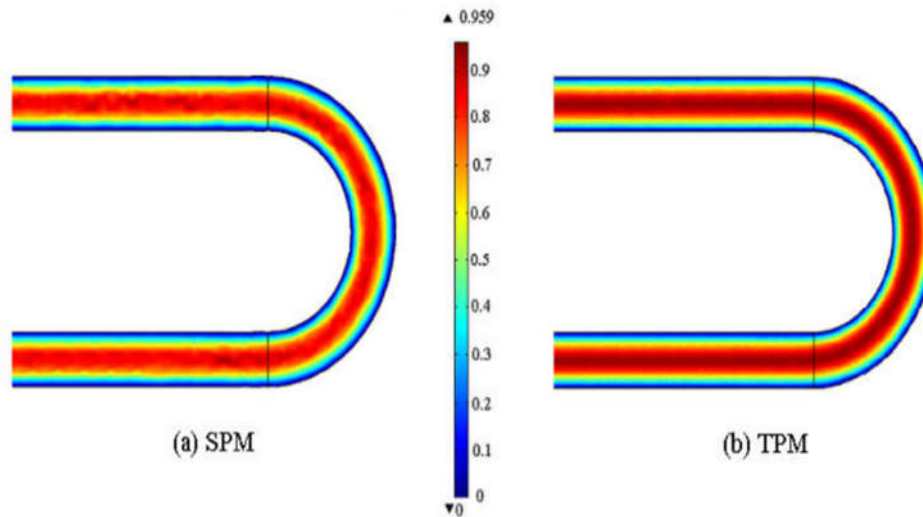
Figure 6-1. Single-phase microalgae flow in a tube (SPM) model (a) and a two-phase microalgae/CO_2 model (TPM) (b).

Figure 6-2b-d capture different geometrical location in the tube and the velocity profile of flow was observed to be affected by the geometry of the flow path. However, this did not appear to quantitatively impact the relationship between the SPM and TPM models' velocities when it was plotted on a graph. The flow pattern from the three graphs in Figure 6-2b-d and their numerical results intuitively indicate that the single-phase fluid dynamics are analogical to the two-phase fluid dynamics without losing generality. Furthermore, it also qualitatively indicates that TPM production is a multiple of SPM. The TPM model that involves the injection of CO_2 in the tube conduit was stated to have enhanced microalgae production. In a similar vein, gases, such as CO_2, are injected into reservoir pores to enhance oil production.
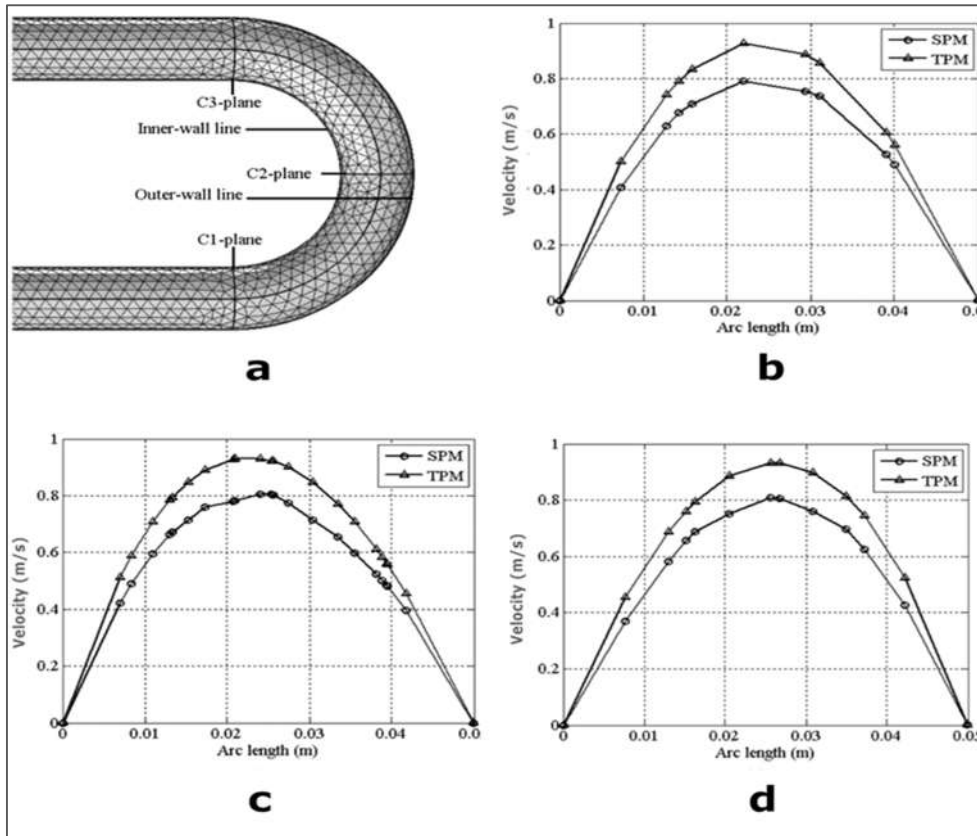
Figure 6-2: The mesh model of a U tube showing three planes for flow investigation (a), and velocity profile obtained from single-phase flow (SPM) and multiphase flow (TPM) at three different cross-sections of the U shape region of the tube: (b) C1, (c) C2 and (d) C3.

Consequently, with the information provided by their study, this research was able to derive a flow velocity analogy between single-phase and two-phase flow for an immiscible system (Darcy 1856, Zeng and Grigg, 2006).

$$Q = \frac{-KA}{\mu'}\frac{dP}{dx}$$

6-1

Given two models: SPM and TPM, this study modified the Darcy equation for each phase as:

$$Q_{SPM} = \frac{-K_{SPM}A}{\mu'_{SPM}}\frac{dP}{dx}$$

6-2

$$Q_{TPM} = \frac{-K_{TPM}A}{\mu'_{TPM}}\frac{dP}{dx}$$

6-3

The volumetric flow rate can be reduced to Darcy velocity by dividing both sides by the cross-sectional area, A, of the flow medium.

$$V_{SPM} = \frac{-K_{SPM}}{\mu'_{SPM}}\frac{dP}{dx}$$

6-4

$$V_{TPM} = \frac{-K_{TPM}}{\mu'_{TPM}}\frac{dP}{dx}$$

6-5

According to Deb, Chayantrakom and Lenbury (2012) and in Figure 6-2, for every timestamp, there is an empirical relationship between the ratio of the velocity of the single-phase (SPM) and two-phase (TPM) flow. This implies:

$$\frac{V_{SPM}}{V_{TPM}} = \frac{\frac{K_{SPM}}{\mu'_{SPM}}\frac{dP}{dx}}{\frac{K_{TPM}}{\mu'_{TPM}}\frac{dP}{dx}}$$

6-6

Eq. 6-6 can be reduced to:

$$\frac{V_{SPM}}{V_{TPM}} = \frac{\frac{K_{SPM}}{\mu'_{SPM}}}{\frac{K_{TPM}}{\mu'_{TPM}}}$$

6-7

Recall mobility is the ratio of permeability to viscosity.

Therefore, Eq.6-7. can be expressed in terms of mobility:

$$\frac{V_{SPM}}{V_{TPM}} = \frac{M_{SPM}}{M_{TPM}}$$

6-8

Eq. 6-8. can be rearranged as:

$$M_{SPM} = \frac{M_{TPM}V_{SPM}}{V_{TPM}}$$

6-9

Eq. 6-9 implies that a plot of M_{SPM} against V_{SPM} should start from the origin and should have M_{TPM}/V_{TPM} as the slope. Eq. 6-9 qualitatively implies that the single-phase (intrinsic) mobility of a fluid through a capillary is proportional to the product of its mobility in a two-phase regime and its velocity in a single-phase regime. For this to be valid, it means that for every saturation or

fractional composition of the fluid in a two-phase system, the slope of a graph of M_{TPM} against V_{TPM} must be linear or constant for the pair of the fluid and capillary system. That is:

$$\frac{M_{TPM}}{V_{TPM}} = constant \qquad\qquad 6\text{-}10$$

Deb, Chayantrakom and Lenbury (2012) stated that different geometry around the tube's U shape (Figure 6-2a) used in their study affected the flow velocity. Nevertheless, the effect was proportionate to both phases. The effect's proportionality can also be observed from the shapes of SPM and TPM in the three graphs of Figure 6-2b-d. These figures represent flow regimes from three different geometry in the U region. Therefore, signifying that the ratios M_{TPM}/V_{TPM}, M_{SPM}/V_{SPM}, M_{SPM}/M_{TPM} and V_{TPM}/V_{SPM} could be assumed significantly constant for any given capillary geometry, assuming other flow conditions and properties are known. However, it is suggested that further study should be carried out in this area to determine the true state.

Although Eq. 6-10 was modelled with respect to the displaced fluid (microalgae), this relationship is expected to also apply to the displacing fluid's (CO_2) flow behaviour. The reason is that the microalgae's enhanced flow in the TPM is a function of the injected CO_2.

Consequently, for the benefit of this research, the relationship between intrinsic mobility and multiphase mobility of a gas in an immiscible gas EOR, at a given saturation or flow composition, can now be expressed by rewriting Eq. 6-9 as:

$$M_{i\infty} = \frac{M_i V_{i\infty}}{V_i} \qquad\qquad 6\text{-}11$$

Where:

$M_{i\infty}$ = intrinsic mobility of gas in mD/cp

M_i = multiphase mobility of gas at a given saturation or fractional compassion in mD/cp

$V_{i\infty}$ = intrinsic Darcy velocity of gas in cm/s

V_i = multiphase Darcy velocity of the gas at a given saturation or fractional compassion in cm/s

This research is interested in comparing the mobility ratio of gases to identify how they approach the favourable condition of M<1.

Accordingly, for a comparative study of the gases used in immiscible gas EOR, where performance is based on gas mobility, the following analogy can be assumed correct.

For gases CH₄, N₂, CO₂ in immiscible displacement,

$$comparing\ M_{CH_4\infty}, M_{N_2\infty}, M_{CO_2\infty} == is\ equavalent\ to == M_{CH_4}, M_{N_2}, M_{CO_2} \qquad \text{6-12}$$

This research is interested in comparing mobility ratio: $M_{N_2@293K\_1atm}$,$M_{CO_2@293K\_1atm}$, $M_{CH_4@293K\_1atm}$ to identify how they approach the favourable condition of M<1 when applied for the respective gases. Therefore, the right side of Eq. 6-12 can be rewritten in the basic form of mobility equation as:

$$comparing\ M_{CH_4\infty}, M_{N_2\infty}, M_{CO_2\infty}$$

$$\xrightarrow[is\ equivalent\ to]{} \left(\left(K/_{\mu'}\right)_{CH_4\infty}\right), \left(\left(K/_{\mu'}\right)_{N_2\infty}\right), \left(\left(K/_{\mu'}\right)_{CO_2\infty}\right) \qquad \text{6-13}$$

The intrinsic mobility values for each gas are a direct outcome of the experiment. The respective gas $K/_{\mu'}$ expressions are an explicit function of the Darcy equation of state (Eq. 6-1), therefore was derived thence. Consequently, the oil displacement competitiveness of the gases in these experiments was interpreted such that: for a gas performance to approach the desired M≤1, it is expected that the experimental results for that gas should indicate a comparatively low intrinsic mobility. Conversely, high intrinsic mobility would signify a relatively high mobility ratio and would be less likely to approach the condition M≤1.

6.1.3 Multiphase Vs Single-Phase Comparison

The experiment was conducted in a single-phase system. In contrast, reservoir processes are usually in two-phase systems. Chin (2002) and Schlumberger (nd) have suggested that most reservoir pressure-transient analyses are conducted in a single phase. The assumption made to validate the experimental outcome's application on the reservoir process is based on engineering principles and several studies and published methods. The principle of critical velocity in immiscible displacement as proposed in Hill (1952), Chuoke, Van der Poel and Killian (1957), Van Meurs, and Van der Poel (1959), and the Klinkenberg theory as developed in Li and Horne (2001b) have been used to prove that for a comparative study, some two-phase expressions can be reduced to a single-phase equivalence. The authors mentioned above have shown the relationship between the behaviour of intrinsic gas properties, such as density, viscosity and permeability in a single-phase and in a two-phase system.

6.1.3.1 Critical Displacement Velocity:

The detailed evolution and derivation of the critical displacement velocity equation are based on simple engineering principles that have been stated in previous sections of this research. The critical displacement velocity as derived from Lu, Weerasooriya and Pope (2014), can be expressed as:

$$\text{v} = Kg\frac{d\rho}{d\mu} = Kg\left(\frac{\rho_o - \rho_g}{\mu_o - \mu_g}\right) \qquad\qquad 6\text{-}14$$

The equation indicates that a measure of displacement efficiency at the pore scale, that is, velocity, is a function of the difference between the oil and gas properties (density and viscosity). Lake and Larry (1989), Al-Abri, Hiwa and Robert (2009), Lu, Weerasooriya and Pope (2014) and Dietz (1953), as mentioned in Dumore (1964), have repeated and applied this concept in their experimental investigation of fluid behaviour, such as surfactant and supercritical CO_2 displacement of oil. There is an extensive validation of the relationship. Therefore, given an oil type with density and viscosity p_o and μ_o, respectively, for a comparative study to evaluate the immiscible displacement

performance of gases, where the driving force is predominantly from the momentum of the gases, but the common permeability of the stable front is controlled by surface volumetric production rate, the following thus holds:

Critical Velocity for oil-CH_4 displacement

$$v_{CH_4} = K_{CH_4} g \left(\frac{\rho_o - \rho_{CH_4}}{\mu_o - \mu_{CH_4}} \right) \qquad 6\text{-}15$$

Critical Velocity for oil-N_2 displacement

$$v_{N_2} = K_{N_2} g \left(\frac{\rho_o - \rho_{N_2}}{\mu_o - \mu_{N_2}} \right) \qquad 6\text{-}16$$

Critical Velocity for oil-CO_2 displacement

$$v_{CO_2} = K_{CO_2} g \left(\frac{\rho_o - \rho_{CO_2}}{\mu_o - \mu_{CO_2}} \right) \qquad 6\text{-}17$$

Taking note of the constants. Eq. 6-15, 6-16 and 6-17 can further lead to equation reduction, such that comparing the critical velocity of the gases is equivalent to comparing the density and viscosity quotients of the respective gases:

$$v_{CH_4}, v_{N_2}, v_{CO_2} ====> \left(K \frac{\rho}{\mu} \right)_{CH_4}, \left(K \frac{\rho}{\mu} \right)_{N_2}, \left(K \frac{\rho}{\mu} \right)_{CO_2} \qquad 6\text{-}18$$

It can be seen from the preceding equations that a two-phase system can be reduced and represented by a single-phase domain space for a comparative immiscible oil-gas displacement investigation.

6.1.3.2   Klinkenberg Theory

Klinkenberg theory has been used by Li and Horne (2001b) to relate gas intrinsic permeability and their apparent permeability in a multiphase system. A classic example of the Klinkenberg equation is expressed in Li and Horne (2001b) as:

$$k_g = k_{g\infty}\left(1 + \frac{4c\lambda}{r}\right)$$

6-19

Where:

K_g = is the effective gas permeability at a mean pressure, P_m (mD);

$k_{g\infty}$ = the intrinsic permeability of gas at an infinite pressure (mD);

c = a proportionality factor which is slightly less than 1;

λ = the mean free path of the gas (cm);

r = the average radius of the capillaries (cm).

The mean free path of a gas is inversely proportional to the mean pressure P_m; thus, Eq. 6-19 could be reduced to:

$$k_g = k_{g\infty}\left(1 + \frac{b}{P_m}\right)$$

6-20

Where:

$$b = \frac{4c}{rP_m}\lambda$$

6-21

Li and Horne (2001b) further published a derived relationship between gas multiphase and single-phase permeability as:

$$k_{g\infty}(S_w) = \left(\frac{k_g(S_w, P_m)}{1 + b_{S_w}/P_m}\right)$$

6-22

Where:

$K_{g\infty}(Sw)$ = intrinsic effective permeability at water saturation, S_w (mD);

b_{Sw} = slip factor of the gas phase at a water saturation of S_w (atm).

Furthermore, in relative permeability terms, they further derived that:

$$k_{rg}(S_w, P_m) = k_{rg\infty}(S_w)\left(1 + \frac{b_{S_w}}{P_m}\right)$$

6-23

Eq. 6-22 and 6-23 show the relationship between the gas intrinsic permeability (i.e., in single-phase) to its apparent permeability (in multiphase).

The experiments can secure values for the variable $k_{g\infty}$. For an immiscible system (two-phase), the fluids' viscosities are considered constant (Muggeridge *et al.,* 2014). Therefore, dividing both sides of Eq. 6-23 with the viscosity of the gas, Eq. 6-24 is arrived at:

$$\frac{k_{g\infty}(S_w)}{\mu'} = \left(\frac{k_g(S_w,P_m)}{\mu'(1+b_{S_w}/P_m)}\right) \xrightarrow{yields} M_{g\infty}(S_w) = \left(\frac{M_g(S_w,P_m)}{(1+b_{S_w}/P_m)}\right) \qquad 6\text{-}24$$

Recall the equation for mobility earlier expressed in Eq. 2-46. In this case, M_i in Eq. 2-46 is equivalent to $M_{g\infty}(S_w)$ in Eq. 6-24. Thus, Eq. 6-24 can be rewritten by substituting for 'b' in Eq. 6-21.

$$M_{g\infty}(S_w) = \left(\left(\frac{1}{\left(1+\left(\frac{4c}{rP_m}\lambda/P_m\right)\right)}\right) M_g(S_w,P_m)\right) \qquad 6\text{-}25$$

For a comparative analysis, all the gases to be compared would experience the same variables (such as P_m and S_w) and constant parameters (c and r) that make up the M_g coefficient in Eq. 6-25. The exception is the parameter λ, the mean free path of the respective gases. For the reason that λ is strictly a unique gas property for each gas. Thus, Eq. 6-25 can be simplified to:

$$M_{g\infty}(S_w) = \left(\frac{M_g(S_w,P_m)}{1+\lambda}\right) \qquad 6\text{-}26$$

Eq. 6-25 signifies that for every measured M_g in a multiphase system at a water/liquid saturation, Sw, the corresponding intrinsic mobility is $M_{g\infty}$. Consequently, comparing the multiphase mobility of gases, $\left(\frac{M_g}{1+\lambda}\right)$ is equivalent to comparing their intrinsic mobility, $M_{g\infty}$.

Therefore, the expression in Eq. 6-12 could be rewritten as:

$$comparing\ M_{CH_4\infty},M_{N_2\infty},M_{CO_2\infty}$$

$$\xrightarrow[is\ equivalent\ to]{} \left(\left(\frac{M_g(S_w,P_m)}{1+\lambda}\right)_{CH_4}\right),\left(\left(\frac{M_g(S_w,P_m)}{1+\lambda}\right)_{N_2}\right),\left(\left(\frac{M_g(S_w,P_m)}{1+\lambda}\right)_{CO_2}\right) \qquad 6\text{-}27$$

The preceding and the expression in Eq. 6-27 could be considered to provide an analytical basis for applying single-phase gas comparison (such as in a laboratory experiment) to a multiphase gas comparison (such as in a reservoir setting).

6.1.4 Darcy Law

There are several fundamental equations of flow state (EOS) present in the industry for PVT analysis and reservoir flow regime evaluation and characterisation. A significant number of these equations were extensively studied, and a careful appraisal method was used to identify which equations should be applied and at what stage. The most applied equations of flow state were classified into three main groups, those derived from experiments, such as the Darcy (1856) and Poiseuille (1940) EOS; from analytical or pseudo-analytical models, such as the Martin-Hou (MH) and Buckley-Leverett fractional flow for immiscible fluid and Welge EOS; and from numerical models. Other EOS also used by investigators are Fick's, Navier-Stoke's, Euler's, Bernoulli's and Poiseuille's equations. Sezgin and Wall (1998) reported their fluid flow investigation using Navier-Stoke EOS. Shehu (2018) have used Ficks EOS to study hydrocarbon recovery and utilisation technology.

Some of these EOS require investigators to estimate or approximate certain constants and parameters, such as in Martin-Hou (MH) equation (Dong *et al*., 2012). The Darcy equation developed by Henry Darcy in 1856 was adopted in this research because of its straightforwardness and explicit variables that can be directly observed and measured in an experimental setup. Nevertheless, other EOSs, such as Poiseuille EOS, have also been applied at a lower degree of relevance in this study. Darcy (1856) conducted some experiments on flow in porous media aptly described in Figure 6-3 and came

up with the mathematical expression for describing the isothermal flow rate of fluid through porous media as a function of the viscosity of the fluid, permeability tensor and pressure gradient across the media. This is represented in Eq. 6-28. Furthermore, it would be observed that quantities described in chapter two and emphasised by Warner and Holstein (2007) to be critical to gas/oil displacement efficiency such as injection rate and mobility are well represented in Eq. 6-28 (Buryakovsky 2001).
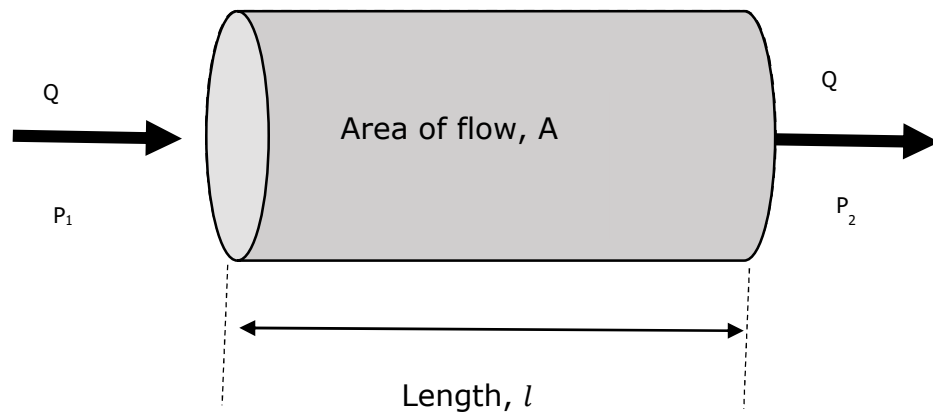
Figure 6-3 Schematic of a linear Darcy Flow through porous media.

$$Q = \frac{-KA}{\mu'}\frac{dP}{dl}$$
6-28

Where:

K = Proportionality constant, also known as the permeability in mD;

A = cross-section area of the core sample in cm^2

μ = Viscosity of flowing fluid in cp;

$\frac{dP}{dl}$ = Pressure drop per unit length in the direction of flow or pressure gradient in atm.cm^{-1};

Q = Volumetric flow rate in cm^3.sec^{-1}.

6.1.5 Modification of Darcy Equation

Authors have suggested and applied various modifications of the original Darcy (1856) equation for single-phase linear flow to analytically solve reservoir problems (Sezgin and Wall 1998, Yu-shu and Karsten 1996, Wang 2010). Buckley and Leverett (1942) modified the Darcy equation by adding a capillary pressure term within the context of conservation of material to characterise the immiscible displacement process. Welge (1952), on the other hand, did away with the capillary terms in the Buckley-Leverett equation and provided a graphical method for estimating oil production based on saturation. Yu-shu and Karsten (1996) modified the equation to include permeability and viscosity terms that allow for a single-phase form of the equation to be valid for a two-phase flow. The Darcy equation has also been modified to develop numerical simulators. Pruess (1991) applied an extension of Darcy's law to develop a numerical simulator, TOUGH2, that describes multiphase fluid flow. Similarly, in this research, the Darcy equation has undergone some essential modifications to account for some reservoir and experimental applicability and engineering principles and assumptions.

6.1.5.1   Modification of Darcy Equation for Radial Flow

This equation represents flow through porous media that is flat sheet configured. However, in this work, a tubular core has been used. Flow is through a radial path. Therefore, Eq. 6-28 has to be modified for radial flow.

For flow through a radially configured media with an internal and external radii r_2 and r_1, respectively, and height h, as shown schematically in Figure 6-4, the Darcy equation would need to be modified.
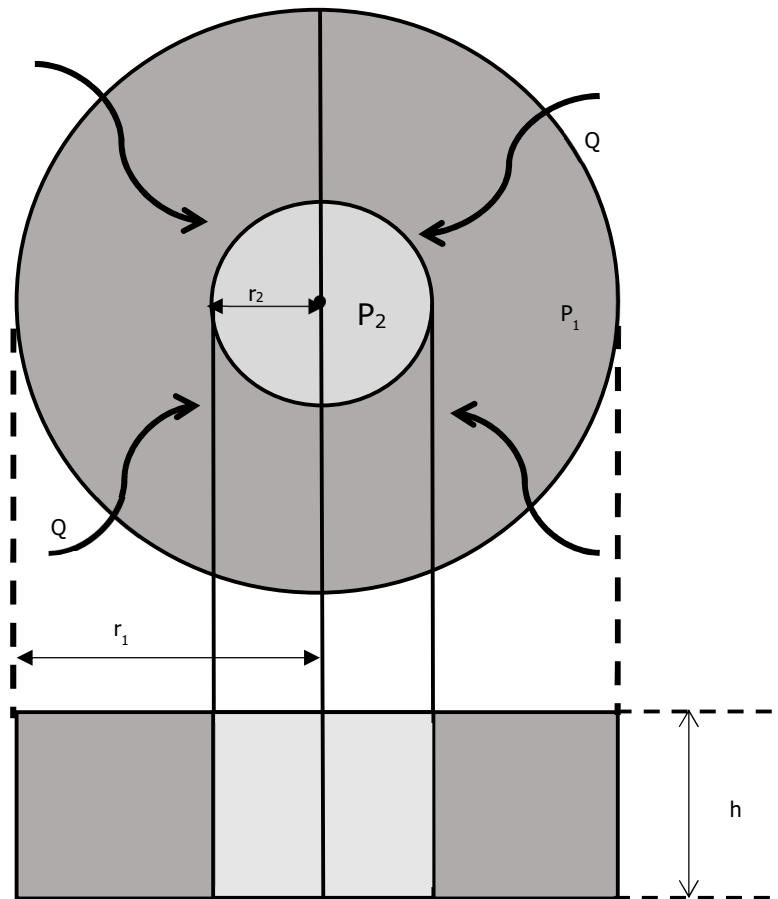
Figure 6-4 Schematic for radial flow showing the flow direction towards to bore.

$$Q = \frac{K.2\pi rh}{\mu'} \frac{dP}{dr}$$

6-29

Notice, the area, A, has become 2πrh to account for the radial configuration. Furthermore, the validity of Eq. 6-29 is based on incompressible fluid, but this study is for gases, which are compressible fluids. Thus, the Darcy equation for compressible fluids needs to be derived from Eq. 6-30.

6.1.5.2 Modification of Darcy Equation for Compressible Fluid

Li and Horne (2001b) and Lui *et al.* (2018) have derived a Darcy equation modification for compressible fluid gas as:

$$Q_g = \frac{K_g A\Delta P}{\mu'_g L} \frac{P_m}{P_{atm}}$$

6-30

Where:

Q_g = *gas* flow rate in cm^3.sec^{-1};

K_g = is the effective gas phase permeability in mD;

μ'_g = viscosity of the gas phase in cp;

P_{atm} = Atmospheric pressure in atm;

P_m = mean pressure in atm;

ΔP = the differential pressure across the core sample in atm;

A = cross-section area of the core sample in cm^2;

L = length of the core sample in cm.

Notice Eq. 6-30 introduced P_m and P_{atm} to the original Darcy equation (Eq. 6-28). This implies that the mobility of a gas is inversely proportional to the mean pressure. Various authors have represented the Darcy equation without considering the temperature. It is important to include temperature due to gas behaviour with respect to temperature variation. Kuuskraa (1982) included a temperature element in his study of gas flow. Although how it was derived was not stated in the study. This study is interested in the potential effects of temperature on the respective mobility of gases used for immiscible gas EOR. Therefore, the Darcy equation was modified to account for the variation between the temperature of the injected gas and the reservoir temperatures. The modification starts with the ideal and combined gas laws that relate both Boyle's law and Charles' law (Slider 1983).

$$PV = znRT \qquad\qquad\qquad 6\text{-}31$$

Where:

P = Pressure (atm).

V = Volume of gas cm^3.

z = is the dimensionless compressibility factor of gas.

n = Numbers of moles (mol).

R = Gas constant (J.mol^{-1}.K^{-1}).

T = Temperature (K).

Rearranging Eq. 6-31 gives:

$$\frac{PV}{zT} = nR = Constant \tag{6-32}$$

It follows that for two sets of pressure, temperature, and volume conditions, the 'nR' term would always be constant. There are different conditions other than standard conditions in which gas activities could be measured or that engineers may be interested in investigating. It is, therefore, proper to bring such measurement to the standard condition of operation. Laboratory and reservoir (res) conditions are some examples of such operating conditions. The following analogy could be drawn based on Eq. 6-32:

$$\left(\frac{PV}{zT}\right)_{res} = \left(\frac{PV}{T}\right)_{std} = Constant \tag{6-33}$$

The subscripts 'res' and 'std' means reservoir and standard conditions, respectively.

With respect to the volumetric rate, it becomes:

$$\frac{PQ}{zT} = \frac{P_{std}Q_{std}}{T_{std}} \tag{6-34}$$

For convenience, the subscript 'res' has been removed from the expression on the left side of Eq. 6-34.

Making Q, the reported volumetric flow rate, the subject of the formula,

$$Q = \frac{zP_{std}Q_{std}}{T_{std}}\frac{T}{P} \tag{6-35}$$

Substituting for Q, in Eq. 6-30 gives:

$$\frac{zP_{std}Q_{std}}{T_{std}}\frac{T}{P} = \frac{K.2\pi rh}{\mu'}\frac{dP}{dr}$$

6-36

Make the volumetric flow rate at the standard condition the subject of the formula,

$$Q_{std} = \frac{K.2\pi rhT_{std}}{z\mu'TP_{std}}\frac{PdP}{dr}$$

6-37

Eq. 6-37 could be rearranged to:

$$Q_{std}\frac{dr}{r} = \frac{K.2\pi hT_{std}P}{z\mu'TP_{std}}dP$$

6-38

Integrating both sides of Eq. 6-39 gives:

$$Q_{std}\int_{r_2}^{r_1}\frac{dr}{r} = \frac{K.2\pi hT_{std}}{z\mu'TP_{std}}\int_{P_2}^{P_1}PdP$$

6-39

Where the boundary conditions are:

r_1 and r_2 = external and internal radii of the flow path, measured in the same direction of pressure growth. This is the reason why the negative sign in the original Darcy equation is taken out.

P_1 and P_2 = injection and exit pressure, respectively.

$$Q_{std}\ln\frac{r_1}{r_2} = \frac{K\pi h\,T_{std}(P_1{}^2 - P_2{}^2)}{z\mu'TP_{std}}$$

6-40

$z\mu'$ could be considered constant in most laboratory pressure conditions in which this experiment falls. This claim is based on some published work by (Zhuang 2020) and John (2007). According to Ahmed and Meehan (2012) and John (2007), series of experimental results indicate that $z\mu'$ is constant for pressure under 2000psi (136atm). This study was operated under 4.00atm pressure, and it was a comparative study; therefore, Eq. 6-40 could further be reduced and rearranged to give:

$$Q_{std} = \frac{K\,\pi h\,T_{std}}{\mu\,TP_{std}}\frac{(P_1{}^2 - P_2{}^2)}{\ln\frac{r_1}{r_2}}$$

6-41

Where:

$\mu = z\mu'$ is a measure of the apparent viscosity of the EOR gases.

Eq. 6-41 is similar to the one in Kuuskraa (1982). The volumetric flow meter used in the study is calibrated by the manufacturer at conditions of P_{std} and T_{std} at 1 and 273K, respectively. Applying these values to Eq. 6-41 yields:

$$Q_{std} = 858 \frac{K\,h}{\mu\,T} \cdot \frac{(P_1{}^2 - P_2{}^2)}{\ln\frac{r_1}{r_2}}$$

6-42

In Eq. 6-42, the following qualification can be made thus:

$\frac{(P_1{}^2 - P_2{}^2)}{\ln\frac{r_1}{r_2}}$ = is the radial pressure gradient.

$\frac{K}{\mu}$ = is mobility.

$\frac{Q_{std}}{h}$ = is a representation of the Darcy velocity.

T = is the temperature of the fluid at the exit that is acquired by the fluid as it permeates through the heated core sample.

6.1.5.3 *Modification of Darcy Equation for Thermal Transfer*

Based on the general principles of continuum mechanics (Andri *et al*., 2017, Berker 2002, Bergstrom 2015, Chandrasekharaiah and Debnath 2014, Coratekin, *et al*., 1999, Malkin 2012, Risby and Hamouda 2011, Pilvin 2019, and Sadd 2018), an analytical process was applied to account for the potential heat transfer that occurs between the core samples and injected gases. For an isobaric flow, there exists an analytical relationship between T, the specific heat of the gas at constant pressure, Cp (in J/g.K) and heat energy supplied H (in J) by the system (or reservoir) to a unit mass, m, of the invading gas. The specific heat capacity at constant pressure, which is the heat energy, in J, required to raise 1g of gas by 1K, is usually represented as (Jin *et al.,* 2021):

$$C_p = \frac{H}{m\Delta T} \qquad\qquad\qquad 6\text{-}43$$

Where:

ΔT = difference between the outlet temperature T_2 and inlet temperature T_1 (T_2 - T_1).

In terms of ΔT, Eq. 6-43 can be rewritten as:

$$\Delta T = (T_2 - T_1) = \frac{H}{mC_p} \qquad\qquad 6\text{-}44$$

In a comparative study to investigate energy transfer between gases and an energy source (porous media or reservoirs), the First and Second thermodynamics laws lend themselves to understanding how temperature could be described. T_1 could be considered a convenient reference temperature and a constant for all gases regardless of what reference value the researcher decides to assign to T_1. For instance, from the source (gas cylinder), each gas can be injected into the reservoir at a standard (273K) or normal (293K) temperature. Therefore, without loss of generalisation, T_1 can be eliminated as a constant and Eq. 6-44 can be reduced to Eq. 6-45.

$$T_2 = \frac{H}{mC_p} - T_1 = \frac{H}{mC_p} \qquad\qquad 6\text{-}45$$

Furthermore, the gases flowing through a reservoir or experimental core would typically experience the same reservoir in-situ heat supply or core heat as regulated by the investigator. Therefore, for a comparative study of gas flow through a core at a controlled heat supply, the H is a constant. Furthermore, if we assume the experiment is conducted with one mole of the respective gases. The denominator m (g) can be dimensionally represented by the molar weight MW (g/mol) of the respective gases. It, therefore, follows that Eq. 6-45 can be represented thuvs:

$$T_2 = \frac{1}{MW C_p} \qquad\qquad\qquad 6\text{-}46$$

T$_2$ in Eq. 6-46 is equivalent to T in Eq. 6-42 for one molar flowrate. Therefore, substituting T$_2$ in Eq. 6-42 yields:

$$Q_{std} = 858\frac{K}{\mu}\frac{hMW\boldsymbol{C_p}(P_1{}^2 - P_2{}^2)}{\ln\frac{r_1}{r_2}}$$ 6-47

For a comparative study that includes temperature variation, Eq. 6-47 should be considered more robust and useful for evaluating flows in reservoir or laboratory cores, especially where temperature data cannot be collected and instrumentation cannot accurately measure outlet gas temperature due to challenges that include unaccounted heat loss in flow lines. The general Darcy equation assumes isothermal flow. However, Eq. 6-47 is an analytical equation that provides qualitative and quantitative solutions for capturing the full extent of the PVT effect on gas properties across a spectrum of pressure change and temperature change. Like the thermal conductivity of gases, $\boldsymbol{C_p}$ assumes different values for gases. The typical values for EOR gases CH$_4$ and CO$_2$ are 2220 and 834 J kg^{-1}K^{-1}, respectively. It, therefore, means that $\boldsymbol{C_p}$ would make a suitable parameter for classifying EOR gases. Furthermore, if the gases are to be compared using media with a similar configuration, this implies that the parameters $\ln\frac{r_1}{r_2}$ and h are constants to all gases. Therefore, Eq. 6-47 can be further reduced to an apparent equation of:

$$Q_{std-apparent} = \frac{K}{\mu}MW\boldsymbol{C_p}(P_1{}^2 - P_2{}^2)$$ 6-48

The respective gas intrinsic mobility is the object of interest; it becomes easy to compute, as molar mass MW and $\boldsymbol{C_p}$ can be easily read off from gas property chart, such as L'Air Liquide (1976).

It should, however, be noted that this equation is only valid for comparative PVT analysis for gas. It is not a true value equation due to the equation reduction that eliminates inlet temperature and heat supplied.

A true value equation would combine Eq. 6-42 and 6-44 to give:

$$Q_{std} = 858 \frac{K}{\mu} \frac{h\left(P_1{}^2 - P_2{}^2\right)}{\ln\frac{r_1}{r_2}} \frac{MW\,C_p}{(\mathrm{H} + MW\,C_p T_1)}$$

$$\text{6-49}$$

6.2 Estimation of Gas Intrinsic Mobility

This research observed that gas intrinsic mobility could be estimated by using graphical and computational methods

6.2.1.1   Graphical Method for Estimating Intrinsic Mobility

For graphical estimation, Eq. 6-47 could be rearranged in 2 ways:

$$\left[\frac{Q_{std}}{85\,8hMW C_p}\right]_i = \left[\frac{K}{\mu}\left(\frac{(P_1{}^2 - P_2{}^2)}{\ln\frac{r_1}{r_2}}\right)\right]_i$$

$$\text{6-50}$$

Whereby for a gas i, the graph of $\frac{(P_1{}^2 - P_2{}^2)}{\ln\frac{r_1}{r_2}}$ against $\frac{Q_{std}MW C_p}{85\,8h}$ would give a plot with slope, $\frac{K}{\mu}$. This is considered to represent the weighed mean intrinsic mobility of the gas, $\dot{\mathrm{M}}_i$ at an isotherm, T. It is a weighed mean value because it would be observed from the curve's shape that it comprises more than one flow regime.

Similarly, another rearrangement of Eq. 6-47 is:

$$\frac{\mu}{K}\left(\frac{Q_{std}\ln\frac{r_1}{r_2}}{858hMW C_p}\right) + P_2{}^2 = P_1{}^2$$

$$\text{6-51}$$

In Eq. 6-51, a plot of $P_1{}^2$ against $\left(\frac{Q_{std}\ln\frac{r_1}{r_2}}{85\,8hMW C_p}\right)$ would give a straight line with a slope that is the inverse of the weighed mean intrinsic mobility of the gas, $\frac{1}{\dot{\mathrm{M}}_i}$ at T isotherm, with an intercept $P_2{}^2$.

6.2.1.2   *Computational Estimation of Intrinsic Mobility*

This method is straightforward when all the required variables are measurable and available. For a given gas, i, Eq. 6-47 could be rearranged with $\frac{K}{\mu}$ as the subject formula to give.

$$M_i = \left(\frac{K}{\mu}\right)_i = \left(\frac{Q_{std}}{85\ \&MW C_p}\frac{\ln\frac{r_1}{r_2}}{(P_1{}^2 - P_2{}^2)}\right)_i \qquad\qquad 6\text{-}52$$

For this experiment, the flowmeter supplies readings for Q_{std}; Thermometer supplied T; Pressure gauge and flowmeter supplied P$_1$, P$_2$; meter rule and calliper supplied h, r$_1$ and r$_2$.

The significant difference between the graphical and computed estimates of intrinsic mobilities is that the computed method can generate instantaneous intrinsic mobility outright, while the graphical method generates a weighed mean intrinsic mobility for the full range of pressure gradient. The graphical method's benefit in this work is that it gives a better view of how the mobility regime is developed along with the pressure, temperature gradient and gas flow rate.

6.2.2 The Rationale for the Operational Range of Parameters

The investigated parameters in the experiments have been inspired by the outcome from phase one of this research and PVT understanding in the literature. However, in designing the experiments, the following underlying motives informed the parameter range.

6.2.2.1   *Operating Temperature:*

According to Charles law, the gas volume is directly proportional to temperature for a fixed mass of gas. Therefore, a temperature contrast between surface gas (as supplied) and reservoir temperature could significantly affect gas volumetric flow behaviour, mobility, momentum, and sensitivities. The expected change in volume is a factor of 273^{-1}K. It is relatively small compared to what is obtainable in Boyles law on pressure.

However, on a reservoir scale, this change could be significant. Therefore, it is important to investigate how the mobility of the respective EOR gases respond to temperature contrast. The temperature range for this experiment has been selected to fit global reservoir reality as reported in the collated database of EOR reservoir and journals. The Zhang, Lu and Li (2019) classification of the Bohai Bay basin, China, indicates a temperature of 402K to 473K. The global EOR survey of the Oil and Gas Journal (2014) revealed an EOR reservoir temperature spectrum of 290K to 416K. Consequently, in this experiment, a temperature spectrum covering the lower and upper temperature limits was used: 293K to 673K.

6.2.2.2   Operating Pressure:

The pressure is a fundamental property of gas in many processes across the oil and gas industry, physical and chemical processing industries. In porous flow, pressure is required to overcome surface energy, friction, and it also couples with permeability to determine flow or flux (Robinson *et al*., 2004). It is usually difficult to set up laboratory experiments at reservoir pressure conditions. However, a reasonable extrapolation can be made from a well-defined laboratory pressure range. In this experiment, the pressure range used is 0.20atm – 3.00atm gauge pressure. It is expected that the different flow behaviour of the gases would have sufficiently revealed themselves within this range to allow a sound extrapolation of higher-pressure gas behaviour below critical pressure (Al-Dahhan *et al., 1*997). The assumption is also based on the hyperbolic nature of the Pressure-Volume curve, which suggests a steady dampening of volume as pressure increases. On the basis that, unlike in miscible EOR, immiscible gas EOR does not need to get to the critical point. Consequently, the laboratory pressure range would have utility for immiscible gas EOR description.

6.2.2.3   Reservoir Pore Size Selection:

The established pore characterisations in the literature review are macropores (d > 50nm), mesopores (d = 2–50nm) and micropores (d < 2nm) (Merlet, *et al.,* 2020, Rouquerol *et al., 1*994, Zhao *et al*., 2015). The core sample pore

sizes have been purposefully selected to fit the global oil reservoir's pore size spectrum. Although the database did not have sufficient information with respect to the pore size of EOR reservoirs, the researcher resorted to journals. Dou *et al.* (2018), Li *et al.* (2020), Wang *et al*. 2020b*,* and Zhang, Lu and Li (2019) studied some reservoirs in the Bohai Bay and Ordos basin, China. They characterised the reservoirs by pore size diameter ranging from micropore (<100nm), mesopores (100-1000nm), and macropores (>1000nm). Their results are similar to Nabawy *et al.* (2009) classification of sandstone in some Egyptian reservoirs and Zhao *et al.* (2015) and Ghanisadeh *et al*. (2015) classifications characteristics of Montney and Bakken reservoirs. Consequently, the mean pore size of the core samples used in this experiment ranges from 15nm to 6000nm. The pore sizes are as determined by the manufacturer (see Table 6-1).

6.2.2.4   Porosity

Similarly, porosity was selected to fit reservoir realities. Some core samples were selected so that two cores might have the same pore size but different porosity. The porosity range in the experiments was informed based on the porosity distribution found in the EOR database in phase one and journals (Satter and Iqbal 2016) as 3-20%. Tiab and Donaldson (2016) classified reservoir quality by porosity as 0–5%—Negligible, 5–10%—Poor, 10–15%—Fair, 15–20%—Good, >20%-Very good.

After a rigorous examination of methods, the core samples' porosities were determined using bulk specific density and particle specific density relation to porosity as suggested in Bess (2019) and Danielson and Sutherland (1986) as represented in Eq. 6-53.

$$Porosity = 1 - \left(\frac{Bulk\ Density}{Particle\ Density}\right) = 1 - \left(\frac{Specific\ Particle\ Density}{Specific\ Bulk\ Density}\right) \qquad \text{6-53}$$

The bulk density was derived from a laboratory measurement of the sample's dimensions. The particulate density of the samples, as provided by the manufacturer, was used. The manufacturer compositional profile and density were consistent with the results from the Energy-dispersive X-ray

spectroscopy (EDS) conducted on the core samples. The comparative porosity results were further validated by the isothermal volumetric rate of He in the respective core samples and the results of porosity determination using the Archimedes principle.

6.2.2.5   *Injected Fluid Thermodynamic Properties utilised:*

The physical properties of gas include critical constants, vapour pressures, viscosities, diffusion coefficients, and surface tension. The thermodynamic properties include densities, enthalpies, entropies, fugacity coefficients, and heat capacities. Since this study involves PVT analysis of EOR gases, it was essential to identify and isolate properties and parameters relevant to the PVT and EOR process for detailed investigation. A rigorous review of journals and texts enabled the selection of key properties. For example, the density of a displacing fluid can either be varied via pressure or by adding a gas with a different molecular weight (Al-Dahhan *et al., 1*997). According to Avogadro (1811), at standard temperature and pressure (STP), 1 mole of all gases occupy 2.4L. This implies that at STP, the densities and specific densities of gases are functions of their molar weights. This knowledge was stretched in estimating the measure of momentum of EOR gases during momentum and permeability contrast analyses. It was further applied to speculate a hypothetical surface tension of the oil-gas systems using the L'Air Liquide (1976), Macleod-Sudgen, and Weinaug and Katz (1943) equations. Al-Dahhan *et al.* (1997), Reid *et al*. (1987), and Sebastian *et al*. (1981) have experimentally investigated the relationship between pressure and some gas properties for Hydrogen at conditions up to 170.00atm and at 410K. Based on their work, some fluid properties such as the heat capacity at constant pressure, mean free path and the kinetic diameter were adopted to study the correlation between gas flow and these properties in porous media.

6.2.3 Introduction to Experiments with the Multichannel, Multi-Layer

6.2.3.1   Materials Used

The key materials used in the experiment include:

I. **Core Sample:** 5 structured tubular ceramic porous core samples were used. The cores sampled are made of similar materials but with different geometrical and structural characteristics, such as pore size, thickness and surface area. To maintain consistency in comparing the gases, the study ensured that all core samples were sourced from the same manufacturer. This guaranteed the material integrity of all the samples used in the research. It was important for the core to bear some similar characteristics. The core samples are assumed to have evenly distributed pore sizes. Yu-shu and Karsten (1996) stated that it is acceptable to study viscosity models, hence flow systems, using experimental data from a capillary analogue of a porous medium. This justifies the use of porous analogues, such as ceramic membranes, filter paper chromatography, packed bed and silicon coating. Similar ceramic core samples have been successfully used for reservoir and gas study in porous media by authors such as Kajama et al. (2016), Mohammed et al. (2016) and Shehu (2018). Table 6-1 highlights the key characteristics of the core samples used in this study.

II. **Samples' Structural Suitability:** The manufacturing specification for the samples used in the experiment is such that the membrane (restrictive) layers are on the outside of the sample and the coarse support layers are on the inside. The direction of flow or pressure gradient is from the outside to the inside. The structural gradient formed by the layers of the membrane and coarse support is analogical to different reservoir scenarios. For instance, typical reservoirs are not structurally continuous (Apostolos *et al.* 2016, Abdullah 2018, and Wang *et al*. 2020b). The different layers of sedimentation make it possible to have different layers with structural uniqueness, where some layered channels are coarser than adjacent layers (Bonnell and Hurich 2008 and Wang *et al*. 2020b), This is similar to what is obtainable in the core

samples used in the experiments. Furthermore, the relatively restrictive section of the layers is often responsible for the control of fluid dynamics through the reservoir, such as experienced in the shale gas and fracking system (Apostolos *et al.* 2016 and Wang *et al*. 2020b). Consequently, for each media sample, it is expected that the flow dynamics is significantly characterised by the restrictive layer on the outer surface.

III.   **Samples' Compositional Suitability**: Gas transport mechanisms in reservoir pores include viscous flow, slip flow, Knudsen diffusion and surface diffusion. Reservoir rocks are usually composed of inorganic and organic materials (Brooks 1979, Hou *et al.*, 2020). The organic nature of the reservoir pore may interfere with the flow dynamic to varying degrees due to the surface diffusion transport mechanism. However, the graphical presentations of gas flow dynamic in Hou *et al.* (2020), Song *et al*. (2018a, 2018b), and Wang *et al*. (2016) suggest that the adsorptive and the consequent surface diffusion mechanism in organic media is only dominant in nanopores below 5nm. Therefore, implying that the effect of the pore's organic nature is not dominant in this study, because conventional reservoirs pore sizes are typically above 5nm (Dou *et al.* 2018, Li *et al.*, 2020, Wang *et al*. 2020b*,* and Zhang, Lu and Li 2019). It is further understood that the most critical parameters for fluid transport, reservoir description and quality are structural, such as pore size, porosity and permeability (Alfarge, Wei, and Bai 2017, Breit 1992, Brooks 1979, and Slatt and Galloway 1992). Consequently, without loss of generalisation, inorganic multilayer channels samples that mimic the heterogenous structural realities of reservoirs were appropriately used in this study.

Table 6-1 Properties of Core used for Gas Mobility Experiment

S/N		Core 1	Core 2	Core 3	Core 4	Core 5
	Code	S15NM	B15NM	S200NM	S6000NM	B6000NM
1.	Manufacturer/Supplier	Ceramiques Techniques et Industrielles (CTI SA), France				
2.	Main material composition	TiO_2 Al_2O_3				
3.	Pore size (nm)	15	15	200	6000	6000
4.	Weight (g)	49.30	494.80	53.20	47.90	274.10
5.	Length (cm)	36.50	65.10	36.60	36.90	37.10
6.	Effective Permeate Length (cm)	33.80	60.20	32.80	32.00	32.00
7.	External Diameter (cm)	1.00	2.56	1.08	1.02	2.57
8.	Internal Diameter (cm)	0.71	2.06	0.77	0.75	2.09
9.	Core Thickness (cm)	0.15	0.25	0.16	0.14	0.24
10.	Permeate Area (2)	105.99	484.22	111.30	102.55	258.40

Figure 6-5 to Figure 6-10 show the different core samples used in the experiment. The Energy Dispersive Spectroscopy (EDS) analysis can be found in Figure B 1-4, APPENDIX B.

Figure 6-5. Areal and Cross-Sectional view of 6000nm and 2.57cm outer diameter core sample.

Figure 6-6 Areal and Cross-Sectional view of 6000nm and 1.02cm outer diameter core sample.

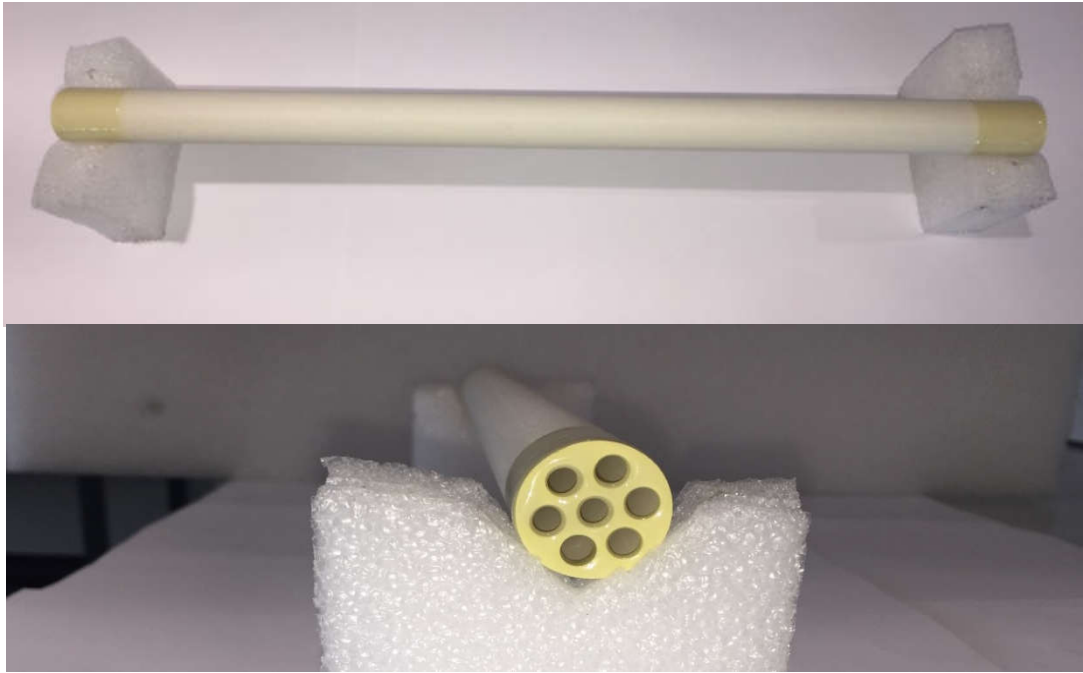*Figure 6-7 Areal view of 200nm and 1.08cm outer diameter core sample.*

Figure 6-8Areal and Cross-Sectional view of 15nm and 2.56cm outer diameter core sample.
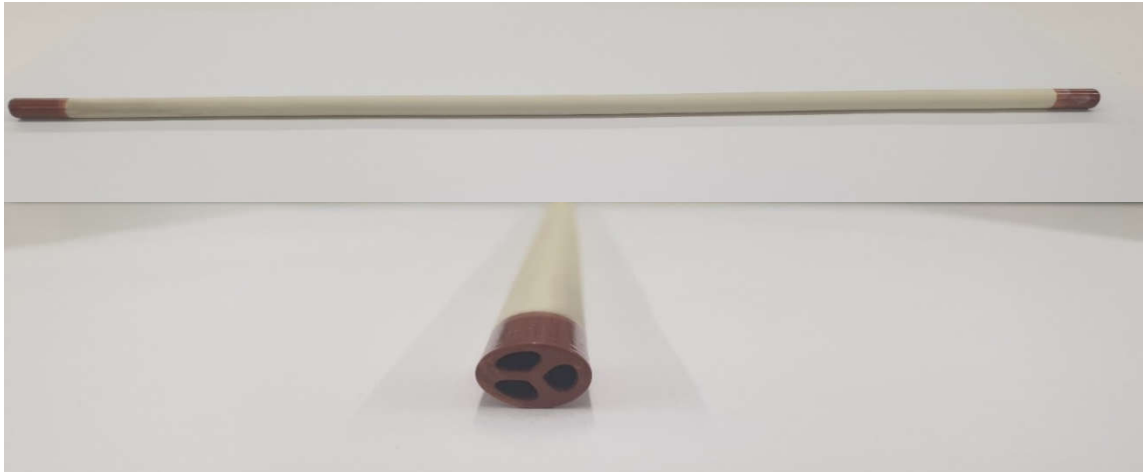
Figure 6-9 Areal and Cross-Sectional view of 15nm and 1.00cm outer diameter core sample.
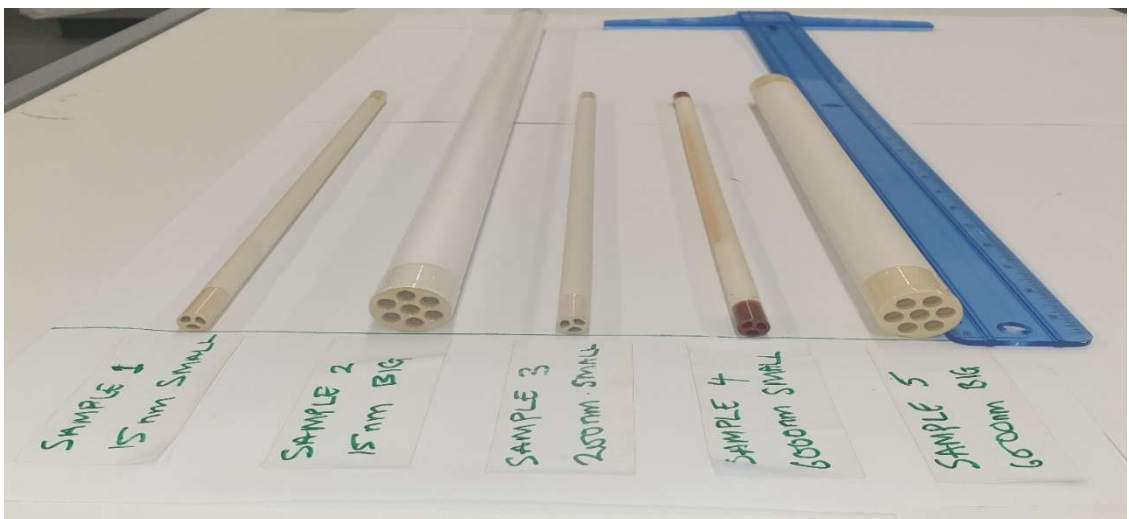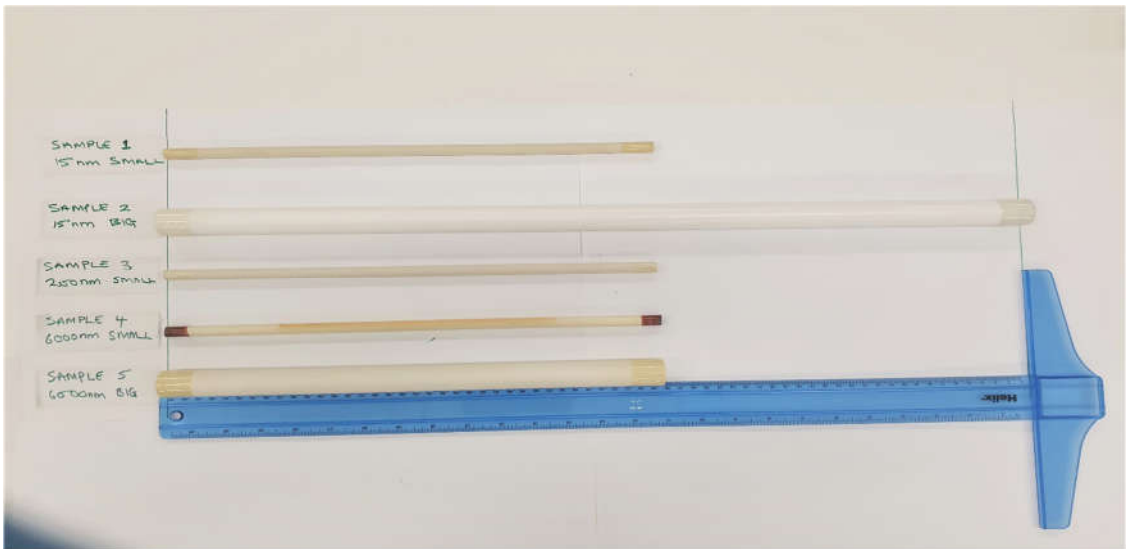

Figure 6-10 Comparing Areal and Cross-Sectional views of the five sample sizes.

IV.   Core Sample Precautions:

In handling the core samples, certain precaution worthy of note was taken during the preparation of the material for the experiments. The core should only be held by their laminated ends. Touching of the permeate surface area was avoided to prevent contamination of sample nanopores. When fixing the core samples into the core holder, sample damage was prevented by ensuring the samples do not contact the stainless-steel core holder's inner walls.

V.   Experimented Gases:

The experiments have been carried out using eight gases and gas mixtures. These gases were selected and grouped based on three considerations.

The first consideration is that they comprise three pure gases and three gas mixtures injected to displace oil in immiscible EOR projects. From previous studies (Gbadamosi 2018) and analysis of data gathered from an EOR global survey conducted in this research, it has been established that these three gases and gas mixtures are the commonly used gases for the immiscible EOR process. Consequently, these gases and gas mixture's effectiveness in EOR application is the primary focus for this research aim and objectives and are therefore categorised as Group1 gases in this research work. See Where d_i, is the kinetic diameter of the component gases. When Eq. 55 is applied to estimate Air kinetic diameter, the equation resolves to

$$d = \frac{1}{2}\sum_{i}^{N=2} d_i = \frac{1}{2}\left(d_{N_2} + d_{O_2}\right) = \frac{1}{2}(364 + 346) = 355 \qquad \text{6-56}$$

Table 6-2 for a list of gases and their key properties that went into the experimental analyses.

The second consideration for selecting the gases is that they comprise two gas mixtures that are potentially obtainable in a reservoir due to injected gas coming in contact with *in-situ* reservoir gases during immiscible EOR implementation. The gas mixture could also be a deliberate injection strategy to improve the density of the injectant. In multiphase flow, gas density can be varied by pressure or by adding gas with a different molecular weight (Al-Dahhan *et al., 1*997). These mixtures' contact with trapped oil is expected to generate a flow dynamism that could significantly affect recovery performance. Whitson (1993) indicated the presence of in-situ CO_2 and N_2 in different samples of reservoir oil. This implies that the presence of *in-situ* reservoir gases can impact the performance of injected gases. Furthermore, in engineering fluid dynamics, viscosity, a determining factor in mobility regime, is not a material constant; instead, it is a material property that depends on fluid mixture composition (Towler 2007). Therefore, consideration of gas mixtures in immiscible EOR is unavoidably important.

The third consideration is that two non-EOR gases (Helium and Argon) were included in the experiment. In Where di, is the kinetic diameter of the component gases. When Eq. 55 is applied to estimate Air kinetic diameter, the equation resolves to

$$d = \frac{1}{2} \sum_{i}^{N=2} d_i = \frac{1}{2}\left(d_{N_2} + d_{O_2}\right) = \frac{1}{2}(364 + 346) = 355 \qquad \text{6-56}$$

Table 6-2, although it is only gases (S/N) 2,3,4,5,6 and 8 that could be implemented in gas EOR practice, the reason for the inclusion of gas 1 and 7 is to provide an expanded spectrum for the investigation of gas physical and thermodynamic properties such as molecular weight and thermal diffusion in the mobility regime development. Furthermore, 10%Carbon Dioxide/Methane and 20%Nitrogen/Methane mixtures were included as a means of studying the varying molecular weight of gas mixtures encountered in EOR practice. For the gas mixtures, a notional average molecular weight was obtained by combining Dalton's and Amagat's laws of partial pressure and volume of gas mixtures, respectively with the ideal gas law (Bejan 2016, Hilgeman, Wilson and Bertrand 2007, Lehmann, Fuentes-Arderiu, and Bertello 1996, Smith and Missen 2005, Weberg., Silberberg, and Weberg 2009). These laws enable the estimation of notional average molecular weight, M, of a gas mixture with N number of gases, with known mole fractions, n_i and molecular weight, M_i. of the respective component gas. This has been reduced in (Mills 1993, Valougeorgis, Vargas, and Naris, 2016, Sharipov 2017 and Wei 2021) to:

$$M = \sum_{i}^{N} n_i M_i \qquad\qquad 6\text{-}54$$

The notional kinetic diameter, d (in pm), of a binary gas mixture is the arithmetic sum of the respective radii, r_i of the component gases as suggested in (Anon 2021, Kandlikar *et al.*, 2005, Mills1993, and Tec 2019).

$$d = \sum_{i}^{N=2} r_i = \frac{1}{2} \sum_{i}^{N=2} d_i \sum_{i}^{N=2} d_i \qquad\qquad 6\text{-}55$$

Where d_i, is the kinetic diameter of the component gases. When Eq. 55 is applied to estimate Air kinetic diameter, the equation resolves to

$$d = \frac{1}{2} \sum_{i}^{N=2} d_i = \frac{1}{2}\left(d_{N_2} + d_{O_2}\right) = \frac{1}{2}(364 + 346) = 355 \qquad\qquad 6\text{-}56$$

Table 6-2 Show some physical and thermodynamic properties (molecular weight, kinetic diameter and reactivity) of the EOR gases evaluated (Baker 2012, Jin et al., 2019, and Mehio et al., 2014).

S/N	Gas	Chemical Formula	Gas Molar Weight, $g.mol^{-1}$	Kinetic Diameter, pm	Specific Heat Capacity at Constant Pressure $J.kg^{-1}K^{-1}$	Reactivity
1.	Helium	He	4	260	5240	Non-Reactive
2.	Methane	CH_4	16	380	2220	Non-Reactive
3.	10%Carbon Dioxide/ Methane	$10\%CO_2/$ CH_4	18.8	355	2050	Non-Reactive
4.	20%Nitrogen/ Methane	$20\%N_2/$ CH_4	25.6	378	1984	Non-Reactive
5.	Nitrogen	N_2	28	364	1040	Non-Reactive
6.	Air	$22\%O_2/N_2$	29	355	993	Reactive
7.	Argon	Ar	40	340	524	Non-Reactive
8.	Carbon Dioxide	CO_2	44	330	834	Non-Reactive

6.2.3.2   Equipment Used

The following items of equipment as pictured in Figure 6-12 to Figure 6-20 were made available for this experiment. Figure 6-21 is a photo shot of some of the connected equipment.

I.   Core Holder
II.   Digital Flowmeter
III.   Pressure gauge
IV.   Temperature indicator
V.   Thermocouple
VI.   Heating jacket
VII.   Gas cylinder
VIII.   Fume cupboard
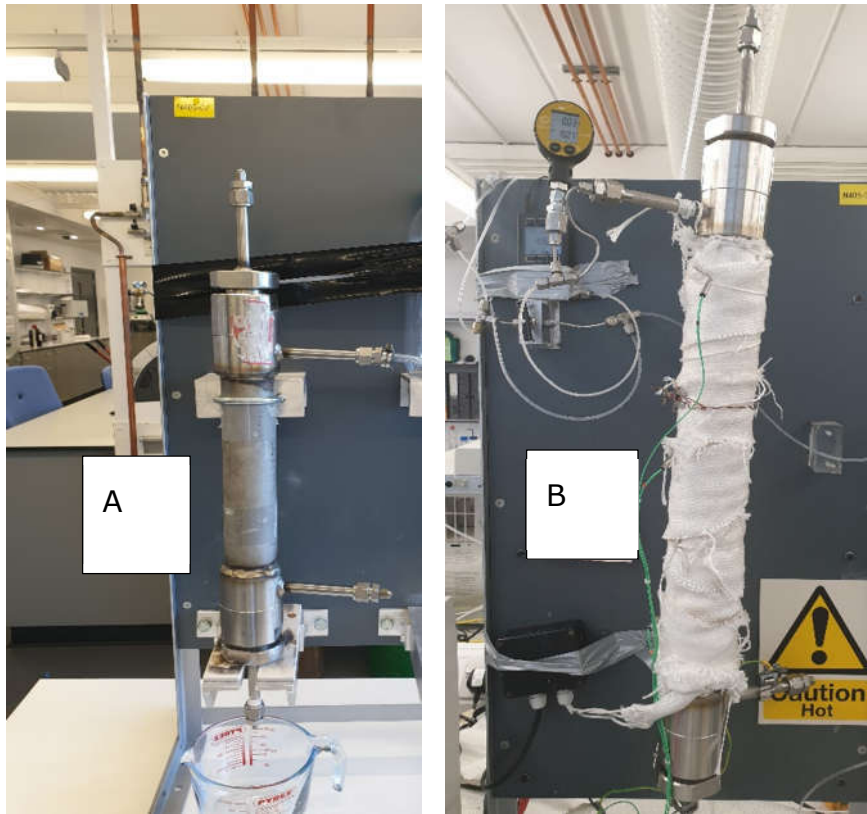
Figure 6-11 Show the core holder (A) and Core holder wrapped with heating tape and fibre insulator to form a heating jacket with attached thermocouples (B).

Figure 6-12 Keller Pressure gauge for controlling and monitory of pressure flow in the core.

Figure 6-13 Cole-Parmer flowmeter for taking flow rate at steady state (x2).

Figure 6-14 3 sizes of granite seal to seal off the core and core holder from gas leaks.

Figure 6-15 Gas cylinder for storing EOR gases at 250Bar ordered from BOC, UK.

Figure 6-16 Fume cupboard for exhausting gas.

Figure 6-17 Barnstead Electrothermal Heat regulator the heat generated by the heating element wrapped around the core holder.
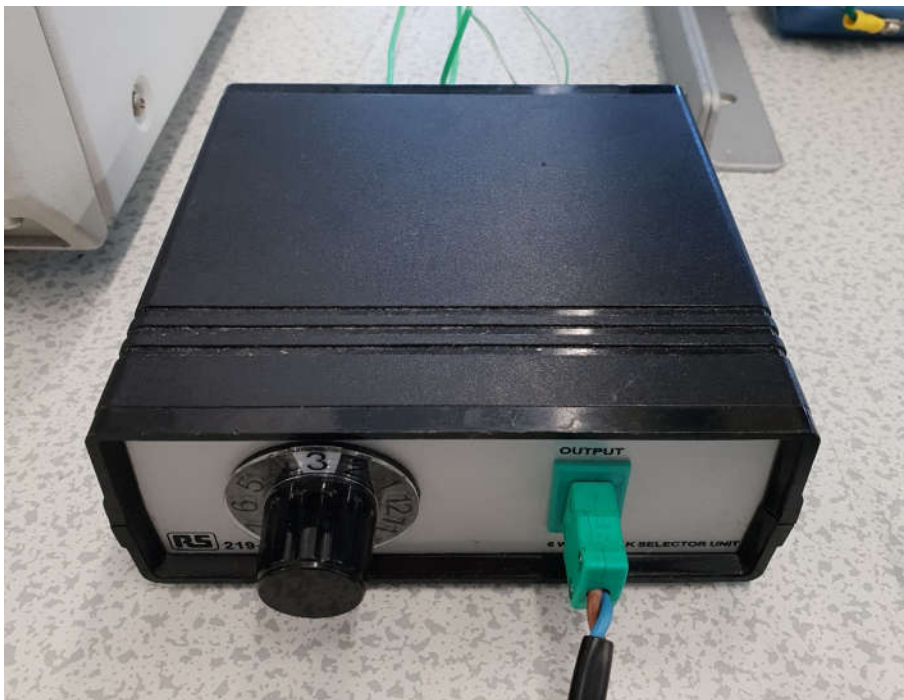
Figure 6-18 A multichannel temperature transducer connected to three thermocouples probes buried in the heating jacket. The transducer is also connected to the Digitron thermometer.

Figure 6-19 Digitron digital thermometer for monitoring and estimating the core temperature.

Figure 6-20 Satorious electronic scale to measure the weight of the core samples.
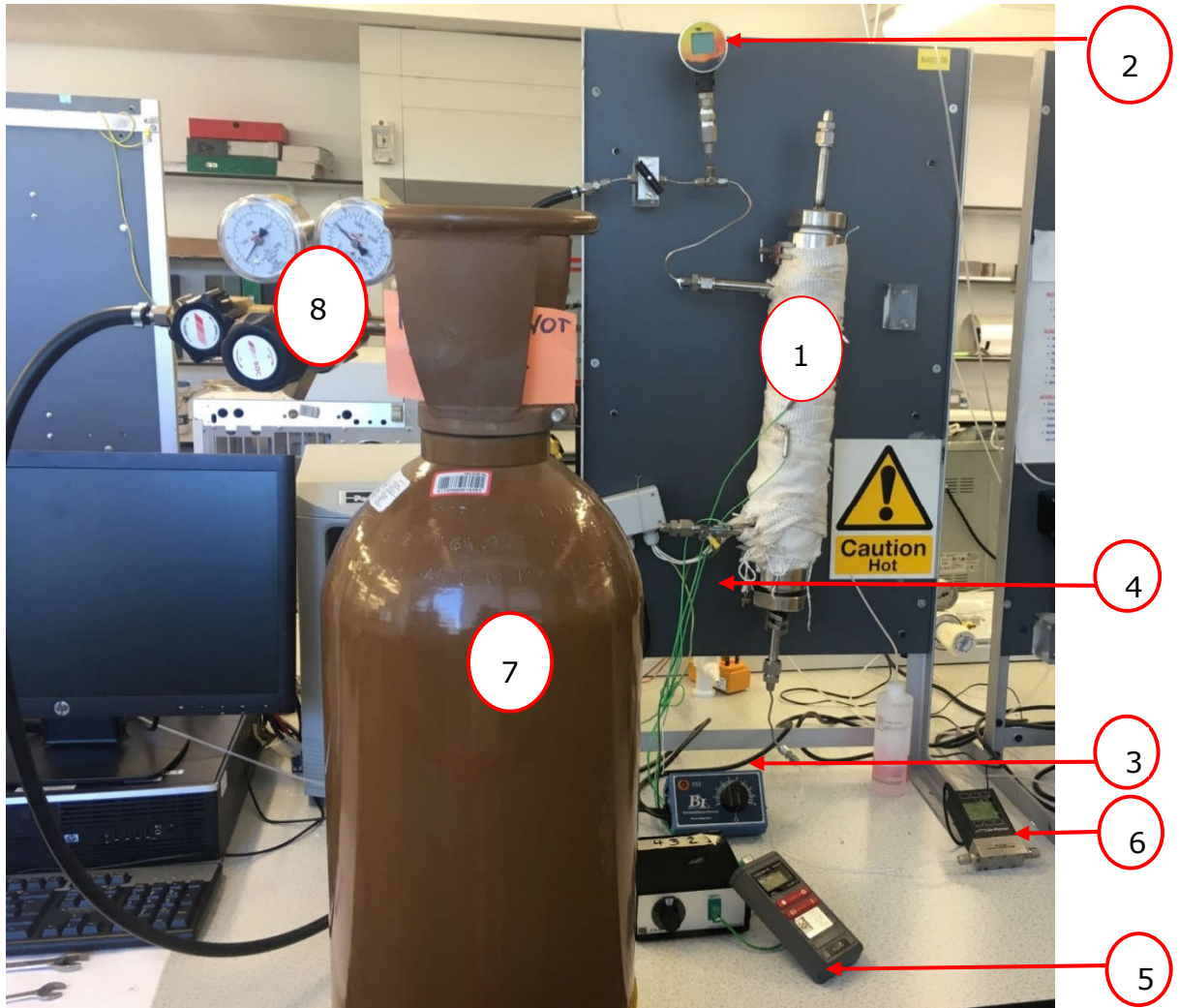
Figure 6-21 Photo shot of experiment in real-time, showing equipment setup: core holder covered in heating tape (1), pressure gauge (2), heat regulator (3), thermocouple (4), temperature indicator (5), volumetric flowmeter (6), gas cylinder (7) and gas

6.2.3.3   Experimental Conditions:

I.   The experiment was conducted under a steady-state condition as suggested and described by Morton-Thompson and Woods (1993)

II.   Gas injection pressure range from 0.20-3.00bar (gauge) at 0.40bar intervals.

III.   The temperature was at intervals 20°C, 50°C, 100°C, 150°C and 400°C, respectively. The phase one temperature classifications informed the temperature distribution in the experiments. Low-temperature is <300C and

High-Temperature >300C in the studies of Gui *et al. (*2010) and Jia *et al.* (2012).

IV.   All units were subsequently converted to be consistent with millidarcy unit, mD, as follows:

- i.   Pressure: atm
- ii.   Temperature: K
- iii.   Length, Height, radius: cm
- iv.   Viscosity: cp

6.2.3.4   *Experimental Setup*

The core samples and core holders were inspected for damage, wear and leak. The core was then placed inside the core holder through one end of the core holder. Once the core was confirmed adequately seated on the seals on both sides of the core holder chamber, the core holder caps were then securely screwed in place on both ends of the core holder. This process was carefully done to prevent any breakage or fracture in the core, as any crack or fracture would affect the experiment's integrity due to the superfluous permeability that would result in the fractured zone. It was then wrapped with the heating jacket. The core holder setup was attached to a core holder rig. Steel clips were used to hold both ends of the core holder in place. Three thermocouple probes were then buried into the heating jacket to measure the core holder system's operating temperature. The purpose of these probes is to enable the researcher to regulate and take various temperature readings of the core holder setup.

A pressure regulator and pressure gauge were connected between the gas supply (gas cylinder with an appropriate gas regulator) and the core holder's gas inlet. This was used to take pressure readings for gas being injected into the core sample. The lower end exit of the core holder (Permeate) was connected to a digital flowmeter to measure the rate by which the respective gases permeate the core at various temperatures and pressure. The gas exiting from the gas flowmeter was then exhausted at atmospheric pressure

into a fume cupboard. Figure 6-22 is a schematic of the experimental arrangement.
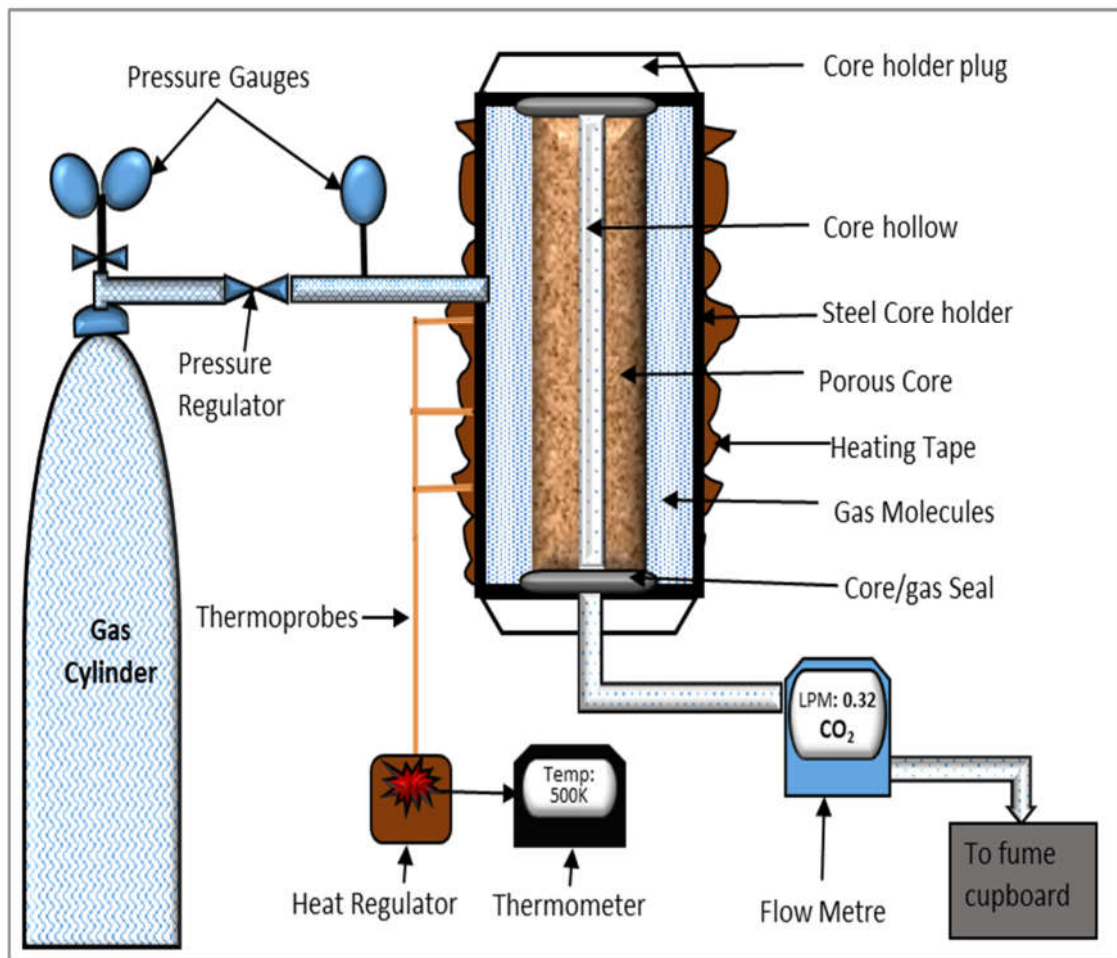
Figure 6-22 A Schematic of Experimental set up for Gas Mobility Investigation

6.2.4 Experimental Procedure

I.   The heat regulator was used to heat the core holder above the desired temperature, usually by 100K, then the core holder system was allowed to cool down to the desired temperature. The aim was to allow for thermal stability to be achieved between the core holder and the core sample. It was observed that when the core holder was initially heated, the temperature drop was rapid. However, as the system approach thermal stability, the temperature drops significantly reduced. It is assumed that at that point, the core holder and core share a similar temperature. Subsequently, the heat

regulator is monitored and adjusted to maintain ±5K of the desired temperature or isotherm. Step I was not required for the first isotherm, being at room temperature, which is approximately 293K.

II.   The desired gas from a gas cylinder or manifold was supplied into the core holder setup through a pressure gauge. The pressure gauge was then used to regulate and monitor the desired pressure. Once the desired pressure is achieved (with an error of ±0.01atm), the system is allowed to operate long enough for the flowmeter to attain steady-state flow.

III.   Once flow stabilisation or steady state is attained, the flowmeter, pressure gauge and thermocouple readings are recorded.

IV.   Procedures II and III are repeated at pressure intervals of 0.4bar starting from 0.20bar until the maximum pressure, 3.00bar, for the experiment is achieved for a particular isotherm.

V.   Steps I to IV are repeated until the maximum temperature, 673K, of the experiment is reached.

VI.   Steps I to V are repeated until all the gases, and the five core analogues have been sampled.

6.2.5 Accuracy and Errors

Temperature and pressure were regulated from low to high (Temp: 293K to 673K and Pressure: 0.20bar to 3.00bar). Temperature readings were collected at ±5K. This translates to 10% and 1.25% error for the lowest (293K) and the highest (673K) adjusted temperature readings, respectively. Pressure gauge readings were collected at ±0.01atm. This translates to 5% and 0.33% error for the lowest (0.20atm) and highest (3.00atm) gauge pressure readings, respectively. Vernier calliper readings were carefully taken, save for possible errors due to parallax. The weight of samples and flow rate were obtained from a calibrated digital weight balance, thereby eliminating certain errors. Electronic devices used were often tared before new measurements are taken.

Efforts were made to always finish all the runs for gas on the same day and setting. This is to avoid or reduce the interference from the change in

operating conditions on experimental data. It was observed from earlier trial runs that stopping and restarting a set of runs for the same gas slightly changed the resulting outcome. Similarly, only one set of apparatus was used for the experiment to avoid calibration errors that might result if a new apparatus or equipment were to be introduced to the setup. Furthermore, between EOR gas runs, such as CO_2 and N_2, an inert gas, such as He and Ar, was used to flush the core by gradually injecting the inert gas from 0.50bar to 3.00bar through the core sample. Although unlikely, however, this was a proactive measure to eliminate any potential physical or chemical reaction that might occur in the core due to gas mixtures at higher temperatures and pressure, although it has been stated that the gases are non-reactive. Furthermore, before reading for a new run, the new gas is first used for flushing the core to expel any residual of the previous gas. It is qualitatively assumed that the new gas should sufficiently displace the older gas due to the pressure difference.

6.2.6 Safety Measures

An ethical and safety assessment was aptly done and approval granted by Robert Gordon University for these experiments. Gas Handling training was done before proceeding with the experiments. Personal Protective Equipment (PPE), such as gloves and goggles, were worn at all times and a lab coat. Electrical and gas leak checks and equipment functionality checks were done before the start of every run and shot down. Gas cylinders were properly secured. The laboratory was adequately ventilated and lighted at all times. Exit gases were appropriately exhausted to a functional fume cupboard. An oxygen detector was in place to measure the safe oxygen level in the laboratory when working with liquid Nitrogen. Fire extinguishers were in place all through the experiment. Importantly, at least one trained gas handler was required to be in the laboratory at all times during the experiment. The opening and closing hour policy of the University laboratory was strictly followed.

6.2.7 Limitations, Constraints and Scope of Research

Gas availability was a major constraint during the experiment, as it takes time for the gases to be ordered and received while the researcher runs out of gases. Some gases, such as CH_4 and $30\%CO_2/CH_4$, were in small cylinders and they often depleted before a full set of runs were completed. Consequently, for some gases, only one run was carried out, while in other gases, such as Ar and CH_4, multiple sets of runs could be afforded for data check purposes. Generally, the COVID-19 presented a significant challenge to research activities. Time constraint was an issue as there was limited time for analysing the various aspects of the experimental results.

6.2.8 Engineering Assumptions

It is assumed that no chemical reaction occurs in the experimental processes for the PVT conditions and gases used. It is assumed that any imperfection in the system should affect the performance of the respective gases equally. Therefore, such imperfection would not significantly affect the comparative analysis and performance evaluation of the EOR gases. Although engineering justifications for using a single-phase mobility experiment to describe multiphase reservoir mobility have been presented in previous sub-sections, care must be taken to avoid the oversimplification of research findings. It is assumed that all analytical application of EOR obey the continuum mechanics.

Chapter Seven

7 EXPERIMENTAL RESULTS AND DISCUSSION

Robust gas experiments have been carried out. Kantzas, Bryan and Taheri (2012) stated that the optimal requirement to secure an accurate experimental measurement of permeability should be at least 12 flow tests, comprising four flow rates at the three isobars. This study used permeability as a building block for other engineering quantities, such as mobility and transmissibility, to evaluate EOR gases. Consequently, this research conducted 1,920 flow tests and obtained 15,360 experimental data points for analyses. The figure is 160 times more than the requirements suggested in Kantzas, Bryan and Taheri (2012). Therefore, the research is confident that the subsequent analyses would present a high level of reliability.

Engineering interpretations and assumptions have been made to explain the phenomena observed in the experiments. The experimental data lend itself to calculating two sets of intrinsic mobilities for the gases. One is derived graphically using Eq. 6-50 or Eq. 6-51. The benefit of these equations is that they allow the opportunity to study how the gases' intrinsic mobilities develop along isotherms and isobars. The other mobility was derived by direct computation of experimental data into Eq. 6-52. The mobility values derived using Eq. 6-52 are the instantaneous mobility at specific pressure and temperature, such as 1.20atm gauge pressure and 293K. Most of the analyses were carried out using computed mobility. Once the individual gas mobility, interstitial velocity and momentum values have been derived, they were then analysed and compared using the expression in Eq. 6-12. The gases' volumetric flow rates were analysed based on the concept of pore volume (PV). Intrinsic mobility was graded based on mobility ratio approaching unity ($M \leq 1$). Interstitial velocity was graded based on its effect on the capillary number and critical velocity. Interstitial momentum and flux

were graded based on the conservation of momentum. The graphs have been plotted to enable the PVT analyses and characterisation of EOR gases. While the evaluations were based on the following five objective functions:

I.   Volumetric Flow rate
II.   Intrinsic Mobility
III.   Interstitial Velocity
IV.   Interstitial Momentum

The graphs produced from the experiments take the forms found in journals for Pore volume vs. Oil recovery graphs for the two-phase study of water and gas flooding, such as in Wu and Pruess (1998). The shape of the mobility graphs is similar to those reported in journals for two-phase oil displacement by water injection, such as in Lyons and Plisga (2011). These similarities give engineering credence to the results presented in the chapter.

7.1 Objectives Achieved

The following have been achieved in the following sections:

I.   Successfully characterised gases used in immiscible gas EOR based on EOR performance as required in Objective II.
II.   Validation of outcomes from data mining as required in Objective I.
III.   PVT characterisation of gas properties as required in Objective III.
IV.   Production of an EOR optimisation curve as required in Objective IV.
        At the end of this chapter, the laboratory analyses of the Rotondi *et al.* (2015) flowchart would have been revealed.

7.2 Data Summary of Phase Two

The experiments recorded 1,920 runs and 15,360 data points. This comprises five core samples, eight gases, eight isobars, and six isotherms. The data includes flow rate, temperature and pressure.

7.3 Presentation of Experimental Results

The experimental data were compiled, and analyses were carried out using techniques, such as graphical methods.

The following series of graphs shows the characterisation of EOR gas in five core samples. For a better visual appreciation of the results, several parameters were simultaneously considered in a single graph. For example, some graphs are plotted so that flow rate, pressure, temperature and core size could be evaluated together. This makes it possible to evaluate more than one relationship in a single graph. Consequently, the primary and secondary axes of the graphs were all used.

Furthermore, a number of the graphs hold multiples of 4 to 5 sub-graphs. Where applicable, the sub-graphs are demarcated from each other with dotted vertical lines. The purpose of using this graphical method is to enable the discovery of trends and their nature of propagation.

Except where stated, the primary x-axis of the graphs holds the pressure variable. The primary y-axis holds flow rate or intrinsic mobility. However, where there are flow rate and intrinsic mobility on one graph, the primary y-axis holds the flow rate while the secondary y-axis holds the intrinsic mobility. Whenever the temperature was considered, the secondary y-axis holds it. Attempts were made to use the same scale within and across all the different graphs to ease visual and qualitative comparison. The following subsections are graphical presentations and discussions of results from the experiments for the eight gases and five core samples.

7.4 Volumetric Flow rate and Mobility Characterisation of EOR Gases in Five Core Samples
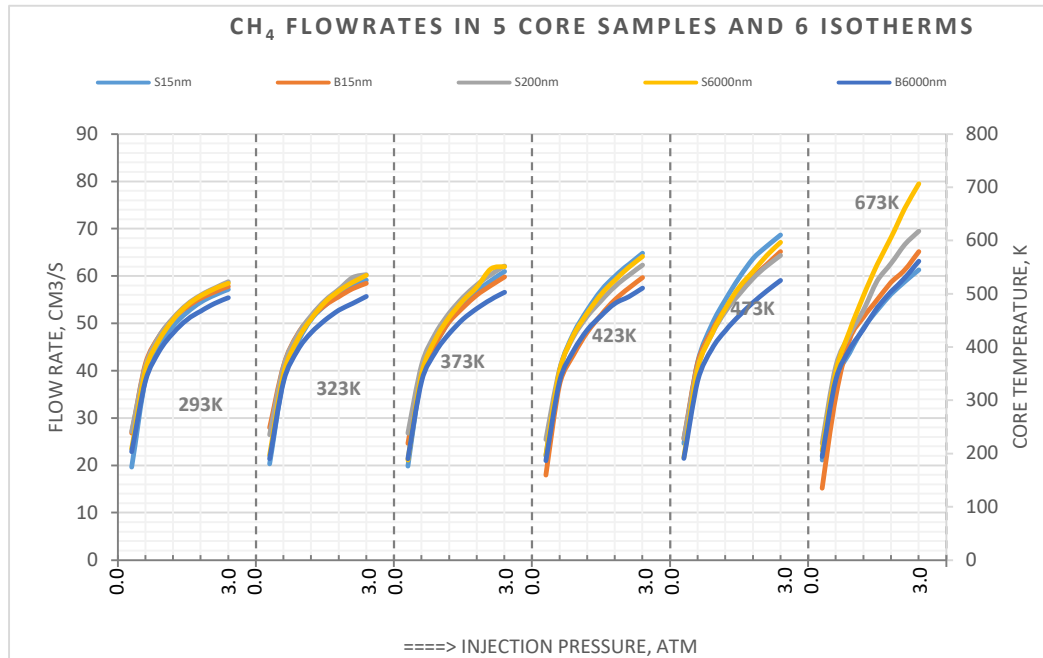
7.4.1 CH₄:

Figure 7-1 shows the flow rate profiles of CH_4 in the five core samples as a function of varying pressure and temperature. The figure is observed to reveal the effect of structural parameters, pressure and temperature on CH_4 flow behaviour in the five core samples. It can be deduced that pressure and temperature could significantly affect the flow rate, hence the displacement of trapped oil by injected CH_4. Figure 7-2 shows a similar graph but for CH_4 mobility.
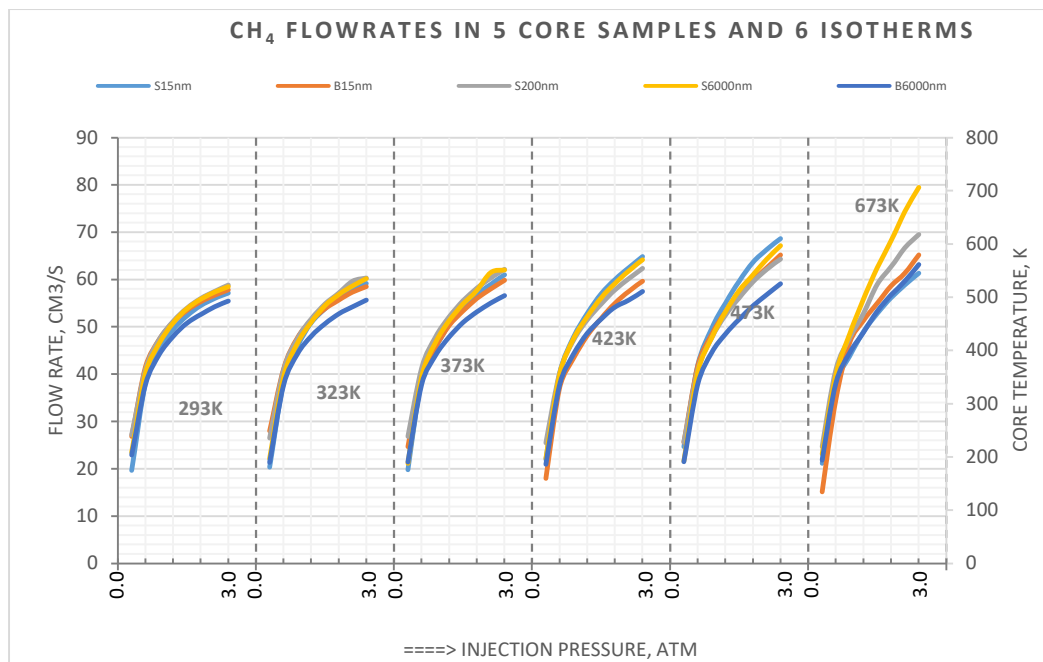
Figure 7-1 Graph showing injected PV profile as a function of pressure, pore size and temperature for CH_4.

The performances of CH_4 in Core 2 and 5 are quite distinct from the other core samples. They indicate that besides pressure and temperature, other factors are detecting the flow and mobility of CH_4 across core samples, such as porosity. The flow profile is significantly characterised by porosity than by pore size. That could explain why Core-1 and Core-2, even though they share the same pore size 15nm) but different porosities, have different flow patterns in Figure 7-1. Temperature is observed to affect gases more in higher porosity samples (Core-1, 3 and 4)) than in tighter samples or reservoirs (Core-2 and 4).
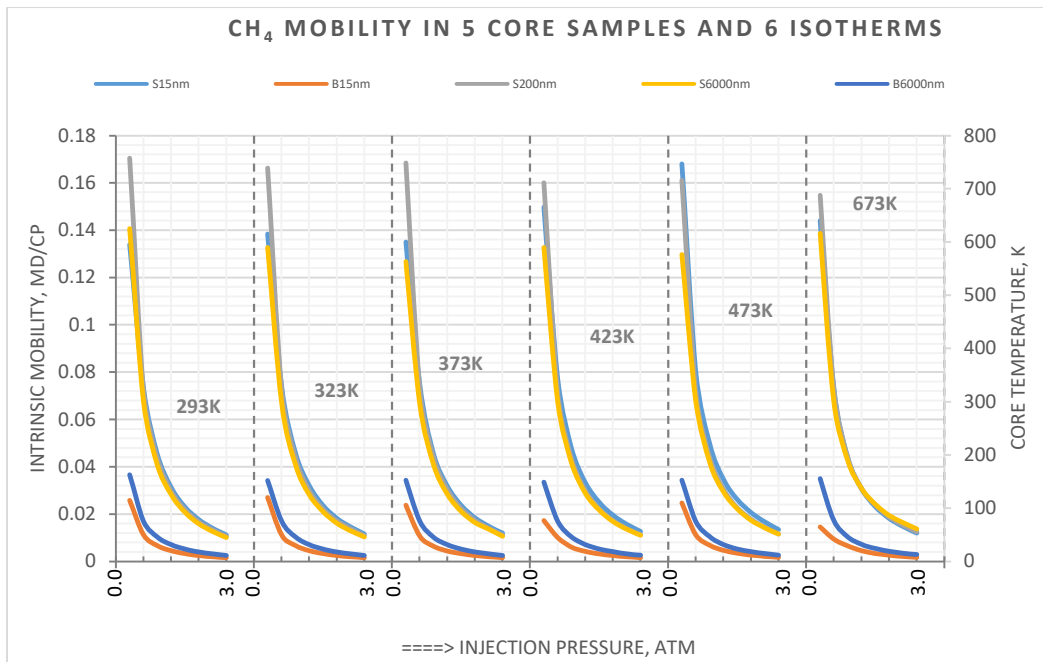
Figure 7-2 Graph showing mobility profile as a function of pressure, pore size and temperature for CH$_4$.

7.4.2 20% CH$_4$/N$_2$:

Figure 7-3 shows the flow rate of 20% CH$_4$/N$_2$ in the five core samples as a function of varying pressure, temperature and structural parameters. It also reveals the growth pattern of flow rate with temperature variation for 20% CH$_4$/N$_2$ in each of the core samples. Figure 7-4 shows a similar graph but for 20% CH$_4$/N$_2$ mobility.

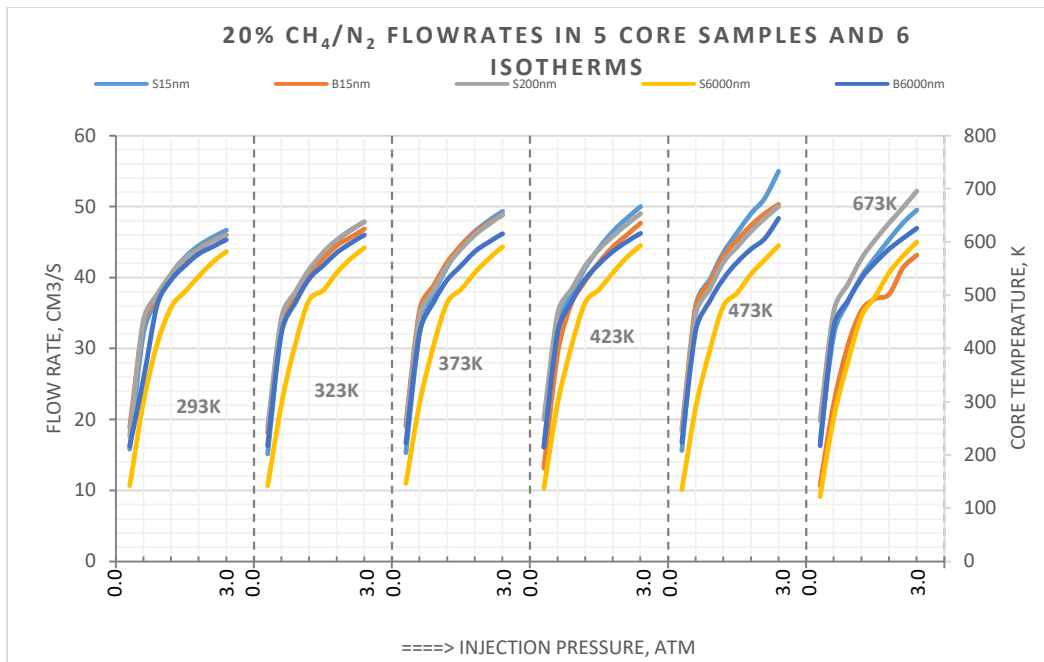Figure 7-3 Graph showing injected PV profile as a function of pressure, pore size and temperature for 20%CH₄/N₂.
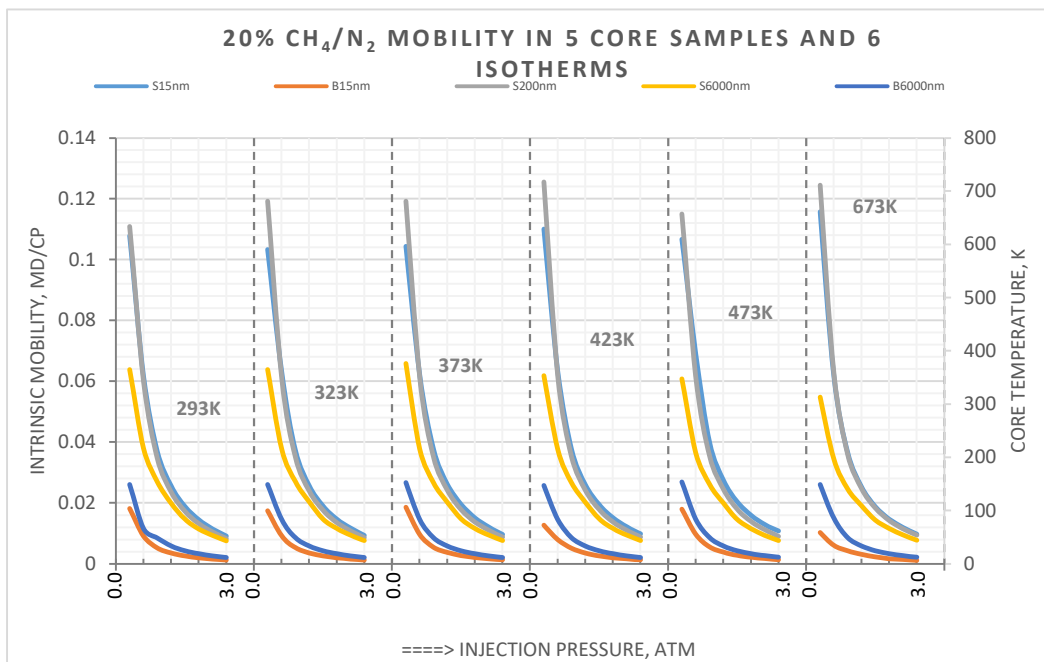
Figure 7-4 Graph showing mobility profile as a function of pressure, pore size, and temperature for 20% CH₄/N₂.

7.4.3 N₂

It is shown in Figure 7-5 that the flow rate of N_2 in the five core samples is a function of varying temperatures. It also reveals the growth pattern of flow rate with temperature variation for N_2 in each of the core samples. It is qualitatively observed that the response to an increase in temperature is not as significant here as in CH_4. Figure 7-6 shows a similar graph but for N_2 mobility. The two graphs show that gas flow and mobility are both segregated by the respective core samples' porosities.

Figure 7-5 Graph showing injected PV profile as a function of pressure, pore size and temperature for N_2

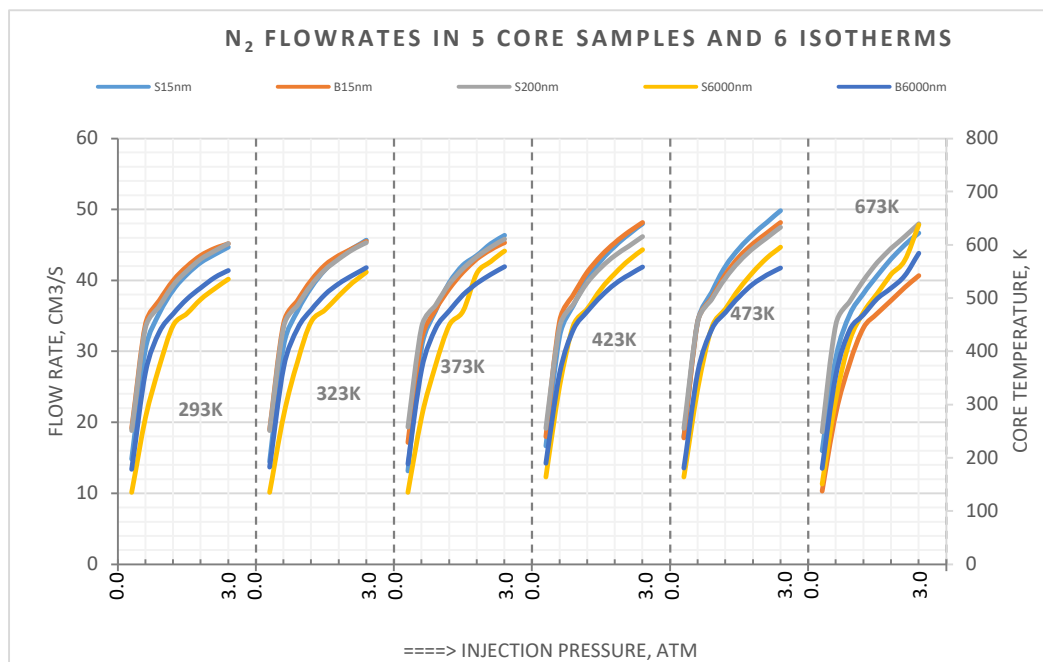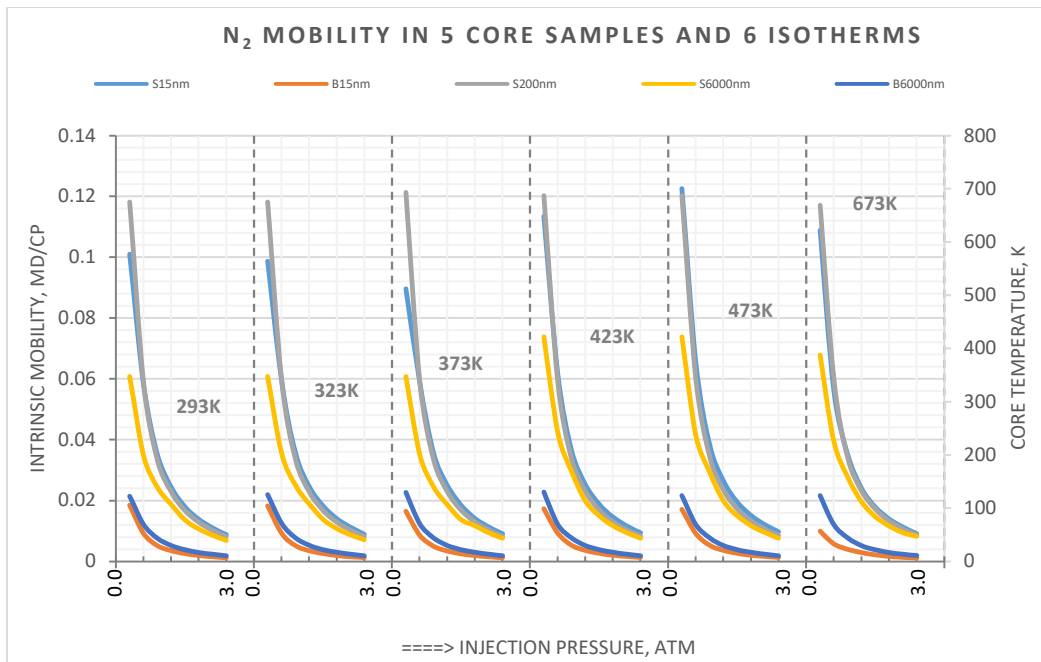*Figure 7-6 Graph showing mobility profile as a function of pressure, pore size and temperature for N_2.*

It was observed that injected PV is generally proportional to pressure for all core samples. However, to attain a certain PV, it was observed that it takes less pressure to achieve it in smaller pore media than in larger pore media. This also reflects the ease of overcoming capillary pressure by assuming the gas is in a hypothetical two-phase system with the solid matrix of the media. This type of analogy is drawn from mercury invasion experiments, where mercury is considered to be in a two-phase system with the media's matrix in determining capillary pressure. The results from this research in terms of capillary pressure contradicts Eq. 2-8 and the results of Andrew, Bijeljic, and Blunt (2014), which state capillary pressure and displacement pressure are inversely proportional to entering pore size. It is speculated that the discrepancy could be due to the porosities of the samples. If the porosity is too low, it means there are fewer capillary channels for the gas to flow through, regardless of the size of the pore.

7.4.4 Air:

The profile of the Air flow rate is shown in Figure 7-7. It reveals the growth pattern of flow rate with temperature variation for Air in each of the core samples. Figure 7-8 shows a similar graph for Air mobility. The experimental and numerical simulation results by authors, such as Yin and Ma (2018), suggest that the oil recovery factor increases with injected PV of Air. From their work, it was observed that the injected PV is greatest in the high permeability core. From the core structural parameters (permeability, porosity, core length, and diameter), it can be deduced that the porosity of the core samples is a determining factor for the injected PV.

Figure 7-7 Graph showing injected Air PV profile as a function of pressure, pore size and temperature.
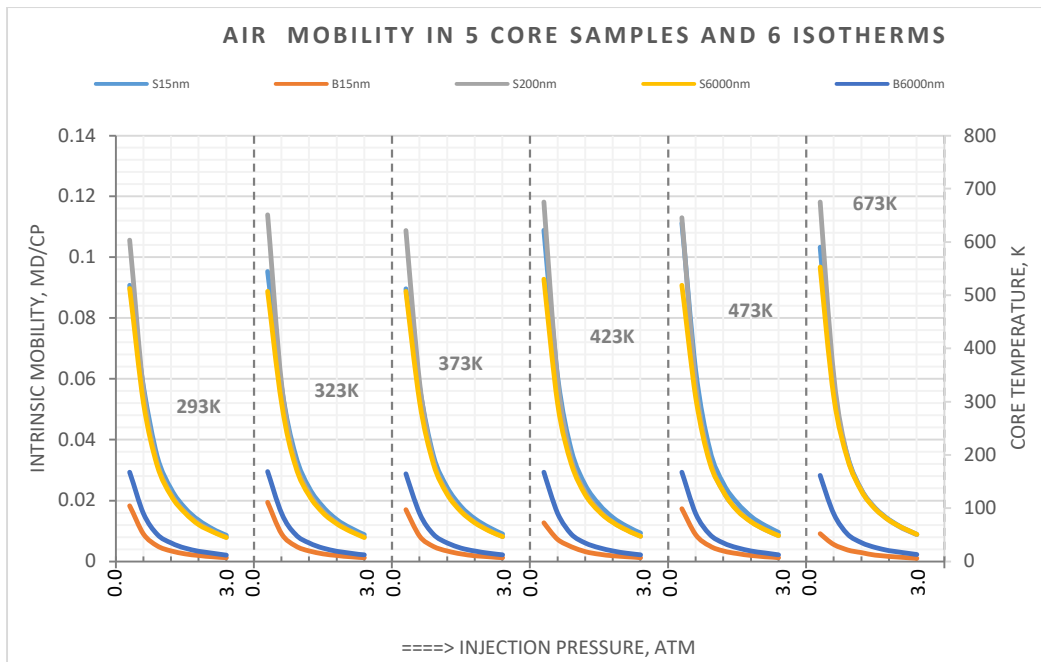
Figure 7-8 Graph showing Air mobility profile as a function of pressure, pore size and temperature.

Yin and Ma (2018) carried out an Air EOR experiment. Their results indicate that higher recovery was recorded at higher permeability core samples. Muggeridge *et al.* (2014) and some other authors have maintained that the recovery factor is a function of relative mobility approaching the condition M≤1. Similarly, Eq. 2-46 and 2-48 suggest that the favourable condition is an explicit function that is inversely proportional to the injected fluid permeability. Therefore, Yin and Ma (2018) experiments could be said to have negated the analytical and empirical expectation of the relationship between oil recovery and injectant permeability. Although Yin and Ma (2018) have reported the phenomenon of oxidation reaction that generated CO_2, CO, flue gas and heat energy that aided oil recovery in the high permeability core sample, there was, however, no qualification of the contribution such reaction

made   to   oil   recovery   in   their   paper.   The   results   depicted   in

AIR MOBILITY IN 5 CORE SAMPLES AND 6 ISOTHERMS

====> INJECTION PRESSURE, ATM
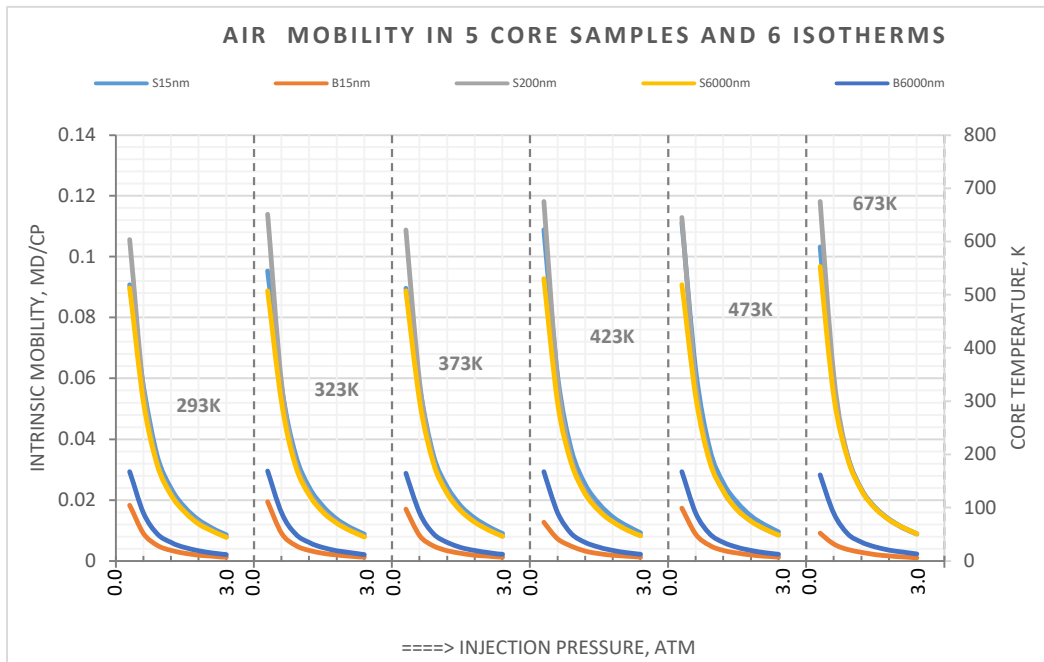
Figure 7-8 contrasts those of Yin and Ma (2018) but are in line with the general principles of mobility suggested in Muggeridge *et al.* (2014).

7.4.5 CO_2

The flow rate of CO_2 is shown in Figure 7-9 for the five core samples as a function of varying temperatures. It also reveals the growth pattern of flow rate with temperature variation for CO_2 in each of the core samples. Figure 7-10 shows a similar graph for CO_2 mobility.
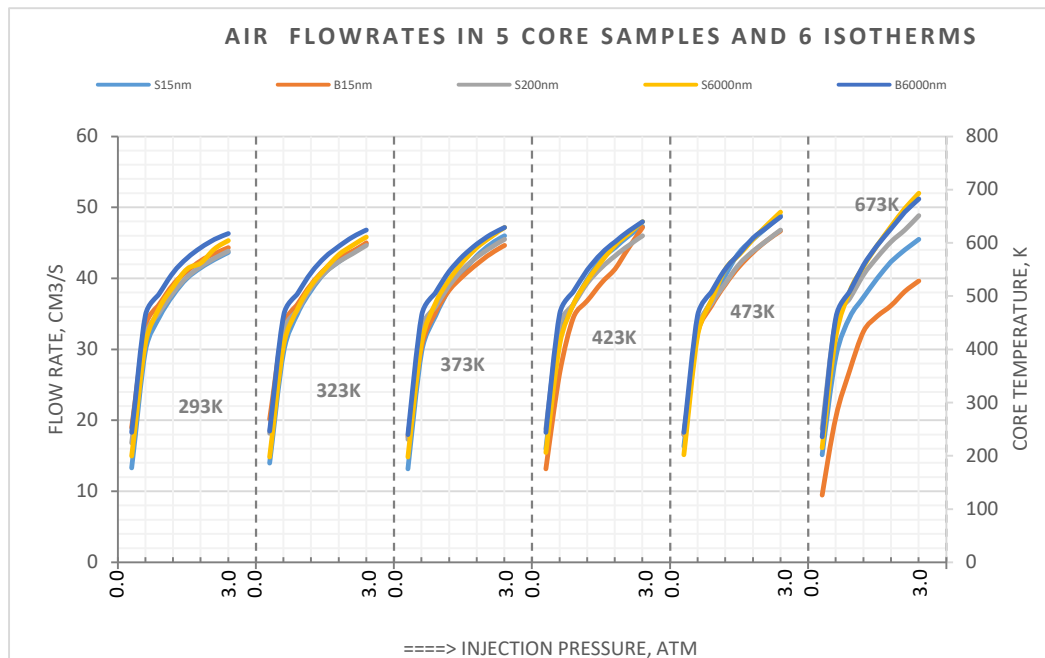
Figure 7-9 Graph showing CO_2 PV profile as a function of pressure, pore size, and temperature.

Figure 7-10 Graph showing mobility profile as a function of pressure, pore size, and temperature for CO_2.

7.4.6 He and Ar:

Figure 7-11 and Figure 7-14 respectively show the flow rates of He and Ar in the five core samples as a function of varying pressure and temperature. The graphs also reveal the growth pattern of flow rate with temperature variation for He and Ar in each of the core samples. Figure 7-13 and Figure 7-14 show a similar graph for He and Ar intrinsic mobilities.
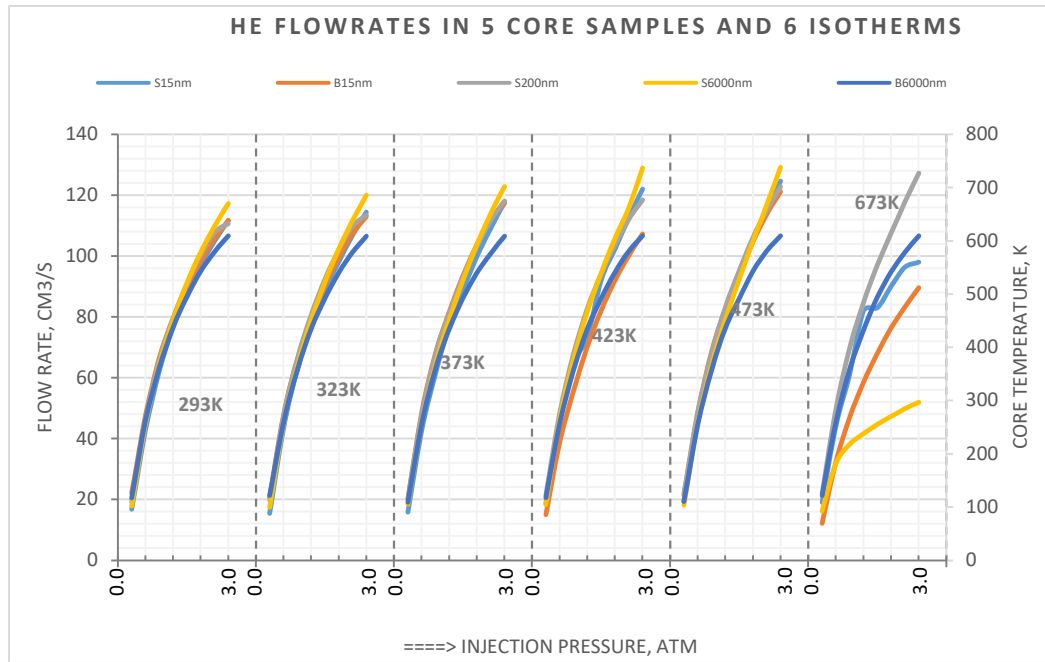
Figure 7-11 Graph showing injected PV profile as a function of pressure, pore size, and temperature for He.
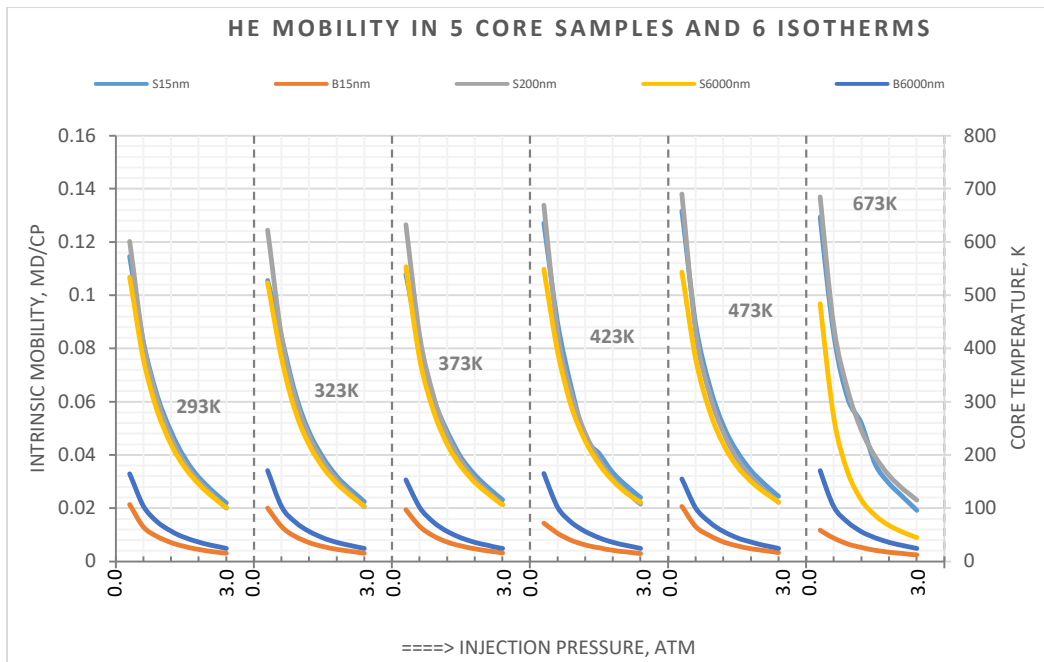
Figure 7-12 Graph showing mobility profile as a function of pressure, pore size and temperature for He.

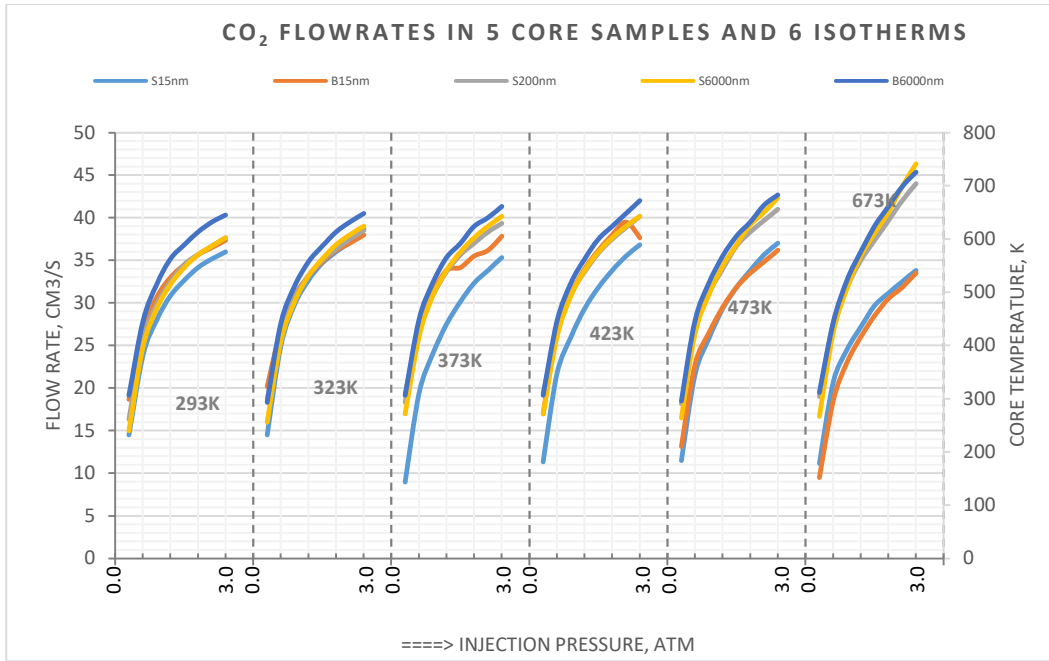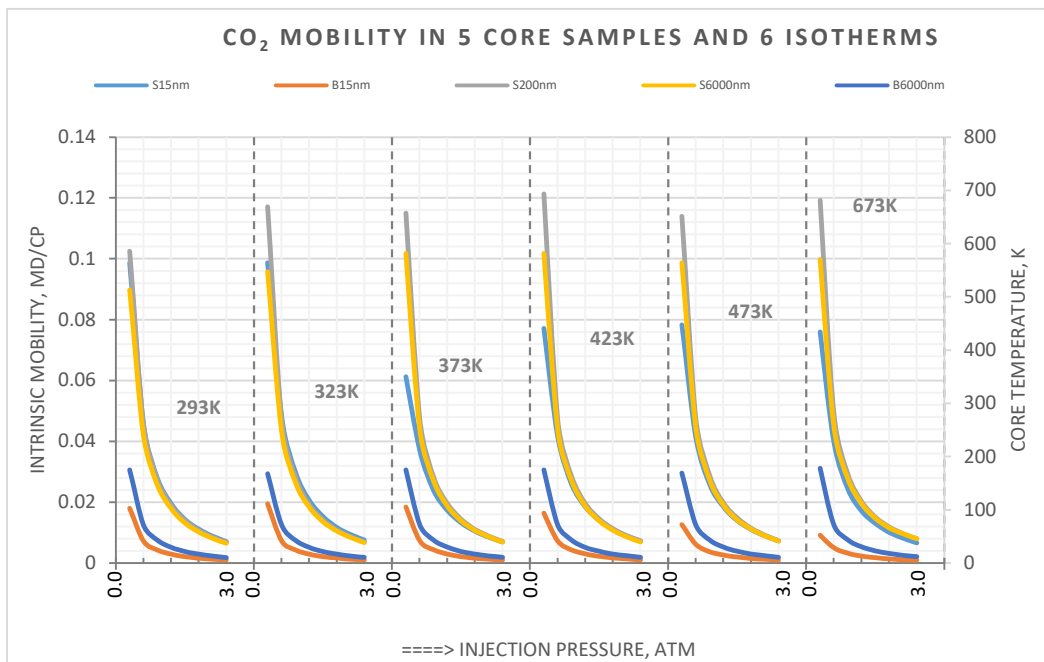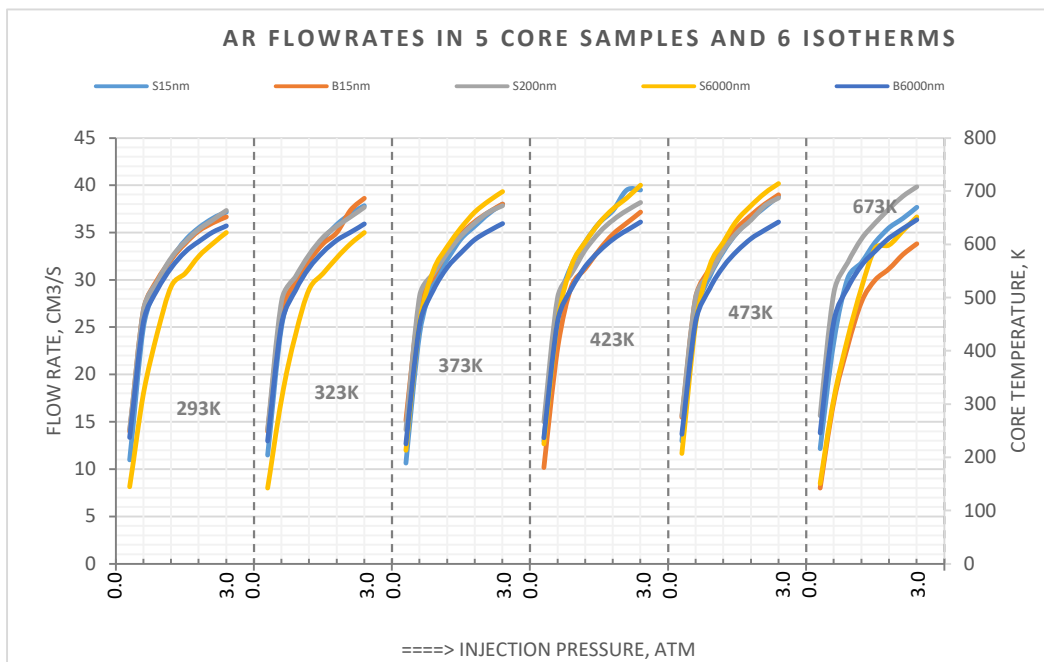Figure 7-13 Graph showing injected PV profile as a function of pressure, pore size and temperature for Ar.
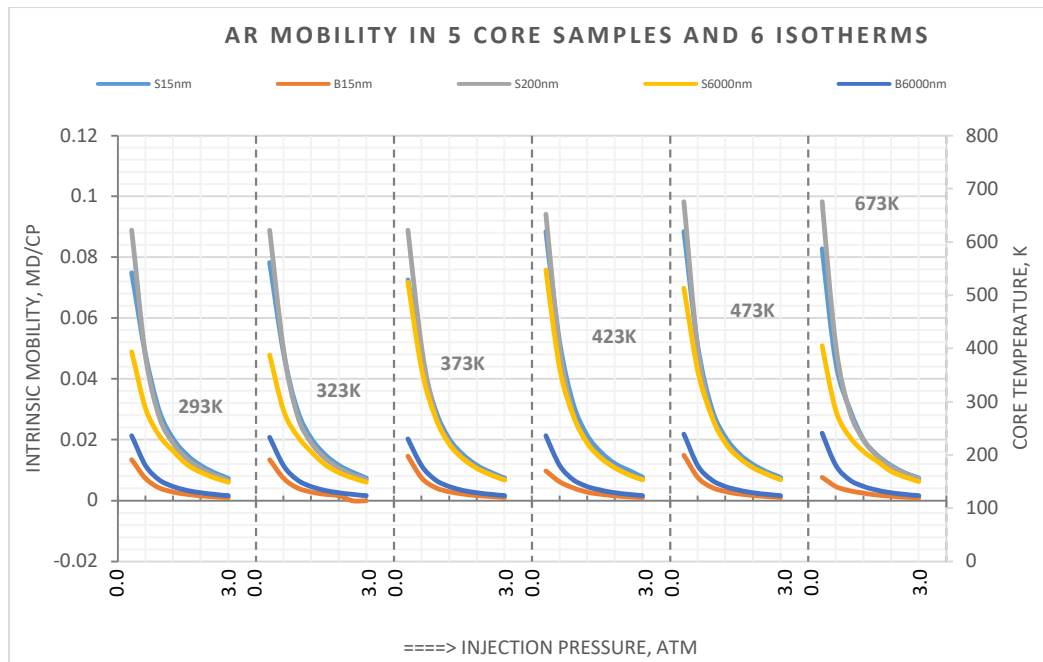
Figure 7-14 Graph showing mobility profile as a function of pressure, pore size and temperature for Ar.

7.5 Volumetric Performance Evaluation of EOR Gases in Core Samples

Figure 7-15 and Figure 7-19 show the volumetric flow rate profile of gases in the five core samples. Recovery efficiency has been evaluated using pore volume factor or cumulative pore volume of various injected fluids (water, surfactants, gases) by authors, such as Cronquist (1977), Fanchi (2002), Feng and Yu (2015), Rob Lavoie (2016), Gomari and Amrouche (2017), Newell and Ilgen (2018) Lake, Lotfollahi and Bryant (2019) and Liu, Ostadhassan and Cai (2019). Their conclusion indicates that increasing pore volume increases the oil recovery factor. Therefore, for a comparative analysis, where time is the basis, the injected fluid that produces the most pore volume within the time basis is considered the fluid that would produce the most oil (Cronquist 1977). This translates to greater oil recovery and performance. These statements are also considered valid for immiscible gas EOR based on the Buckley-Leverett immiscible flow principle in porous media.
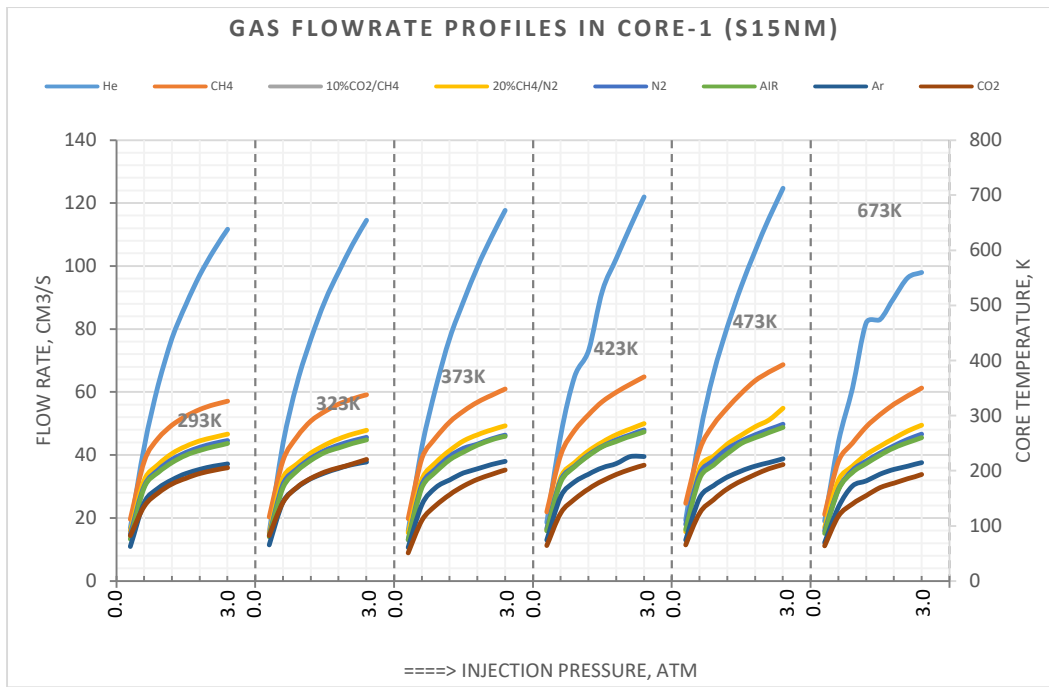
Figure 7-15 Graph comparing the volumetric flow rate profile of gases in Core-1, 15nm pore size at the temperature range of 293-673K.
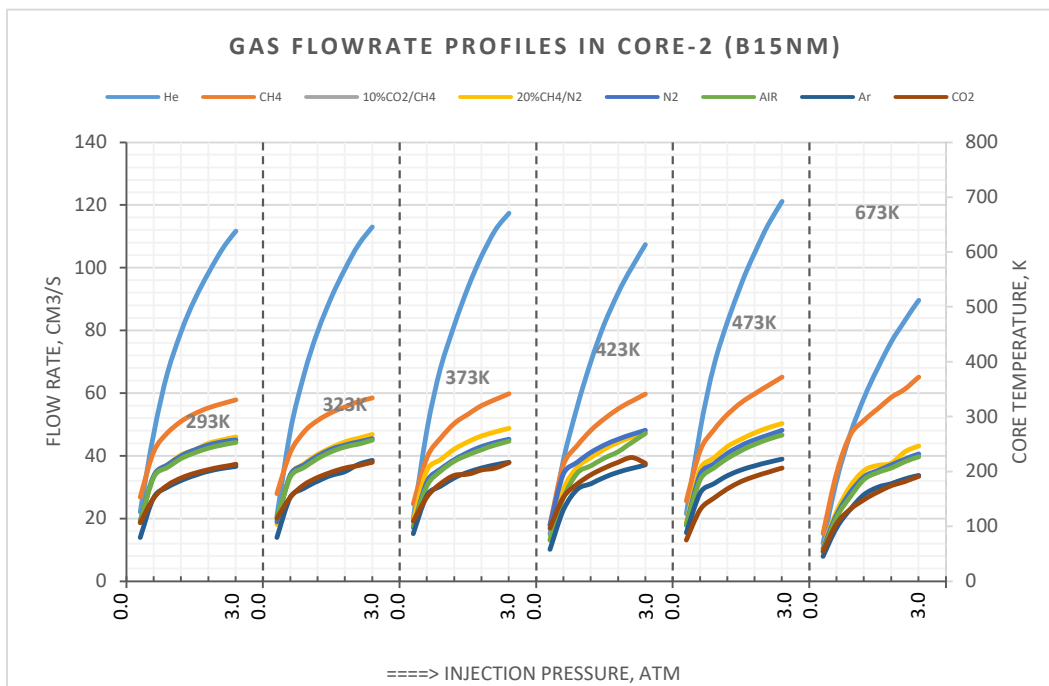
Figure 7-16 Graph comparing the volumetric flow rate profile of gases in Core-2, 15nm pore size at the temperature range of 293-673K.
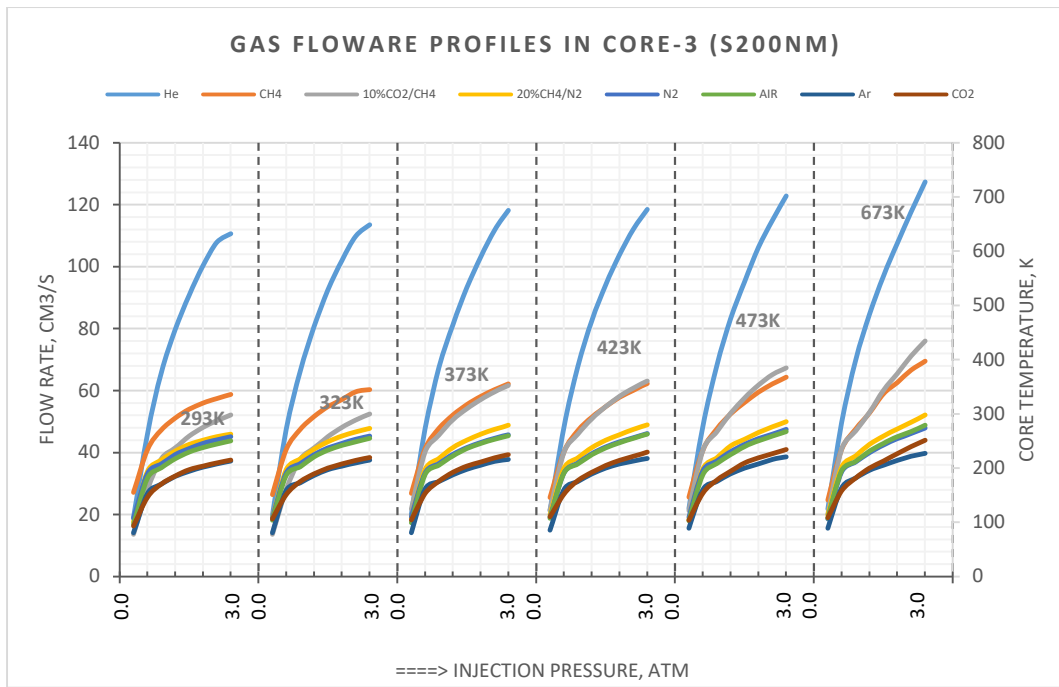
Figure 7-17 Graph comparing the volumetric flow rate profile of gases in Core-3, 200nm pore size at the temperature range of 293-673K.
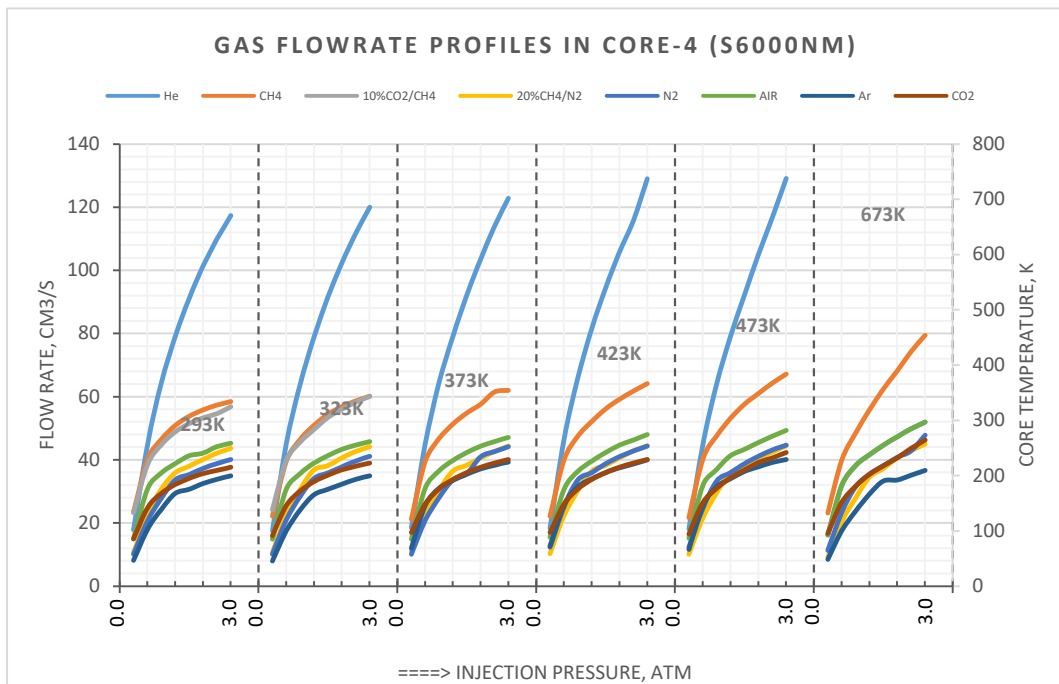
Figure 7-18 Graph comparing the volumetric flow rate profile of gases in Core-4, 6000nm pore size at the temperature range of 293-673K.
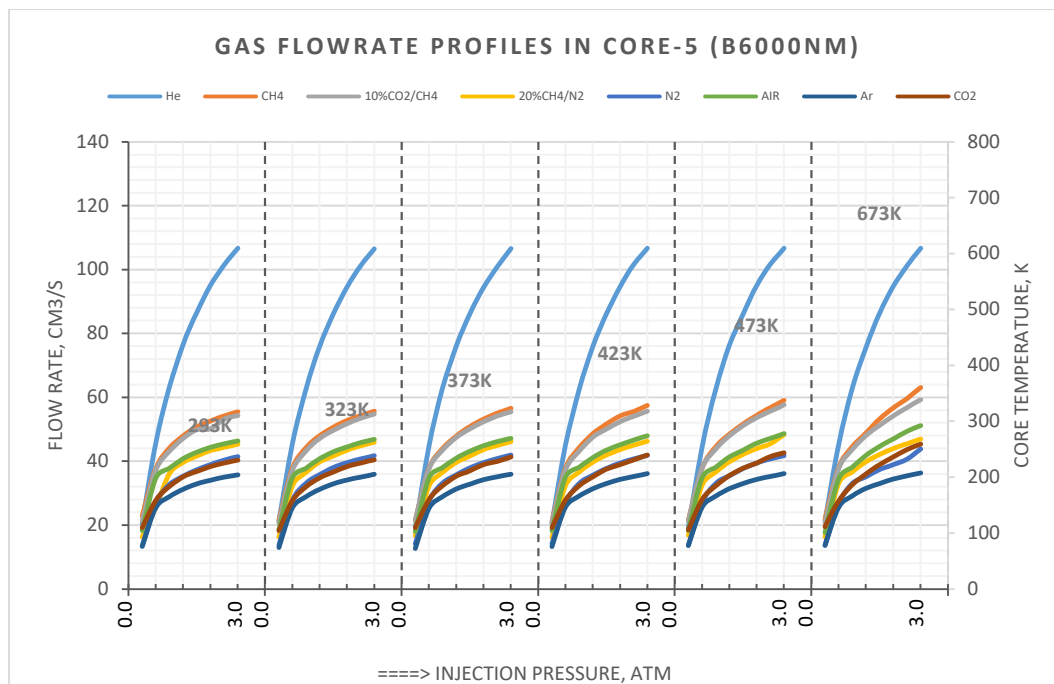
Figure 7-19 Graph comparing the volumetric flow rate profile of gases in Core-5, 6000nm pore size at the temperature range of 293-673K.

Applying these findings and principles to the results from the experiments conducted in this study reveal that CH_4 is consistently the most competitive gas for all pore sizes and distribution sampled. This volumetric performance of CH_4 was observed through the gauge pressure (0.20-3.00atm) and temperature (293-673K) range of the experiments. It reconfirmed that the flow per area of porous media is a function of applied pressure (Robinson *et al*., 2004). This implies that in evaluating and characterising gases based on the objective function of volumetric flow rate or pore volume, CH_4 should be considered the most suitable gas in displacing oil. This experimental finding cannot explain Al Adasani and Bai's findings in Figure 2-5, where the oil recovery factor from CO_2 is reported to be more than the ones reported for CH_4 and N_2. This result, however, validates the finding from the data mining phase in Figure 5-8, where CH_4 (hydrocarbon) gas EOR process is observed to form a cluster at the topmost end in the displacement efficiency graph compared to other gas EOR processes. The recovery factor is reported by Thomas (2001) and Muggeridge *et al.* (2014) to be the sum of E_V (volumetric sweep efficiency) and E_D (displacement efficiency or capillary level recovery).

The CH_4 may only be significantly effective in enhancing E_D than E_V. If this is correct, it implies that CH_4 is a better injection gas for overcoming capillary forces that exist at residual saturation and reservoirs with small pores size and low effective porosity and permeability. Figure 5-3 (data mining) lends itself to this assertion, as CH_4 was found to be implemented in low to high porosity reservoirs. It is worth mentioning that the volumetric flow rate graphs here take the form similar to the one found in the Pore volume vs Oil recovery efficiency graph in two-phase water flooding reported in Wu and Pruess (1998). Therefore, implying that these comparative results can be qualitatively accepted for characterising EOR gases in oil reservoirs.

Table 7-1 shows the gases' quantitative ranking based on their respective volumetric output (performance) in each of the core samples. A qualitative inspection of

Table 7-1 shows that the volumetric output is not aligned with the molecular weight of the gases and mixtures. As earlier mentioned in a previous section, the gases investigated in the experiments include gas mixtures and non-EOR gases (He and Ar). The main aim of including them is to enable a broader data spectrum for a robust investigation of fluid properties' effect on performance.

The colour code is the same as the colours assigned to the respective gases in the previous graphs. The scattering of the colour codes in columns 3 to 8 indicates there could be a flow mechanism that is inspired by the porous media and gas properties, which significantly cause the gases to behave differently in the five core samples. Suffice to state that this mechanism is not noticeable in He and CH_4 gases, as both gases maintained their relative ranking in the five core samples.

Table 7-1 Volumetric flow rate performance ranking of gases vis-a-vis gas properties

Original MW Order	4	16	24.4	18.4	28	29	40	44
Flow Ranking	**1**	**2**	**3**	**4**	**5**	**6**	**7**	**8**
Core-1	He	CH_4	$20\%N_2/CH_4$	N_2	Air	Ar	CO_2	$10\%CO_2/CH_4$
Core-2	He	CH_4	$20\%N_2/CH_4$	N_2	Air	CO_2	Ar	$10\%CO_2/CH_4$
Core-3	He	CH_4	$10\%CO_2/CH_4$	$20\%N_2/CH_4$	N_2	Air	CO_2	Ar
Core-4	He	CH_4	Air	$20\%N_2/CH_4$	N_2	CO_2	Ar	$10\%CO_2/CH_4$
Core-5	He	CH_4	$10\%CO_2/CH_4$	Air	$20\%N_2/CH_4$	CO_2	N_2	Ar
All Cores	He	CH_4	$10\%CO_2/CH_4$	$20\%N_2/CH_4$	Air	N_2	CO_2	Ar

Although columns 3 to 8 quite deviate from the actual molecular weight order for the gases, however, when their ranked flow rate was plotted against gas properties-the inverse of the square root of molecular weights, and specific heat capacities, the R^2 was up to 97% for all the core samples (Figure 7-20). This indicates that the flow behaviour of the respective gases and their competitiveness can be significantly described by gas molecular weight and specific heat capacity. However, the R^2 between flow rate and gas *kinetic diameter* was less than 50%. Indicating Kinetic diameter does not contribute as much as the molecular weight to the gas flow behaviour in this study.
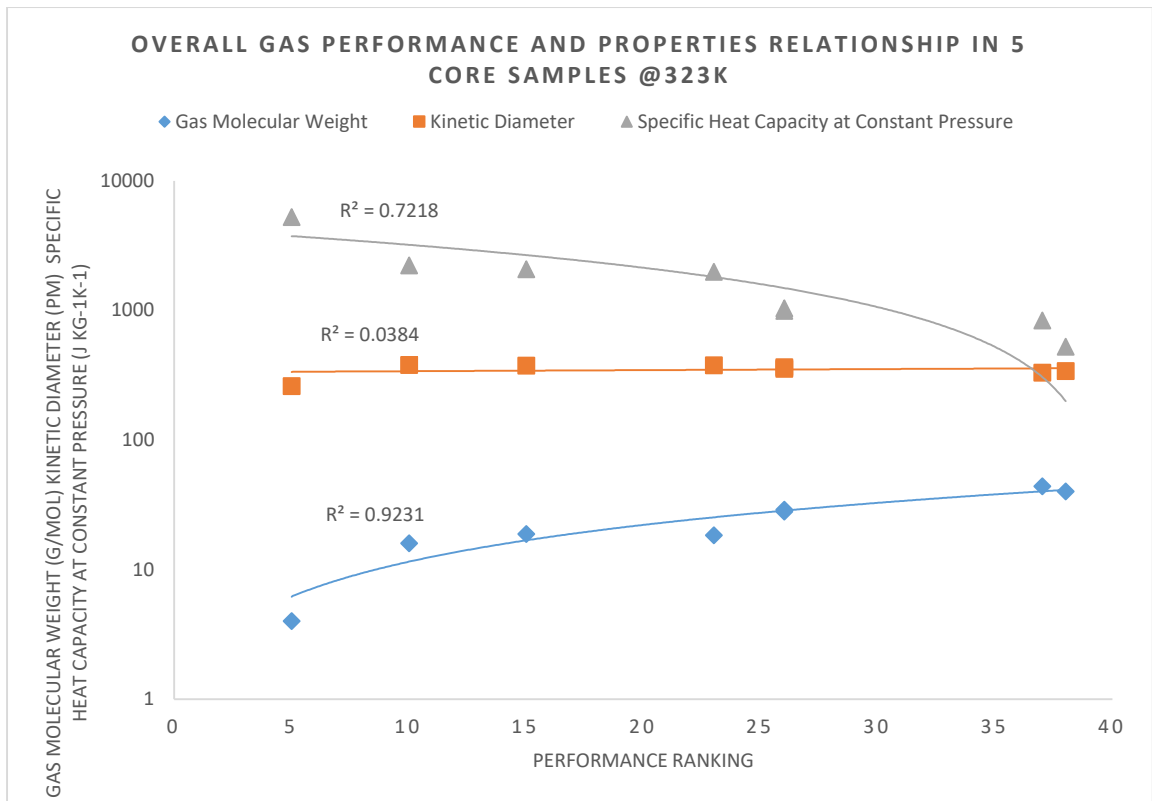
Figure 7-20 Effect of gas properties (molecular weight, Kinetic diameter and specific heat) on gas volumetric performance ranking.

The significance of

Table 7-1 and Figure 7-20 in reservoir engineering is that it enables engineers to predict the potential volumetric performance behaviour of resultant gas mixtures that may occur before and during injection and oil displacement.

7.6 Intrinsic Mobility Performance Evaluation of EOR Gases in Core Samples

The series of graphs in the subsection are multivariable graphs used to simultaneously evaluate and compare the gases' intrinsic mobility in each of the five-core samples. Each of the plots is colour coded and is assigned to a particular gas. For all the graphs in this subsection, care was taken to order the colour coding according to the gases' molecular weight. Consequently, the graph's legend begins with the lightest gas (He) and ends with the heaviest gas (CO_2). This is to intuitively test whether the intrinsic mobilities of gases are aligned according to their molecular weight. The graphs are also based on temperature variation. Each band of the plots is a temperature block. There are six temperature bands, beginning from 293K to the maximum experimental temperature of 673K. Banding the intrinsic mobilities together allows investigating the nature of the propagation of EOR gases' intrinsic mobilities as core or reservoir temperature increases.

7.6.1 Core-1 (S15NM)

Figure 7-21 is the graph that compares the mobility of the gases in Core-1 (S15NM) with pressure and temperature variations. Although the graph indicates that mobility decreases with pressure and temperature for all gases, however, the rate and extent of the decrease are not the same for all gases. While the response to pressure is significant, the response to temperature is marginal. Furthermore, the mobility of the gases is not consistent with molecular weight. He and CH_4 are light and therefore have comparatively higher mobility by way of their molecular weight. This could not be applied to the intrinsic mobilities of N_2 and Air. Per the molecular weight principle, N_2 is expected to be more mobile than Air and, therefore, should have higher mobility than Air. Nevertheless, the reverse was observed to be the case in

Core-1. CO_2 consistently had the least mobility in all pressure and temperature range.

Figure 7-21 Graph comparing the mobility profile of gases in Core-1, 15nm pore size at the temperature range of 293-673K.

7.6.2 Core-2 (B15NM)

Figure 7-22 is the graph that compares the mobility of the gases in Core-2 (B15NM) with pressure and temperature variations. The graph indicates that mobility decreases with pressure and temperature for all gases, similar to the gases' behaviour in Core-1. Some differences were, however, observed for all gases; these include:

The intrinsic mobilities were significantly lower than the intrinsic mobilities in Core-1. The gases were tightly clustered. This implies EOR gases are not significantly discriminated with respect to mobility.

While the response to pressure is significant, the response to temperature is insignificant. Recall that Core-1 and Core-2 have the same pore size (15nm); the difference between the two cores is their entering surface area, radial thickness and porosity. As shown in the Core-1 and Core-2 graphs, intrinsic

mobilities in the latter are quite lower than intrinsic mobilities in the former by a factor greater than 5. Assumably, the magnitude of this factor could be attributed to the ratio between the entering surface area of Core-2 to Core-1, which is 4.7. Another explanation could be the low porosity of Core-2, which implies less internal porous surface area to conduct flow. If this assumption is correct, then a revisit to the data mining graphs should reveal that in lower porosity reservoirs, gas EOR processes are not significantly discriminated. However, in higher porosity reservoirs, the gases should show some pattern of discrimination.

Although He and CH_4 are more mobile than the other gases in Core-1, this is not the case in Core-2, where helium is significantly affected by the flow mechanism that generally dampened mobility in Core-2. It can be concluded that EOR gases would perform far better in Core-2 than in Core-1 due to the gases' generally low mobility. Therefore, it should be more cost and production effective to implement gas EOR in low porosity reservoirs. This validates the observations in Figure 5-2 and Figure 5-3 (data mining section), where gas EOR are mostly implemented in low porosity reservoirs compared to other EOR technologies, such as Thermal EOR. It has earlier been stated in Table 5-3, based on data mining, that porosity is not a selection criterion for gas EOR processes. However, it was included in the experiment to evaluate if there are any performance advantages. It can be concluded that with respect to mobility and Core-2, there is no performance discrimination for the gases. However, in its pore size cohort (i.e., Core-1), EOR gases are segregated with respect to mobility.
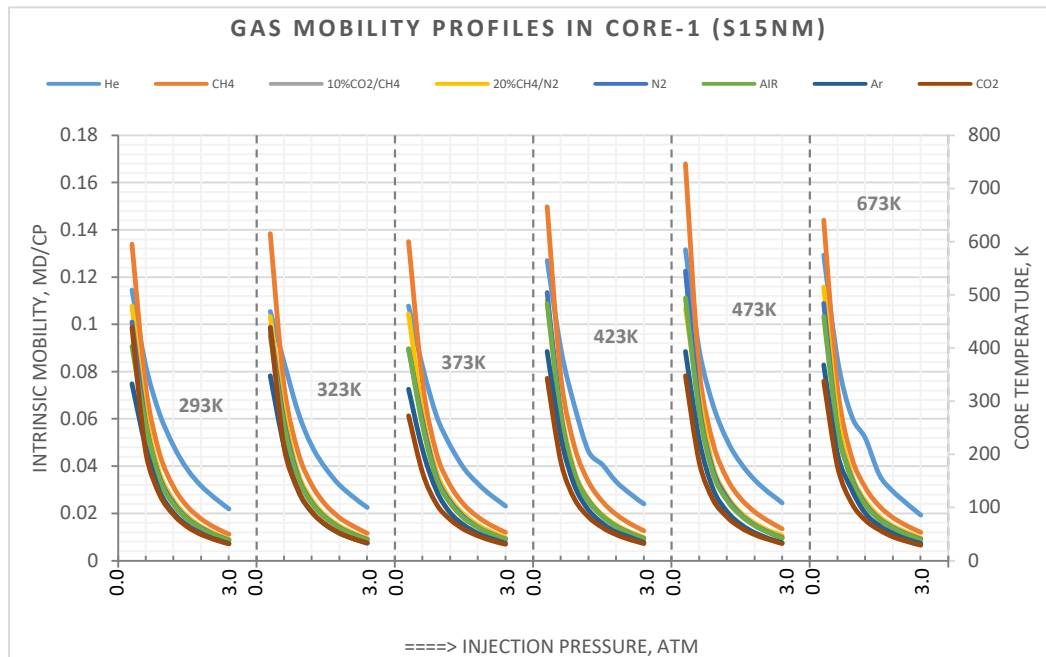
GAS MOBILITY PROFILES IN CORE-2 (B15NM)

Figure 7-22 Graph comparing the mobility profile of gases in Core-2, 15nm pore size at the temperature range of 293-673K.

7.6.3 Core 3 (S200NM)

Figure 7-23 is the graph that compares the mobility of the gases in Core-3 (S200NM) with pressure and temperature variations. Although the graph indicates that mobility decreases with pressure and temperature for all gases, however, the rate and extent of the decrease are not the same for all gases. While the response to pressure is significant at lower pressure, however, as the pressure increase beyond the median pressure of 1.60atm, the rate of change to pressure reduces significantly. The response to temperature variation is observed to be marginal after the median pressure point. It is important to state that the nature of the graph for Core-1 and Core-3 are similar even though their pore sizes are 15nm and 200nm, respectively, and the porosity of Core-3 is higher than that of Core-1. This is an early indication that the effect of pore size may not be as strong as the effect of surface area and porosity on gas mobility, considering that Core-1 (**15nm** and 114cm^2) shares mobility similarities with Core-3 (200nm and 124cm^2) than with Core-2 (**15nm** and 524cm^2). The pore size of Core-1 is 13 times that of Core-3

(that is a pore size ratio of 1:13), and their surface area ratio is 1:1. However, the pore size and area ratios of Core-1 and Core-2 are 1:1 and 1:4, respectively. Therefore, it does not matter how much the magnitude of the pore size difference is. What matters in gas mobility is the entering surface area of permeation and the porosity of the reservoir rock. This finding can be related to the observation in Hartmann, Beaumont and Coalson (2000). The authors have highlighted a limitation in the Darcy equation with respect to the surface area variable, where it is considered unrepresentative of the pore and porosity effects on the magnitude of flow.
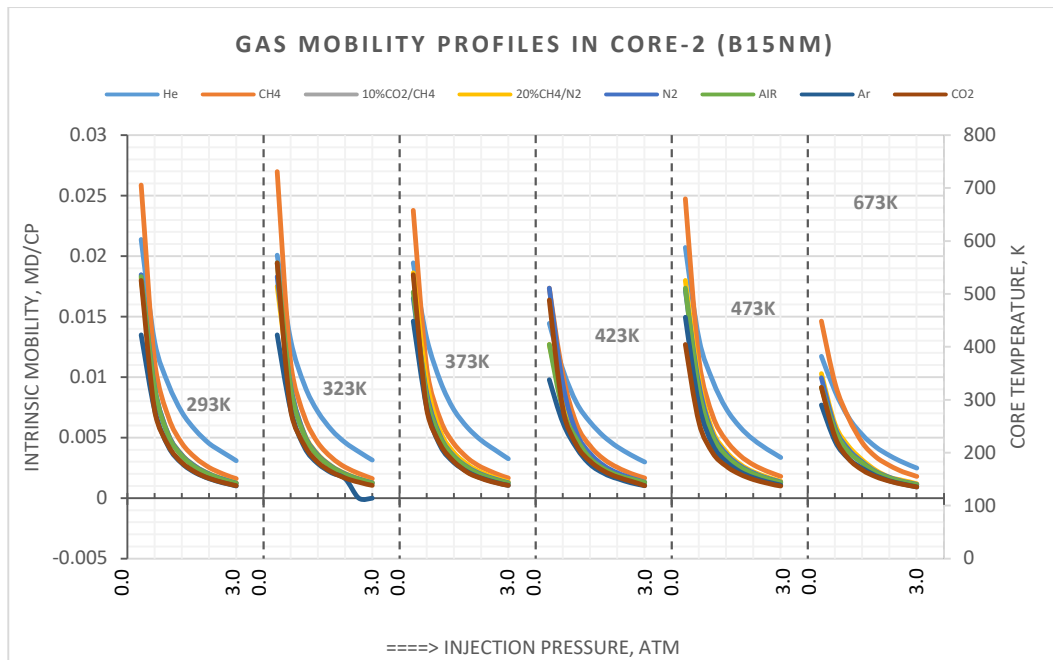

Figure 7-23 Graph comparing the mobility profile of gases in Core-3, 200nm pore size at the temperature range of 293-673K.

7.6.4 Core 4 (S6000NM)

Figure 7-24 is the graph that compares the mobility of the gases in Core-4 (S6000NM) with pressure and temperature variations. Although the graph indicates that mobility decreases with pressure and temperature for all gases, however, the rate and extent of the decrease are not the same for all gases. Furthermore, the response to pressure is significantly higher at a lower pressure than at higher pressure. The response to temperature is noticeable

at pressures lower than the median gauge pressure of 1.60atm. Above this pressure, the effect of temperature is little or insignificant in several gases. Like Core-1, the order of the gases' intrinsic mobilities is not consistent with the order of their molecular weight. He and CH_4 are light, therefore, could be expected to have comparatively higher mobility by way of their molecular weight in that order. This cannot be said with respect to the intrinsic mobilities of N_2 and Air. Following the molecular weight expectation, N_2 is expected to be more mobile than Air and, therefore, should have higher mobility than Air.

It is further observed that the nature of graphs for Core-1, Core-3, and Core-4 are similar with respect to mobility propagation and mobility ranges. This could be attributed to their surface area and porosity similarity since they have significantly different pore sizes. Consequently, it could be stated that amongst three variables: pore size, porosity, and surface area, mobility is more defined by surface area and porosity than by pore size.
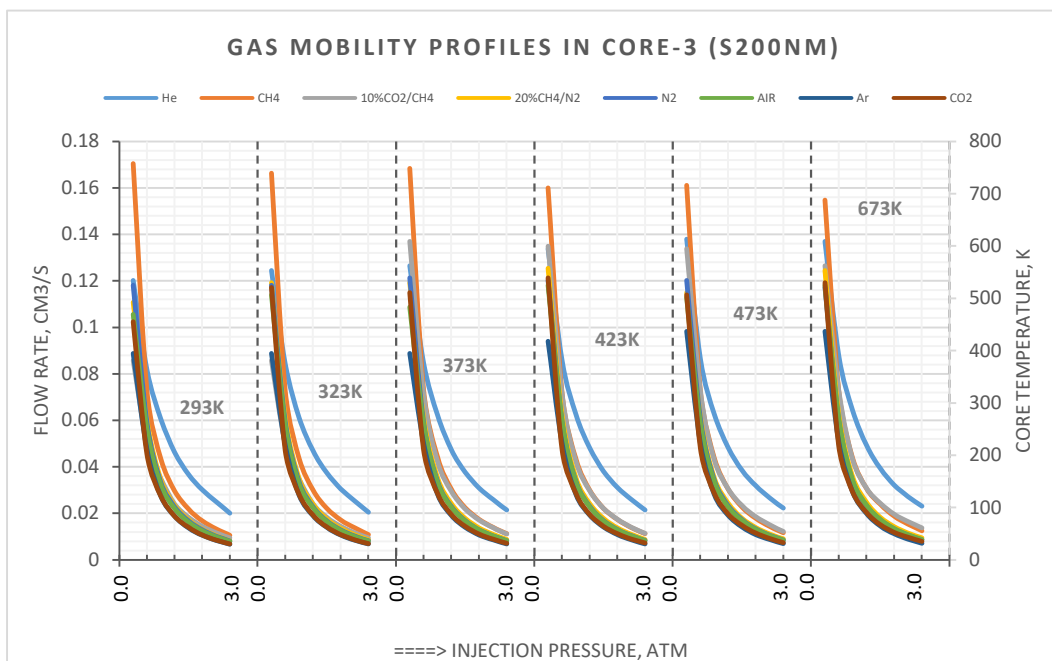

Figure 7-24 Graph comparing the mobility profile of gases in Core-4, 6000nm pore size at the temperature range of 293-673K.

7.6.5 Core 5 (B6000NM)

Figure 7-25 graph compares the mobility of the gases in Core-5 (B6000NM) with pressure and temperature variations. This graph indicates that mobility decreases with pressure and temperature for all gases in a similar vein to the graphs of Core-1, 2, 3, and 4. However, the difference is that the values of the rate and extent of the decrease are quite clustered together for all gases. Furthermore, the pressure response is more significant at a pressure below the median pressure of 1.60atm (gauge pressure). The response to temperature is insignificant at a pressure above the median pressure.

However, Core-4 and Core-5 have the same pore size. It is striking to note that the nature of the respective graphs is markedly different, as evident in the mobility range and clustering of points on the graphs. The main difference in parameters between the two cores is their surface area, porosity, and radial thickness. Therefore, it is correct to argue that surface area, porosity, and the radial thickness could be responsible for the observed discrepancy in the mobility regime of gases in the respective cores. When Core-5 parameters and mobility profiles are compared with Core-2, it is noted that the mobility clustering is similar in tightness; however, the intrinsic mobilities in Core-5 are generally higher than the intrinsic mobilities in Core-2. In terms of parameters, the two cores are similar in radial thickness and porosity. At the same time, they are different in surface area and pore size. It has been previously shown in the comparison of Core-1, 3, and 4 that the pore size effect on mobility is relatively smaller than the effect of other factors. Therefore, it could be stated that the mobility difference between Core-5 and Core-4 is not a result of pore size but a result of surface area.
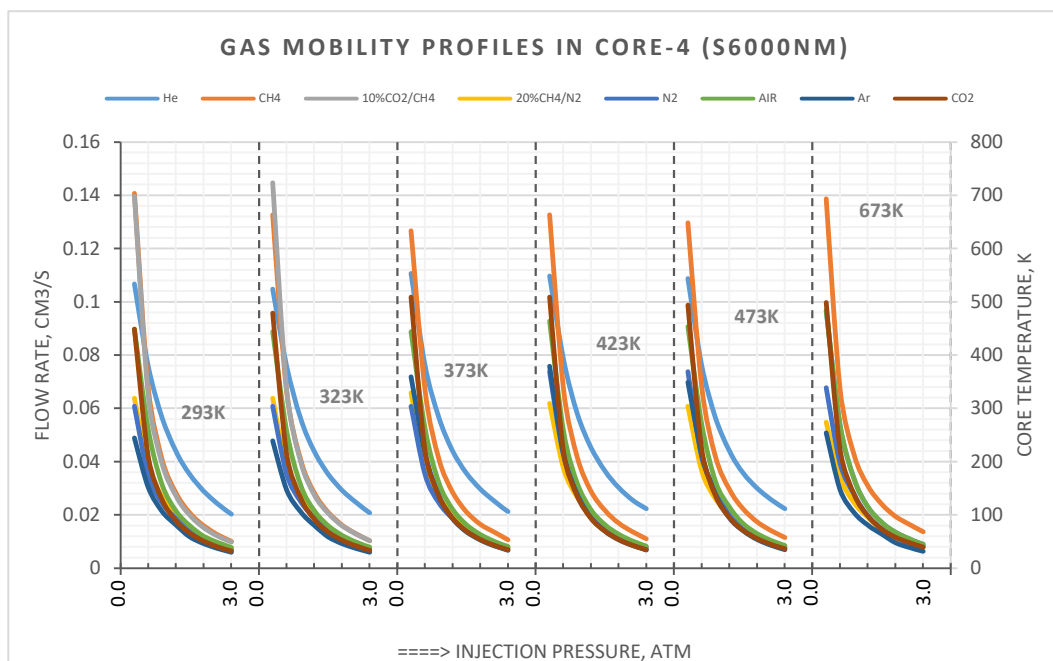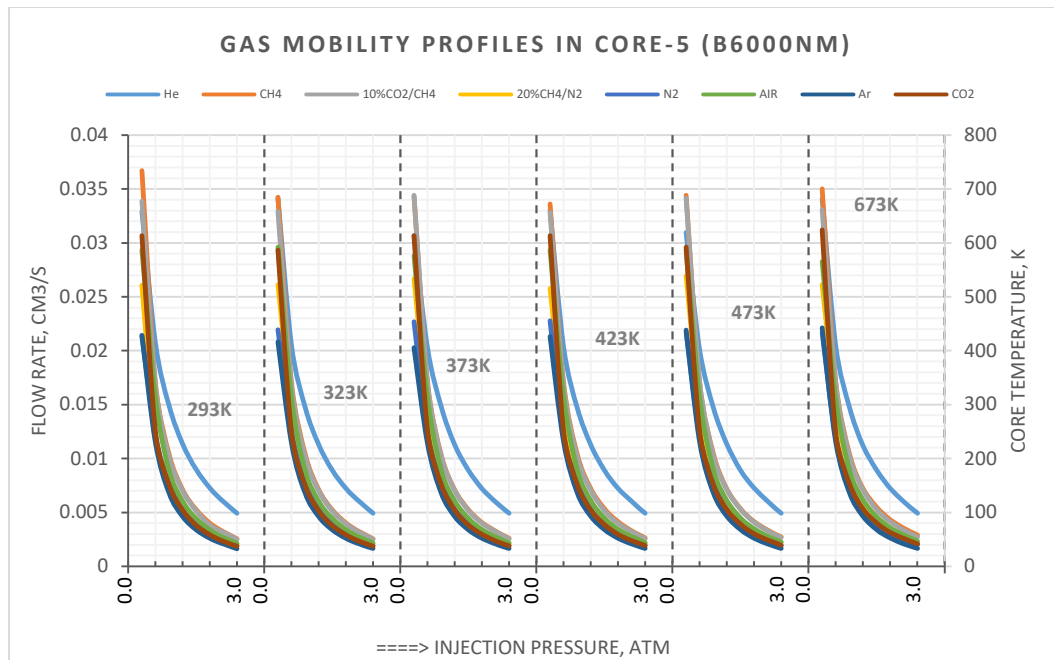
Figure 7-25 Graph comparing the mobility profile of gases in Core-5, 6000nm pore size at the temperature range of 293-673K.

The summary of the mobility analyses of the five cores and eight gases are as follows:

Intrinsic mobility generally responds to pressure change than temperature. The entering surface area and internal surface area are factors consistently affecting the quality and magnitude of mobility. Intrinsic mobility of gases is not significantly discriminated in porous media with poor porosity. This has also been validated by the results of the mobility profiles in the data mining phase. In terms of performance evaluation and gas competition, CO_2 is considered as the gas most likely to approach the favourable relative mobility condition of M≤1. The mobility profiles of the respective gases are not correlated to their respective molecular weights.

7.6.6 Flow rate and Intrinsic Mobility vs. Molecular Weight, Specific Heat Capacity

There was a need to investigate the relationship between the gases' intensive properties with their PVT (Pressure, Volume, and Temperature) behaviour.

For instance, a gas mixture would assume an average molecular weight different from the individual component gases. This knowledge is expected to facilitate the understanding and management of planned and accidental gas mixtures in EOR processes. Consequently, the respective gases' flow rates and intrinsic mobilities were plotted against the gases' molecular weights. The results indicate that flow rate and mobility relationships to molecular weight, specific heat capacity, and kinetic diameter of the gases are all complicated. Although the nature of the relationships at lower pressure differs from that at a pressure greater than the 1.60atm. The nature of the relationships at a lower temperature, 293K, differs from that of 400K. Nevertheless, the relationship could only be described with a higher-order polynomial, up to the 5th order. Therefore, it would be difficult to analytically predict gas mixture displacement potential in immiscible EOR processes based on these three intensive properties. Mobility is a combinatorial objective function derived from permeability and viscosity.

Although, Mason (2020) has stated that there is no obvious correlation between viscosity and molecular weight and Fanchi (2007) has mentioned that permeability is a function of gas molecular weight and applied pressure, the regression analyses on the experimental data show otherwise. The viscosity correlated to molecular weight to the extent of $R^2 = 0.98$, while that of permeability is 0.20. Therefore, permeability could be the reason for the poor correlation between gas mobility and molecular weight.

7.7 Optimisation Curve Domain and Buckley-Leverett Immiscible Flow Theory

The proposed optimisation curve can also provide an optimisation model for the balance between the two areal sweep parameters (injection volume and mobility) at any given pressure within the optimisation domain. It was discovered that the solutions from the optimisation curve domain, which are ratio factors of flow rate and mobility, could be analytically imposed on the Buckley-Leverett theory for immiscible displacement given an oil saturation (S_o) and injection pressure.

7.7.1 Flow-Intrinsic Mobility Optimisation Curve

A Flow-Intrinsic mobility optimisation curve was proposed and developed in this study. The aim was to advance the studies by Dyes, Caudle and Erickson (1954) and Holstein (2007). These authors claim that an immiscible EOR's displacement efficiency depends on the combined effort of the volume and the mobility of the displacing fluid. This suggests that combinatorial optimisation curves can be developed where flow rate, mobility, temperature and saturation are the optimisation constraints, and pressure is the variable. In Figure 7-26 to Figure 7-28, below are graphs showing the combined plot of flow rate (on the primary y-axis) and intrinsic mobility (on the secondary y-axis) as a function of pressure (x-axis). The respective graphs show the optimisation curve for the EOR gases in each of the core samples investigated. Although it is a laboratory-scale optimisation with respect to the magnitude of pressure used in the study, the general principle could be upscaled for reservoir conditions. A total of six isotherms have been sampled in this study. However, only two points were investigated (373k and 673K).

The choice of these three temperature points is based on their frequency in the data mining results collected from the reservoir temperature cluster. It was observed that most immiscible gas EOR reservoirs are around 373K temperature. The other temperature point, 673K, represent high-temperature reservoirs.
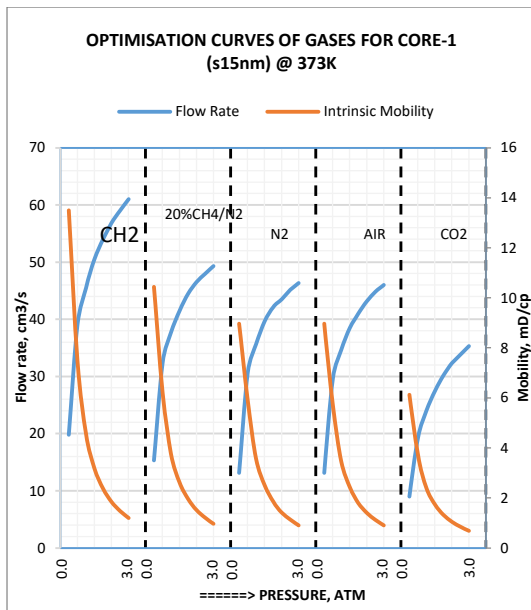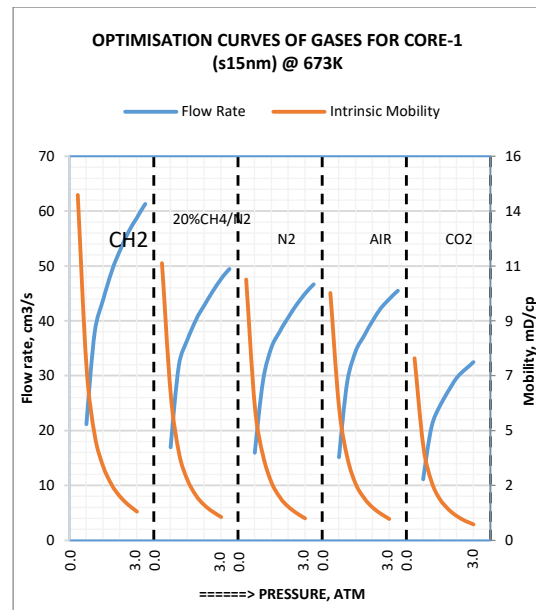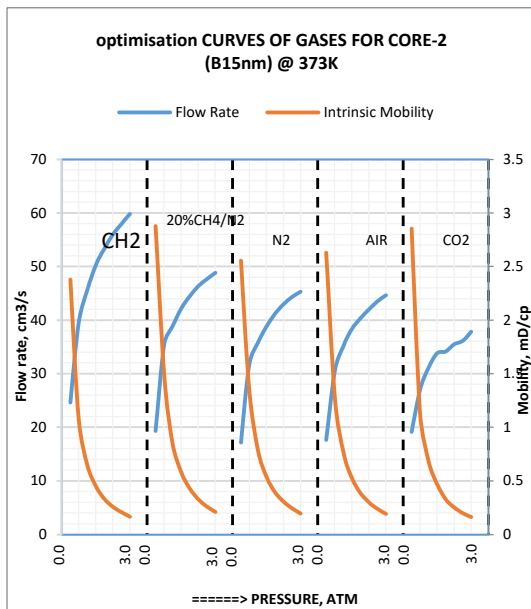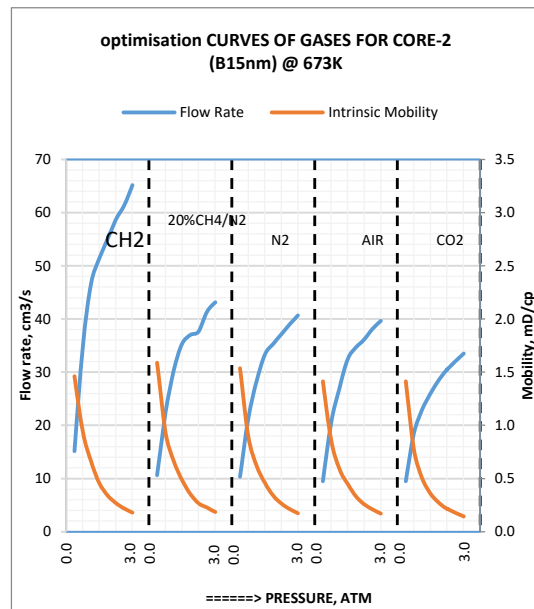
Figure 7-26 Comparing PVT optimisation of gases in Core-1 and 2, 15nm pore size at 373 and 673K.

The optimisation curve's interpretation follows that the point on the graph where the gas flow rate and intrinsic mobility intercept should be considered the threshold of optimisation, and the pressure is the threshold pressure. The area inside the curve is the vector domain for valid solutions to improve oil recovery for any EOR gas with respect to injection pressure, operating reservoir temperature and geometry. Any vertical line drawn from the

horizontal axis (injection pressure) would intercept the optimisation curve at two vector points. These two intercepts theoretically define the boundaries of optimisation. The lower intercept is traced to a mobility value on the secondary y-axis, while the upper intercept is traced to a volumetric rate or pore volume (PV factor) value on the primary y-axis. Therefore, there should be a corresponding pair of volume rate and mobility values for every pressure greater or equal to the optimisation curve's threshold pressure. According to Dyes, Caudle and Erickson (1954) and Holstein (2007) findings and the Buckley-Leverett equation for immiscible flow, the recovery factor of an immiscible EOR process increases with injected pore volume and decreases with mobility of the displacing fluid.

a.

b.
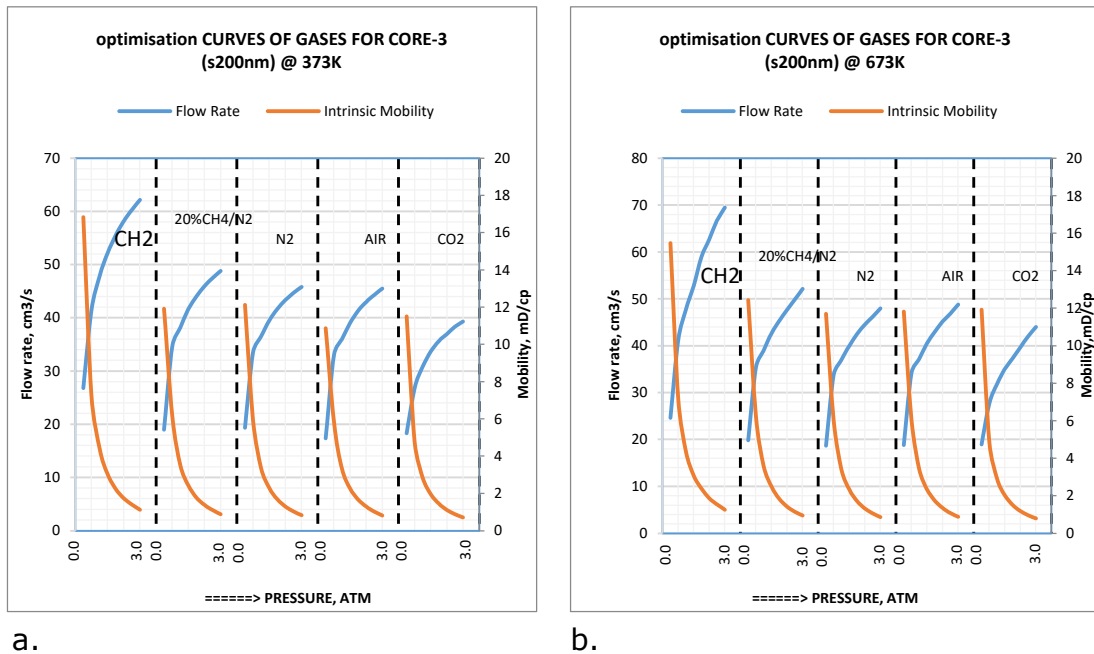
Figure 7-27 Comparing PVT optimisation of gases in Core-3, 200nm pore size at 373 and 673K.

Consequently, the ratio from the pair of values for pore volume and mobility in these graphs could be considered to represent a Sweep Optimisation Parameter (SOP) that hypothetically determines the recovery quality of a gas EOR process. This can therefore be applied to evaluate the competitiveness of EOR gases in immiscible gas EOR.
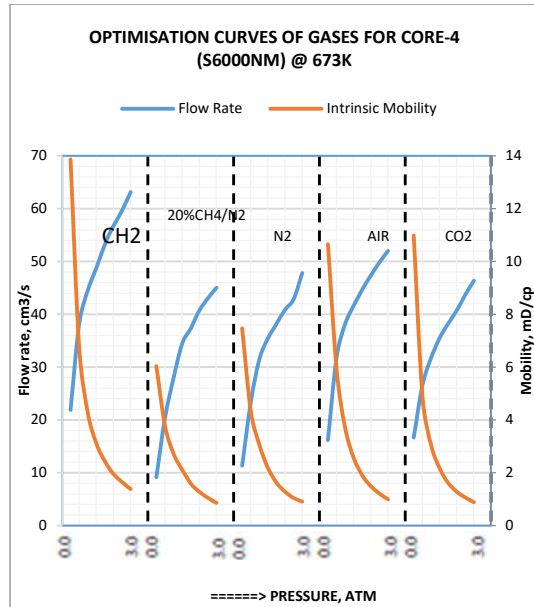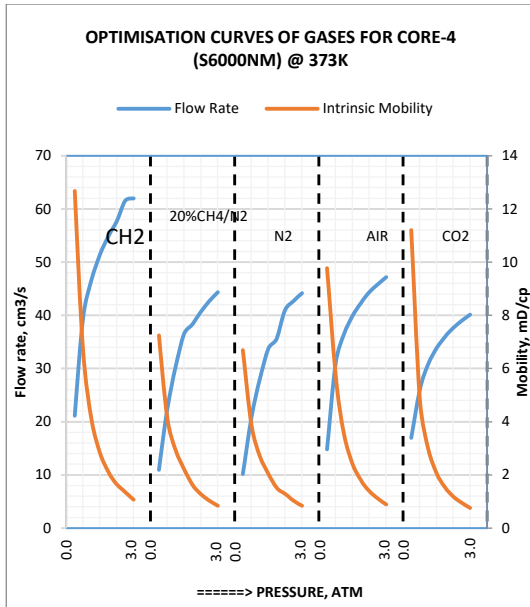
a.

b.
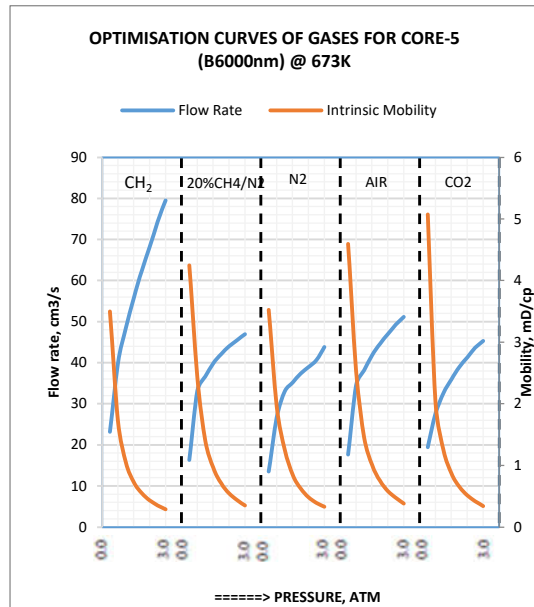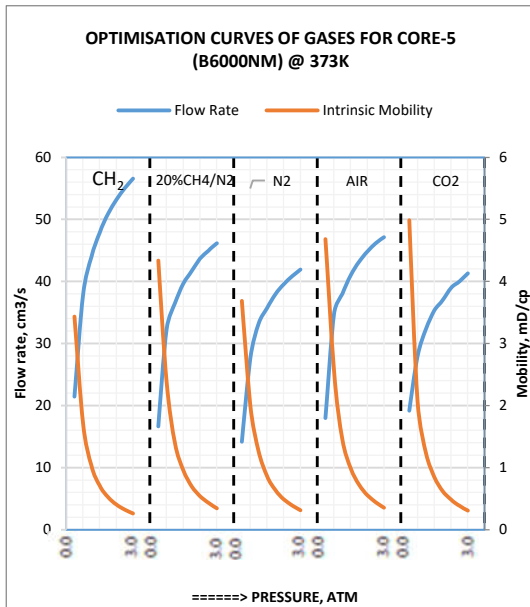
c.

d.

Figure 7-28 Comparing PVT optimisation of gases in Core-4 and 5, 6000nm pore size at 373 and 673K.

A high volume to mobility ratio would imply a high SOP. For a reservoir system with known reservoir parameters, the SOP of the respective gases can be compared for any given injection pressure P, using the respective gases' optimisation curves as proposed above.

P needs to meet the conditions: $P_o \leq P \leq P_\infty$

Where:

P_o and P_∞ are the threshold pressure and pressures at infinity, respectively.

When more than one gas is evaluated, the gas with the highest SOP is considered the most competitive because it fulfils the Dyes, Caudle and Erickson (1954) and Holstein (2007) assertion. The gas with the lowest SOP is considered the least competitive.

The graph was modelled and the values computed for threshold pressure, P_0 and at a pressure of 2atm. The values of the gas SOP have been sorted in decreasing order for each core sample in the table below. Based on the above, CH_4 was identified to be the most competitive gas for immiscible EOR for Core 1, 2 and 5. In contrast, CO_2 is the least competitive for Core 4. Generally, the low porosity improves SOP. It is observed that the threshold SOP values are the same for all gases in each core sample. This indicates that at very low pressure, or pressure gradient, the gases do that have a comparative advantage with respect to SOP.

For a gas/oil displacement mechanism that is predominantly gas-driven; where the displacing velocity of the EOR gas front is equal, but behind that of the displaced oil front (implying piston-like displacement of oil with no viscous fingering); and the well is producing below critical flow rate, the graphs in Figure 7-29 above could be used to assess the performance of the respective gases based on their translational influence on an oil well Productivity Index. For a better comparison, Js' specific productivity index can be derived by dividing J by the reservoir thickness- which is equivalent to the length of the radial core samples. J lends itself to another performance parameter termed the Inflow Performance Relationship (IPR), which is mathematically the inverse of J. Another important equivalence on the volumetric-Inverse pressure graph is the Bulk Modulus. It is the ratio of pressure change to the normalised volume change. It is a measure of the extent of gas strain caused by the applied pressure stress.

Table 7-2 Showing volume-mobility optimisation computation for Core 1 to 5 and the performance of the gases.

Core 1	CH_4	AIR	$20\%CH_4/N_2$	N_2	CO_2
SOP@P_o	3.33	3.33	3.33	3.20	3.33
SOP@2.0atm	16.67	15.85	15.84	15.52	15.28

Core 2	CH_4	$20\%CH_4/N_2$	CO_2	N_2	AIR
SOP@P_o	19.41	19.41	19.23	20.00	20.00
SOP@2.0atm	113.64	72.72	72.00	71.93	71.29

Core 3	$20\%CH_4/N_2$	AIR	CO_2	CH_4	N_2
SOP@P_o	3.89	3.33	3.38	3.89	3.33
SOP@2.0atm	20.84	18.57	18.50	17.39	16.67

Core 4	CO_2	CH_4	$20\%CH_4/N_2$	N_2	AIR
SOP@P_o	5.00	5.01	5.00	5.01	5.10
SOP@2.0atm	17.17	16.44	16.36	16.36	16.34

Core 5	CH_4	$20\%CH_4/N_2$	AIR	CO_2	N_2
SOP@P_o	10.00	10.00	10.67	10.00	10.00
SOP@2.0atm	73.86	42.38	41.34	41.29	41.27

Although the optimisation algorithm used for this evaluation is based on assertions of authors, such as Dyes, Caudle and Erickson (1954) and Holstein (2007), the outcome, however, does not support the EOR gas recovery performance reported by Al Adasani and Bai (2011) in Figure 2-5. Al Adasani and Bai (2011) reported that immiscible CO_2 EOR offers relatively higher recovery efficiency than immiscible CH_4 EOR. There could be other multivariant reservoir or operational factors responsible for the discrepancy that have not been considered in this research.

For temperature effect on gas EOR optimisation (Figure 7-26 to Figure 7-28), it was observed that, for all the gases, the temperature effects on the position of the optimisation threshold and the constraints curvature are inconsistent in core-1 (S15nm) for temperature 293K and 673K (Figure 7-26a and b). However, this was not the case with Core-3, 4, and 5. Furthermore, core samples with relatively lower radial thickness and surface area have the

broadest optimisation curvature, Core-1, Core-3 and Core-4. This implies a broader solution matrix for optimisation.

The preceding analysis has partly fulfilled the second and third objectives of this research, which are focused on identifying the most competitive EOR gas using an optimisation model.

7.7.2 Gas Flow rate Sensitivity to Pressure

Figure 7-29 consists of 5 graphs showing plots of the pore volume of gases as a function of pressure at isotherm, 373K. As stated earlier, this isotherm was often selected for detailed analysis in this research because it is the closest to the modal and mean temperature in the global data of EOR reservoirs.

There was a strong correlation between the pore volume rate and the inverse of the gauge pressure in all the plots. For comparative purposes, this relationship was discussed here as gas pore volume sensitivity to pressure. This enables a qualitative and quantitative comparison to be carried out among the gases investigated. The gradients from the plots indicate that the gases respond to pressure differently. Sensitivity to pressure variation was assessed based on the steepness of the slope of each gas. For the EOR gases, CH_4 pore volume is the most sensitive to pressure variation. This was observed to be consistent across pore size and radial thickness.

The slopes of the graphs have the unit of $cm^3.s^{-1}.atm$. This dimension represents the equivalence factor of some important reservoir parameters such as the Productivity Index and the gases' bulk modulus. In reservoir terms, the productivity index, J, is the ratio of the total volumetric flow rate to a well to the pressure drawdown (Ahmed 2018, Ahmed and Meehan, 2012), with units of $cm^3.s^{-1}.atm^{-1}$. Through dimensional analysis that involves multiplying the respective slopes by the ratio $atm.atm^{-1}$, the Productivity Index's true values were calculated.
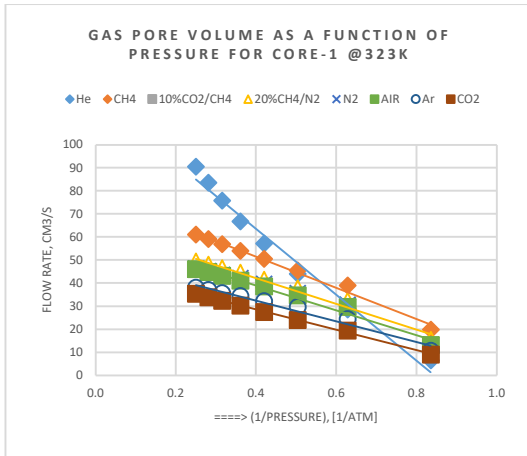
a.
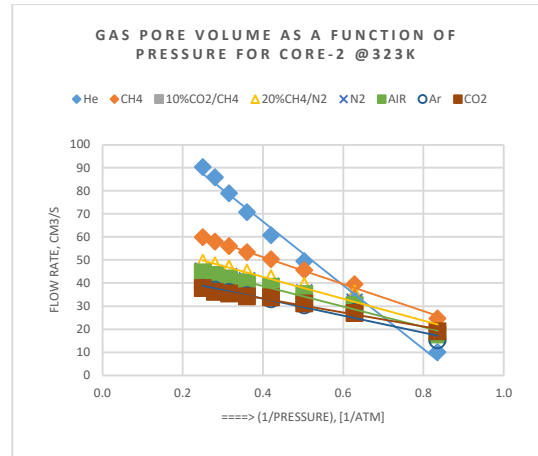
b.
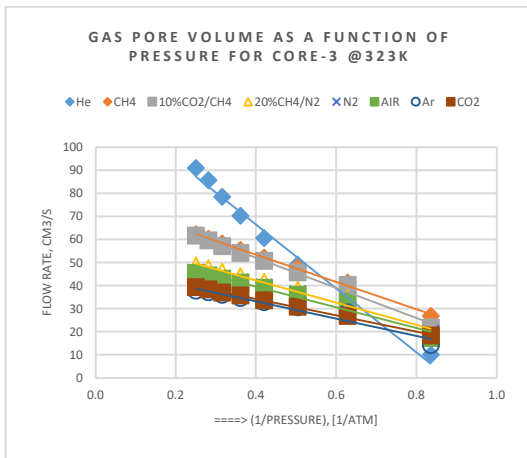
c.
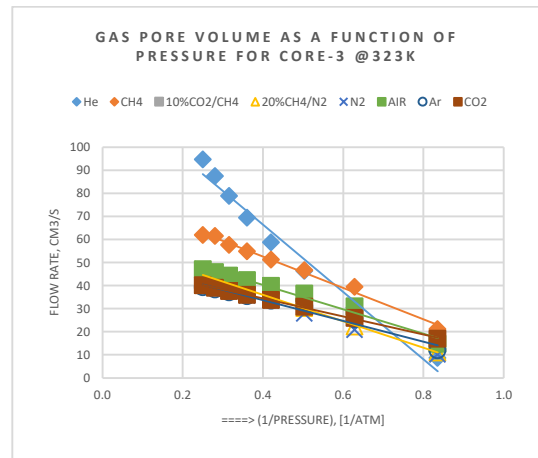
d.
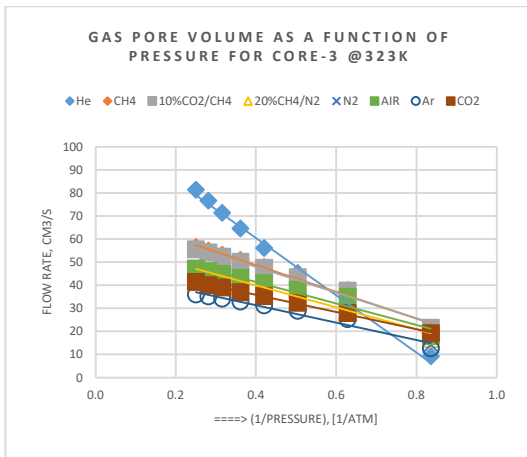
e.

Figure 7-29 Graphs showing the response of gas pore volume to pressure variation in 5 core samples.

Theoretically, the negative slope between gas pore volume and the inverse gauge pressure reflected in these plots appears to violate Boyle's law. The true Boyle's law position should allow gas pore volume to be positively related to the inverse of pressure (Avison 2014). The data were reconsidered severally in an attempt to overcome or explain the seeming violation. The probable analogy that could be employed is the filling of a balloon by Air. Pressure and volume are observed to be directly proportional, enabling the balloon to increase with increasing pressure. It is determined that Boyle's law is only valid for a finite mass, as Avison (2014) emphasised. Hence, injecting more Air into the balloon increases Air mass, which consequently translates to more volume (moles) due to Avogadro's law. It is assumed that increasing the gas inlet pressure for the steady-state flow through the core is equivalent to injecting an additional mass of gas, hence the reason the graphs in Figure 7-29 appear to violate Boyle's law.

7.7.3 Gas Intrinsic Mobility Sensitivity to Pressure

For all the cores sampled, the mobility sensitivity to pressure variation formed a strong correlation. It can be seen in Figure 7-30a-e that the gradient, which is the measure of sensitivity, is different for each gas and core sample. For instance, it can be qualitatively deduced that CH_4 has a steeper slope than the other gases in Figure 7-30c.

Consequently, Figure 7-31 was drawn to highlight and quantify the respective gases and gas mixtures' mobility sensitivity. The effect of pressure variation on mobility is observed to be stronger than that of temperature. It is also noticed that, unlike temperature, the relationship between mobility and pressure can best be described with a linear regression model for all the gas samples regardless of the injected mass, pore size, porosity, and operating reservoir temperature. The Coefficient of Determination, R^2, is above 90%, while the CVs are generally very low. This implies that the variation in pressure significantly explains the variation in mobility.
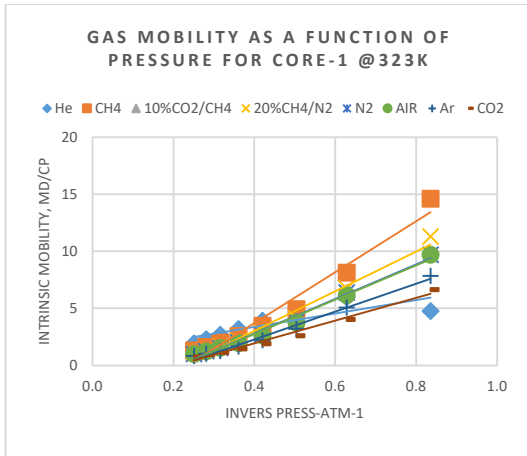
a.
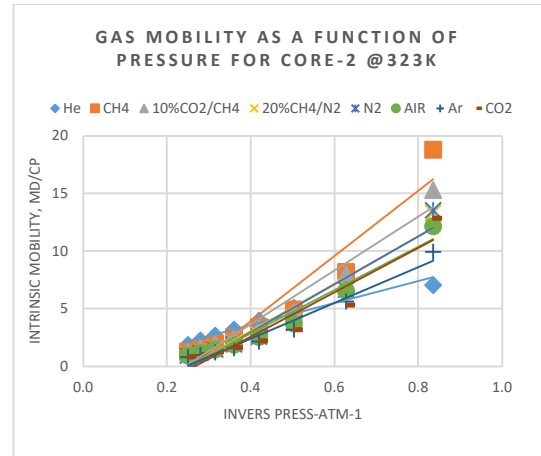
b.
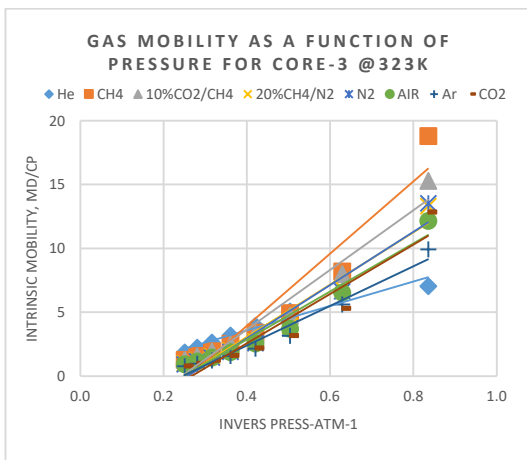
c.
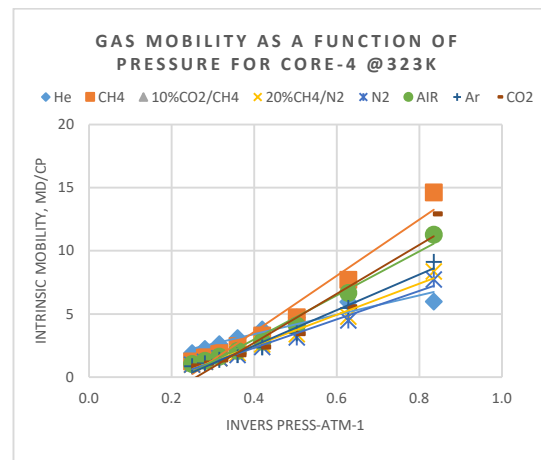
d.
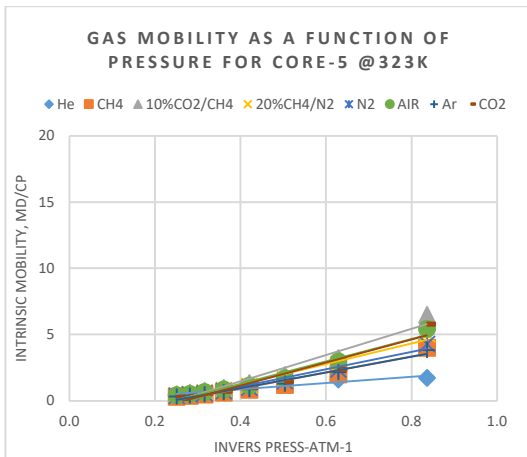
e.

Figure 7-30a-e Graphs showing the relationship between mobility and pressure for five cores samples and eight gases.

CH$_4$ mobility was observed to be consistently most responsive to finite change in pressure in all the core samples, as demonstrated in Figure 7-31. The magnitude of response is affected by porosity and pore sizes. As can be seen, the pore size of Core-1 and 2 are the same (15nm); however, the gas intrinsic mobilities are generally more sensitive to pressure in Core-1 (porosity 13%) than in Core-2 (porosity: 3%). Porosity variation is deduced to explain the response in this case. This phenomenon was also observed between Core-4 and 5 (6000nm). Nevertheless, when the porosities are close or similar, such as in the case of Core-1 (13%) and Core-4 (14%), it is observed that the pore effect becomes dominant.

It should be noted that the magnitude of the effect of porosity is generally higher than that of pore size. This confirms that large pore size is not useful to fluid flow if there are less of it in the porous media's bulk volume or when they are not effectively connected. This information is useful for injection, mobility control and reservoir heterogeneity (permeability) management of EOR gases
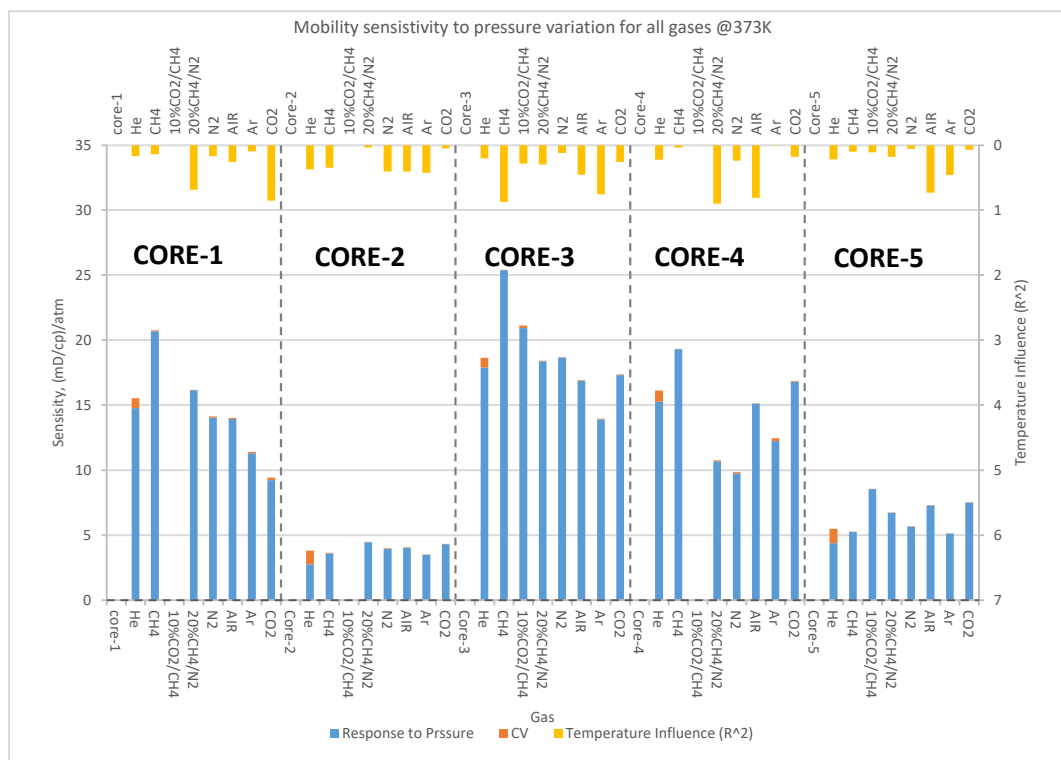
Figure 7-31 Intrinsic mobility response to pressure change as a measure of sensitivity.

When the temperature was added to the analysis to investigate the influence of temperature variation on mobility response to pressure, it was observed that the R^2 (yellow bars in Figure 7-31) between temperature variation and mobility-pressure sensitivity is generally below 50% for the gases and core samples, except for some EOR gases and mixtures, such as CO_2 in Core-1, and CH_4 in Core-3. However, the behaviour is not consistent across the core samples and gas properties, such as molecular weight. This inconsistency may be due to other flow mechanisms not covered in this research.

Consequently, numerical analysis of the experimental data reveals that CH_4 mobility responded to change in pressure the most in Core-1, 3, 4 with a gradient of 23, 27, and 23 mD.atm^{-1}, respectively. For Core-1 and 3, CO_2 mobility is observed to be the EOR gas least sensitive to pressure. Interestingly, for Core-2 and 5, CO_2 mobility is the most sensitive to pressure variation in the cores, followed by Air, N_2, and then CH_4. Considering the experimental parameters and conditions that generated these data, the intuitive explanation for the observed reversal of mobility sensitivity to pressure between CH_4 and CO_2, other than porosity, could be traced to the radial thickness and surface area of the cores. Core-2 (15nm) and Core-5 (6000nm) are thicker than Core-1 (15nm) and Core-4 (6000nm) and have more surface area. This information would be necessary when selecting a gas for EOR implementation in a reservoir that has a greater radial extent. It would also lend utility to determining the distance between injection and production wells.

The mobility sensitivity of the eight gases could not be linearly traced to gas properties of molecular weight, kinetic diameter and specific heat. The relationship's complexity is at best described by a higher-order polynomial equation (4th order).

In summary, mobility sensitivity to pressure has been found to exist for EOR gases. The magnitude and impart of reservoir parameters and conditions can be analogically drawn from the experiments. The factor determining the order of mobility sensitivity was found to be based on porosity, radial thickness and

surface area but not pore size. Overall, the temperature has an impact on how mobility sensitivity responds to pressure for some gases. Gas properties could not explain the mobility sensitivity to pressure. These plots would be useful in reservoir engineering to estimate gas mobility variation that may occur during gas injection. This section has also contributed to fulfilling the third objective of this research.

7.7.4 Gas Flow rate Sensitivity to Temperature

Figure 7-32 to Figure 7-34 show the responses of EOR gases to temperature in each of the core samples. Two pressure isobars have been selected for investigation. These are low pressure (0.20atm) and high pressure (3.00atm). The graphs in Figure 7-32a-d show that the flow rate relationship to temperature in a reservoir with mesopore size (15nm) is complicated perhaps due to the flow mechanism. The gas volume-temperature relationship for all the gases sampled in Core-1 (15nm, 13%) and Core-2 (15nm, 3%) was between 4th and 5th order polynomial. These results negate Charles law that states that volume is directly proportional to temperature at constant pressure. The porosity, thickness and surface area were irrelevant in affecting the flow pattern in Core-1 and 2. This phenomenon could be attributed to the type of flow mechanism taking place in the media, the pore size and mean free path of the gases being relatively close to the mesopore's size compared to the larger pore core samples may be responsible.
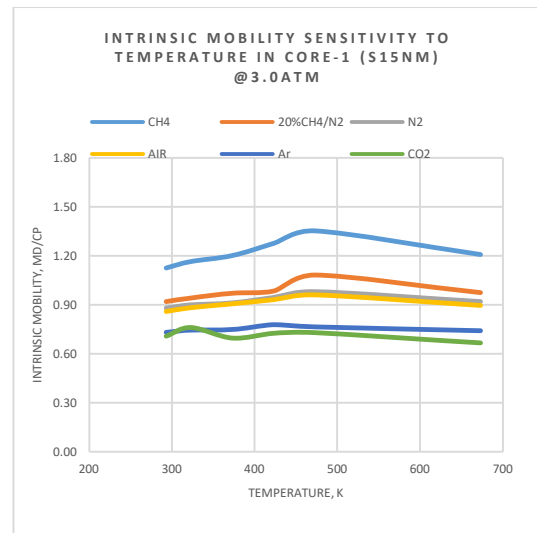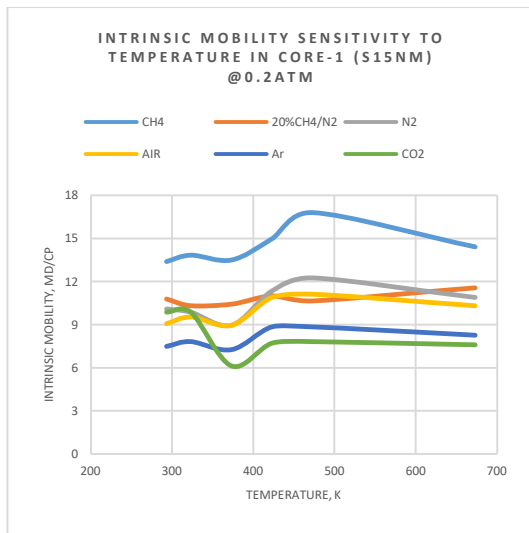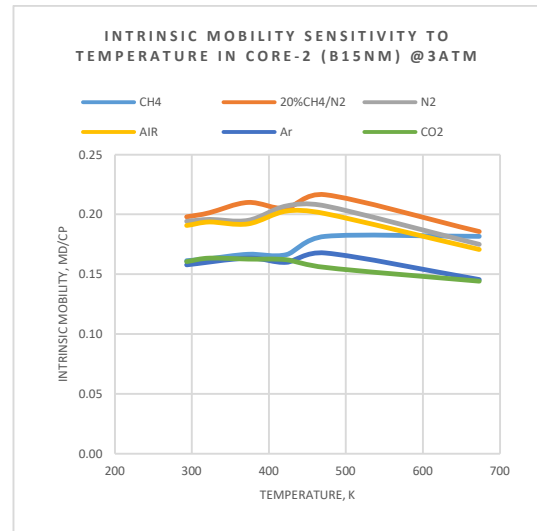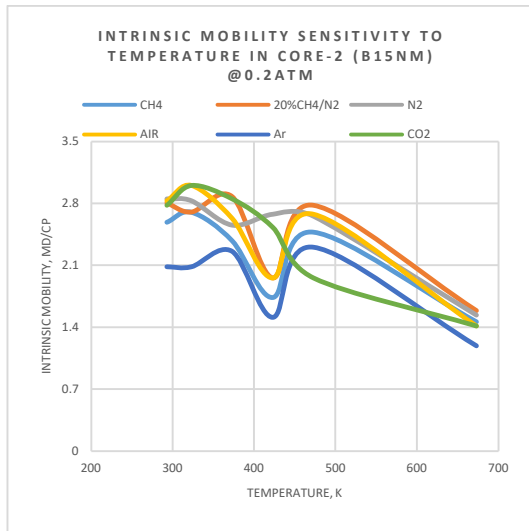
Figure 7-32 EOR gas injected PV sensitivity to core temperature in core-1 and 2 (15nm) at injection pressure points 0.20 and 3.00atm.

It is theoretically expected that a larger pore would encourage a higher flow rate or increased pore volume (assuming the mean pore size is proportional to the pore throat size distribution). It was observed that in Core-3, 4 and 5 with pore sizes of 200nm, 6000nm and 6000nm, respectively, Charles law was aptly obeyed. The gradients of the plots are an indication of the sensitivity of the gases to change in temperature. They depict the potential measure of the change in injected gas volume due to temperature variation between injected gas temperature and *in situ* core (reservoir) temperature.

CH$_4$ was observed to be the most sensitive to temperature variation for the Core-3, 4, and 5 with gradients of 0.027cm^3/K, 0.055 cm^3/K, 0.022 cm^3/K, respectively. Notice that at 3.00atm, all the gases PV sensitivity to temperature in Core-4 is higher than that of Core-5 even though they are both 6000nm in pore size. The intuitive explanation for this would be the difference in porosity, surface areas (entering and internal), and thickness. It is expected that a longer radial thickness (Core-5) would imply a longer residence time for heat exchange to take place between the permeating gas and the hot porous wall than in slimmer radial thickness (Core-4). However, it appears the thickness is not a strong factor to influence heat exchange compared to the other three factors. Therefore, it can be concluded that the effective internal surface area is sovereign to effective length for a porous media. It further explains why heat transfer flux is a quotient of the area and not length.

It was also observed that the operating or injecting pressure is also critical to how gases respond to temperature. As shown in Figure 7-33a and Figure 7-34a and c, the plots are taken at a low gauge pressure of 0.20atm. At this pressure and in all the core samples, the gas flow rate response to temperature cannot be described by simple proportionality. However, in Figure 7-33b and Figure 7-34b and d, at 3.00atm gauge pressure, the temperature responses could be characterised by linear regression for most of the gases and core samples, unlike Core-1 and 2. Expectedly due to the small pore size (15nm) of the two samples rather than their respective porosity of 13% and 3%.
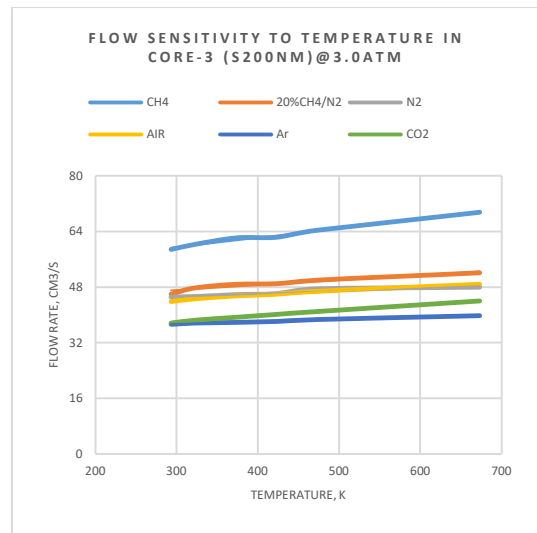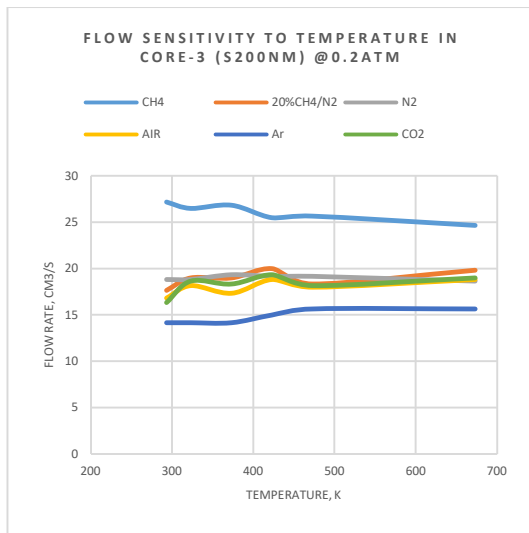
a.   b.

Figure 7-33 EOR gas injected PV sensitivity to core temperature in Core-3 (200nm) at injection pressure points 0.20 and 30atm.

Furthermore, in Figure 7-35, the respective gas properties were plotted against the respective sensitives for the EOR gases, non-EOR gases, and gas mixtures. The graph indicates that PV-temperature sensitivity does not correlate with the gas properties.

In summary, Charles law cannot be used to describe gas PV sensitivity to temperature in mesopore porous media for pressure range 0.20-3.00atm. Charles law cannot also be used to describe gas PV sensitivity to temperature at low pressure (0.20atm) for pores sizes 200nm and 6000nm. However, at 3.00atm, Charles law begins to manifest in the PV-Temperature relationship. For core samples that obey Charles law, it is observed that CH_4 PV is the most sensitive to temperature.
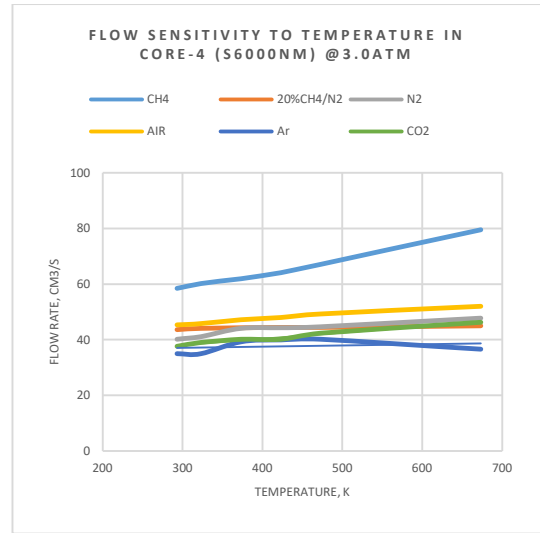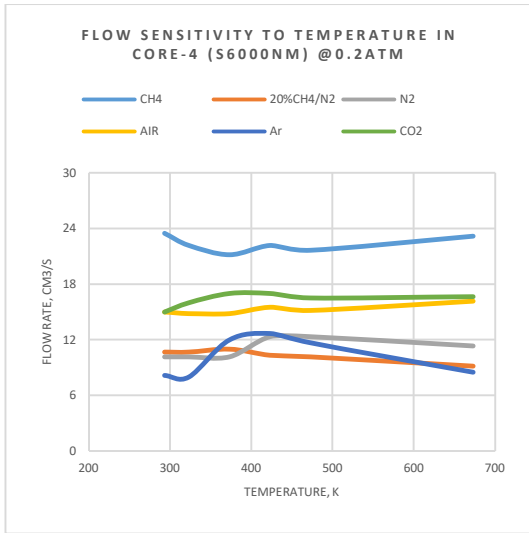
a.

b.
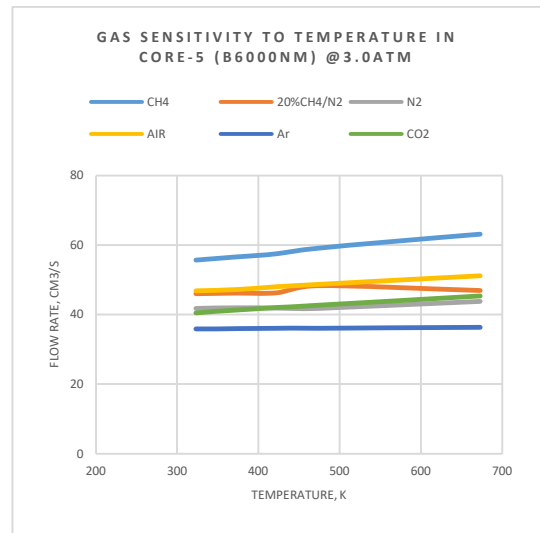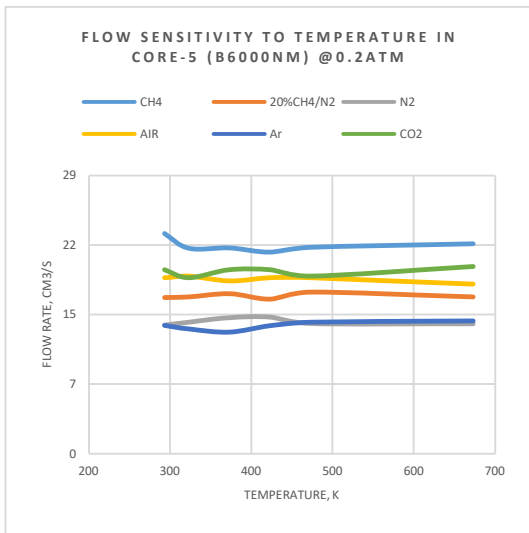
c.

d.

Figure 7-34 EOR gas injected PV sensitivity to core temperature in Core-4 and 5 (6000nm) at injection pressure points 0.20 and 3.00atm.
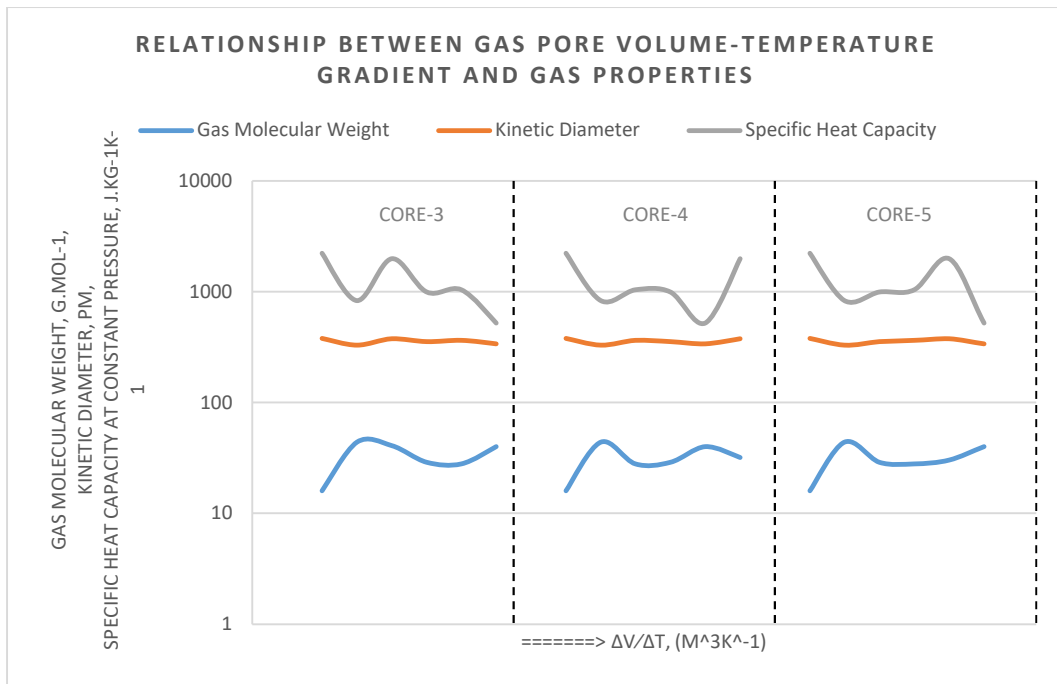
Figure 7-35 Effect of gas properties on gas PV-temperature sensitivity in Core-3, 4 and 5

Porosity influences PV sensitivity. Molecular weight, Kinetic diameter and Specific heat do not correlate with PV sensitivity to pressure.

7.7.5 Intrinsic Mobility Sensitivity to Temperature

The temperature effect on all the gases in Core-1 and 2 was difficult to describe for all pressure points (Figure 7-36a-d). It was observed that the effect of variation in temperature on the intrinsic mobility of the gases was not significant for core-3, 4 and 5 at an injection pressure of 3.00atm (Figure 7-36a,b and Figure 7-37b,d). Like the PV sensitivity graph, the intrinsic mobility response to temperature at a low injection pressure of 0.20atm was found to be a complicated polynomial of a higher order.
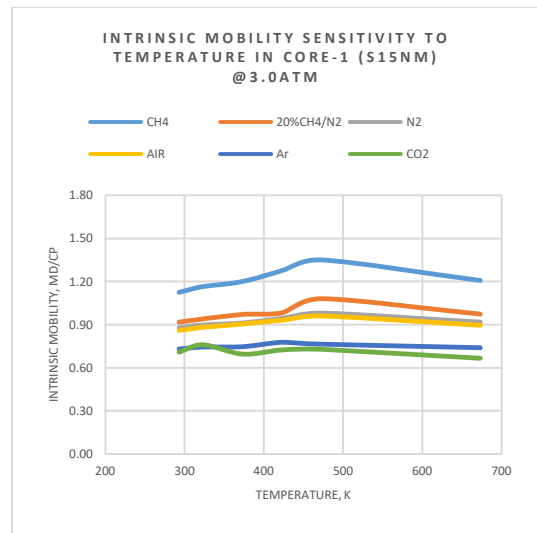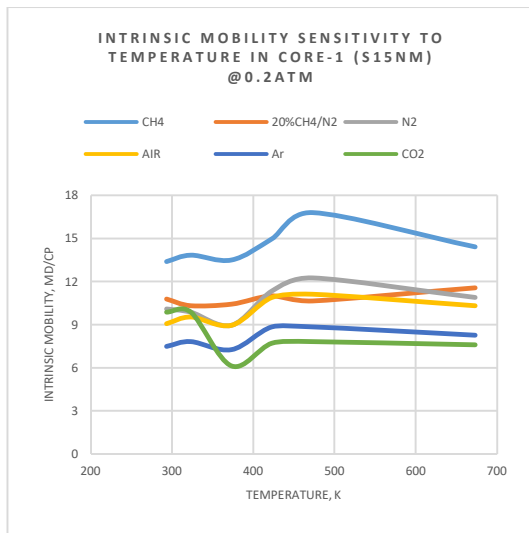
a.

b.
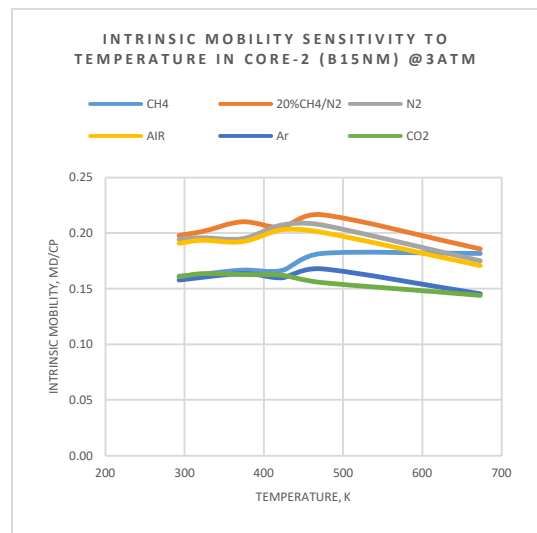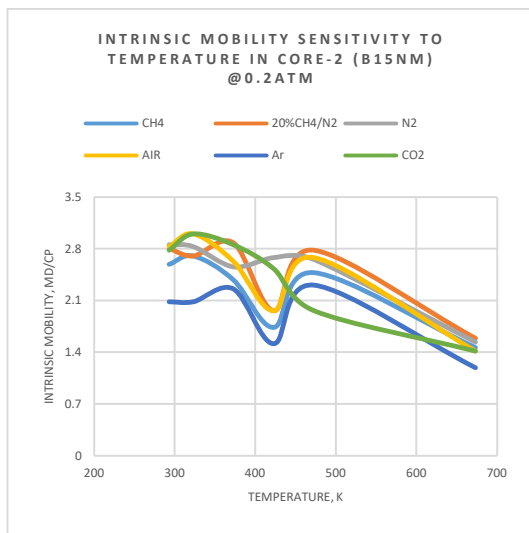
c.

d.

Figure 7-36 EOR gas intrinsic mobility sensitivity to core temperature in Core-1 and 2 (15nm) at injection pressure points 0.20 and 3.00atm

From the data mining and experiment analyses, it has been deduced that, although reservoir temperature discrimination occurs for CH_4 EOR in Figure 5-5 (data mining Phase I), it is not an effective criterion for selecting gases for immiscible gas EOR processes based on intrinsic mobility. Nevertheless, this does not undermine the observed positive temperature effect on the gas flow rate. Therefore, based on the flow rate, the temperature is significant for selecting EOR gases. Since the optimisation curve is a matrix that

combines intrinsic mobility and flow rate, the net effect of temperature is considered to be captured by the optimisation curves.
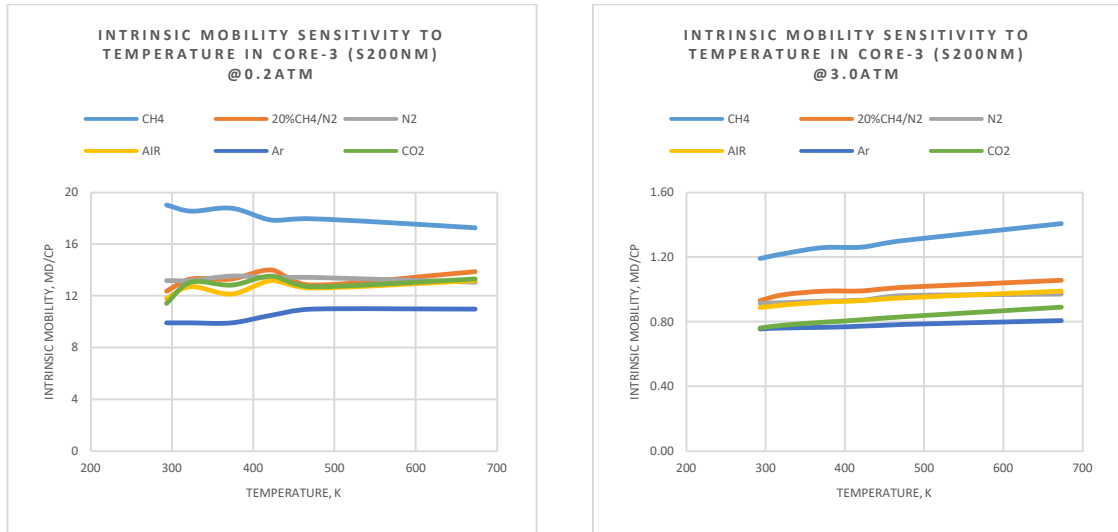
a.   b.

Figure 7-37 EOR gas intrinsic mobility sensitivity to core temperature in Core-3 (200nm) at injection pressure points 0.20 and 3.00atm.
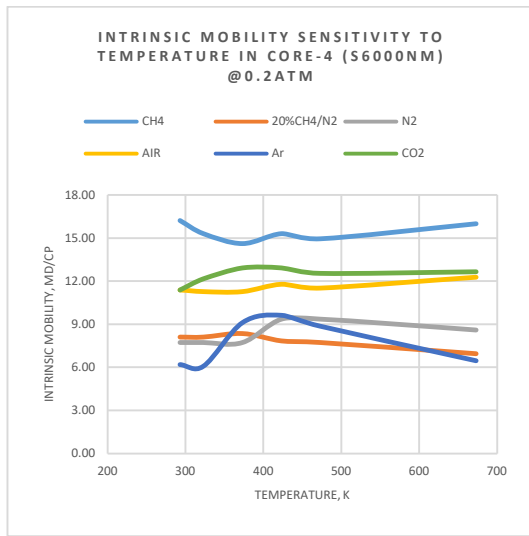
a.
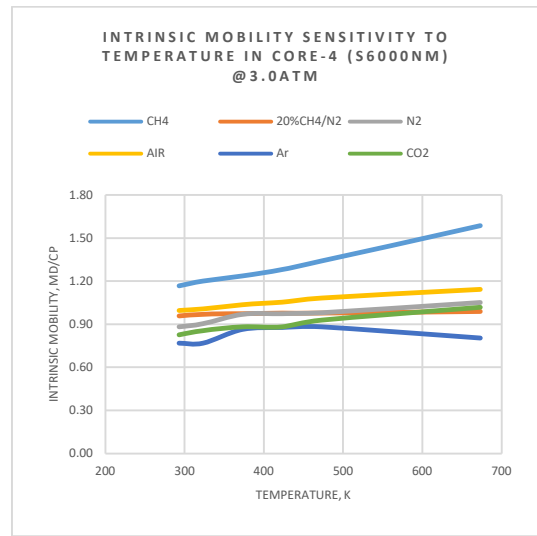
b.
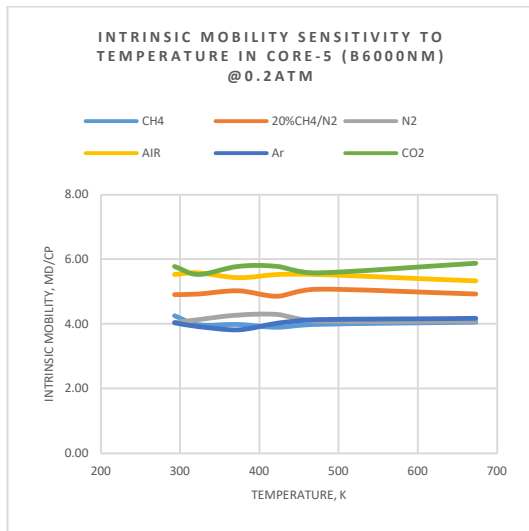
c.
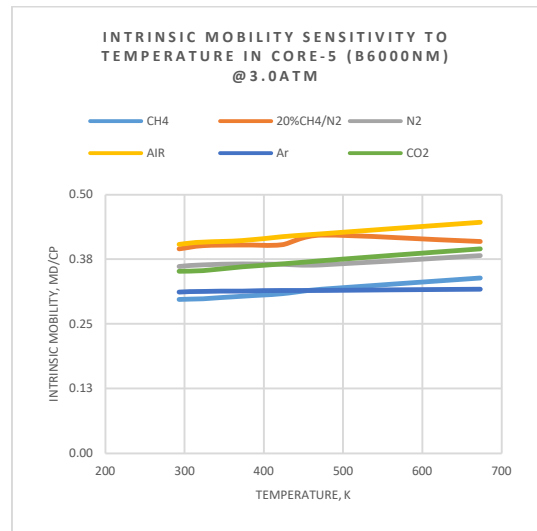
d.

Figure 7-38 EOR gas intrinsic mobility sensitivity to core temperature in Core-4 and 5 (6000nm) at injection pressure points 0.20 and 3.00atm.

7.8 Velocity Performance Evaluation of EOR Gases in Core Samples

Figure 7-39a and b, Figure 7-40, and Figure 7-41a and b are graphs showing the velocity performance of EOR gases as a function of pressure and temperature of the five core samples. It was observed that He consistently has the highest interstitial velocity. While the least velocity switches between

Ar and CO_2. Ar and CO_2 behaviour is observed to depend on porosity and operating temperature. Porosity and pore size were observed to affect the magnitude of gas interstitial velocity.
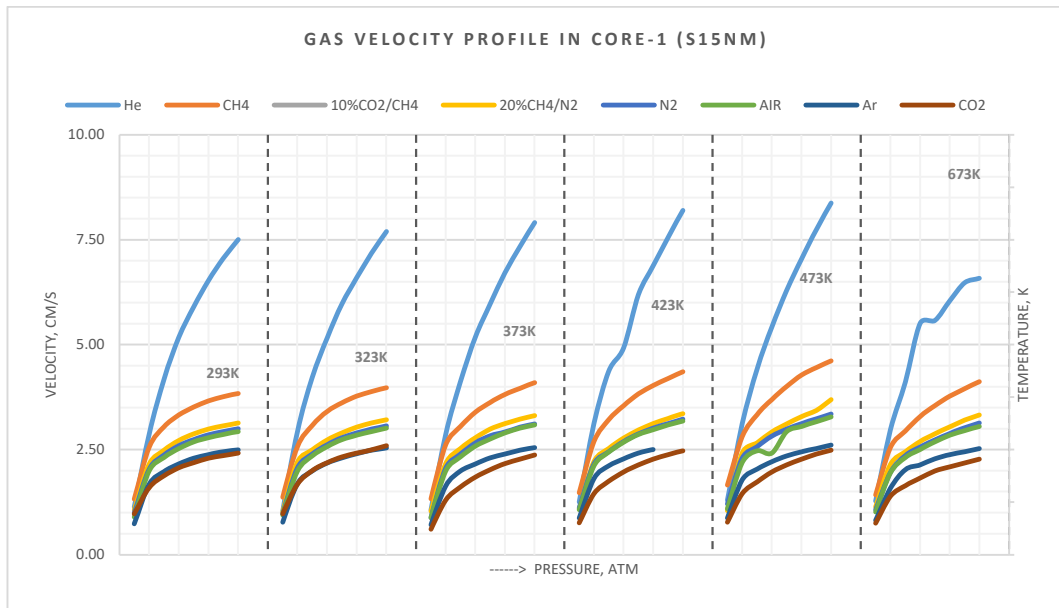
a.
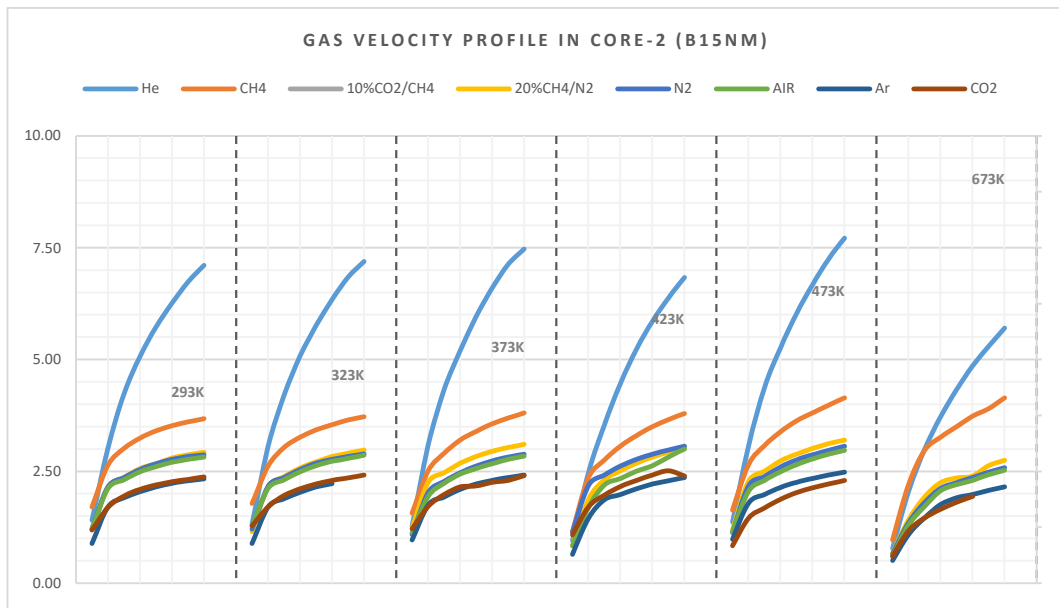
b.

Figure 7-39 Graphs showing the velocity performance of EOR gases as a function of pressure and temperature in samples (a) Core-1, 14nm, (b) Core-2, 15nm.

The lowest velocity is recorded in Figure 7-40, Core 3, which is a relatively higher porosity (20%). The highest set of values for velocity was registered

in Figure 7-41b, Core-5, which is a low porosity (4%) and large pore (6000nm) sample. Suppose this observation is attributed to Bernoulli's theorem, which is a statement of continuity favouring higher velocity for flow through a constriction. In that case, the observation in Figure 7-41b suggests that porosity is a stronger measure of bulk constriction than the pore size. Bernoulli's explanation runs into problems when one applies the same explanation to Figure 7-39b, Core-2, which has both lower macroscopic (porosity 3%) and microscopic (15nm) constriction. However, the general velocity profile is lower in Core-2 than in Core-5.
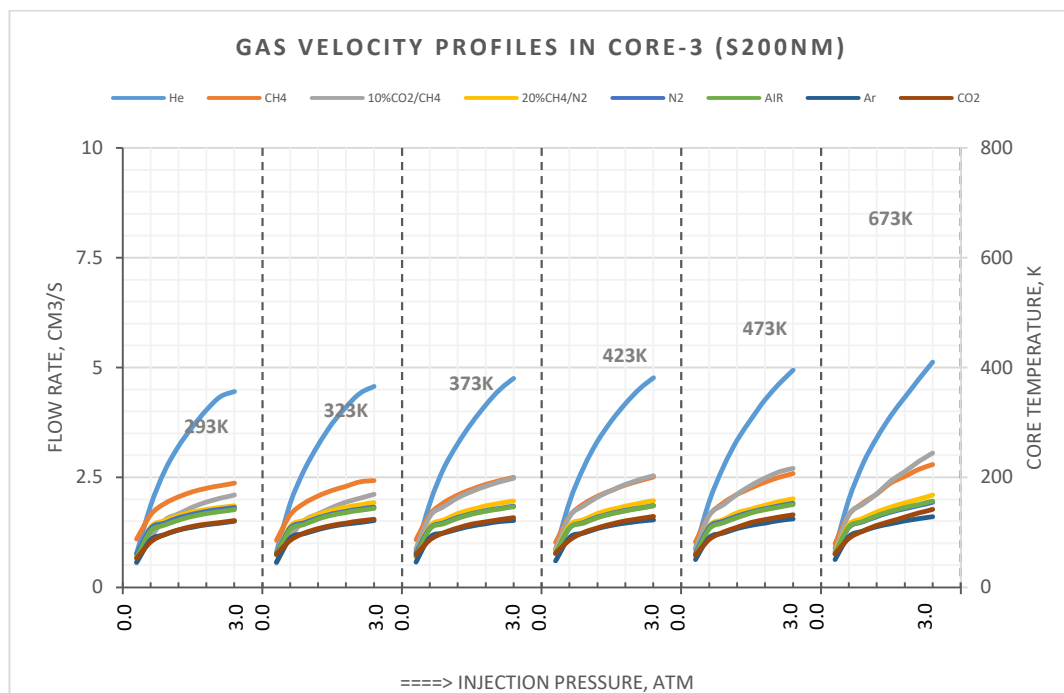
Figure 7-40 Graphs showing the velocity performance of EOR gases as a function of pressure and temperature in sample Core-3, 200nm.

Overall, CH_4 was observed to have the highest velocity among the EOR gases in all core samples. Determining the gas with the least interstitial velocity depends on the core samples' characteristics and operating temperature. In Core-4 and 5, N_2 and CO_2 shared similar velocity values (Figure 7-41b). The parameter these two samples share in common is pore size. Therefore, it could be deduced that pore size influences the dynamism for gas interstitial velocity grading.
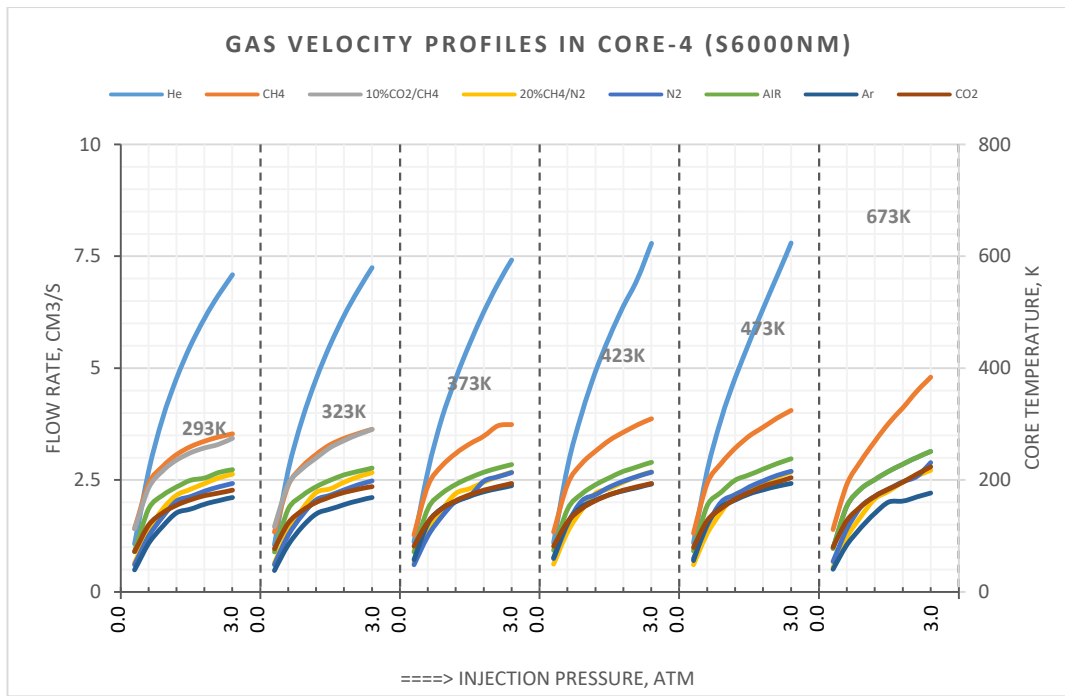
a.
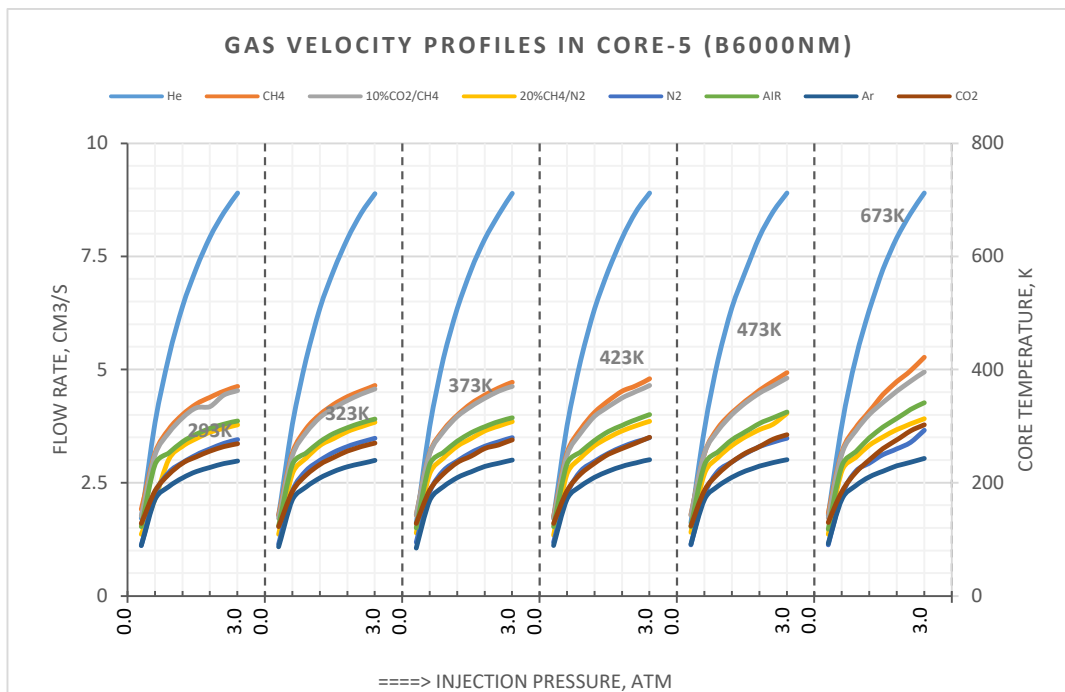
b.

Figure 7-41 Graphs showing the velocity performance of EOR gases as a function of pressure and temperature in samples (a) Core-4, 6000nm (b) Core-5, 6000nm.

In summary, it has been demonstrated that CH_4 consistently possesses the highest interstitial velocity in all the core samples, pressure and temperature

points investigated. Considering the velocity position switching among the other EOR gases, based on these experiments, it can be concluded that velocity is not discriminated by molecular weight. The evaluation of EOR gases based on velocity is not well documented in journals like other properties. The few available documentations have conflicting conclusions. Therefore, it was difficult to find material to compare these results.

Furthermore, the implication of high or low velocity was based on other oil production concepts and analogies, such as the critical oil production rate, transfer of momentum, coning and liquid loading as described in journals (James, Henry and Mike 2008). It is, therefore theoretically, expected that when in contact with an oil droplet, the incoming gas would use its velocity to displace oil in line with the principles of conservation and transfer of momentum; otherwise, the gas would break the displacement front and cause viscous fingering. Furthermore, recall the capillary number parameter discussed in section 2.3.1.6, and Eq. 2-18 indicate that the Capillary number can be favourably increased by increasing the interstitial velocity. The coupling of positive injection velocity and recovery has been stated in experiments, such as Lu and Pope (2017). There are also investigators whose experimental claims are contrary to this equation, such as Al-Abri, Hiwa and Robert (2009) and Lu, Weerasooriya and Pope (2014). In the transport of water droplets in liquid loading problem, Guo (2019) defined a minimum gas velocity required to produce trapped liquid droplets as the sum of the minimum gas velocity required for floating the liquid droplets, that is keeping the droplets in suspension and the displacement velocity of the droplets. If this is applied to the gas displacement of oil droplets in reservoir pores, it, therefore, means that high velocity is a favourable expectation to compensate for the carriage and displacement components. Consequently, CH_4, being the gas with the highest velocity in these experiments, is the most competitive EOR gas.

7.9 Momentum Performance Evaluation of EOR Gases in Core Samples

A measure of the interstitial momentum profiles of the various gases has been investigated to determine which of the EOR gases is most competitive in the domain of this parameter. Figure 7-42, Figure 7-43 and Figure 7-44 show that gas momentum is affected by pressure and temperature. The effect of temperature is not as marked as the effect of pressure. Their molecular weight quite influenced the magnitude of the momentum of the respective gases. However, the coefficient of determination R^2 between momentum and molecular weight hardly attained 0.70 for all pressure and temperature range sampled. Generally, CO_2 was observed to have the highest momentum, while CH_4 is the least momentous of the EOR gases for temperatures less than 473K.
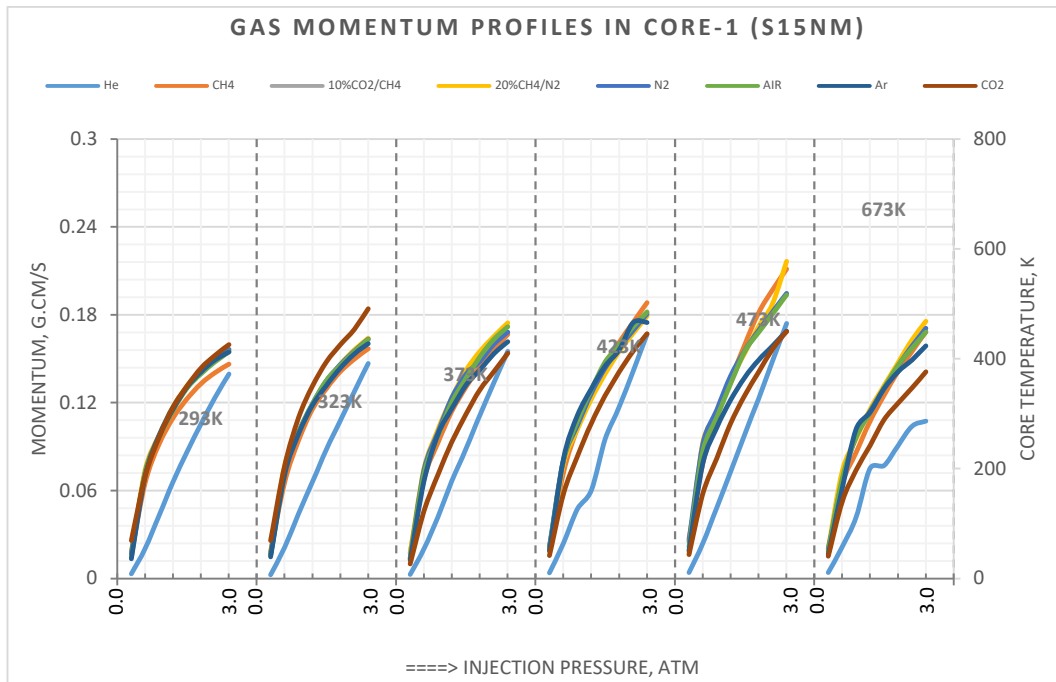
a.
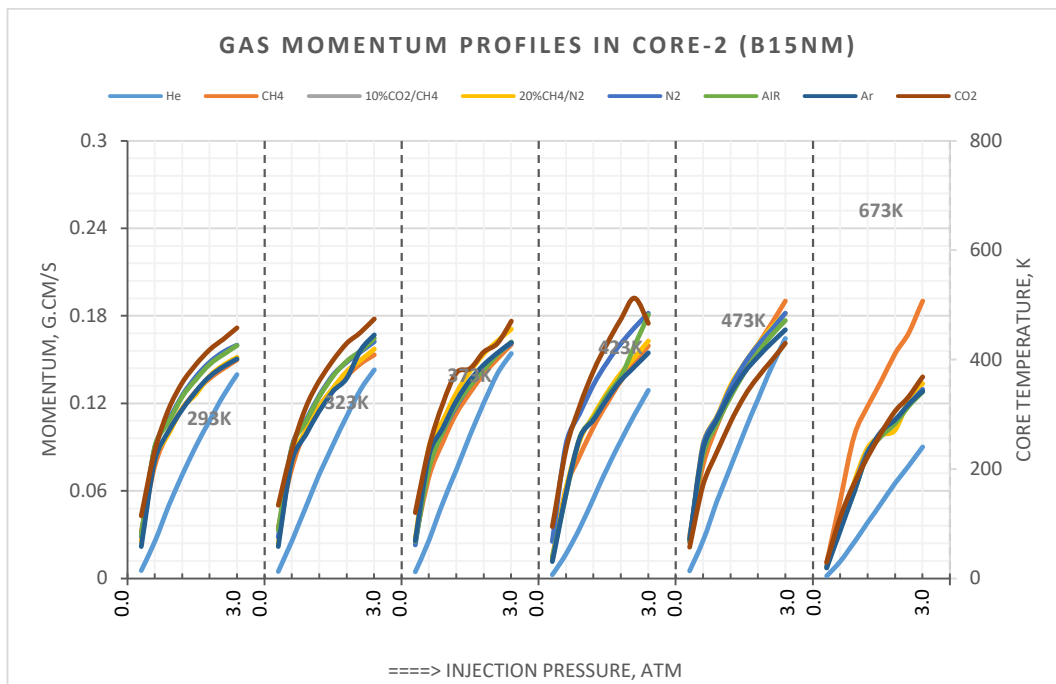
b.

Figure 7-42 Graphs showing the momentum performance of EOR gases as a function of pressure and temperature in samples (a) Core-1, (b) Core-2.
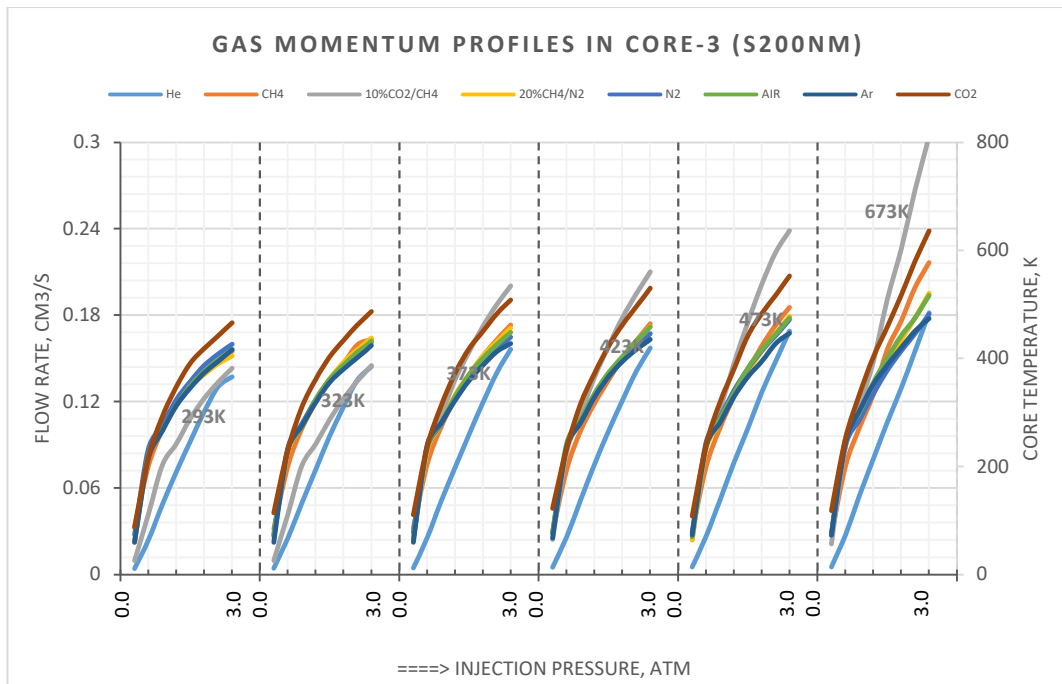
Figure 7-43 Graphs showing the momentum performance of EOR gases as a function of pressure and temperature in the Core-3 sample.

The effect of pore size and porosity on momentum is quite established across the graphs. Figure 7-43 shows that the momentum of the gases is generally low in higher porosity samples (Core-3:20%, Core-4:14%, and Core-1:13%) than the other lower porosity core samples (Core-2:3% and Core-5:4%). In Figure 7-44a and b, values for Core-4 (14%) are lower than values for Core-5 (4%), even though they share the same large pore size (6000nm). Figure 7-42a and Figure 7-44a values for Core-1 (15nm) are higher than Core-4 values, even though they both share similar porosity and surface area. All these indicate that pore size and porosity are determining factors for the interstitial momentum available to gas in displacing oil from reservoir pores. The velocity and momentum profile significantly mirror each other.
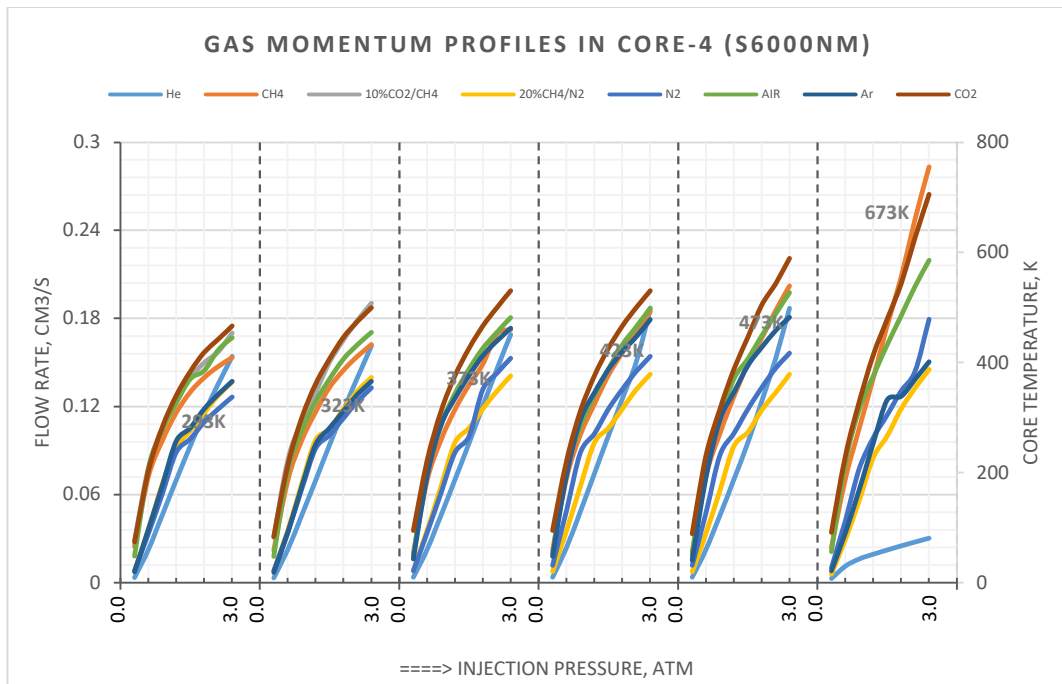
a.
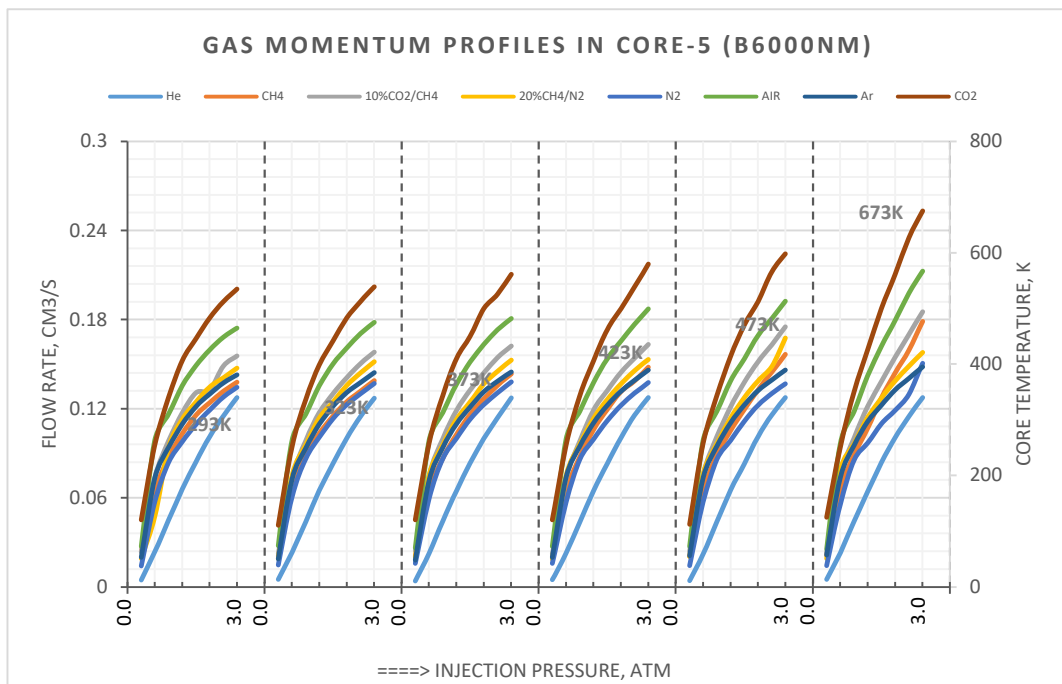
c.

Figure 7-44 Graphs showing the momentum performance of EOR gases as a function of pressure and temperature in samples (a) Core-4, (b) Core-5.

The gas momentum concept has not been discussed in journals with respect to gas-oil displacement. However, based on the conservation of energy, it is expected that there should be momentum transfer between the displacing

fluid and the stagnant oil droplets at the point of first contact and displacement front. Consequently, favourable momentum should be the one that is high enough to displace the oil in the direction of the producing well. Therefore, high momentum is the desired optimisation objective in enhancing oil recovery.

In summary, the interstitial magnitude has been observed to be affected by pore size and porosity. On the momentum parameter basis, it has been established that CO_2 is the most competitive and CH_4 is the least.

7.10 Summary of Phase II

Rigorous analyses of the experimental data within the context of 24 geological and engineering quantities have been concluded. The analogy of the selectivity index was successfully applied to quantitatively compare and rank the gas performances. Selectivity index is used here as a quantitative method to assign a numerical ranking to various competing gas alternatives. Given an EOR property or parameter for evaluation (e.g., gas cost), the gas with the desired outcome (in this case, gas with the lowest cost value) is used to divide itself and the cost values of the other competing gases. The quotients thereof are the selectivity indexes of the respective alternatives. The optimisation requirement for the evaluated EOR quantity ensures that all the selectivity indexes are usually less than one except that of the desired gas, which should be equal to unity. Selectivity and permselectivity have been extensively used to evaluate fluid processes such as gas and ion separation, and transport rates of various components through porous media (Castricum *et al.* 2015, Grot 2011, Millet 2011, Ranade and Bhandari 2014, and Tonezzer *et al.* 2019). In this study, 24 EOR parameters and properties were evaluated using this method. And the respective selectivity indexes of each gas were summed up to give the grand values that are considered a measure of the relative competitiveness (or Competitive Index) of the gases, as shown in Table 7-3.

It has been demonstrated in Table 7-3 that CH_4 and CO_2 are the most competitive when all the selectivity indexes were summed up. The least is N_2, with 17.2 index points. It is also shown that overall, the comparative performance of all the gases in percentage is above 90%.

Table 7-3 shows the overall competitive indexes of the respective EOR gases for 23 examined quantities.

	CH_4	CO_2	Air	N_2
Competitive Index	18.37	18.32	17.32	17.17
Comparative Performance	100%	100%	94%	93%

Therefore, based on the gas performance in the sample, it is concluded that CH_4 offers relatively more EOR opportunities.

8 PHASE III: DATA MINING AND EXPERIMENT COUPLING

It was essential to couple the results from the data mining and the experimental phases. This facilitates understanding the common parametric relationships between the displaying fluids and the displaced fluid. Functional reservoir parameters and properties have been coupled here. The objective functions were also coupled for performance evaluation in the following sections.

8.1 Parameters and properties

These coupled reservoir parameters and fluid properties have been extensively described in the literature review and have been experimented on.

8.1.1 Viscosity coupling

Figure 8-1a and b show the viscosity characterisation of oil in gas EOR reservoirs and the laboratory results from the viscosity characterisation of gases used in displacing reservoir oil. Both graphs share similar characterisation features from CH_4 to Air. The viscosity ranking of the gases is qualitatively related to their respective molecular weight. Furthermore, the CVs of both graphs have the same shape. This is a strong indication that there are possible synergistic opportunities between the reservoir oil and the EOR gases. Based on the CVs, N_2 EOR processes and gas are the most sensitive to viscosity variation. The graphs generally indicate that viscosity increases with pressure for all gases. The result in this research validates Qasem *et al*. (2016).

a.

b.
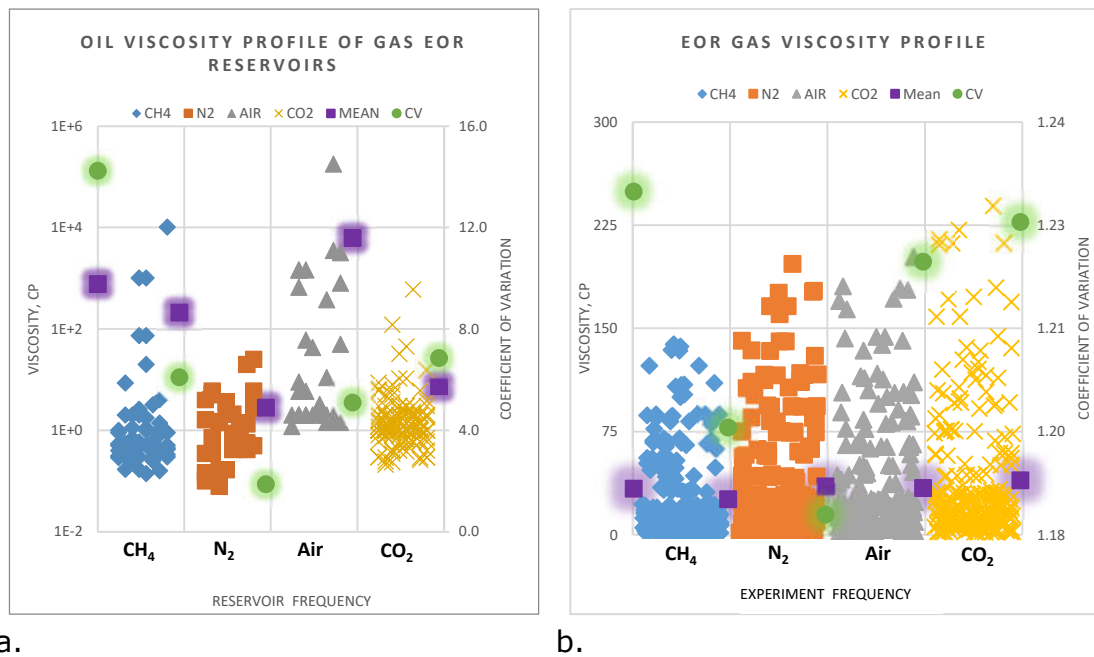
Figure 8-1 Viscosity coupling of (a) reservoir and (b) experimental data.

Similarly, the two viscosity sets correspond significantly. It is suggestive that CH_4 is suitable for low viscous oil, and CO_2 is most appropriate for high viscous oil. However, for competitive evaluation, based on the role of viscosity in capillary number, viscosity ratio, and mobility ratio in estimating oil recovery, CO_2 could be considered the most competitive coupling gas by its sheer comparatively high viscosity in the experimental data. The competitive ranking for viscosity is, therefore: CO_2, N_2, Air and CH_4.

8.1.2 Permeability coupling

Figure 8-2a and b couple permeability characterisation of EOR oil and gases. In Figure 8-2a, the permeability and CV distribution suggest CH_4 EOR projects are strongly correlated to high permeability reservoirs, but CH_4 does not possess corresponding conduction in the pores, as shown in Figure 8-1b. N_2 and CO_2 meet a more comprehensive range of reservoir permeability. The shape of the mean values and CVs for the field and gas clusters are closely related. Kantzas, Bryan, and Taheri (2012) showed that different gas would have different permeability, this is so in Figure 8-2b. The result here does not fully support Amirkhani, Harami and Asghari (2020), where the authors

stated that gas permeability in increasing order is $CH_4 > N_2 > CO_2$. The order in this study is $N_2 > CH_4 > CO_2$. Amirkhani, Harami and Asghari (2020) acknowledged significant adsorption mechanisms in their porous media, this may have contributed to how the respective gases permeability manifest themselves, thus the difference between this study and theirs. It is seen in Figure 8-2b that permeability to gases is not related to their molecular weight, as suggested by Fanchi (2007). Further regression analysis gave the relationship an R^2 less than 0.02. In addition to pressure, there may be other mechanisms at play, such as pore heterogeneity, that may have caused the permeability to deviate from the molecular weight model. Mobility is a function of permeability, such that high displacement fluid permeability increases mobility ratio, which is undesired. CO_2 has the least permeability; therefore, it is the most competitive. The competitive ranking for permeability is, therefore: CO_2, CH_4, N_2 and Air.

a.   b.
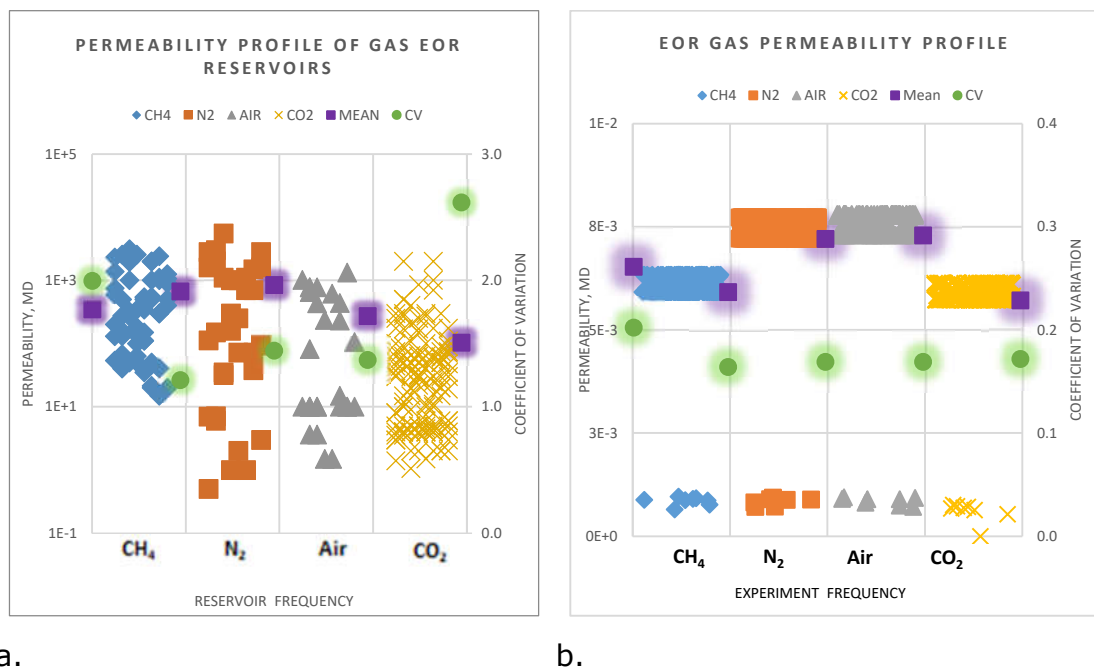
Figure 8-2 Permeability coupling of (a) reservoir and (b) experimental data.

8.1.3 Molecular weight coupling

The molecular weight profile in Figure 8-3a and b show that field data is somewhat segregated by molecular weight. The mean molecular weight distribution for the field cluster corresponds with the EOR gas molecular weight in Figure 8-3b except for Air. CH_4 and N_2 correspondingly favour reservoirs with lighter oil. In contrast, CO_2 and N_2, which are heavier gases, favour relatively heavier oil. There is no competitive basis for ranking here.

a.   b.
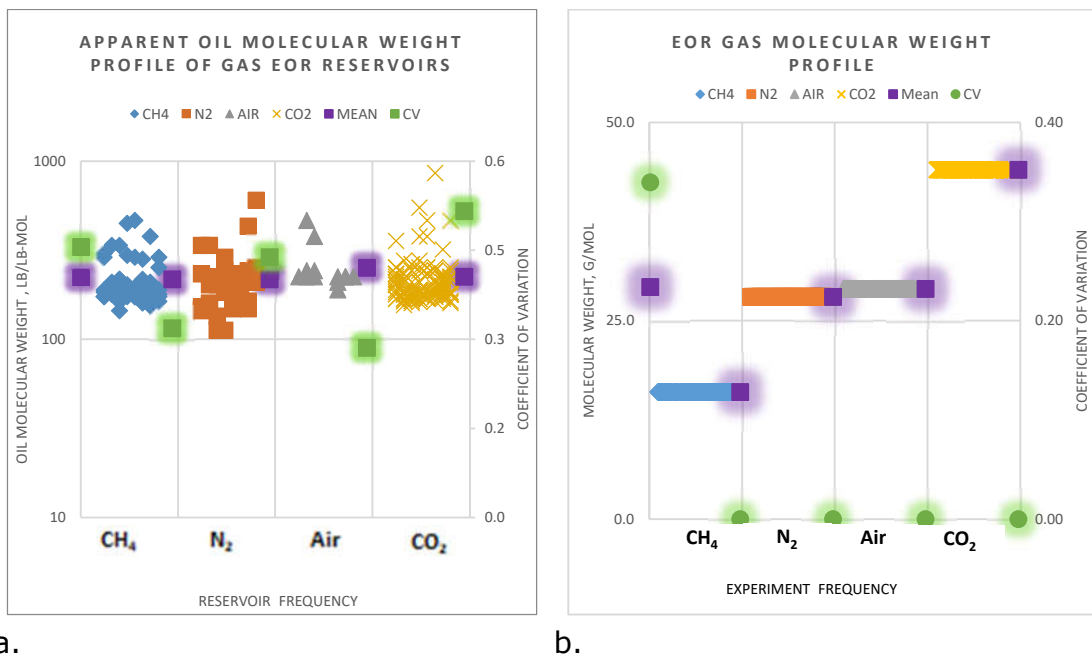
Figure 8-3 Molecular weight coupling of (a) reservoir and (b) experimental data.

8.2 Objective functions

The objective functions facilitate performance evaluation and quantity optimisation.

8.2.1 Potential Volume rate coupling

Figure 8-4a characterised the potential volume available for gas EOR displacement. Figure 8-4b is the experimental characterisation of gas volume. EOR reservoir volume is demonstrated not to be strongly characterised (Figure 8-4a). Nevertheless, it has been earlier stated that the oil recovering

factor increases with the injected pore volume. Therefore, in this coupling, CH_4 offers the most pore volume for equivalent pressure (Figure 8-4b), hence the most competitive. The competitive ranking for potential volume is, therefore: CO_2, N_2, Air, and CH_4.
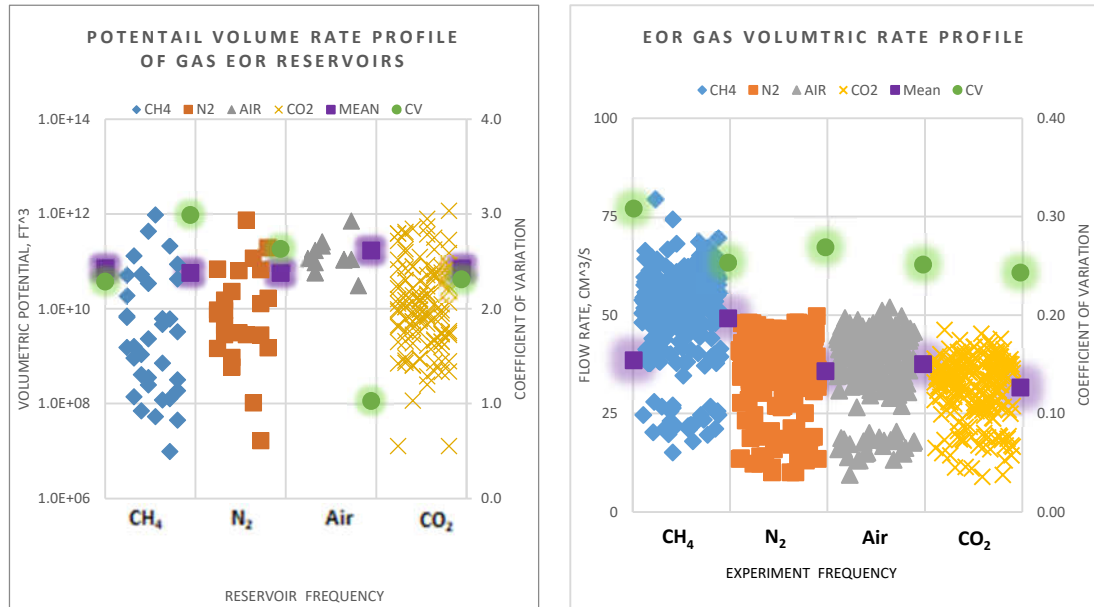
a.   b.

Figure 8-4 Potential Volume rate coupling of (a) reservoir and (b) experimental data.

8.2.2 Mobility coupling

It has been earlier mentioned (Abunumah, Ogunlude, and Gobina 2021a), that the intrinsic mobility ratio (a simplified relative mobility term) between the displacing gas is a measure of the displacement performance of the respective displacing fluids and oil recovery. The coupling in Figure 8-5a and b indicates that the reservoir oil in EOR projects ranks similar to the displacement gases. A visual and mathematical comparison reveal that the mobility ratio with CO_2 gas provides the least intrinsic mobility ratio for all the reservoirs in Figure 8-5a.
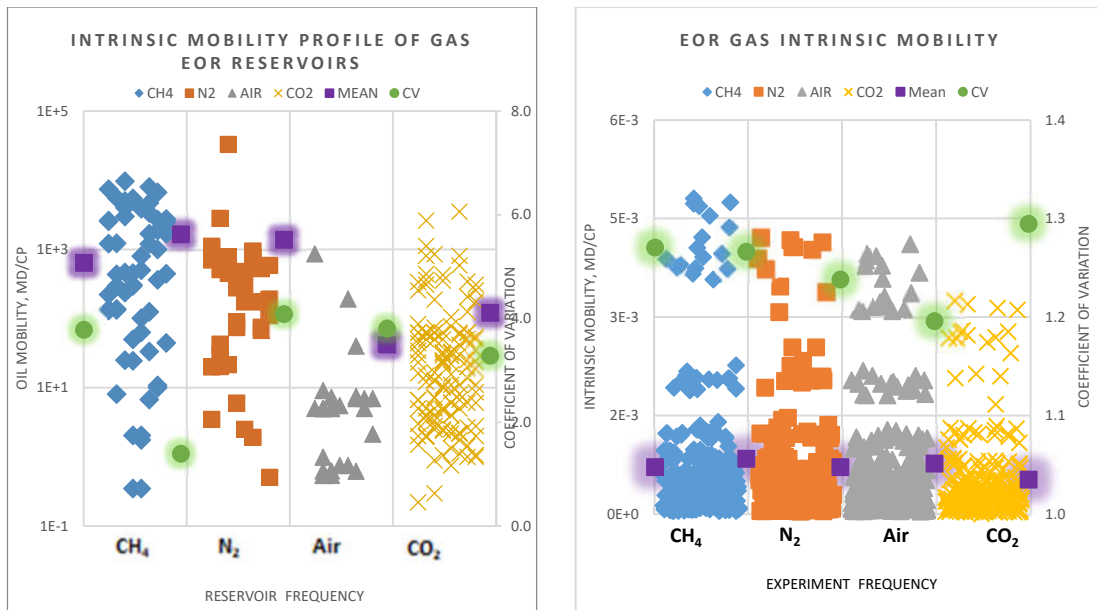
a.   b.

Figure 8-5 Mobility coupling of (a) reservoir and (b) experimental data.

The mean mobility and CV values in each graph contrast each other. The CVs in the field clusters have a convex shape (Figure 8-5a), while the gases have a concave shape (Figure 8-5b). It is seen that CH_4 EOR projects are very sensitive and may be significantly affected by mobility variation (Figure 8-5a). In contrast, CH_4 mobility easily varies when disturbed (Figure 8-5b). It was noted that the magnitude of the respective gas mobilities corresponds with their molecular weight. Based on the intrinsic mobility ratio, CH_4 has been demonstrated to be the most competitive. The competitive ranking for mobility is, therefore: CO_2, N_2, Air, and CH_4.

8.2.3 Velocity coupling

Figure 8-6a and b describe the coupling of velocity. The velocity profile of the EOR gases does not correspond with their molecular weight. CH_4 EOR projects are implemented in low-velocity reservoirs compared to other EOR processes. The critical velocity mentioned previously, which is the velocity required to keep a stable displacement front, enables the balancing of the displacement velocity between the displacing fluid in Figure 8-6b and the displaced fluids in Figure 8-6a. Viscous fingering is a useful criterion to consider in velocity

balance. In an immiscible displacement, a high displacing velocity might cause the displacing CH_4, for example, to break the critical velocity in the porous matrix between it and the oil boundary. Subsequently causing viscous fingering, poor sweep efficiency, and ultimately low oil recovery. The capillary number is a direct function of velocity. It is considered that a higher velocity would improve the capillary number and consequently the recovery factor. CH_4 comparatively has the highest velocity, therefore the most competitive. The competitive ranking for velocity is, therefore: CH_4, Air, N_2 and CO_2.
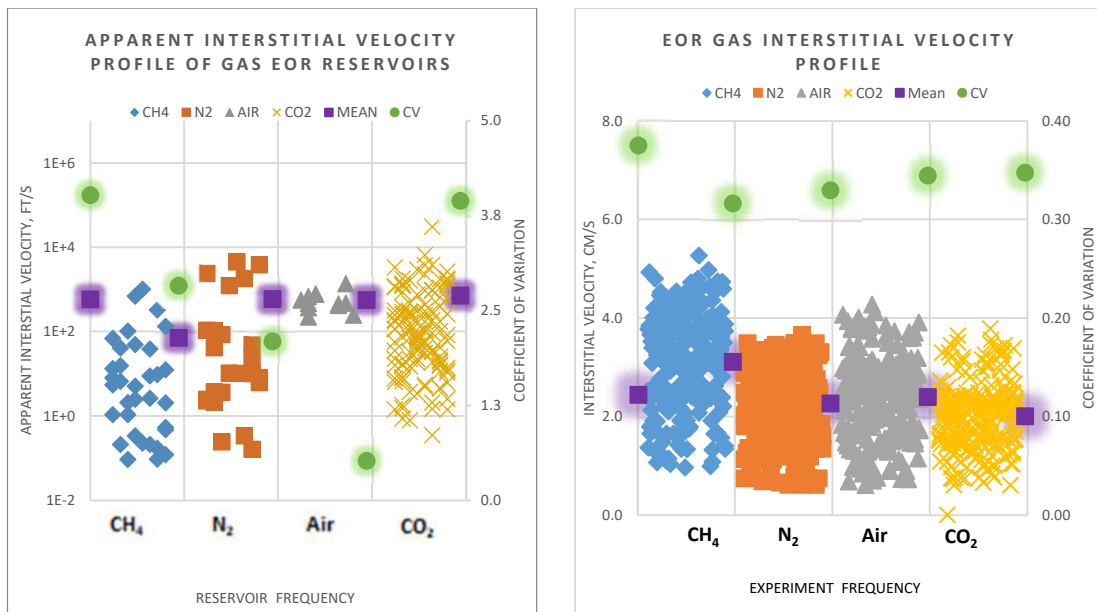
a.   b.

Figure 8-6 Velocity coupling of (a) reservoir and (b) experimental data.

8.2.4 Momentum Coupling

Figure 8-7a and b show that the magnitude ranking for the momentum in the oil field is the inverse of the EOR gas ranking, except for air. Although CO_2 gas had the lowest velocity in Figure 8-6b, it has the highest momentum in Figure 8-7b, probably due to its comparatively large molecular weight (44g/mole). Nevertheless, the segregation is not based strictly on molecular weight. It is noted that CH_4 (16g/mole) has a higher mean momentum than that of N_2 (28g/mole). Comparing Figure 8-4b and Figure 8-6b with Figure 8-7b demonstrates that mass is sovereign to velocity and volume rate in

defining gas momentum. In an immiscible displacement, CO_2 would be a better gas option for the reservoirs in Figure 8-7a. The optimisation is to identify the gas with the highest momentum potential. With respect to momentum, using CH_4 or N_2 gas to displace the oil in Figure 8-7b would not provide optimal results than using CO_2 and Air. The competitive ranking for momentum is, therefore: CO_2, Air and N_2, CH_4.
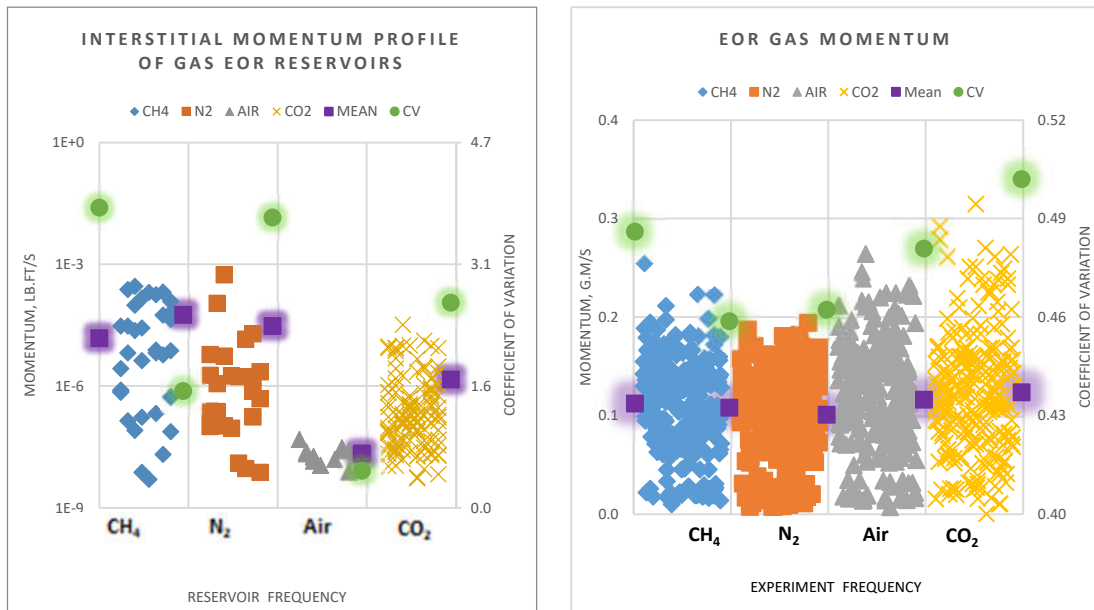
a.   b.

Figure 8-7 Momentum coupling of (a) reservoir and (b) experimental data.

8.2.5 Momentum Flux coupling

Momentum flux is used here as a measure of the rate of momentum interaction, diffusivity and transfer. Figure 8-8a and b couple the characterisation cluster for EOR reservoirs and EOR gases. The optimisation is to identify the gas that has the highest propensity to transfer momentum. The competitive ranking for momentum flux is, therefore: CH_4, N_2, Air and CO_2.
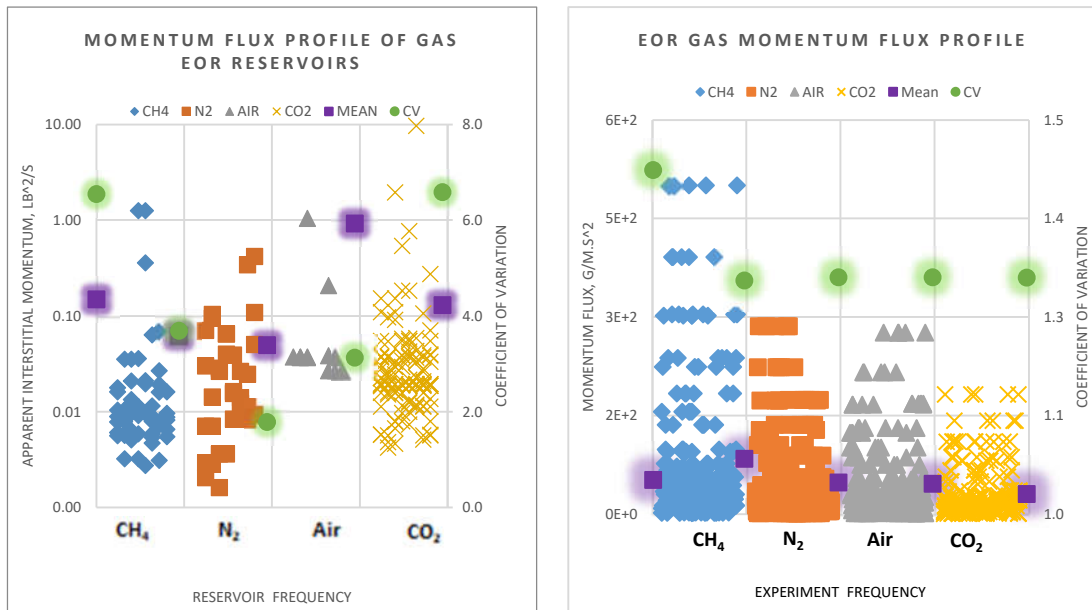
a.   b.

Figure 8-8 Momentum Flux coupling of (a) reservoir and (b) experimental data.

8.2.6 Inherent energy loss coupling

Fluid flow through porous media involves an energy continuum. The energy interaction could be caused by the geological structure or by contact with other fluids. It has been previously mentioned that in the momentum interaction process, there would be energy loss by the displacing fluid. Shelton and Maurice (1973) stated that energy supplied by injected gas is proportional to oil recovery. The coupling in Figure 8-9a and b enables the research to evaluate the reservoir and gas energy balances and losses. The optimisation is to identify which gas would suffer the least energy loss in a coupled system. In Figure 8-9b the experiments show CH_4 has the least energy loss and N_2 has the highest. However, in the reservoirs in Figure 8-9a, oils that implement CH_4 and N_2 EOR have the highest energy losses. It has been mentioned that for an idealised immiscible and perfectly inelastic displacement, the measure of energy loss is the energy difference between the displacing and the displaced fluid, divided by the displacing fluid energy. It could be intuitively concluded that by ranking and combining Figure 8-8a and b, CO_2 and Air experience the least energy loss. The energy loss paradigm

in Figure 8-8a and b fits into the analytical model derived in Eq. 2-66 ($\phi_E = \left(\frac{m_0}{m_g + m_0}\right)$). It states that the fraction of energy loss, ϕ_E is inversely proportional to the mass of the displacing gas, m_g. On a single mole basis, the mass of the injected gas can be represented by their respective molecular weight. Consequently, the energy loss can be characterised by the molecular weight of the respective gases. Therefore, the mass model is validated by the Kinetic model coupling in Figure 8-8a and b, save for CH_4 gas. It can also be deduced that the energy loss between gas and oil interaction is sovereign to velocity. Nevertheless, it is observed that N_2 EOR projects and the N_2 gas do not fit with the mass model. The optimisation goal is to minimise energy loss. The competitive ranking for energy loss is, therefore: CH_4, CO_2, Air, and N_2.

a.   b.
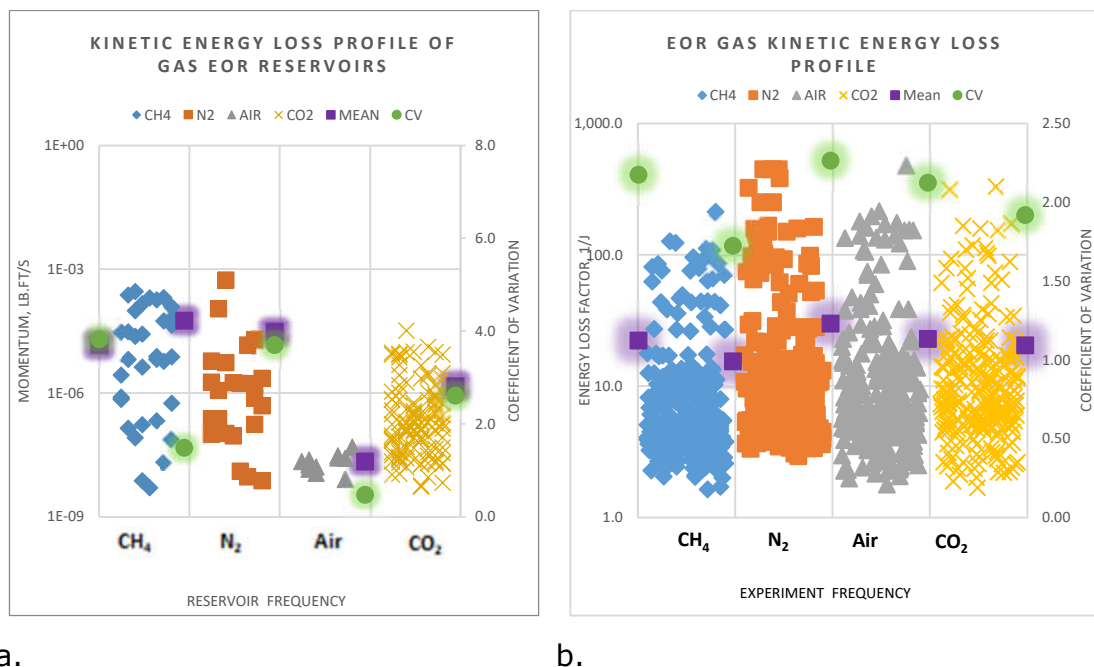
Figure 8-9 Inherent energy loss coupling of (a) reservoir and (b) experimental data.

8.2.7 Transmissibility Coupling

The importance of transmissibility has been previously mentioned. Figure 8-10a and b show that transmissibility profiles for EOR project and gas experiments and significantly related, save for CO_2. A synergetic coupled transmission between CH_4 gas in Figure 8-10b and CH_4 reservoir oil in Figure

8-10a means quicker and higher recovery at the production well. The competitive ranking for transmissibility is, therefore: CH_4, Air, N_2 and CO_2.
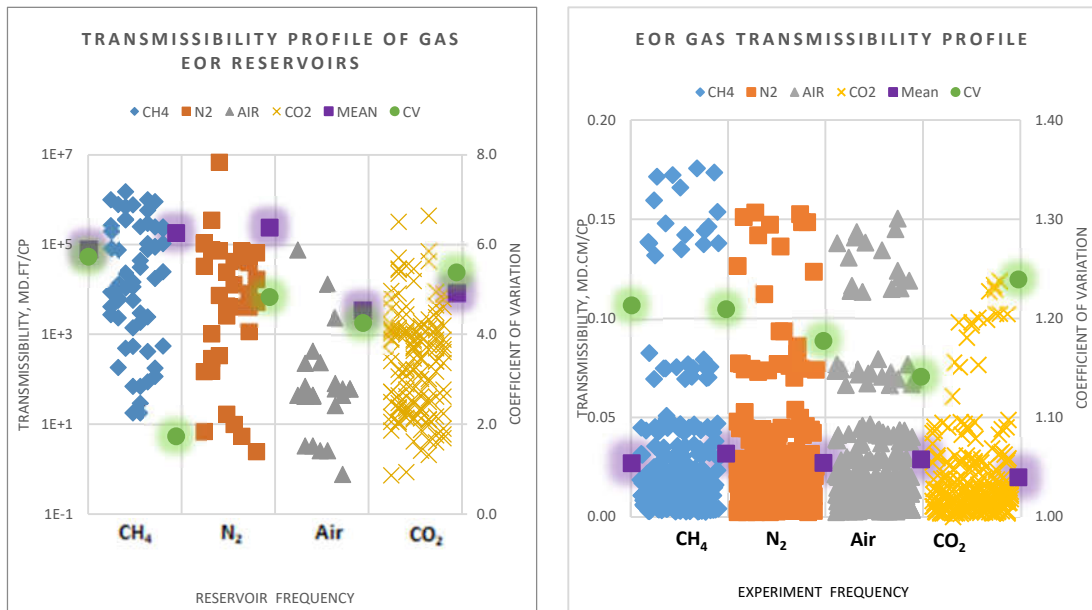
a.   b.

Figure 8-10 Transmissibility Coupling of (a) reservoir and (b) experimental data.

8.2.8 Capillary Number coupling

Figure 8-11a and b show that the capillary number for the EOR reservoirs and the EOR gases is only dramatic for CH_4. It has been mentioned previously that oil displacement occurs at a capillarity number greater than 10^{-5}. It is seen from the experiments that CH_4 tends to readily approach this condition than the other gases (Figure 8-11b). Therefore, CH_4 would be most suited for the four types of gas EOR reservoirs in Figure 8-11a. This suggests that performance would be greatest where CH_4 is applied to N_2, Air and CO_2 EOR reservoirs than when applied to CH_4 EOR reservoirs, because CH_4 EOR reservoirs (as noticed in Figure 8-11a) possess the least capillary number potential, therefore would comparatively dampen the injected gas capillary number. The CV profile curves are similar, and they show that Air mixture and Air EOR projects would be more sensitive to Capillary number variation

than others. In contrast, the mean profile curves are inverse. The competitive ranking for capillary number is, therefore: CH_4, Air, N_2 and CO_2.
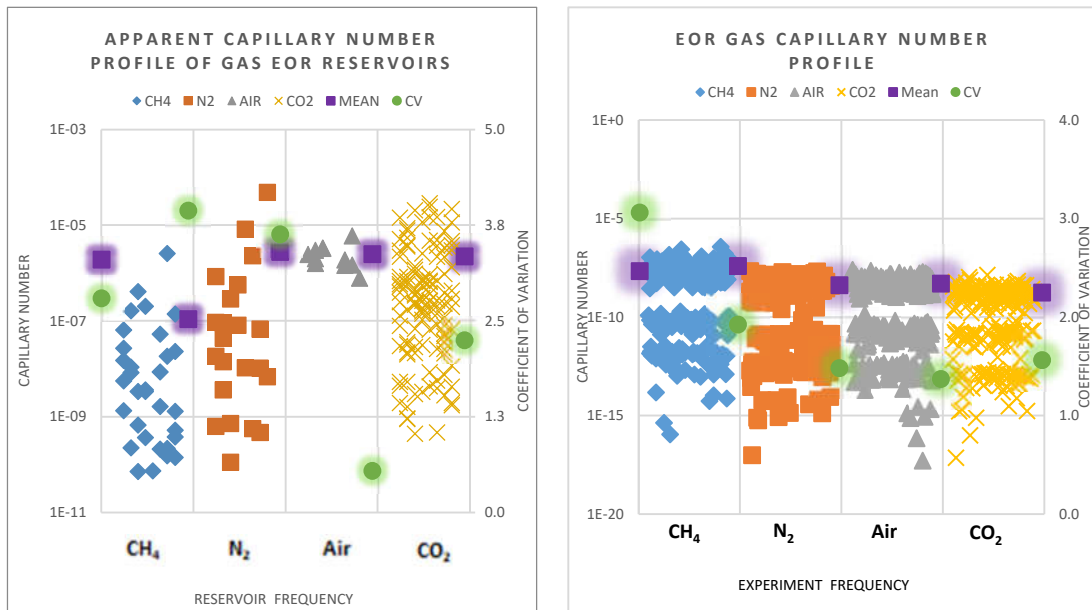
a.   b.

Figure 8-11 Capillary Number.

8.2.9 Displacement Efficiency Coupling

The clusters in Figure 8-13a and b show the displacement efficiency of the respective EOR systems as a function of end oil saturation. Figure 8-13a indicates that at the end of the CO_2 EOR process, CO_2 injection into reservoir pores would have recovered 43% of the trapped oil. The highest reported recovery is for the CH_4 EOR process, which is 75%. Air displacement efficiency is between these two extremes. There was not enough data to characterise N_2 saturation. The experimental data were presented in Figure 8-13b. It shows clusters estimating pore-scale displacement efficiency based on immiscible gas-liquid displacement mechanism in capillary tubes. The mean displacement efficiency values in Figure 8-13b are functions of the oil film thickness (proportional to end saturation) un-displaced by the gas slug injected through the capillary tube. It is shown that the CO_2 slug displaces more trapped oil than other gases. CH_4 gas has the least displacement

efficiency\. It is noted that the experimental data in Figure 8-13b matches Al Adasani and Bai (2011) work in Figure 2-5 with respect to the comparative displacement efficiency of CO_2. However, these two do not match the field data and Sakthikumar, Madaoui, and Chastang (1995). The optimisation goal is to maximise displacement efficiency. Consequently, based on the experimental data in Figure 8-13b, the competitive ranking for displacement efficiency is, therefore: CO_2, N_2, Air, and CH_4.
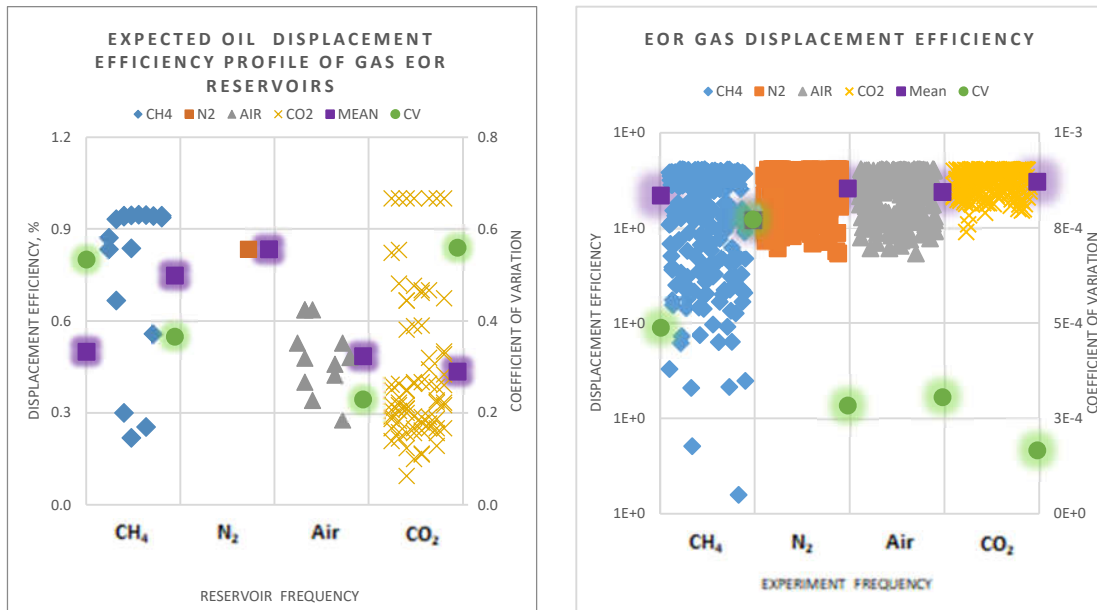
a.   **b.**

Figure 8-12 Displacement efficiency coupling of (a) reservoir and (b) experimental data.

8.3 Cost Centres

8.3.1 Displacement and Capillary Pressure

Figure 8-13b shows that CO_2 has the lowest displacement pressure, which measures its capacity to overcome capillary forces and displace oil. Comparing Figure 8-13a and b suggest that CO_2 would serve the four types of reservoirs in Figure 8-13a more effectively and at a reduced pressure than the other gases. This would save costs on injection pumps and power ratings. It would also make it easy to manage other engineering events and

quantities, such as mobility and velocity. On this basis, N_2, which has the highest displacement pressure, would be the costliest to implement and manage; therefore, it is the least to optimise the objective function of capillary pressure. It is noted that the CV and Mean profiles for both graphs are quite validated, although the mean profiles are inversely related. Therefore, the competitive ranking for capillary/displacement pressure is CO_2, Air, CH_4, and N_2.
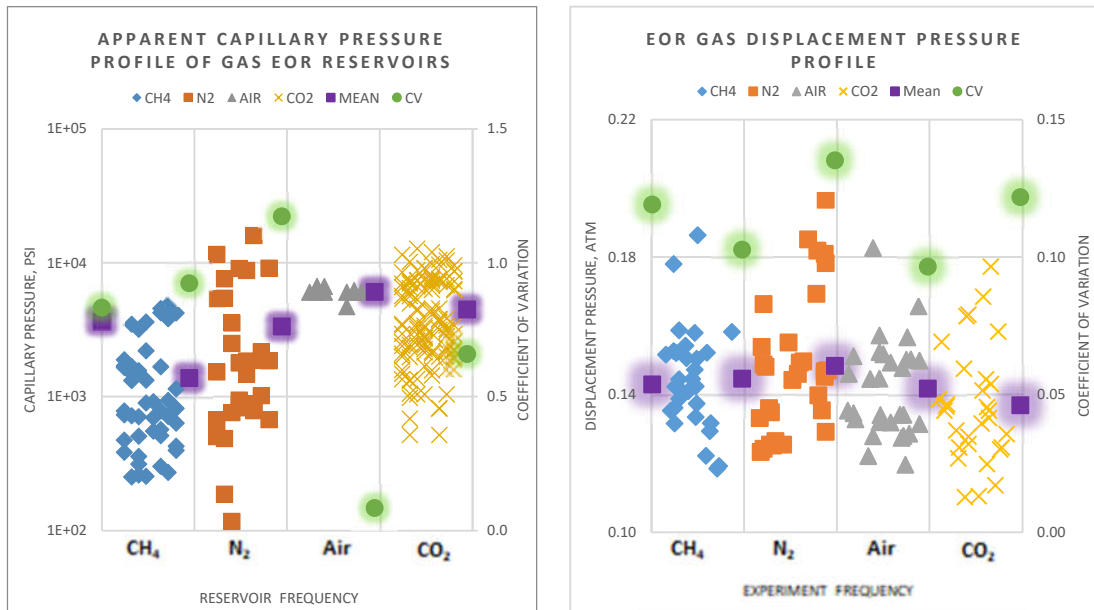
a.   b.

Figure 8-13 Displacement and Capillary Pressure.

8.3.2 Well Density coupling

Figure 8-14a and b show that the experimental well density significantly couples with the EOR gas projects. From the mean well density profiles, it is concluded that CH_4 require the least number of wells for effective reservoir drainage and coverage. In the field data, it is shown in Figure 8-14a that CO_2 (0.07 well.acre^{-2}) would require about three times the number of wells required by CH_4 (0.02 well.acre^{-2}) for the same reservoir coverage. This is validated by the experimental outcome in Figure 8-14b, where CO_2 (1.50 well.cm^{-2}) requires about twice the number of wells required by CH_4 (0.96 well.cm^{-2}) for the same area coverage. Combined with the fact that the CVs

in both graphs indicate CO_2 performance is sensitive to well density, the implication to engineering economics and technical complexity is significant.
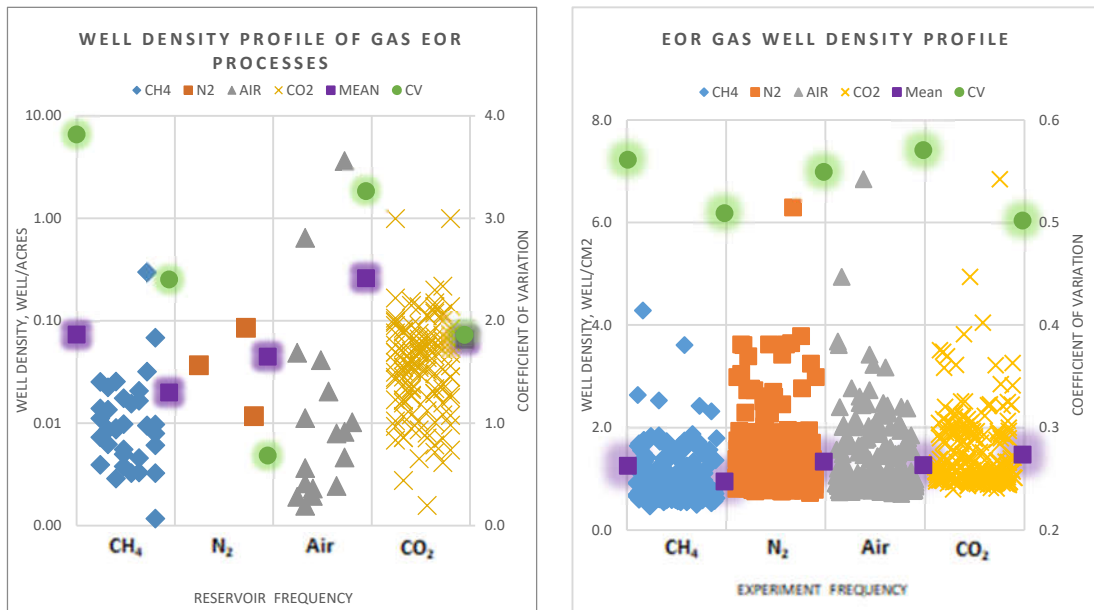
a.   b.

Figure 8-14 Well Density coupling of (a) reservoir and (b) experimental data.

Selecting CH_4 EOR over CO_2 EOR would invariably save cost on well drilling, avert the operational risk and downtime required to drill new infill wells, and the shutdown time to maintain existing ones. Consequently, the competitive ranking for well density is, therefore: CH_4, Air, N_2 and CO_2.

8.3.3 Cumulative gas cost coupling

It has been mentioned previously that EOR volume recovery is proportional to the injected volume of the displacing fluid. Therefore, without loss of generalisation, the potential oil volume trapped in the reservoir can be intuitively considered as a measure and a factor of the injected gas volume required to displace it. Given that the data mining results have significantly validated the experimental results, it is intuitive to assume the experimented injected volume can consequently couple with the potential trapped oil volume revealed in the data mining analysis. A cost analysis of the two volumes has been presented in Figure 8-15a and b. The research used a

January 1st 2021 BOC gas pricing quotation. The gas price was normalised to United States dollars of January 1st 2021. Figure 8-15a indicates it would cost more to sweep trapped oil volume in CH_4 EOR reservoirs than in other EOR reservoirs. CO_2 gas sweep of trapped oil comparatively cost the lowest. The cost sensitivity is highest for Air EOR. The cumulative cost pattern is significantly mirrored in Figure 8-15b. The cost of CH_4 volume is distantly above the other gases. It has been criticised previously that CH_4 is often implemented where access to the gas market is limited, and where there are gas flaring challenges.

a.   b.
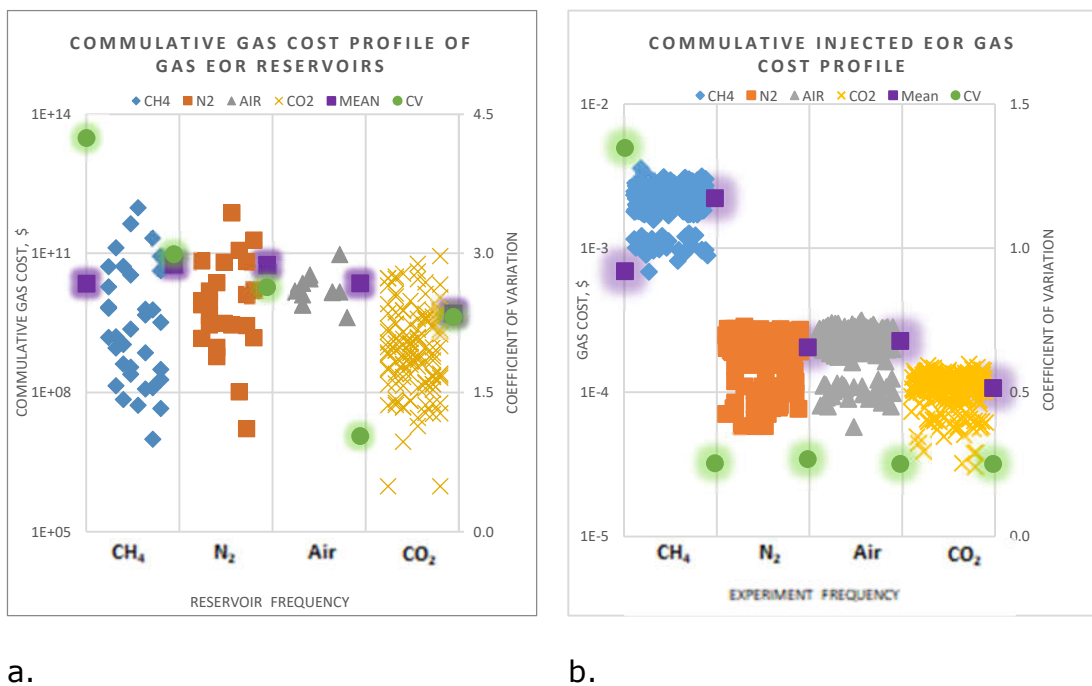
Figure 8-15 Cumulative gas cost coupling of (a) reservoir and (b) experimental data.

Figure 8-15a and b seem to have explained that. Surprisingly, the cumulative cost of injecting and N_2 and Air is higher than that of CO_2 in both reservoir and experimental data. Considering the availability of Air has been previously mentioned to be a cost opportunity for Air EOR projects. The study takes exception to this finding. The cost of processing Air for injection in an oil field should not be as expensive as the BOC quotation. However, for theoretical purposes, the ranking of the cost competitiveness of EOR gases is, therefore: CO_2, N_2, Air, and CH_4.

Three explicit cost centres (well density, displacement pressure, and injected gas cost) analysed have revealed useful information on the opportunity cost of selecting an EOR process and gases. Although it is observed that CH_4 would sweep a significant amount of trapped oil, the cost of doing that beats other cost advantages that it has, such as well density. The cost difference in cumulative injected gas between the extremes of CH_4 ($\$10^{10}$) and CO_2 ($\$10^9$) has a higher cost implication than the cost difference in well density CH_4 (1 well/acre) and CO_2 (2 well/acres). This is coupled with the fact that CO_2 would require less utility cost in pressure pump, power and gas storage due to its comparatively low displacement pressure.

The summary of Figure 8-13b, Figure 8-14b and Figure 8-15b, suggests that in an immiscible EOR screening process, selecting CH_4 over CO_2 means less well cost but more gas and utility cost. Selecting CO_2 is the direct opposite of CH_4 cost. Selecting N_2 offers high utility and gas costs but a relatively lower well cost than CO_2. These are some cost centres that EOR engineers must consider before selecting an EOR process. However, it is common to see produced EOR gases being reinjected in a perpetual cycle. The analysis has not considered the magnitude of gas recycling. It is assumed that this would reduce the cost outlook proportionately for the respective EOR gas.

8.4 Heterogenous Performance Evaluation

Reservoir activities usually experience heterogeneities. This ranges from permeability, porosity, pore size, pay zone thickness, radial thickness, oil viscosity, and pressure heterogeneities. It is expected that the selected EOR process should be the one that is robust enough to perform within the heterogeneity domain. In the previous sections, the gases have been investigated using criteria, such as Volumetric flow rate (PV), Intrinsic mobility, Interstitial Velocity, and Momentum as the objective functions for optimising enhanced oil recovery. Those examinations were conducted by considering a single parameter at a time. It was, however, important to investigate how the gases compare in a heterogeneous system.

Using the statistical technique, all the experimentally generated data were evaluated, and the results are presented in Figure 8-16 to Figure 8-19. Each of the graphs contains a series for the heterogeneous values and coefficient of variation CV of the respective gases for a particular parameter. The CV here is a measure of how the gases respond to heterogeneity.
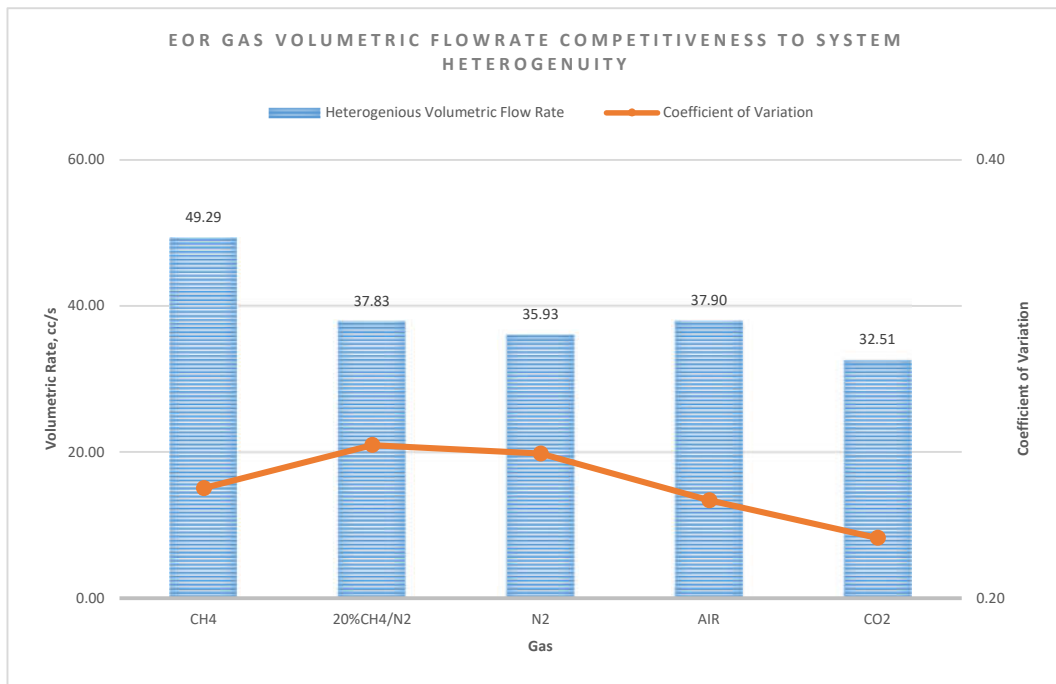
Figure 8-16 Volumetric performance of EOR gases in a heterogeneous system.

In Figure 8-16, for the volumetric flow rate, it was observed that CH_4 offers the best solution. Although the least competitive gas is CO_2, it, however, has the lowest CV, meaning it is the gas that is least affected by system heterogeneity. In contrast, N_2 is the most affected or sensitive to system heterogeneity.
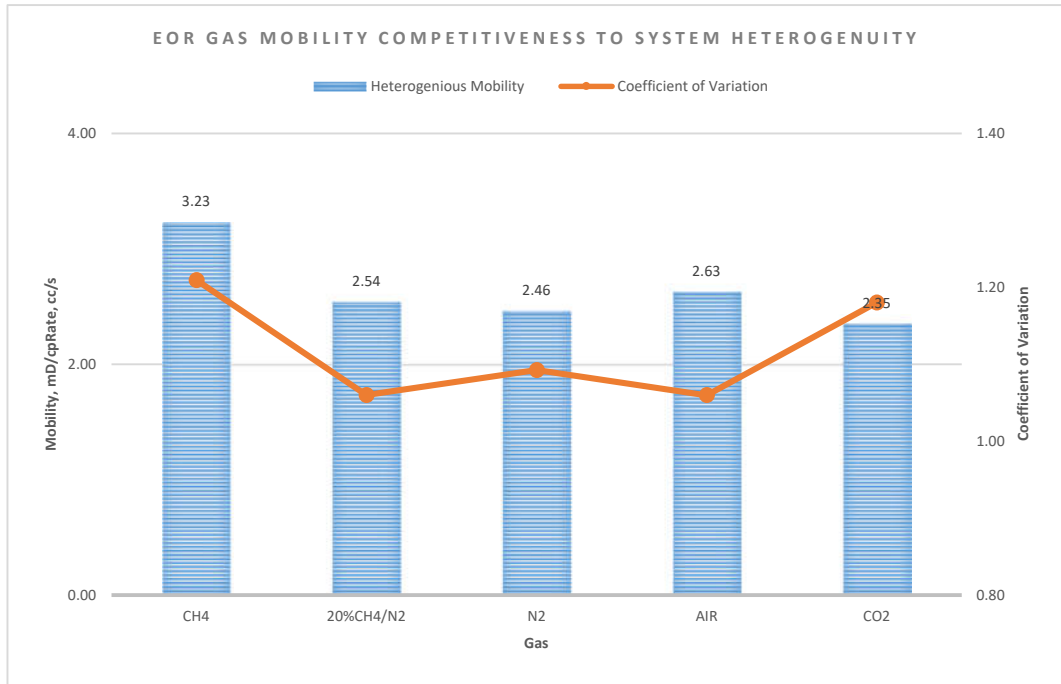
Figure 8-17 Intrinsic mobility performance of EOR gases in a heterogeneous system.

For intrinsic mobility, the lower the intrinsic mobility, the better. Therefore, in Figure 8-17, CO_2 is observed to offer the desired intrinsic mobility in a heterogeneous system. This is followed by N_2, Air, and CH_4. Air's intrinsic mobility performance is least affected by system heterogeneity, while CH_4 is most affected by system heterogeneity.
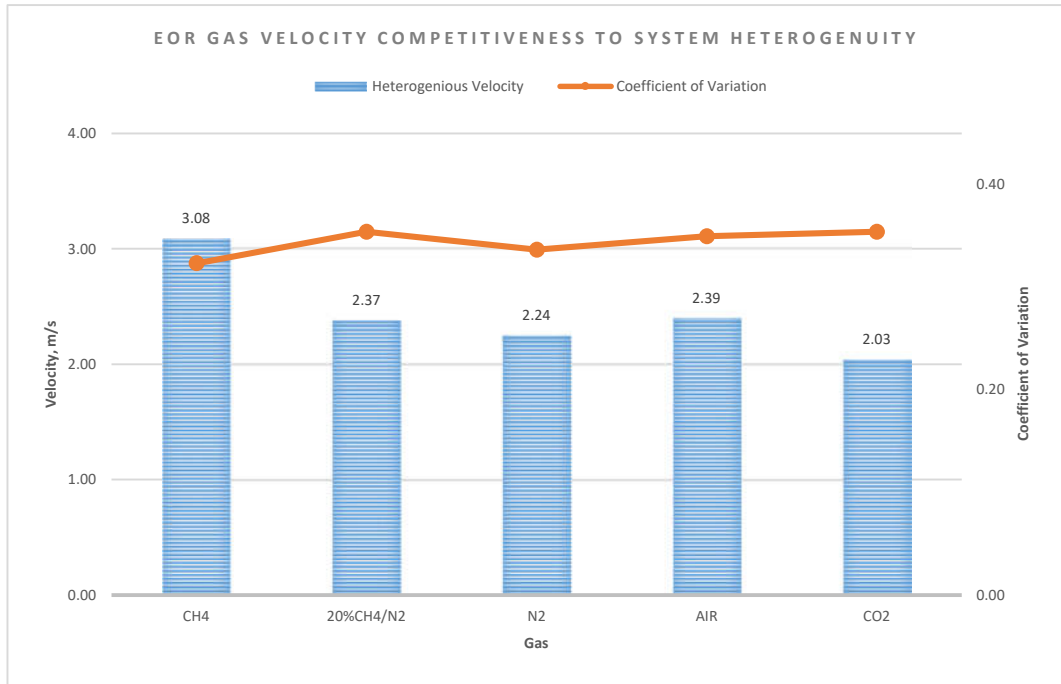
Figure 8-18 Interstitial velocity performance of EOR gases in a heterogeneous system.

In Figure 8-18, for interstitial velocity, it has been observed that CH_4 offers the most competitive velocity, followed by Air, N_2, and CO_2. Based on the CV profile, it could be stated that the effect of system heterogeneity is not very different for the gases, although CO_2 CV is marginally above others.
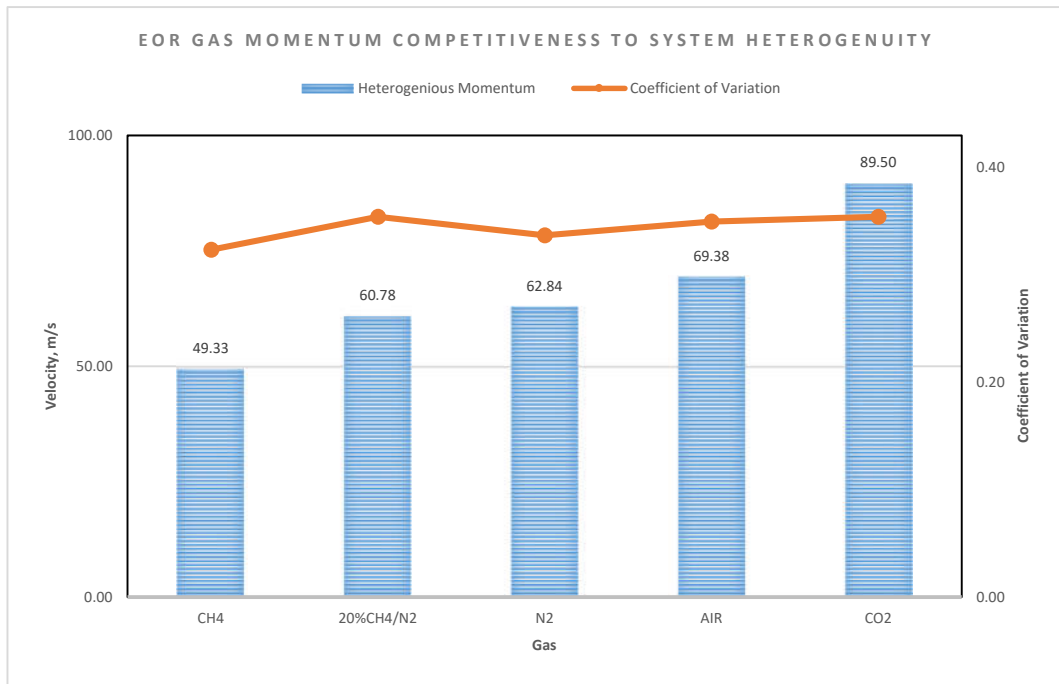
Figure 8-19 Momentum performance of EOR gases in a heterogeneous system.

In Figure 8-19, for Momentum, it was observed that CO_2 is the most competitive EOR gas, followed by Air and N_2. In this case, CH_4 is the least competitive. The CV is highest in CO_2 also.

In summary, it can be seen from the preceding that the range of competitiveness of EOR gases lies between CH_4 and CO_2. N_2 was the closest alternative in the Volumetric and Intrinsic mobility criteria, while Air is the closest alternative in Velocity and Momentum criteria.

8.5 Reservoir Permeability Contrast

8.5.1 Well Topology Optimisation

The well topology optimisation analysis investigates how the respective gas performances in an EOR process would affect well placement, type and density in reservoirs with certain permeability contrast.

Where the volumetric rate is the sole objective in an EOR process, wells are expectedly placed in locations that maximise the gas volumetric flow rate.

Conversely, where intrinsic mobility is the sole objective, wells are placed to minimise intrinsic mobility. However, in the real world, EOR gases are engineered to meet these two conditions simultaneously, hence the need for optimisation. Given a reservoir with a certain permeability contrast or heterogeneity, the best well topology optimisation would occur where the well placement (including type and density) required to achieve optimal volumetric flow rate also simultaneously achieves optimal intrinsic mobility vice-versa. In this case, the optimisation is marked as mutually inclusive for volumetric rate and intrinsic mobility at the heterogeneity. The optimisation is marked as mutually exclusive where it is not practicable for volumetric rate and intrinsic mobility to share the same well topology.

To test this evaluation, the synergy of flowrate and intrinsic mobility was analysed using momentum transfers as a criterion. Gas-Oil displacement occurs between injection and production wells. Momentum transfer occurs between the gas and oil droplets through the porous media, such that the displacing gas momentum diminishes as it transfers momentum to displace the oil droplets in the direction of the Producer well. Core-1, 3 and 4 were selected for the evaluation because they have similar dimensions but different pore sizes and porosity to create the desired permeability contrast that can be estimated by Dykstra and Parsons method. The core samples are considered hypothetical blocks or discretised grids of a reservoir with varying parameters such as pore size and porosity stacked together in a continuous series such that it exhibits geometric heterogeneity. The gases were allowed to generate their respective topology, using a momentum profile similar to Harrison and Chauvel (2007) pressure profile between a producer well and a reference point, usually an injection well or the reservoir's external boundaries.
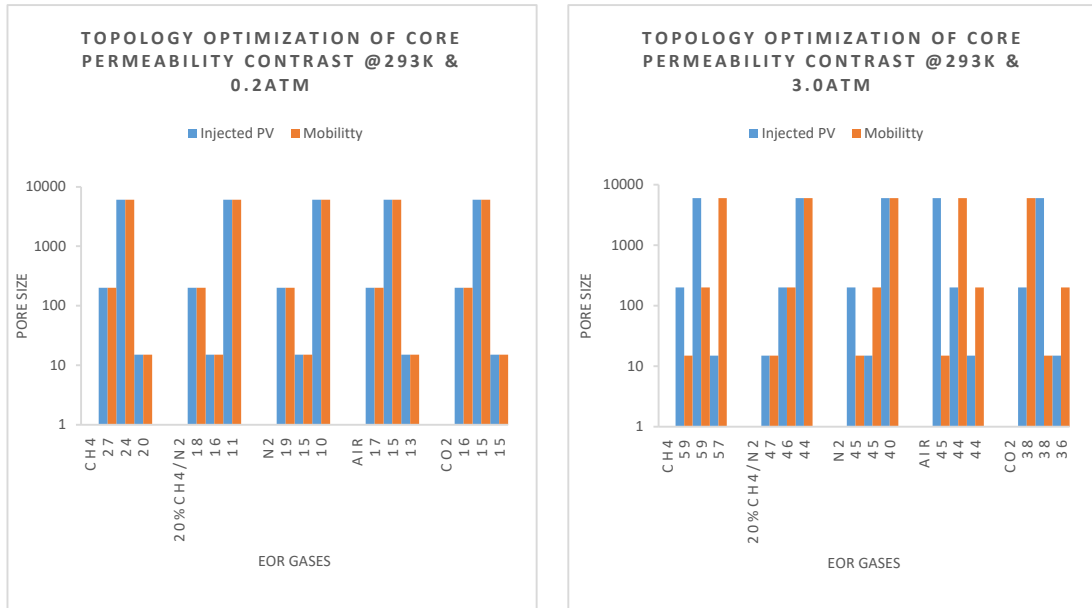
a.

b.

Figure 8-20 Potential Performance of EOR gases to permeability contrast when the core temperature is 293K: (a) at 0.20atm (b) at 3.00atm.

It is shown in Figure 8-20a and b that at 0.20atm and room temperature of 293K, the two parameters: Injected PV and intrinsic mobility, are mutually inclusive for all gas and three core samples because the PV and mobility both align with each other for all the gases. Hence the topology is straightforward.

In this case, all five gases and mixture favour the injection well being placed in the 200nm (porosity: 20%) side of the reservoir. CH_4, Air and CO_2 favour the producer to be placed at the 15nm (13%) side of the reservoir. In contrast, 20%CH_4/N_2 and N_2 favours being produced from the 6000nm (14%) side. Although a number of the previous analyses done in this research had shown hard-to-describe flow behaviour for the gases at low pressure, the response of the gases to permeability contrast is interestingly describable and stable. Granted, this may not apply to oil reservoirs because reservoir pressures are large multiples of 0.20atm; however, this finding may find utility in other industries that flow gases through porous media at low pressure.

Figure 8.5a and b at 3.00atm and 293K show that only 20%CH_4/N_2 is suggestive of mutual inclusivity. The other gases have a situation where the volumetric flow rate and intrinsic mobility suggest a different well pattern, indicating a lack of synergy between the two parameters. Their optimisation is therefore considered mutually exclusive.
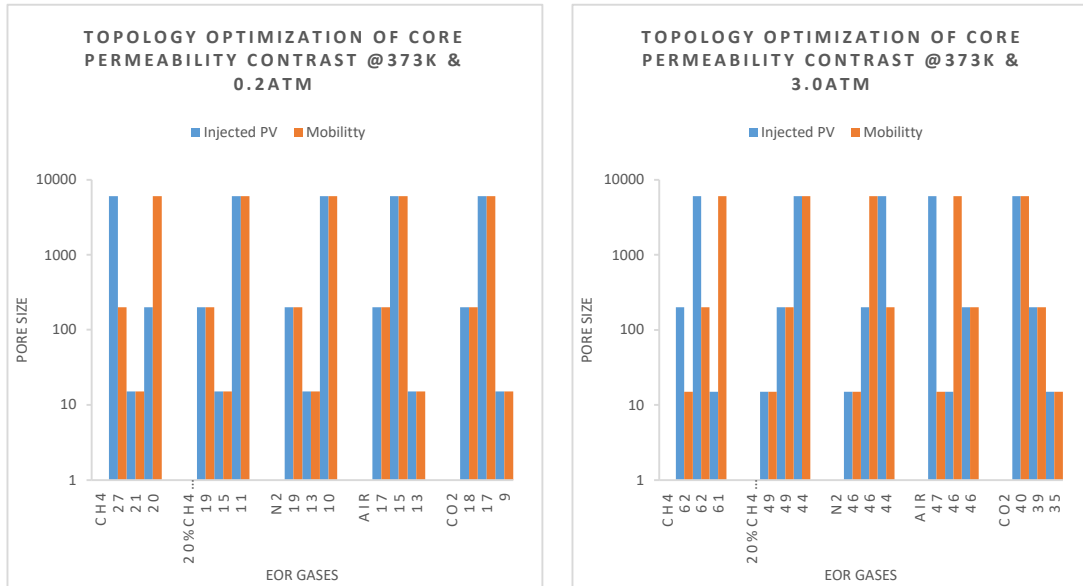
a.

b.

Figure 8-21 Potential Performance of EOR gases to permeability contrast when the core temperature is 323K: (a) at 0.20atm (b) at 3.00atm.

Figure 8-21a and b show similar profiles at conditions of 0.20atm and 3.00atm gauge pressure and 373K. The 3.00atm gauge pressure and 373K are extrapolatable to reservoir conditions, unlike the analysis in Figure 8-20a and b. It is observed that at 0.20atm and 373K, the histogram profile formed here is similar to the profile in Figure 8-20a, except for CH_4 parametric constraints whose optimisations are not synergetic. Similarly, in Figure 8-21b, 20%CH_4/N_2 and CO_2 gases have parametric constraints whose optimisations are mutually inclusive at a Dykstra–Parsons Coefficient of 1.16. In contrast, CH_4 gas volumetric flow rate is optimised when the injection well is placed before the 200nm section of the reservoir, and the producer well is placed after the 15nm section of the reservoir, while its intrinsic mobility is optimised only when the injection well is placed before the 15nm side of the

reservoir and the producer well at the 6000nm side of the reservoir. This indicates that the volumetric rate and intrinsic mobility optimisations are mutually exclusive at a Dykstra–Parsons Coefficient of 1.161 for CH_4. To manage this situation, the engineers are left with three possible choices:

I. Optimise either volumetric injection rate or intrinsic mobility ratio (Remark: Low oil productivity).

II. Sectionalise the reservoir and drill additional pairs of infill wells at each section to achieve sectional mutual inclusivity (Remark: increased well expenses).

III. Reconsider using alternative gas, such as 20% CH_4/N_2 and CO_2, that allows simultaneous well topology optimisation at a Dykstra–Parsons Coefficient of 1.161 (Figure 8-21b) (Remark: a better option but must be considered early in the screening stage).

For clarity purposes, Figure 8-22a-d are used to depict the well number, well type and placement development plans for four of the gases analysed. The figures also show the pore size gradient, which is defined as the difference between the outlet and inlet pore radius divided by the thickness of the pore contrast l in the direction of flow ($\lambda=(r_o-r_i)/l$). As stated in the literature review, λ can assume values of zero and positive or negative numbers. It is observed that CH_4 (Figure 8-22a) would apparently require six wells to be able to optimise volumetric flow rate and intrinsic mobility simultaneously. Here, the λ between injection and production well is zero. Due to the mutual inclusivity of the volumetric rates and intrinsic mobilities of 20%CH_4/N_2, and CO_2 (Figure 8-22a and d), only two wells are required to produce and enhance oil recovery. There are some opportunities for N_2 (Figure 8-22c), as it only requires four wells to optimise volumetric rates and intrinsic mobilities overall.

Interestingly, Figure 8-22d correspond with Rabbani *et al.* (2018) experimental result in a two-phase displacement of silicon oil by water. The authors suggest that recovery efficiency is enhanced when the pore size gradient is negative, *λ<0*. Although 20%CH_4/N_2 in Figure 8-22b and

Volumetric-Intrinsic mobility performances at 0.20atm (Figure 8-20a and Figure 8-21a) suggest recovery performance can be achieved with a positive pore gradient. The authors did mention that λ does not act alone; it couples with the capillary number. Therefore, this could likely be one of the reasons 20%CH_4/N_2 deviates from their findings.
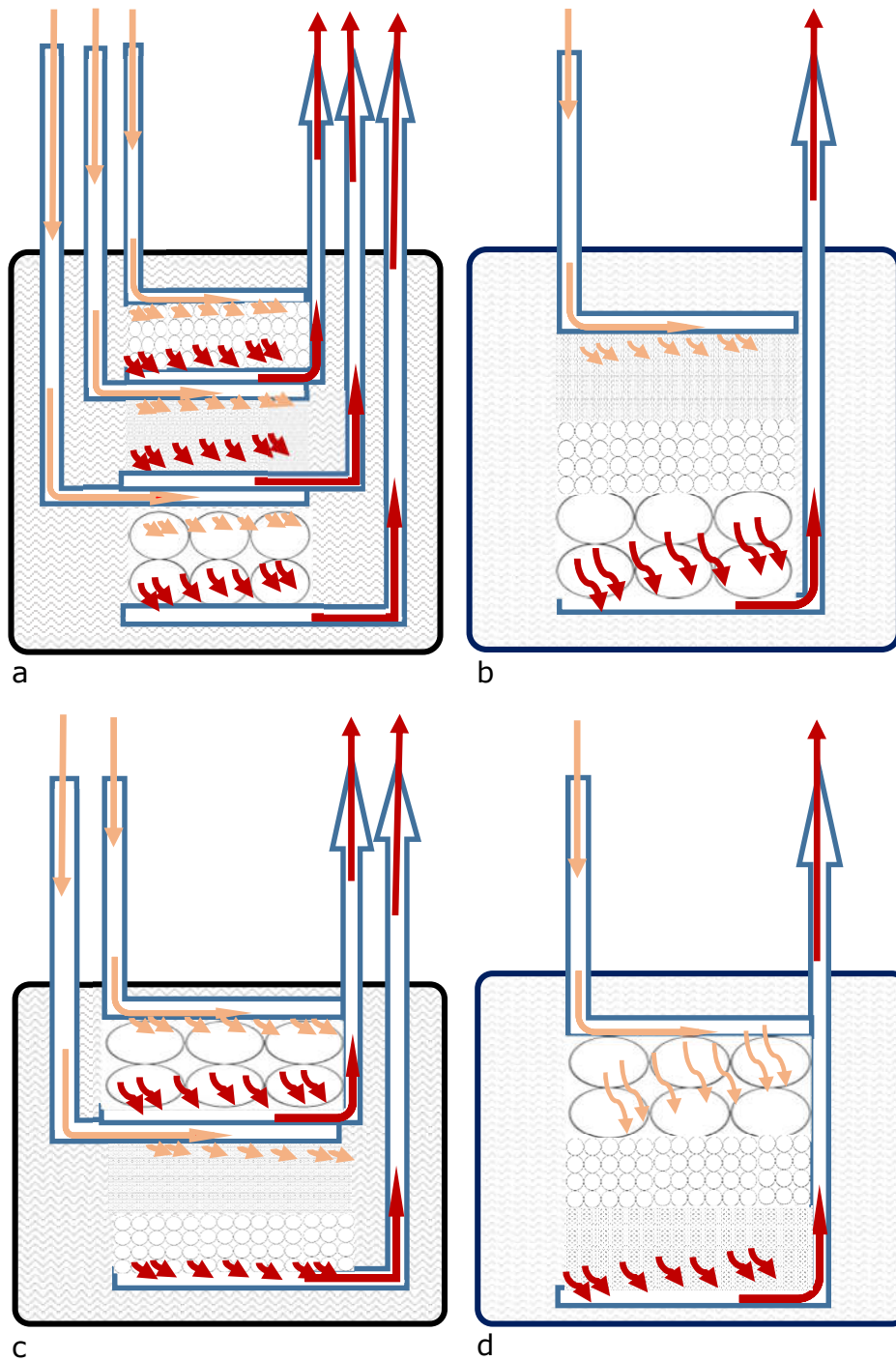
Figure 8-22 Graphs showing different numbers of well and well placements due to EOR gas response to reservoir heterogeneity in Figure 7-41 : (a) CH_4 requires six wells due to complete mutual exclusivity of parameters and compound permeability rhythm (b) 20%CH_4/N_2 requires two wells due to mutual inclusivity of parameters and the reverse pore size rhythm (c) N_2 requires four wells due to partial the mutual inclusivity of the parameters (d) CO_2 requires two wells due to mutual inclusivity of the parameters and a positive pore size rhythm.

Similarly, Figure 8-23a and b can be described in the same manner as the previous figures. Figure 8-23b shows that 20%CH_4/N_2, N_2, and CO_2 are the only gases that enjoy mutually inclusive optimisation. It is observed that, for N_2, mutual inclusivity was not achieved at 373K but was attained at 473K. This indicates that the temperature of the porous media or reservoir could be critical to N_2 Volumetric-Intrinsic mobility optimisation performance.
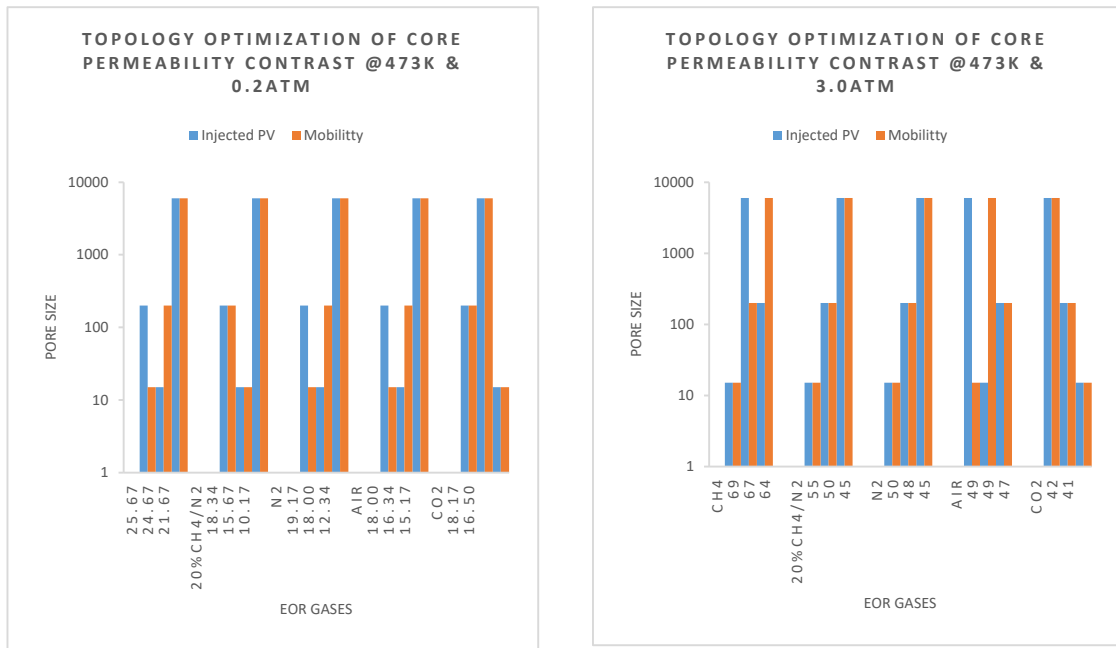
a.

b.

Figure 8-23 Potential Performance of EOR gases to permeability contrast when the core temperature is 473K: (a) at 0.20atm (b) at 3.00atm.

In summary, the performance of EOR gases to permeability contrast, measured as Dykstra–Parsons Coefficient of 1.16, has been investigated. It is observed that at low pressure and temperature, all the gases volumetric rate and intrinsic mobility formed a mutually inclusive optimisation. As the temperature increased from 273K to 473K, the gases except for 20%CH_4/N_2 and CO_2 began to lose their ability to retain a common well topology optimisation. At 3.00atm, and temperature 273K to 473K, only 20%CH_4/N_2, N_2 and CO_2 possessed optimisation that could be considered mutually inclusive. The thermodynamics behind this observation is not very clear at

this time. It cannot be explained by basic gas properties, such as molecular weight or density.

Furthermore, there are few works to compare these results. Although, in tight reservoirs or very low permeability reservoirs (0.001-0.1 mD), Wu *et al.* (2020) found that N_2 is not effective compared to CO_2 or CO_2/N_2 mixture in displacing oil, while the authors observed CO_2 alternate N_2 injection to be the most effective than CO_2 alone. Furthermore, CO_2/N_2 mixture was found to be better than the individual gases. Jia (2018) stated in a numerical simulation investigation of Air that reservoir heterogeneity was observed to be favourable to Air performance. Unfortunately, this is not the case with the results of this research.

Air is a mixture of about 70%N_2; the common gas between the research and Jia (2018) and Wu *et al*. (2020) investigation is N_2. Unfortunately, the fraction of N_2 in the CO_2/N_2 mixture used by Wu *et al*. (2020) is not clear. This hinders access to compare the two studies further. In the research and the ones of authors cited above, N_2 gas performs better as a mixture, whether with CH_4 (as shown in this study) or with CO_2, as shown in Wu *et al.* (2020). It is recommended that further study be carried out in this area to understand the mechanism and property relationship that exists. The import of this knowledge is economical and technological for the oil industry and other porous media industries. It is expected that results from this analysis could cut the additional cost of infill wells or facilitate effective EOR development plans.
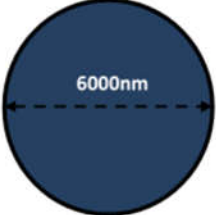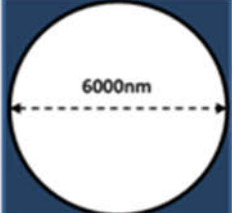
Finally, the competitiveness of EOR gases based on reservoir permeability contrast indicates that CO_2 is the most competitive gas while CH_4 is the least gas. N_2 in the mixture has been confirmed to be consistently competitive in heterogeneous reservoirs.

8.6 Reservoir Rhythm

As part of investigating the competitiveness of the EOR gas, it is also valuable to investigate the reservoir rhythm that favours optimising the engineering

quantities so far examined. Reservoir rhythm is usually a function of the geological structure, such as permeability, pore size and porosity. To conduct the rhythm analysis, the engineering quantities were optimised based on EOR optimisation requirements; then the structural rhythm that created the quantity optimisation was recorded and presented in Figure 8-24 and Figure 8-25 cells. The configuration for each cell assumes there is a horizontal gas injection well located on top of a reservoir pack with five porous layers of different structural parameters, and a horizontal oil producer well is located at the bottom of the reservoir. It is also assumed that the flow direction is top to bottom. The effect of gravity is not required. Eleven quantities were optimised. In this study, the structural parameters include five porosity and three pore sizes. The available porous media structural parameters are shown in Table 8-1.

Table 8-1 Shows the cores sample used in the experiment and their structural parameters, this media diagrams can be used as a legend for Figure 8-24 and Figure 8-25 cells.

Media	Pore Diameter (nm)	Porosity	Core
15nm	15	$\varphi = 13\%$	**Core-1**
15nm	15	$\varphi = 3\%$	**Core-2**
200nm	200	$\varphi = 20\%$	**Core-3**
6000nm	6000	$\varphi = 14\%$	**Core-4**
6000nm	6000	$\varphi = 4\%$	**Core-5**

The media in Table 8-1 are sized arbitrarily proportional to their pore sizes. Hence the table can be qualitatively and quantitatively used as a legend for studying Figure 8-24 and Figure 8-25.

For CH_4, the cells highlighted with yellow colour in Figure 8-24 indicate that the reservoir rhythm can simultaneously achieve flow rate and gas cost optimisation. It implies that these two quantities are mutually inclusive. The interpretations and utility of the observation to reservoir engineers are significant. It suggests that for flowrate and gas cost to be optimised in a heterogeneous reservoir, the injection wells should be placed on the reservoir side with the largest pore size and lower porosity, and the production well should be located at the reservoir side with the largest pore size and highest porosity. Simply put, a pair of injection and producer wells can be used to optimised the two quantities. In this case, the structural gradients are zero 5pore gradient and positive porosity gradient.

The other nine quantities are mutually exclusive because their rhythms are unique and do not synchronise with any other quantities. It is also seen that some quantities are optimised in a positive pore gradient, while the others fall into negative gradients, such as capillary number, N_c, and displacement pressure, P_d. This gradient phenomenon is also observed in porosity. Finally, most of the quantities prefer the injection wells to be located on the larger pore size and low porosity side of the reservoir. Similarly, N_2 experiences rhythm synchronisation for flow rate and gas cost optimisation.
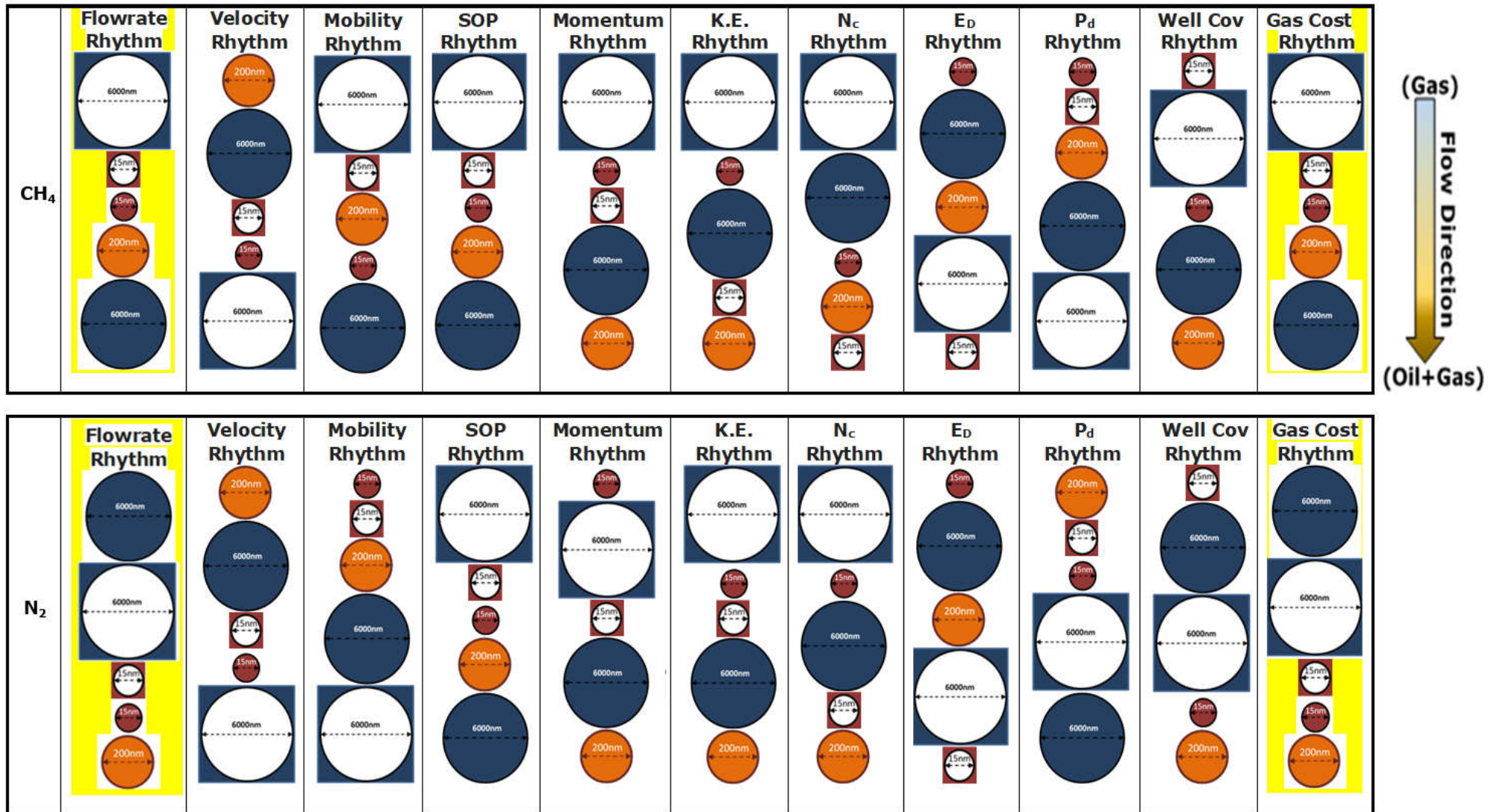
Figure 8-24 Shows pore size and porosity rhythm mapping for CH₄ and N₂, each cell consist of an engineering quantity that has been optimised and its supporting rhythm, the location of each porous media is in relation to the injection and production wells.

For Air, Figure 8-25 shows four quantities that can be optimised using two geological rhythms. Here, flow rate and Well Cov (well coverage) share rhythm highlighted in yellow colour. While mobility and gas cost share the same rhythm.
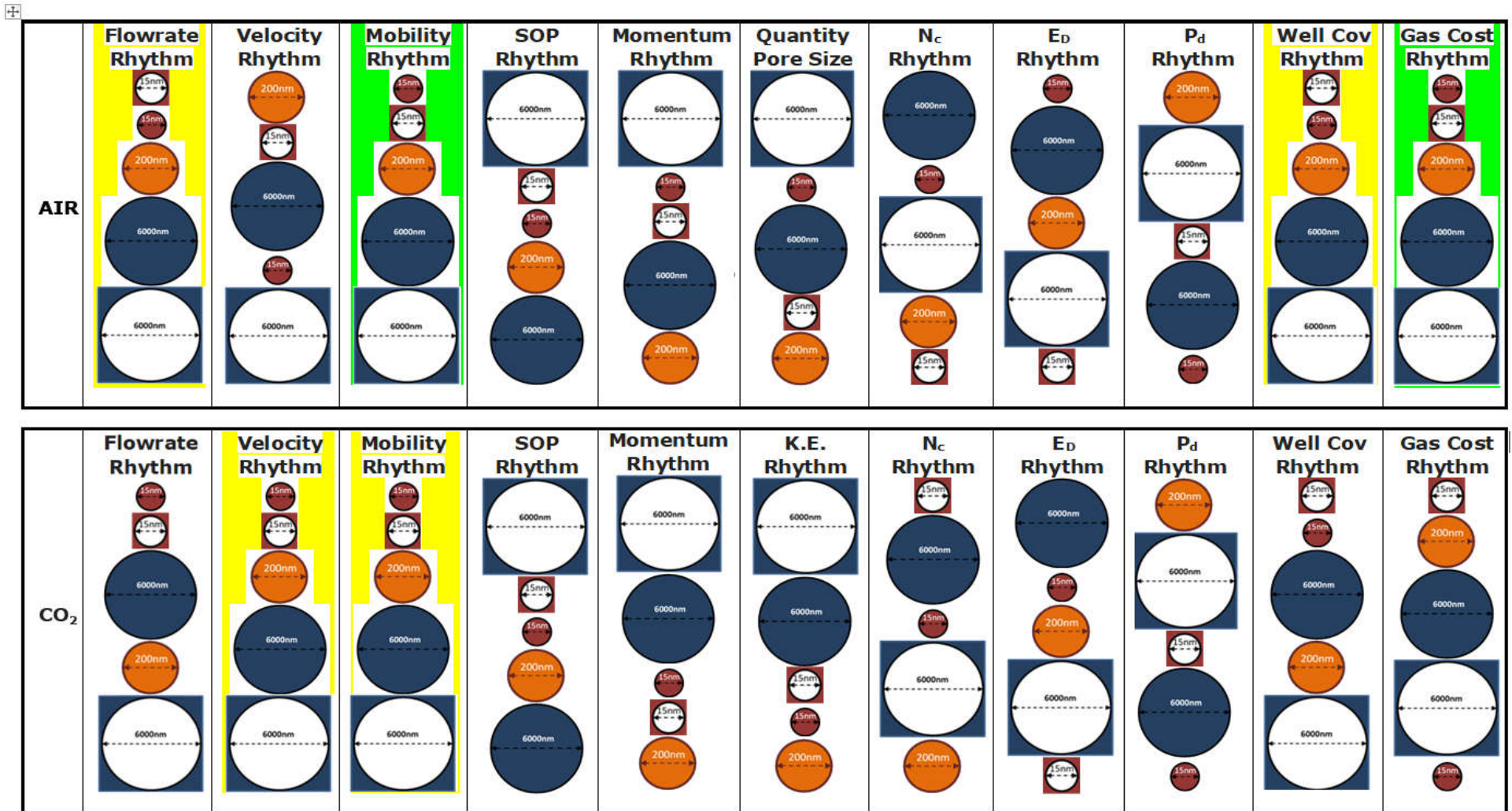
Figure 8-25 Shows pore size and porosity rhythm mapping for Air and CO₂, each cell consist of an engineering quantity that has been optimised and its supporting rhythm, the location of each porous media is in relation to the injection and production wells.

The gradients here are positive for pore size and porosity, unlike CH_4 in Figure 8-24 that only experiences a porosity gradient. For CO_2, in Figure 8-25, velocity and mobility are mutually inclusive with respect to optimisation and reservoir rhythm. It is observed that seven of the quantities are optimised when the injection wells are located in the smaller pore size region of the reservoir, unlike CH_4 optimisation that responds better when injection wells are placed at the larger pore side of the reservoir.

Although the optimisation analyses were carried out with EOR in mind, nonetheless, understanding the rhythm mapping presented here would find great utility in other industries, such as in membrane technology, gas separation, and catalytic reaction systems. Furthermore, and most importantly, this analysis gives a sound solution for well density and well pattern optimisation given a reservoir with known structural rhythm

Chapter Nine

9 CONCLUSION AND RECOMMENDATION

The suitability and performance of gases used for displacing trapped Oil during immiscible gas EOR have been comparatively characterised using data mining techniques and laboratory experiments. The research was divided into three phases based on the industry standard for the EOR project work plan. The phases include Data mining, Experiments, and Phase coupling.

The optimisation of 21 geological and engineering quantities, which include some objective functions, has been applied to evaluate the competitiveness of EOR gases. Some common objective functions applied include volumetric, intrinsic mobility, optimisation curve, interstitial velocity, and momentum. Volumetric flow rate and intrinsic mobility respectively have a direct and inverse relationship with recovery efficiency. In contrast, velocity and momentum have a direct relationship with recovery efficiency. The desired relative mobility for effective gas EOR has been identified to be the one that approaches the condition M<1. This condition has been demonstrated in Figure 2-8a and b to be favourable for improving areal sweep and pore-scale displacement efficiency while simultaneously preventing viscous fingering and early gas breakthrough. Out of the four EOR gases and fourteen geological quantities evaluated in the data mining phase, eight were identified and selected for experimental investigation in this study's second phase. In the second phase, eight gases were investigated in a rigorous experimental PVT study vis-à-vis the eight gas properties and reservoir parameters obtained from the data mining phase. Relevant graphs and tables were used to highlight key observations, such as gas intrinsic mobility sensitivity to operating temperature, injection pressure, kinetic diameter/mean free path, and molecular weight. A performance evaluation process, referred to as Sweep Optimisation Parameter (SOP), was proposed that optimises two of

the objective functions, pore volumetric flow rate, PV, and gas intrinsic mobility, M. Consequently, the best gas for EOR, based on certain common reservoir conditions for each objective function were identified.

9.1 Optimised Gases

After a rigorous analysis of Phase I, II, and III, an optimisation table was completed, as shown in Table 9-1. For each quantity studied, the gas that met a certain optimisation goal was selected and tabulated into three subgroups- fluid properties, reservoir parameters, and cost centres. It has been concluded that out of the twenty-one quantities optimised, CH_4 is the most competitive in ten of the quantities. CO_2 is the most competitive in ten other unique quantities, and N_2 is competitive only in injected gas cost per area. Air is not the best in any of the quantities, however, it came out second-best in some quantities, as shown in the subsequent research summary. The results from Table 9-1 suggest CO_2 and CH_4 are equally competitive.

A further attempt was made to find a segregated and quantitative ranking for the EOR gases. A selectivity index similar to the one applied in perm-selectivity studies was applied to each quantity investigated. CH_4 is found to be the most competitive with a score of 18.37 points, but this is insignificantly above CO_2 at 18.32 points. Air scored 17.32points, and N_2 scored 17.17points. So far, the overall performance metric of EOR gases is not based on their molecular weight order.

Table 9-1 Shows the gas that is most optimised for each quantity related to EOR performance.

Fluid Properties			Reservoir Parameters			Cost Centres		
S/N	Quantity	Optimised Gas	S/N	Quantity	Optimised Gas	S/N	Quantity	Optimised Gas
1.	Capillary number	CH_4	1.	Permeability	CO_2	1.	Well coverage	CH_4
2.	Interstitial velocity	CH_4	2.	Transmissibility	CO_2	2.	Well density	CH_4
3.	Energy loss	CH_4				3.	Commutative gas cost	CO_2
4.	Kinetic energy	CH_4				4.	Displacement pressure	CO_2
5.	Surface tension	CH_4				5.	Gas cost/Area	N_2
6.	Flowrate	CH_4						
7.	Momentum flux	CH_4						
8.	SOP	$CH4$						
9.	Mass flow rate	CO_2						
10.	Mobility	CO_2						
11.	Viscosity	CO_2						
12.	Momentum	CO_2						
13.	Density	CO_2						
14.	Displacement Efficiency	$CO2$						

9.2 Gas Competitive Summary for Select Geological and Engineering Quantities

The competitiveness of the EOR gases has been summarised using their respective performances in a heterogeneous system. Using this instead of their performances in each core sample makes this section concise.

The research has demonstrated the following:

Evaluating the gases based on flow rate indicates that CH_4 offers the highest flow rate for most reservoir conditions and parameters investigated. Therefore, it is the most competitive gas because it has the potential to displace more oil from the reservoir pore by its sheer pore volume rate. CO_2 was the least competitive gas. The suitability order based on maximising this objective function is thus: CH_4 >Air >$20\%CH_4/N_2$ >N_2 >CO_2.

Evaluating the gases based on intrinsic mobility indicates that CO_2 is the least mobile for most reservoir conditions and parameters. Therefore, it is the most competitive gas because it has the greatest potential to achieve the favourable condition of intrinsic mobility ratio M ≤ 1 (as slug or WAG) before other gases. CH_4 was the least competitive gas on this ground. The suitability order based on the minimisation of the objective function is thus: CO_2 >N_2 >$20\%CH_4/N_2$ >Air >CH_4.

Evaluating the gases based on the SOP (Sweep Optimisation Parameter) curve indicates that CH_4 offers the widest solution domain for the reservoir conditions and parameters investigated. The ratio from the pair of values for volumetric rate and intrinsic mobility reflected by the Sweep Optimisation Parameter (SOP) is highest for CH_4. It implies that CH_4 employs the two objectives function's synergy in a heterogeneous system better than the other gases. Therefore, it can be concluded that based on this quantity, CH_4 gas is the most competitive EOR gas for the immiscible gas EOR process. In contrast, the other gases switched competitive performance among themselves based on operating conditions, such as porosity and temperature.

Evaluating the gases based on interstitial velocity indicates that CH_4 has the highest velocity available at the pore scale for most conditions and parameters investigated. Therefore, it is the most competitive gas because it has the potential to attain the minimum velocity required to lift or suspend and displace oil droplets towards producing well. However, there is a downside to this advantage concerning critical velocity, which is the velocity required to keep a stable displacement front. CH_4 has the most propensity to violate the critical velocity if it is not well managed. The suitability order based on optimizing this objective function is thus: CH_4 >Air >20%CH_4/N_2 >N_2 >CO_2.

Evaluating the gases based on interstitial momentum indicates that CO_2 consistently has the highest momentum. Therefore, it is the most competitive gas because, based on the concept of momentum conservation and transfer, the experimental results indicate that CO_2 has the highest momentum in the pores. Suffice to state that this is the only objective function among the five that coincides with the molecular weight order of the gases investigated. The suitability order based on maximising this objective function is thus: CO_2 >Air >N_2 >20%CH_4/N_2 >CH_4.

This momentum diffusion is essential to maintain the displacement front in steady motion at the pore level. CH_4 offers better pore-scale momentum diffusivity between itself and the oil droplets. CO_2 was the least competitive gas on this ground. The suitability order based on maximising this objective function is thus: CH_4> N_2> Air> CO_2.

Energy is required to push trapped droplets across reservoirs. In doing so, energy could also be lost through mechanisms such as friction. It has been demonstrated that CH_4 losses the least energy, and the competitiveness is CH_4> CO_2> Air > N_2.

It has been validated through the field and experimental data that CH_4 requires the least well density. Consequently, the competitive ranking for well density is, therefore: CH_4>Air>N_2>CO_2.

The cost of injectant is a major EOR cost, and the research had demonstrated that CO_2 incurs the least injectant cost. With respect to the other gases, the order of superiority is $CO_2 > N_2 > Air > CH_4$.

9.3 Objective Functions Response to Reservoir Parameters and Fluid Properties

The volumetric rate of EOR gases in the reservoir could be significantly affected by reservoir temperature and injection pressure. Although at low injection pressure (0.20atm) or low-pressure gradient, the relationship between volumetric rate and pressure could not be explained by Boyles laws for all pore sizes. It is assumed that mass influx is causing the gas plots not to obey Boyle's law. This was also observed in small pore size (15nm) for all pressure and temperature range sampled. The gases were observed to respond more to pressure than temperature. CH_4 volumetric rate was the most responsive to injection pressure and temperature, while CO_2 was the least responsive. Therefore, in a reservoir condition, the presence and level of free *in situ* CH_4 should be factored into immiscible CH_4 gas EOR project design.

The intrinsic mobilities of EOR gases were responsive to injection pressure but not to core temperature. This result couples well with the data mining results, as there was no temperature segregation (distinct clusters) observed across EOR technologies or within Gas technology in the database analyses. Meanwhile, there was depth (implying pressure in reservoir context) segregation across EOR technologies and within Gas technology. This implies that temperature is not a critical parameter for selecting gases to be injected in EOR processes, but the pressure is a sound criterion for consideration.

Intrinsic mobility response at low pressure (0.20atm) or pressure gradient is a complicated function for all gases and pore sizes sampled. CH_4 gas intrinsic mobility was the most responsive to injection pressure, and CO_2 was the least responsive. Similarly, in reservoir conditions, the presence and level of *in situ*

CH_4 should be factored into immiscible CH_4 gas EOR project design with respect to mobility.

The R^2 for the relationship between volumetric rate and the inverse of the square root of molecular weight for the system increases with pressure, temperature and porosity but decreases with increasing pore size. Intrinsic mobility of the respective gases did not follow the order of molecular weight. Therefore, they could not be characterised by molecular weight. This may create potent problems for managing gas mixture, where the mixture's weight can vary according to mixture composition due to the potential mixture that could be formed when injected gas, such as N_2, comes in contact with *in-situ* reservoir gases such as CH_4. It was, however, discovered that the intrinsic mobility and volumetric rate are related to the fractional volume composition of the gas mixture. This, therefore, suggests an analytical solution can be offered for injected or *in situ* gas mixtures.

Pore size only affected the volumetric rate and intrinsic mobility when other geometrical factors, such as porosity, radial extent and surface area, were held constant. This extensively corroborates the data mining results in Figure 5-3. It justifies the non-inclusion of porosity as a selection critical within gas EOR technology. However, it is not a sufficient justification for the absence of porosity in the general EOR screening criteria because Figure 5-3a indicates that other EOR technologies are distinctly clustered with respect to porosity.

The surface and radial extent significantly affected the flow rate and intrinsic mobility of gases. This indicates that reservoir size would significantly affect the performance of immiscible Gas EOR. Interestingly, gas flow rate response to temperature reduces as radial thickness increases. Flow rate and intrinsic mobility are generally inversely related to the radial thickness in the experiments, but this could be traced to porosity, as the cores with the highest thickness also have the lowest porosity. The data mining in Figure 5-6a identified that radial extents could characterise EOR reservoirs, EOR technologies, and processes. Therefore, this parameter should be considered as a screening criterion. The well density concept is akin to the radial extent

parameter. It was shown that Well Density could characterise EOR processes. Immiscible gas EOR processes were found to require the least wells per acre compared to other technologies such as Thermal technology. This implies reduced well cost for gas EOR in general.

9.4 Recommendation for Further Study

I.   This study has undergone the optimisation of more than five objective functions with respect to immiscible gas EOR. It is recommended that a numerical model should be developed using the findings from this research so that the volumetric-intrinsic mobility optimisation can be estimated from any given PVT analysis and petrophysical parameters and properties (such as viscosity, mixture molecular weight and radial extent).

II.   Furthermore, this study was conducted using intrinsic mobility as the basis for evaluation both in the data mining and experimental phases. Although each approach results converge for immiscible gas EOR, it is recommended that a further study should be carried out using relative mobility as the basis for evaluation.

III.   The data from the experiments have been analysed using simple models. There is more information that can be derived from the data set than this research has provided. Therefore, it is recommended that more advanced numerical techniques be applied to analyse the data generated in this study.

IV.   This study has been conducted using laboratory conditions. Although a number of the quantities were set to reservoir conditions, such as temperature and porosity, there could be the challenge of oversimplification and scaling of findings in this study to reservoir size and conditions. It is recommended that this research be conducted using additional reservoir conditions.

REFERENCES

Abbas, E. and Song, C.L., 2011. Artificial intelligence selection with capability of editing a new parameter for EOR screening criteria. *Journal of Engineering Science and Technology*, *6*(5), pp.628-638.

Abdullah, M.R., 2018. The Fracturing Behavior in Layered Rocks: Modeling and Analyses of Fractured Samples. Available from: http://resolver.tudelft.nl/uuid:73622e8e-4cec-4add-8f51-ebf9c0061e99. [Access 10/09/2021]

Abdus, S. and Ghulam, M.I., 2016. 16-Waterflooding and waterflood surveillance. Reservoir Engineering; Abdus, S., Ed.; Gulf Professional Publishing: Amsterdam, The Netherlands, pp.289-312.

Abu-Elbashar, O.B., Daltaban, T.S., Wall, C.G. and Archer, J.S., 1990, September. Application of analytical methods in predicting waterflood performance of reservoirs with stochastic sand bodies. In *ECMOR II-2nd European Conference on the Mathematics of Oil Recovery* (pp. cp-231). European Association of Geoscientists & Engineers.

Abunumah, O., Ogunlude, P. and Gobina, E., 2021a. Experimental Evaluation of the Mobility Profile of Enhanced Oil Recovery Gases. *Advances in Chemical Engineering and Science*, *11*(02), p.154.

Abunumah, O., Ogunlude, P. and Gobina, E. 2021b. The effect of pressure and porous media structural parameters coupling on gas apparent viscosity. In Proceedings of the ICANM 2021: 8th International conference and exhibition on advanced and nanomaterials 2021 (ICANM 2021), 9-11 August 2021, [virtual conference]. Ontario: ICANM, pages 42-46. Available from: https://rgu-repository.worktribe.com/output/1427964.

Abunumah, O., Ogunlude, P. and Gobina, E. 2021c. Cost description and characterisation of gas enhanced oil recovery processes. In 2021 TUBA (Turkish Academy of Science) World conference on energy science and technology (TUBA WCEST-2021) book of abstracts, 8-12 August 2021, [virtual conference]. Ankara: Turkish Academy of Sciences. https://doi.org/10.53478/TUBA.2021.017.

Adewumi, M., 2009. PNG 520 phase relations in reservoir engineering. *Pennsylvania State University, Retrieved September 9*, 2019, https://www.e-education.psu.edu/png520/m18_p9.html

Ado, M.R., 2020. Effect of reservoir pay thickness on the performance of the THAI heavy oil and bitumen upgrading and production process. *Journal of Petroleum Exploration and Production Technology*, *10*(5), pp.2005-2018.

Agarwal, V.C., 2012. *Groundwater hydrology*. PHI Learning Pvt. Ltd.

Ahmed, T. And Meehan, D.N., 2012. Chapter 6 - Introduction To Enhanced Oil Recovery. In: T. Ahmed And D.N. Meehan, Eds, Advanced Reservoir Management And Engineering (Second Edition). Boston: Gulf Professional Publishing, Pp. 541-585.

Ahmed, T., 2010. Principles of waterflooding. *Reservoir engineering handbook*, pp.909-1095.

Ahmed, T., 2010a. Chapter 5 - Relative Permeability Concepts. In: T. Ahmed, ed, *Reservoir Engineering Handbook (Fourth Edition).* Boston: Gulf Professional Publishing, pp. 288-330.

Ahmed, T., 2010b. Chapter 4–Fundamentals of Rock Properties. In: T. Ahmed, ed, *Reservoir Engineering Handbook (Fourth Edition).* Boston: Gulf Professional Publishing, pp.189-287.

Ahmed, T., 2018. *Reservoir engineering handbook*. Gulf professional publishing.

Al Adasani, A. and Bai, B., 2011. Analysis of EOR projects and updated screening criteria. Journal of Petroleum Science and Engineering, 79(1-2), pp.10-24.

Al-Abri, A., Hiwa, S. and Robert, A., 2009. Experimental investigation of the velocity-dependent relative permeability and sweep efficiency of supercritical CO_2 injection into gas condensate reservoirs. *Journal of Natural Gas Science and Engineering*, *1*(4-5), pp.158-164.

Al-Dahhan, M.H., Larachi, F., Dudukovic, M.P. and Laurent, A., 1997. High-pressure trickle-bed reactors: a review. *Industrial & engineering chemistry research*, *36*(8), pp.3292-3314.

Alfarge, D., Wei, M. and Bai, B., 2017. Factors affecting CO_2-EOR in shale-oil reservoirs: numerical simulation study and pilot tests. *Energy & Fuels*, *31*(8), pp.8462-8480.

Alhashmi, N.F., Torres, K., Faisal, M., Cornejo, V.S., Bethapudi, B.P., Mansur, S. and Al-Rawahi, A.S., 2016, September. Rock typing classification and hydraulic flow units definition of one of the most prolific carbonate reservoir in the onshore Abu Dhabi. In *SPE Annual Technical Conference and Exhibition*. Society of Petroleum Engineers.

AlHomadhi, E.S., 2014. New correlations of permeability and porosity versus confining pressure, cementation, and grain size and new quantitatively correlation relates permeability to porosity. Arabian Journal of Geosciences, 7(7), pp.2871-2879.

Allen, M.D., and Raabe O.G. (1985). Slip correction measurements of spherical solid aerosol particles in an improved Millikan apparatus. Aerosol Sci Technol 4(3):269–286

Al-Marhoun, M.A., 1988. PVT correlations for Middle East crude oils. *Journal of Petroleum Technology*, *40*(05), pp.650-666.

Al-Mayan, H., Winkler, M., Kamal, D., AlMahrooqi, S. and AlMaraghi, E., 2016. Integrated EOR Screening of Major Kuwait Oil Fields Using Qualitative, Quantitative and Risk Screening Criteria. In SPE EOR Conference at Oil and Gas West Asia. Society of Petroleum Engineers.

Al-Shammasi, A.A., 2001. A review of bubblepoint pressure and oil formation volume factor correlations. *SPE Reservoir Evaluation & Engineering*, *4*(02), pp.146-160.

Alvarado, V. and Manrique, E. 2010a. Chapter 8 - EOR's Current Status, In Enhanced Oil Recovery, Gulf Professional Publishing: Boston, Pages 133-156.
(https://www.sciencedirect.com/science/article/pii/B9781856178556 000140)

Alvarado, V. and Manrique, E., 2010b. Enhanced oil recovery: an updated review. *Energies*, *3*(9), pp.1529-1575.

Alvarado, V., Ranson, A., Hernandez, K., Manrique, E., Matheus, J., Liscano, T. and Prosperi, N., 2002, October. Selection of EOR/IOR opportunities based on machine learning. In *European Petroleum Conference*. OnePetro.

Aminzadeh, F. and Dasgupta, S.N., 2013. Fundamentals of Petroleum Geophysics. In *Developments in Petroleum Science* (Vol. 60, pp. 37-92). Elsevier.

Amirkhani, F., Harami, H.R. and Asghari, M., 2020. CO_2/CH_4 mixed gas separation using poly (ether-b-amide)-ZnO nanocomposite membranes: Experimental and molecular dynamics study. *Polymer Testing*, *86*, p.106464.

Andrew, M., Bijeljic, B. and Blunt, M.J., 2014. Pore-by-pore capillary pressure measurements using X-ray microtomography at reservoir conditions: Curvature, snap-off, and remobilisation of residual CO_2. *Water Resources Research*, *50*(11), pp.8760-8774.

Andri, B., Lebrun, P., Dispas, A., Klinkenberg, R., Streel, B., Ziemons, E., Marini, R.D. and Hubert, P., 2017. Optimization and validation of a fast supercritical fluid chromatography method for the quantitative determination of vitamin D3 and its related impurities. *Journal of Chromatography A*, *1491*, pp.171-181.

Annie., 2015. Efficiency of a Displacement Process. [Online] Available from < http://slideplayer.com/slide/4142747/ >

Anon, 2021. Collisional Cross Section. Available at: https://chem.libretexts.org/@go/page/1403 [Accessed September 8, 2021].

Apostolos, K., Jonathan, B. and Saeed, T. 2016. Fundamentals of Fluid Flow in Porous Media. [Online] Available from. < http://perminc.com/resources/fundamentals-of-fluid-flow-in-porous-media/> [Accessed 12/10/2017]

Atangana, A. (2018). Chapter 2 - principle of groundwater flow. In A. Atangana (Ed.), *Fractional operators with constant and variable order with application to geo-hydrology* (pp. 15-47) Academic Press. doi:https://doi.org/10.1016/B978-0-12-809670-3.00002-3 Retrieved from https://www.sciencedirect.com/science/article/pii/B9780128096703000023

Atkins, A.G., Atkins, T. and Escudier, M., 2013. A dictionary of mechanical engineering. Oxford University Press.

Avison, J., 2014. *The world of physics*. Nelson Thornes, Cheltenham, Glasgow.

Avogadro, A., 1811. Essay on a manner of determining the relative masses of the elementary molecules of bodies, and the proportions in which they enter into these compounds. *Journal de physique*, *73*, pp.58-76.

Ayan, C., Colley, N., Cowan, G., Ezekwe, E., Wannell, M., Goode, P., Halford, F., Joseph, J., Mongini, A., Obondoko, G. and Pop, J., 1994. Measuring

permeability anisotropy: the latest approach. Oilfield Review, 6(4), pp.24-35.

Aziz, H., 2017. Comparison between field research and controlled laboratory research. Fortune Journal, 1(2), pp.102-104 http://www.fortunejournals.com/articles/comparison-between-field-research-and-controlled-laboratory-research.pdf

Babadagli, T., 2020. Philosophy of EOR. *Journal of Petroleum Science and Engineering*, *188*, p.106930.

Babadagli, T., Al-Bemani, A., Boukadi, F. and Iyoho, A.W., 2001. EOR possibilities for development of a mature light-oil reservoir in Oman. In *SPE Asia Pacific Improved Oil Recovery Conference*. Society of Petroleum Engineers.

Bachu, S., 2016. Identification of oil reservoirs suitable for CO_2-EOR and CO_2 storage (CCUS) using reserves databases, with application to Alberta, Canada. *International Journal of Greenhouse Gas Control*, *44*, pp.152-165.

Bagci, A.S., 2007. Immiscible CO_2 flooding through horizontal wells. *Energy Sources, Part A*, *29*(1), pp.85-95.

Bahadori, A., 2018. Fundamentals of enhanced oil and gas recovery from conventional and unconventional reservoirs. Gulf Professional Publishing.

Baker, R., 1998. Reservoir Management for Waterfloods-Part II. Petroleum Society of Canada. doi:10.2118/98-01-DA

Baker, R.W., 2012. *Membrane technology and applications*. John Wiley & Sons.

Bamidele O., 2014. Ebok Marginal Field Comes on Stream. Quarterly In-House Journal of the Department of Petroleum Resources. Vol. 6 (2) pp.2 http://dpr.gov.ng/index/wp-content/uploads/2014/10/DPR%20Newsletter%20SEPT%202011.pdf]

Bank, G. C., Riestenberg, D. and Koperna, G.J., 2007. 'CO$_2$-Enhanced Oil Recovery Potential of the Appalachian Basin.' SPE: *Conference Paper, Eastern Regional Meeting,* Kentucky

Baojun, F., Xingjia, D. and Cai, Y., 1997. Pilot Test of Water Alternating Gas Injection in Heterogeneous Thick Reservoir of Positive Rhythm Sedimentation of Daqing Oil Field. *SPE Advanced Technology Series*, *5*(01), pp.41-48.

Beal, C., 1946. The viscosity of air, water, natural gas, crude oil and its associated gases at oil field temperatures and pressures. *Transactions of the AIME*, *165*(01), pp.94-115. Chew, J.N. and Connally Jr, C.A., 1959. A viscosity correlation for gas-saturated crude oils. *Transactions of the AIME*, *216*(01), pp.23-25.

Beaumont, E.A. and Fiedler, F., 1999. Treatise of Petroleum Geology/Handbook of Petroleum Geology: Exploring for Oil and Gas Traps. Chapter 5: Formation Fluid Pressure and Its Application.

Beggs, H.D., 1987. Oil System Correlations (1987 PEH Chapter 22). *Petroleum Engineering Handbook*.

Bejan, A., 2016. *Advanced engineering thermodynamics*. John Wiley & Sons.

Belyadi, H., Fathi, E. and Belyadi, F., 2019. Hydraulic fracturing in unconventional reservoirs: theories, operations, and economic analysis. Gulf Professional Publishing.

Ben, S. and Randall, E., 2015. Unlocking marginal fields. [Online] Available from <http://www.oedigital.com/component/k2/item/7889-unlocking-marginal-fields> [Accessed 6/10/2017]

Berenblyum, R., Calderon, G.R., Kollbotn, L. and Surguchev, L.M., 2008. Modelling CO 2 Injection: IOR Potential after Waterflooding. In *SPE Symposium on Improved Oil Recovery*. Society of Petroleum Engineers.

Bergman, D.F. and Sutton, R.P., 2007. An update to viscosity correlations for gas-saturated crude oils. In *SPE annual technical conference and exhibition*. Society of Petroleum Engineers.

Bergstrom, J.S., 2015. *Mechanics of solid polymers: theory and computational modeling*. William Andrew.

Berker, A., 2002. *Rheology for adhesion science and technology* (pp. 443-498). Amsterdam: Elsevier Science BV.

Bess, R., 2019, How to Calculate Porosity. Available [online] https://www.wikihow.com/Calculate-Porosity#aiinfo (accessed: 12/06/2020)

Bonnell, B. and Hurich, C., 2008. Characterization of reservoir heterogeneity: An investigation of the role of cross-well reflection data. *CSEG Recorder*, *33*(2), pp.31-37.

Brashear, J.P. and Kuuskraa, V.A., 1978. The potential and economics of enhanced oil recovery. *Journal of Petroleum Technology*, *30*(09), pp.1-231.

Breit, V.S., 1992. Enhanced oil recovery: part 10. Reservoir engineering methods. In Morton-Thompson, D. and Woods, A.M. eds., 1993. *Development geology reference manual: AAPG methods in exploration series, no. 10* (No. 10). AAPG.

Bretherton, F.P., 1961. The motion of long bubbles in tubes. *Journal of Fluid Mechanics*, *10*(2), pp.166-188.

Brian, W., 2017. The Next Frontier: EOR in unconventional Resources. Exploration and Production. 90(8) pp 48-49

Brooks, R. and Corey, T., 1964. HYDRAU uc properties of porous media. *Hydrology Papers, Colorado State University*, *24*, p.37.#

Brooks, R.A., 1979. *The Geologic Parameters Affecting In-situ Leaching of Uranium Deposits*. US Department of the Interior, Geological Survey.

Buckley, S.E. and Leverett, M., 1942. Mechanism of fluid displacement in sands. *Transactions of the AIME*, *146*(01), pp.107-116.

Buikema T. A., Mair C., Williams D., Mercer D., Webb K. J., Hewson A., Reddick C. E. A. and Robbana E. 2011. Low salinity enhanced oil recovery—laboratory today one field implementation—LoSal EOR into the Clair Ridge project. In Proc. EAGE IOR Symp. Cambridge, UK, 12–14 April 2011. See http://www.earthdoc.org

Buryakovsky, L.A., Chilingar, G.V. And Aminzadeh, F., 2001. Chapter 10 - Mathematical Models In Oil And Gas Exploration And Production (Static Geologic Systems). In: L.A. Buryakovsky, G.V. Chilingar And F. Aminzadeh, Eds. *Petroleum Geology Of The South Caspian Basin.* Burlington: Gulf Professional Publishing. Pp. 248-346

Buynevich, I.V., Jol, H.M. and FitzGerald, D.M., 2009. Coastal environments. *Ground penetrating radar: Theory and applications*, pp.299-322.

Carlo, P., 2017. Unlocking marginal fields UKCS opportunity. [Online] Available from <https://www.ogauthority.co.uk/media/3325/oga-subsea-expo-c-procaccini-final.pdf> [Accessed 6/10/2017]

Carman, P.C., 1937. Fluid flow through granular beds. *Trans. Inst. Chem. Eng.*, *15*, pp.150-166.

Cash, P., Stanković, T. and Štorga, M., 2016. An introduction to experimental design research. In *Experimental Design Research* (pp. 3-12). Springer, Cham.

Castricum, H.L., Qureshi, H.F., Nijmeijer, A. and Winnubst, L., 2015. Hybrid silica membranes with enhanced hydrogen and CO_2 separation properties. *Journal of membrane science*, *488*, pp.121-128.

Caudle, B.H. and Dyes, A.B., 1958. Improving miscible displacement by gas-water injection. *Transactions of the AIME*, *213*(01), pp.281-283.

Cerpa, N.G., Wada, I. and Wilson, C.R., 2019. Effects of fluid influx, fluid viscosity, and fluid density on fluid migration in the mantle wedge and their implications for hydrous melting. *Geosphere*, *15*(1), pp.1-23.

Chandrasekharaiah, D.S. and Debnath, L., 2014. *Continuum mechanics*. Elsevier.

Chanson, H., 2012. Momentum considerations in hydraulic jumps and bores. *Journal of Irrigation and Drainage Engineering*, *138*(4), pp.382-385.

Chapman, S., Cowling, T. G., and Burnett, D. (1970). The mathematical theory of non-uniform gases: an account of the kinetic theory of viscosity, thermal conduction and diffusion in gases. Cambridge university press.

Charles L V, John G K and Robert M S 1993, 'Capillary Pressure' in Morton-Thompson, D. and Woods, A M (eds), *Development geology reference manual: AAPG methods in exploration series*, 10 edn. AAPG, Tulsa, Oklahoma

Chen, Z.Y., Song, H., Zhang, X.P., 2012. Air Foam Injection for EOR in Light Oil Reservoirs with High Heterogeneity. Advanced Materials Research 524–527, 1322–1326. https://doi.org/10.4028/www.scientific.net/amr.524-527.1322

Cheng, H., Hills, J.H. and Azzorpardi, B.J., 1998. A study of the bubble-to-slug transition in vertical gas-liquid flow in columns of different diameter. *International Journal of Multiphase Flow*, *24*(3), pp.431-452.

Chin, W.C., 2002. *Quantitative methods in reservoir engineering*. Gulf Professional Publishing. Woburn, New York

Christou, C., & Kokou Dadzie, S. (2015). Direct simulation Monte Carlo method in porous media with varying Knudsen number. In SPE Reservoir Simulation Symposium. Society of Petroleum Engineers.

Chuoke, R.L., Van Meurs, P. and van der Poel, C., 1959. The instability of slow, immiscible, viscous liquid-liquid displacements in permeable media. *Transactions of the AIME*, *216*(01), pp.188-194.

Civan, F., 2015. *Reservoir formation damage: fundamentals, modeling, assessment, and mitigation*. Gulf Professional Publishing.

Clancy, J.P., Gilchrist, R.E., Cheng, L.H.K. and Bywater, D.R., 1985. Analysis of nitrogen-injection projects to develop screening guides and offshore design criteria. *Journal of petroleum technology*, *37*(06), pp.1-097.

Colin, S., 2006. Single-phase gas flow in microchannels. *Heat transfer and fluid flow in minichannels and microchannels*, pp.9-86.

Coll, R., Peña, G., Guitián, J., Mancera, A. and Escobar, E., 2017, November. Surface Facilities for a Giant Thermal EOR Project-Cost and HSE Implications of Alternative Fuels for Steam Generation. In SPE Abu Dhabi International Petroleum Exhibition & Conference. Society of Petroleum Engineers.

Compernolle, T., Welkenhuysen, K., Huisman, K., Piessens, K. and Kort, P., 2017. Off-shore enhanced oil recovery in the North Sea: The impact of price uncertainty on the investment decisions. *Energy Policy*, *101*, pp.123-137.

Cone, M.P. and Kersey, D.G., 1992. "Porosity: Part 5. Laboratory Methods." in Morton-Thompson, D. and Woods, A M (eds), Development geology reference manual: AAPG methods in exploration series, 10 edn. AAPG, Tulsa, Oklahoma

Coratekin, T., Schubert, A. and Ballmann, J., 1999. Assessment of Eddy Viscosity Models in 2D and 3D Shock/Boundary-Layer Interactions.

In *Engineering Turbulence Modelling and Experiments 4* (pp. 649-658). Elsevier Science Ltd.

Corey, A.T., 1954. The interrelation between gas and oil relative permeabilities. *Producers monthly*, *19*(1), pp.38-41.

Cragoe, C.S., 1929. Thermodynamic Properties of Petroleum Products. *Miscellaneous Publications No. 97, Bureau of Standards, US Department of Commerce, Washington, DC, 22.*

Cronquist, C., 1977. Tertiary Recovery of Crude Oil. In Meyer, R.F. ed., 2013. *The Future Supply of Nature-Made Petroleum and Gas: Technical Reports*. Pergamon, Elmsford, New York.

Curtis, C., Kopper, R., Decoster, E., Guzman-Garcia, A., Huggins, C., Knauer, L., Minner, M., Kupsch, N., Linares, L.M., Rough, H. and Waite, M., 2002. Heavy-oil reservoirs. *Oilfield Review*, *14*(3), pp.30-51.

Cutler Jr, W.W., 1924. Estimation of underground oil reserves by oil-well production curves. [35 references] (No. BM-BULL-228). Bureau of Mines, Washington, DC (USA).

Danielson, R.E. and Sutherland, P.L., 1986. Porosity. In A. Klute (Ed.) *Methods of Soil Analysis: Part 1 Physical and Mineralogical Methods*, *5*, pp.443-461. doi:10.2136/sssabookser5.1.2ed.c18

Darcy, H., 1856. *Les fontaines publiques de la ville de Dijon: exposition et application...*. Victor Dalmont.

David, F. M., and Robert M. C., 1996. Enhanced Oil Recovery Methods. In Lyons, W. C. (ed.) *Standard Handbook of Petroleum and Natural Gas Engineering: Volume 2.* Texas: Gulf Professional Publishing.

Davies, R.M. and Taylor, G.I., 1950. The mechanics of large bubbles rising through extended liquids and through liquids in tubes. *Proceedings of the Royal Society of London. Series A. Mathematical and Physical Sciences*, *200*(1062), pp.375-390.

Davim, J.P. ed., 2012. *The design and manufacture of medical devices*. Elsevier, Woodhead Publishing Limited, Cambridge

de Sousa, D.A., Soares, E.J., de Queiroz, R.S. and Thompson, R.L., 2007. Numerical investigation on gas-displacement of a shear-thinning liquid and a visco-plastic material in capillary tubes. *Journal of non-newtonian fluid mechanics*, *144*(2-3), pp.149-159.

Deb, U.K., Chayantrakom, K. and Lenbury, Y., 2012. Comparison of Single-phase and Two-phase Flow Dynamics in the HLTP for Microalgae Culture. International journal of mathematics and computers in simulation, 6(5), pp.496-503.

Delamaide, E., Bazin, B., Rousseau, D. and Degre, G., 2014b. Chemical EOR for heavy oil: the Canadian experience. In *SPE EOR Conference at Oil and Gas West Asia*. Society of Petroleum Engineers.

Delamaide, E., Zaitoun, A., Renard, G. and Tabary, R., 2014a. Pelican Lake field: first successful application of polymer flooding in a heavy-oil reservoir. *SPE Reservoir Evaluation & Engineering*, *17*(03), pp.340-354.

Dellinger, S.E., Patton, J.T. and Holbrook, S.T., 1984. CO_2 mobility control. *Society of Petroleum Engineers Journal*, *24*(02), pp.191-196.

Desbarats, A.J. and Dimitrakopoulos, R., 1990. Geostatistical modeling of transmissibility for 2D reservoir studies. *SPE formation evaluation*, *5*(04), pp.437-443.

Dielman, S.A., 2005. Hydraulic Conductivity/Transmissibility. *Water Encyclopedia*, *5*, pp.507-514.

Dietz, D.N., 1953. A theoretical approach to the problem of encroaching and by-passing edge water. *Proc. Akad. van Wetenschappen*, *56*, pp.83-92.

Dindoruk, B. and Christman, P.G., 2001, January. PVT properties and viscosity correlations for Gulf of Mexico oils. In *SPE annual technical conference and exhibition*. Society of Petroleum Engineers.

DOE/NETL, 2010. Carbon Dioxide Enhanced Oil Recovery Untapped Domestic Energy Supply and Long Term Carbon Storage Solution, [Online] Available From http://www.netl.doe.gov/technologies/oil-gas/publications/EP/small_CO$_2$_eor_primer.pdf [Accessed 23/10/2017]

Donaldson, E.C, Chilingarian, G.V. and Yen, T.F., 1989. Enhanced Oil Recovery, II: Processes and Operations. Amsterdam: Elsevier Science Publishers

Donaldson, E.C. and Alam, W., 2008. "Wettability and Production," *Wettability*, pp. 121–172. doi:10.1016/B978-1-933762-29-6.50009-0.

Donaldson, E.C. And Alam, W., 2008. Chapter 3 - Wettability And Production. In: E.C. Donaldson And W. Alam, Eds, Wettability. Gulf Publishing Company, Pp. 121-172.

Dou, W., Liu, L., Wu, K., Xu, Z., Liu, X. and Feng, X., 2018. Diagenetic heterogeneity, pore throats characteristic and their effects on reservoir quality of the Upper Triassic tight sandstones of Yanchang Formation in Ordos Basin, China. *Marine and Petroleum Geology*, *98*, pp.243-257.

DPR (Department of Petroleum Resources), 2014. List of Marginal Fields. [Online] Available from https://dpr.gov.ng/index/list-of-marginal-fields/# [Accessed 10/5/2017]

Duda, J.R. and Il, A.B.Y., 2010. Carbon Dioxide Enhanced Oil Recovery: Untapped Domestic Energy Supply and Long Term Carbon Storage Solution. *US Department of Energy: Washington, DC, USA*.

Dumore, J.M., 1964. Stability considerations in downward miscible displacements. *Society of Petroleum Engineers Journal*, *4*(04), pp.356-362.

Durham University. 2010. North Sea oil recovery using carbon dioxide is possible, but time is running out, expert says. *ScienceDaily*. Retrieved October 25, 2017, from www.sciencedaily.com/releases/2010/10/101013193533.htm

Dyes, A.B., Caudle, B.H. and Erickson, R.A., 1954. Oil production after breakthrough as influenced by mobility ratio. *Journal of Petroleum Technology*, *6*(04), pp.27-32.

Dykstra, H. and Parsons, R.L., 1950. The prediction of oil recovery by waterflood. *Secondary recovery of oil in the United States*, *2*, pp.160-174.

Eain, M.M.G., Egan, V. and Punch, J., 2013. Film thickness measurements in liquid–liquid slug flow regimes. *International Journal of Heat and Fluid Flow*, *44*, pp.515-523.

El Ela, M.A. and Sayyouh, H., 2014. An integrated approach for the application of the enhanced oil recovery projects. Journal of Petroleum Science Research.

El Ela, M.A. and Sayyouh, H., 2014. An integrated approach for the application of the enhanced oil recovery projects. *Journal of Petroleum Science Research*, *3*(4), pp.176-188.

El Ela, M.A. and Sayyouh, H., 2014. An integrated approach for the application of the enhanced oil recovery projects. *Journal of Petroleum Science Research*, *3*(4), pp.176-188.

Elsharkawy, A.M. and Alikhan, A.A., 1999. Models for predicting the viscosity of Middle East crude oils. *Fuel*, *78*(8), pp.891-903.

Engineering ToolBox, 2014. Gases - Dynamic Viscosity. [online] Available at: https://www.engineeringtoolbox.com/gases-absolute-dynamic-viscosity-d_1888.html [Accessed 2 August, 2018].

Espinoza, D.N. and Santamarina, J.C., 2010. Water- CO_2-mineral systems: Interfacial tension, contact angle, and diffusion—Implications to CO_2 geological storage. *Water resources research*, *46*(7).

Ezekiel, J., Wang, Y., Liu, Y., Zhang, L., Deng, J. and Ren, S., 2014, November. Case study of Air injection IOR process for a low permeability light oil reservoir in Eastern China. In *SPE Annual Caspian Technical Conference and Exhibition*. Society of Petroleum Engineers.

Fadili, A., Kristensen, M. R., & Moreno, J. 2009. Smart Integrated Chemical EOR Simulation. International Petroleum Technology Conference. doi:10.2523/IPTC-13762-MS.

Faghri, A. and Zhang, Y., 2020. Flow and heat transfer in porous media. In *Fundamentals of Multiphase Heat Transfer and Flow* (pp. 687-745). Springer, Cham.

Fairbrother, F. and Stubbs, A.E., 1935. 119. Studies in electro-endosmosis. Part VI. The "bubble-tube" method of measurement. *Journal of the Chemical Society (Resumed)*, pp.527-529.

Falode, O. and Manuel, E., 2014. Wettability effects on capillary pressure, relative permeability, and irreducible saturation using porous plate. *Journal of Petroleum Engineering*, *2014*. Volume 2014 (465418)

Fanchi, J., 2010. *Integrated reservoir asset management: principles and best practices*. Gulf Professional Publishing.

Fanchi, J.R., 2002. Measures of Rock-Fluid Interactions, *Shared Earth Modeling*, pp. 108–132. doi:10.1016/B978-075067522-2/50007-0.

Fanchi, J.R., 2002a. Chapter 7 - Measures Of Rock-Fluid Interactions. In: J.R. Fanchi, Ed, Shared Earth Modeling. Woburn: Butterworth-Heinemann. pp. 108-132.

Fanchi, J.R., 2002b. Shared Earth Modelling: Methodologies for Integrated Reservoir Simulations. Gulf Professional Publishing, Woburn, MA.

Fanchi, J.R., 2007. Volume I–General Engineering. *Petroleum Engineering Handbook; Lake, LW, Ed.; Society of Petroleum Engineers: Richardson, TX*.

Fanchi, J.R., 2010. 10 - Rock–Fluid Interactions. In: J.R. Fanchi, Ed, Integrated Reservoir Asset Management. Boston: Gulf Professional Publishing, pp. 167-185.

Fanchi, J.R., 2010a. Fluid Displacement, *Integrated Reservoir Asset Management*, pp. 205–222. doi:10.1016/B978-0-12-382088-4.00012-8.

Fanchi, J.R., 2010b. Rock–Fluid Interactions, *Integrated Reservoir Asset Management*, pp. 167–185. doi:10.1016/B978-0-12-382088-4.00010-4.

Fassihi, M.R., Yannimaras, D.V. and Kumar, V.K., 1997. Estimation of recovery factor in light-oil air-injection projects. *SPE Reservoir Engineering*, *12*(03), pp.173-178.

Feng, G. and Yu, M., 2015. Characterisation of pore volume of cumulative water injection distribution. *Petroleum*, *1*(2), pp.158-163.

Fink, J., 2015. *Petroleum engineer's guide to oil field chemicals and fluids*. Pages 477-565. Gulf Professional Publishing.

Firoozabadi, A. and Ramey Jr, H.J., 1988. Surface tension of water-hydrocarbon systems at reservoir conditions. *Journal of Canadian Petroleum Technology*, *27*(03).

Forrest, J., Marcucci, E. and Scott, P., 2005. Geothermal gradients and subsurface temperatures in the northern Gulf of Mexico.

Frashad, F., LeBlanc, J.L., Garber, J.D. and Osorio, J.G., 1996, January. Empirical PVT correlations for Colombian crude oils. In *SPE Latin America/Caribbean petroleum engineering conference*. Society of Petroleum Engineers.

Gbadamosi, A.O., Kiwalabye, J., Junin, R. and Augustine, A., 2018. A review of gas enhanced oil recovery schemes used in the North Sea. Journal of Petroleum Exploration and Production Technology, 8(4), pp.1373-1387.

George, E., 2013. DPR Sponsors Forum to Boost Exploration…Aims TO Meet National Reserves Target. Quarterly In-House Journal of the Department of Petroleum Resources. Vol. 7 (2) pp.1

George, O., 2014. FG sets March 2015 as deadline for non-performing marginal fields. Available [online] from: https://dpr.gov.ng/index/fg-sets-march-2015-as-deadline-for-non-performing-marginal-fields-2/ [accessed 5/09/2017]

Gerber, A.S. and Green, D.P., 2008. Field experiments and natural experiments. In *The Oxford handbook of political science*.

Germic, L., Ebert, K., Bouma, R.H.B., Borneman, Z., Mulder, M.H.V. and Strathmann, H., 1997. Characterisation of polyacrylonitrile ultrafiltration membranes. *Journal of membrane science*, *132*(1), pp.131-145.

Ghani, A.A., 2014. Experimental Research Methods for Students in Built Environment and Engineering. In *MATEC Web of Conferences* (Vol. 10, p. 01001). EDP Sciences.

Ghanizadeh, A., Clarkson, C.R., Aquino, S., Ardakani, O.H. and Sanei, H., 2015. Petrophysical and geomechanical characteristics of Canadian tight oil and liquid-rich gas reservoirs: I. Pore network and permeability characterisation. *Fuel*, *153*, pp.664-681.

Gharbi, R.B., 2000. An expert system for selecting and designing EOR processes. *Journal of Petroleum Science and Engineering*, *27*(1-2), pp.33-47.

Ghoodjani, E. and Bolouri, S.H., 2015. Green Balance Software: An Integrated Model for Screening of CO_2-EOR and CCS Projects. *Energy Sources, Part A: Recovery, Utilization, and Environmental Effects*, *37*(14), pp.1479-1486.

Gidley, J.L., 1992. Stimulation: Part 9. Production Engineering Methods. In Morton-Thompson, D. and Woods, A.M. eds., 1993. *Development geology reference manual: AAPG methods in exploration series, no. 10* (No. 10). AAPG.

Glassman, I., and Harris, B. L., 1952. Collision Diameters of Some Gases as a Function of Temperature. The Journal of Physical Chemistry, 56(6), 797-799.

Glover, P., 2000. Petrophysics. *University of Aberdeen, UK*.

Godec, M., Kuuskraa, V., Van Leeuwen, T., Melzer, L.S. and Wildgust, N., 2011. CO_2 storage in depleted oil fields: The worldwide potential for carbon dioxide enhanced oil recovery. *Energy Procedia*, *4*, pp.2162-2169. doi:https://doi.org/10.1016/j.egypro.2011.02.102.

Golan, M., 1992. Fundamentals of Fluid Flow: Part 10. Reservoir Engineering Methods. in Morton-Thompson, D. and Woods, A.M. eds., 1993. *Development geology reference manual: AAPG methods in exploration series, no. 10* (No. 10). AAPG.

Gomari, S.R. and Amrouche, F., 2017, July. Investigating the Effect of Rock Pore Size Distribution on Reservoir Production Performance. In *8th International Conference on Computational Methods*.

Goodlett, G.O., Honarpour, M.M., Chung, F.T. and Sarathi, P.S., 1986, January. The role of screening and laboratory flow studies in EOR process evaluation. In SPE Rocky Mountain Regional Meeting. Society of Petroleum Engineers.

Grot, W., 2011. 9 - Experimental Methods. In: W. Grot, Ed. *Fluorinated Ionomers (Second Edition).* William Andrew Publishing. Pp. 211-233

Guerillot, D.R., 1988, January. EOR screening with an expert system. In *Petroleum Computer Conference*. Society of Petroleum Engineers.

Gui, B., Yang, Q.Y., Wu, H.J., Zhang, X. and Lu, Y., 2010. Study of the effects of low-temperature oxidation on the chemical composition of a light crude oil. Energy & Fuels, 24(2), pp.1139-1145.

Guo, H., Dong, J., Wang, Z., Liu, H., Ma, R., Kong, D., Wang, F., Xin, X., Li, Y. and She, H., 2018, April. 2018 EOR Survey in China-part 1. In *SPE Improved Oil Recovery Conference*. Society of Petroleum Engineers.

Guo, H., Dou, M., Hanqing, W., Wang, F., Yuanyuan, G., Yu, Z., Yansheng, W. and Li, Y., 2015, October. Review of Capillary Number in Chemical Enhanced Oil Recovery. In SPE Kuwait Oil and Gas Show and Conference. Society of Petroleum Engineers.

Hamid, S. A., & Muggeridge, A. H., 2018. Analytical solution of polymer slug injection with viscous fingering. Computational Geosciences, 22(3), 711-723.

Hamid, S.A. and Muggeridge, A., 2018, April. Viscous fingering in reservoirs with long aspect ratios. In *SPE Improved Oil Recovery Conference*. Society of Petroleum Engineers.

Hanafy, H.H., Macary, S.M., ElNady, Y.M., Bayomi, A.A. and El Batanony, M.H., 1997, January. Empirical PVT correlations applied to Egyptian crude oils exemplify significance of using regional correlations. In *International Symposium on Oilfield Chemistry*. Society of Petroleum Engineers.

Harrison, D. and Chauvel, Y. 2007. Reservoir Pressure and Temperature. In Holstein, E.D., 2007. Volume V–Reservoir Engineering and

Petrophysics. *Petroleum Engineering Handbook; Lake, LW, Ed.; Society of Petroleum Engineers: Richardson, TX*.

Hartmann, D.J. and Beaumont, E.A., 1999. Treatise of Petroleum Geology/Handbook of Petroleum Geology: Exploring for Oil and Gas Traps. Chapter 9: Predicting Reservoir System Quality and Performance.

Hartmann, D.J., Beaumont, E.A. and Coalson, E., 2000. Prediction sandstone reservoir system quality and example of petrophysical evaluation. *Search and discovery*, *40005*. What is permeability? - AAPG Wiki

Heath, R.C., 1980. *Basic elements of ground-water hydrology with reference to conditions in North Carolina* (Vol. 80, No. 44). US Department of the Interior, Geological Survey.

Henrie, M., Carpenter, P. and Nicholas, R.E., 2016. Chapter 4 - Real-Time Transient Model–Based Leak Detection. In: M. HENRIE, P. CARPENTER and R.E. NICHOLAS, eds, *Pipeline Leak Detection Handbook.* Boston: Gulf Professional Publishing, pp. 57-89.

Henry A. and David G. 1993, 'Permeability' in Morton-Thompson, D. and Woods, A M (eds), *Development geology reference manual: AAPG methods in exploration series*, 10 edn. AAPG, Tulsa, Oklahoma

Hilgeman, F.R., Wilson, B. and Bertrand, G., 2007. Using Dalton's law of partial pressures to determine the vapor pressure of a volatile liquid. *Journal of chemical education*, *84*(3), p.469.

Hill, S., 1952. Channeling in packed columns. *Chemical Engineering Science*, *1*(6), pp.247-253.

Hoffman, B. T., 2012. Comparison of Various Gases for Enhanced Recovery from Shale Oil Reservoirs. Society of Petroleum Engineers. Doi: 10.2118/154329-MS

Holdich, R.G., 2002. Filtration of liquids. *Fundamentals of Particle Technology, Midland Information Technology and Publishing*, pp.29-35.

Holditch, S.A., 1992. Well Completions: Part 9. Production Engineering Methods. In Morton-Thompson, D. and Woods, A.M. eds., 1993. *Development geology reference manual: AAPG methods in exploration series, no. 10* (No. 10). AAPG.

Holm, L.W., 1980. Infill Drilling vs. Tertiary Oil Recovery vs. More Imports (includes associated papers 9737 and 9738). Journal of Petroleum Technology, 32(07), pp.1-169.

Holstein, E.D., 2007. Volume V–Reservoir Engineering and Petrophysics. In Lake, LW (Ed.) *Petroleum Engineering Handbook; Society of Petroleum Engineers: Richardson, TX*.

Hosseininoosheri, P., Hosseini, S. A., Nunez-Lopez, V., & Lake, L. W. (2018). Evolution of CO_2 Utilization Ratio and CO_2 Storage under Different<break/>CO_2 - EOR Operating Strategies: A Case Study on SACROC Unit Permian Basin. Society of Petroleum Engineers. doi:10.2118/190038-MS

Hou, J., Zhang, Y., Wang, D., and Zhou, K., 2016. Numerical simulation of reservoir parameters' synergetic time-variability on development rules. *Journal of petroleum exploration and production technology*, 6(4), pp.641-652.

Hou, P., Gao, F., He, J., Liu, J., Xue, Y. and Zhang, Z., 2020. Shale gas transport mechanisms in inorganic and organic pores based on lattice Boltzmann simulation. *Energy Reports*, 6, pp.2641-2650.

Huang, K., Zhu, W., Sun, L., Wang, Q. and Liu, Q., 2019. Experimental study on gas EOR for heavy oil in glutenite reservoirs after water flooding. *Journal of Petroleum Science and Engineering*, 181, p.106130.

Hubbert, M.K., 1953. Entrapment of petroleum under hydrodynamic conditions. *Aapg Bulletin*, *37*(8), pp.1954-2026.

Hugill, J.A. and Van Welsenes, A.J., 1986. Surface tension: a simple correlation for natural gas+ condensate systems. *Fluid Phase Equilibria*, *29*, pp.383-390.

Ibatullin, R.R., Ibragimov, N.G., Khisamov, R.S., Podymov, E.D. and Shutov, A.A., 2002, April. Application and method based on artificial intelligence for selection of structures and screening of technologies for enhanced oil recovery. In *SPE/DOE Improved Oil Recovery Symposium*. OnePetro.

IEA, 2018. Whatever happened to enhanced oil recovery?, IEA, Paris. [Online] From https://www.iea.org/commentaries/whatever-happened-to-enhanced-oil-recovery Accessed (29/10/2021)

IEA, 2020. *Global* CO_2 *emissions in 2019*, IEA, Paris. [Online] From https://www.iea.org/articles/global-co2-emissions-in-2019 Accessed (29/10/2021)

IEA, 2008. *World Energy Outlook 2008*, OECD Publishing, Paris. [Online] From http://dx.doi.org/10.1787/weo-2008-en Accessed (29/10/2021)

IEA, 2014. *World Energy Outlook 2014*, IEA, Paris. [Online] From http://dx.doi.org/10.1787/weo-2014-en Accessed (29/10/2021)

Ikiensikimama, S.S. and Ogboja, O., 2009. Evaluation of empirically derived oil viscosity correlations for the Niger Delta crude. *Journal of Petroleum Science and Engineering*, *69*(3-4), pp.214-218.

International Energy Agency (IEA), 2013. Technology roadmap carbon capture and storage – 2013 Edition. [Online] From https://iea.blob.core.windows.net/assets/bca6758e-9a74-4d2a-9c35-b324d81fc714/TechnologyRoadmapCarbonCaptureandStorage.pdf Accessed (29/10/2021)

International Energy Agency (IEA), 2013. *Technology roadmap carbon capture and storage – 2013 Edition.* https://iea.blob.core.windows.net/assets/bca6758e-9a74-4d2a-9c35-b324d81fc714/TechnologyRoadmapCarbonCaptureandStorage.pdf Accessed (29/10/2021)

Ismail, A.F., Khulbe, K.C. and Matsuura, T., 2015. Gas separation membranes. *Switz. Springer*, *10*, pp.978-3.

Jacques M. 2015. "For every marginal or mature field, there is a cost-effective solution to maximize your profits." [Online] Available from < http://www.frames-group.com/getattachment/bbe5d857-b014-4889-ba9b-a6c8ffe64e3b/Whitepaper-Marginal-Fields.pdf.aspx?ext=.pdf> [Accessed 6/10/2017]

Jahangiri, H.R. and Zhang, D., 2012. Ensemble based co-optimization of carbon dioxide sequestration and enhanced oil recovery. *International Journal of Greenhouse Gas Control*, *8*, pp.22-33.

James F. L., Henry V. N., Mike R. W., 2008, CHAPTER 1 - INTRODUCTION. In James F. L., Henry V. N., Mike R. W. (ed.) Gas Well Deliquification 2nd Edn., Pgs 1-11. Gulf Professional Publishing.

Jerez, J.M., Molina, I., García-Laencina, P.J., Alba, E., Ribelles, N., Martín, M. and Franco, L., 2010. Missing data imputation using statistical and machine learning methods in a real breast cancer problem. *Artificial intelligence in medicine*, *50*(2), pp.105-115.

Jia, H. and Sheng, J.J., 2017. Discussion of the feasibility of air injection for enhanced oil recovery in shale oil reservoirs. *Petroleum*, *3*(2), pp.249-257.

Jia, H., 2018. Effect of reservoir heterogeneity on air injection performance in a light oil reservoir. *Petroleum*, *4*(1), pp.15-24.

Jia, H., Yin, S.P. and Ma, X.P., 2018. Enhanced oil recovery mechanism of low oxygen air injection in high water cut reservoir. *Journal of Petroleum Exploration and Production Technology*, *8*(3), pp.917-923.

Jia, H., Yuan, C.D., Zhang, Y., Peng, H., Zhong, D. and Zhao, J., 2012, January. Recent progress of high-pressure air injection process (HPAI) in light oil reservoir: laboratory investigation and field application. In SPE Heavy Oil Conference Canada. Society of Petroleum Engineers.

Jiaona, L., Pengsong, C., and Di, Z., 2012. Characteristics of the Heterogeneity of Wang 9 Well Area in Wangji Oilfield. *IOSR Journal of Engineering (IOSRJEN).* 2(11), pp47-53.

Jin, L., Noraldeen, S.F., Zhou, L. and Du, X., 2021. Molecular study on the role of solid/liquid interface in specific heat capacity of thin nanofluid film with different configurations. *Fluid Phase Equilibria*, *548*, p.113188.

Jin, Y., Fan, Y., Meng, X., Zhang, W., Meng, B., Yang, N. and Liu, S., 2019. Theoretical and experimental insights into the mechanism for gas separation through nanochannels in 2D laminar MXene membranes. *Processes*, *7*(10), p.751.

John, L., 2007, Fluid Flow Through Permeable Media. In Holstein, E.D., Ed., *Volume V–Reservoir Engineering and Petrophysics*. In Lake, LW, Ed., *Petroleum Engineering Handbook*, Pgs. 719-894. Society of Petroleum Engineers: Richardson, TX.

Jordan, C.L., 2015, November. Quick Tricks, Tips, Analytical Methods and Other Proxy Tools for the Unconventional Reservoir Engineer. In *SPE Asia Pacific Unconventional Resources Conference and Exhibition*. Society of Petroleum Engineers.

Kamali, F. and Cinar, Y., 2014. Co-optimizing enhanced oil recovery and CO_2 storage by simultaneous water and CO_2 injection. *Energy exploration & exploitation*, *32*(2), pp.281-300.

Kandlikar, S., Garimella, S., Li, D., Colin, S. and King, M.R., 2005. *Heat transfer and fluid flow in minichannels and microchannels*. elsevier.

Kang, P.S., Lim, J.S. and Huh, C., 2014, August. Screening criteria for application of EOR processes in offshore fields. In The Twenty-fourth International Ocean and Polar Engineering Conference. International Society of Offshore and Polar Engineers.

Kantzas, A., Bryan, J. and Taheri, S., 2012. Fundamentals of fluid flow in porous media. *Pore size distribution*.

Kantzas, A., Chatzis, I. and Dullien, F.A.L., 1988, January. Enhanced oil recovery by inert gas injection. In *SPE enhanced oil recovery symposium*. Society of Petroleum Engineers.

Kargarpour, M.A., 2017. Investigation of reservoir temperature in a gas reservoir in Middle East: case study. *Journal of Petroleum Exploration and Production Technology*, *7*(2), pp.531-541.

Karović-Maričić, V., Leković, B. and Danilović, D., 2014. Factors influencing successful implementation of enhanced oil recovery projects. *Podzemni radovi*, *22*(25), pp.41-50

Keller, W.O. and Callaway, F.H., 1950. Critical analysis of the effect of well density on recovery efficiency. Journal of Petroleum Technology, 2(09), pp.269-280.

Kemp, A.G. and Stephen, L., 2014. The Economics of Enhanced Oil Recovery (EOR) in the UKCS and the Tax Review. *Aberdeen Centre for Research in Energy Economics and Finance. Aberdeen: University of Aberdeen*.

Kennedy, M., 2015. Core and Other Real Rock Measurements. In *Developments in Petroleum Science* (Vol. 62, pp. 73-88). Elsevier.

Kern, L.R., 1981. Effect of Spacing on Waterflood Recovery Efficiency. Society of Petroleum Engineers. [Online] Available from https://www.onepetro.org/general/SPE-10538-MS

Khataniar, S. and Peters, E.J., 1992. The effect of reservoir heterogeneity on the performance of unstable displacements. *Journal of Petroleum Science and Engineering*, *7*(3-4), pp.263-281.

Khodaei Booran, S., Upreti, S.R. and Ein-Mozaffari, F., 2016. Enhanced oil recovery with air injection: effect of the temperature variation with time. Energy & Fuels, 30(4), pp.3509-3518.

Khojastehmehr, M., Madani, M. and Daryasafar, A., 2019. Screening of enhanced oil recovery techniques for Iranian oil reservoirs using TOPSIS algorithm. *Energy Reports*, *5*, pp.529-544.

Klobes, P. and Munro, R.G., 2006. *Porosity and specific surface area measurements for solid materials*. Special Publication 960-17, Natl. Inst. Stand. Technol., Washington, DC.

Knight, B. L., and Rhudy, J. S. (1977, October 1). Recovery Of High-Viscosity Crudes By Polymer Flooding. Petroleum Society of Canada. doi:10.2118/77-04-07

Ko, D., Doh, S., Park, H.S. and Kim, M.H., 2018. The effect of through plane pore gradient GDL on the water distribution of PEMFC. *International Journal of Hydrogen Energy*, *43*(4), pp.2369-2380.

Kokal, S. and Al-Kaabi, A., 2010. Enhanced oil recovery: challenges & opportunities. *World Petroleum Council: Official Publication*, *64*, pp.64-69.

Koneshloo, M., Aryana, S.A. and Hu, X., 2018. The impact of geological uncertainty on primary production from a fluvial reservoir. *Petroleum Science*, *15*(2), pp.270-288.

Kovscek, A.R. and Cakici, M.D., 2005. Geologic storage of carbon dioxide and enhanced oil recovery. II. Cooptimization of storage and recovery. *Energy conversion and Management*, *46*(11-12), pp.1941-1956.

Kulasingam R. 2014. Marginal fields in Nigeria: recent developments. Available [online] from: https://www.scribd.com/document/318813899/Marginal-Fields-in-Nigeria-21-May-2014 [accessed 10/05/2017]

Kuuskraa, V., 1982. Unconventional Natural Gas. *In Advances in Energy Systems and Technology (pp. 1-126)*. Academic Press.

Labedi, R., 1992. Improved correlations for predicting the viscosity of light crudes. *Journal of Petroleum Science and Engineering*, *8*(3), pp.221-234.

Lake, L.W. and Carroll, H.B. 2016 "Reservoir Characterization," *Reservoir characterization.*, pp. 583–640. doi:10.1016/B978-0-12-803188-9.00010-3.

Lake, L.W., Fanchi, J.R., Arnold, K., Clegg, J.D., Holstein, E.D. and Warner, H.R. eds., 2007. *Petroleum engineering handbook: reservoir engineering and petrophysics* (Vol. 5). Society of Petroleum Engineers.

Lake, L.W., Lotfollahi, M. and Bryant, S.L., 2019. CO_2 Enhanced Oil Recovery Experience and its Messages for CO_2 Storage. In Newell, P. and Ilgen, A. eds., 2018. *Science of Carbon Storage in Deep Saline Formations: Process Coupling Across Time and Spatial* (pp. 15-31). Elsevier Science Publishing Co Inc, Cambridge, MA.

Lake, Larry W., 1989, Enhanced Oil Recovery. Austin, TX: University Co-op. Print.

Lane-Serff, G.F., 2001. Overflows and cascades. Academic Press.

Lasater, J.A., 1958. Bubble point pressure correlation. *Trans. AIME*, *213*(379), p.22A.

Latil, M., 1980. *Enhanced oil recovery*. Éditions Technip.

Laugier, A. and Garai, J., 2007. Derivation of the ideal gas law. *Journal of Chemical Education*, *84*(11), p.1832.

Lee, 2010 Innovative Energy Technologies Program Application 01-023 Taber S Mannville B Alkaline-Surfactant-Polymer Flood Warner ASP Flood 2009 Annual Report. [Online] Avaiable from: <http://www.energy.alberta.ca/xdata/IETP/IETP%202009/01-023%20Taber%20S%20Alkaline-Surfactant-Polymer%20Flood/2009%20Annual%20Report%20Application%2001-023%20Final.pdf> [Accessed 17/08/2017]

Lehmann, H.P., Fuentes-Arderiu, X. and Bertello, L.F., 1996. Glossary of terms in quantities and units in Clinical Chemistry (IUPAC-IFCC Recommendations 1996). *Pure and Applied Chemistry*, *68*(4), pp.957-1000.

Li, C., Wang, H., Wang, L., Kang, Y., Hu, K. and Zhu, Y., 2020. Characteristics of tight oil sandstone reservoirs: a case study from the Upper Triassic Chang 7 Member in Zhenyuan area, Ordos Basin, China. *Arabian Journal of Geosciences*, *13*(2), pp.1-19.

Li, J.J., Jiang, H.Q., Xiao, K., Zhang, Z.T. and Wang, Y.C., 2017. The relationship between the sweep efficiency and displacement efficiency of function polymer in heterogeneous reservoir after polymer flood. *Particulate Science and Technology*, *35*(3), pp.355-360.

Li, K. and Horne, R.N., 2001a. An experimental and analytical study of steam/water capillary pressure. *SPE Reservoir Evaluation & Engineering*, *4*(06), pp.477-482.

Li, K. and Horne, R.N., 2001b, January. Gas slippage in two-phase flow and the effect of temperature. In *SPE Western Regional Meeting*. Society of Petroleum Engineers.

Li, Y., Xu, W., Xiao, F., Liu, L., Liu, S. and Zhang, W., 2015. Optimization of a development well pattern based on production performance: A case

study of the strongly heterogeneous Sulige tight sandstone gas field, Ordos Basin. *Natural Gas Industry B*, *2*(1), pp.95-100.

Lindsay, M. 2016. A picture is worth a thousand words: A regression is worth a few pictures. Available [Online] from: http://viewer.zmags.com/publication/4e07ca29#/4e07ca29/1. Accessed 23/07/2017.

Liu, G., Fan, Z., Lu, Y., Li, S., Feng, B., Xia, Y., & Zhao, Q., 2018. Experimental Determination of Gas Relative Permeability Considering Slippage Effect in a Tight Formation. Energies, 11(2), 467.

Liu, K., Ostadhassan, M. and Cai, J., 2019. Characterising Pore Size Distributions of Shale. In Cai, J. and Hu, X. eds., 2019. *Petrophysical characterisation and fluids transport in unconventional reservoirs*. Elsevier, Cambridge, MA.

Lohman, S.W., 1988. *Definitions of selected ground-water terms, revisions and conceptual refinements*. U.S. Geological Survey, Water Supply Paper.

Lorsong, J., 2013. *CO 2 EOR and Storage*. [Online] From: https://ieaghg.org/docs/General_Docs/Summer_School_2013/ CO_2_EOR_Lorsong_July_13SEC.pdf. Accessed (29/10/2021)

Loudon, C. and McCulloh, K., 1999. Application of the Hagen—Poiseuille equation to fluid feeding through short tubes. *Annals of the Entomological Society of America*, *92*(1), pp.153-158.v

Lu, J. and Pope, G.A., 2017. Optimization of gravity-stable surfactant flooding. *SPE Journal*, *22*(02), pp.480-493.

Lu, J., Weerasooriya, U.P. and Pope, G.A., 2014. Investigation of gravity-stable surfactant floods. *Fuel*, *124*, pp.76-84.

Lucia, F. J., 2007, Reservoir geology, in Holstein, E. D., ed., Volume V– Reservoir Engineering and Petrophysics. *Petroleum Engineering*

Handbook; Lake, LW, Ed.; Society of Petroleum Engineers: Richardson, TX. p. 1-12

Lyons, W., 2009. Working guide to reservoir engineering. Gulf professional publishing.

Lyons, W.C. and Plisga, G.J., 2011. *Standard handbook of petroleum and natural gas engineering*. 2 Edn. Elsevier, Gulf Professional Publishing, Burlington.

Lyons, W.C., 2010. Chapter 5 - Enhanced Oil Recovery Methods. In: W.C. Lyons, Ed, Working Guide to Reservoir Engineering. Boston: Gulf Professional Publishing, Pp. 279-310.

Lyons, W.C., 2010. Enhanced Oil Recovery Methods, *Working Guide to Reservoir Engineering*, pp. 279–310. doi:10.1016/B978-1-85617-824-2.00005-8.

Ma, H. and Hsiao, B.S., 2019. Electrospun nanofibrous membranes for desalination. In *Current trends and future developments on (bio-) membranes* (pp. 81-104). Elsevier.

Ma, T., Tang, T., Chen, P., Li, Z. and Liu, S., 2020. Numerical investigation of gas-liquid displacement between borehole and gassy fracture using response surface methodology. *Energy Science & Engineering*, *8*(3), pp.740-754.

Magnini, M., Beisel, A.M., Ferrari, A. and Thome, J.R., 2017. Pore-scale analysis of the minimum liquid film thickness around elongated bubbles in confined gas-liquid flows. *Advances in Water Resources*, *109*, pp.84-93.

Mahdavi, E and Zebarjad, F.S., 2018. Screening Criteria of Enhanced Oil Recovery Methods. *In* Bahadori, A., (ed). *Fundamentals of enhanced oil and gas recovery from conventional and unconventional reservoirs*. Gulf Professional Publishing. Pp 41-59

Majumder, A., Mehta, B. and Khandekar, S., 2013. Local Nusselt number enhancement during gas–liquid Taylor bubble flow in a square mini-channel: an experimental study. *International journal of thermal sciences*, *66*, pp.8-18.

Malkin, A.Y., 2012. Rheology: concepts, methods and applications. prof. dr. *Alexander Ya. Malkin, prof. dr. Avraam I. Isayev. 2nd edition: Toronto: ChemTec Publishing*.

Mamudu, A., Olalekan, O. and Uyi, G.P., 2015. Analytical study of viscosity effects on waterflooding performance to predict oil recovery in a linear system. *Journal of Petroleum & Environmental Biotechnology*, *6*(3), p.1.

Manrique, E.J., Izadi, M., Kitchen, C.D. and Alvarado, V., 2009. Effective EOR decision strategies with limited data: field cases demonstration. SPE Reservoir Evaluation & Engineering, 12(04), pp.551-561.

Marino, M.A. and Luthin, J.N., 1982. Seepage and groundwater. in Developments in Water Science. (13) Pages vii-viii Elsevier. https://doi.org/10.1016/S0167-5648(08)70572-0.

Masalmeh, S.K., Wei, L. and Blom, C., 2011, January. Mobility control for gas injection in heterogeneous carbonate reservoirs: comparison of foams versus polymers. In SPE Middle East Oil and Gas Show and Conference. Society of Petroleum Engineers.

Mason, E. A., 2020. "Gas". Encyclopedia Britannica, https://www.britannica.com/science/gas-state-of-matter. Accessed 1/02/2021.

Masoudi, R., 2012. How to get the most out of your Oil Rim Reservoirs? Reservoir management and hydrocarbon recovery enhancement initiatives. *Distinguished Lecturer Program, PETRONAS*.

Masoudi, R., Karkooti, H. and Othman, M.B., 2013, March. How to get the most out of your oil rim reservoirs? In *IPTC 2013: International Petroleum Technology Conference* (pp. cp-350). European Association of Geoscientists & Engineers.

Matthew, D., 2017. Here's how much it costs both Saudi Arabia and the US to produce oil. [Online] Available from http://markets.businessinsider.com/commodities/news/how-much-it-costs-both-saudi-arabia-and-the-us-to-produce-oil-2017-3-100186804. Accessed 20/11/2017

Matthews, M.D., 1999. Treatise of Petroleum Geology/Handbook of Petroleum Geology: Exploring for Oil and Gas Traps. Chapter 7: Migration of Petroleum.

Mehio, N., Dai, S., and Jiang, D. E., 2014. Quantum mechanical basis for kinetic diameters of small gaseous molecules. The Journal of Physical Chemistry A, 118(6), 1150-1154.

Merlet, R.B., Pizzoccaro-Zilamy, M.A., Nijmeijer, A. and Winnubst, L., 2020. Hybrid ceramic membranes for organic solvent nanofiltration: State-of-the-art and challenges. *Journal of membrane science*, *599*, p.117839.

Meyer, J.P., 2007. Summary of carbon dioxide enhanced oil recovery (CO_2EOR) injection well technology. *American Petroleum Institute, Washington, DC*.

Miao, T., Long, Z., Chen, A. and Yu, B., 2017. Analysis of permeabilities for slug flow in fractal porous media. *International Communications in Heat and Mass Transfer*, *88*, pp.194-202.

Mike, T. 2016. Unlocking Marginal Fields Unlocking Marginal Fields Unlocking Marginal Fields – What does the economics tell us? [Online] Available from https://www.subseauk.com/documents/presentations/mike%20thole

n%20-%20oil%20and%20gas%20uk%20-%20unlocking.pdf
[Accessed 6/10/2017]

Millet, P., 2011. 18 - Membrane Electrolysers For Hydrogen (H2) Production. In: A. Basile And S.P. Nunes, Eds. *Advanced Membrane Science And Technology For Sustainable Energy And Environmental Applications.* Woodhead Publishing. Pp. 568-609

Mills, I., 1993. *Quantities, units and symbols in physical chemistry/prepared for publication by Ian Mills...[et al.].* Oxford; Boston: Blackwell Science; Boca Raton, Fla.: CRC Press [distributor],

Mohammed N. K., Habiba S., Edidiong O., Ify O., and Edward G., 2016. VOC oxidation in excess of oxygen using flow-through catalytic membrane reactor. International Journal of Hydrogen Energy, Vol 41(37)

Mohammed, N. K., Ngozi C. N. and Edward, G., 2016. Preparation and characterisation of inorganic membranes for hydrogen separation. International Journal of Hydrogen Energy, Vol 41(19)

Morton-Thompson, D. and Woods, A.M. eds., 1993. Development geology reference manual: AAPG methods in exploration series, no. 10 (No. 10). AAPG.

Moura, A.C. and Toralles, B.M., 2019. Correlation between Permeability and Porosity for Pervious Concrete (PC). *Dyna*, *86*(209), pp.151-159.

Muggeridge, A., Cockin, A., Webb, K., Frampton, H., Collins, I., Moulds, T. and Salino, P., 2014. Recovery rates, enhanced oil recovery and technological limits. *Philosophical Transactions of the Royal Society A: Mathematical, Physical and Engineering Sciences*, *372*(2006), p.20120320.

Müller-Petke, M. and Yaramanci, U., 2015. Tools and techniques: Nuclear magnetic resonance. In Schubert, G., (2015). *Treatise on Geophysics, 11 Volume Set (2nd Edition) - 1.02.1 Introduction.* Elsevier. Retrieved

from
https://app.knovel.com/hotlink/pdf/id:kt00UCKWZ2/treatise-geophysics-11/introduction

Nabawy, B.S., Basal, A.M.K., Sarhan, M.A. and Safa, M.G., 2018. Reservoir zonation, rock typing and compartmentalization of the Tortonian-Serravallian sequence, Temsah Gas Field, offshore Nile Delta, Egypt. *Marine and Petroleum Geology*, *92*, pp.609-631.

Nabawy, B.S., Rochette, P. and Géraud, Y., 2009. Petrophysical and magnetic pore network anisotropy of some cretaceous sandstone from Tushka Basin, Egypt. *Geophysical Journal International*, *177*(1), pp.43-61.

Nageh, M., El Ela, M.A., El Tayeb, E.S. and Sayyouh, H., 2015, September. Application of using fuzzy logic as an artificial intelligence technique in the screening criteria of the EOR technologies. In *SPE North Africa Technical Conference and Exhibition*. OnePetro.Nagel, W.A. and Byerley, K.A., 1992. Core-Log Transformations and Porosity-Permeability Relationships: Part 5. Laboratory Methods.

Naseri, A., Nikazar, M. and Dehghani, S.M., 2005. A correlation approach for prediction of crude oil viscosities. *Journal of Petroleum Science and Engineering*, *47*(3-4), pp.163-174.

Nazari, J., Nasiry, F., Seddiqi, N. and Honma, S., 2015. Influence of relative permeability and viscosity ratio on oil displacement by water in petroleum reservoir. *Proceedings of School of Engineering of Tokai University*, *40*, pp.15-20.

Neele, F., Quinquis, H., Read, A., Wright, M., Lorsong, J., & Poulussen, D. F. 2014. CO_2 Storage Development: Status of the Large European CCS Projects with EEPR Funding. *Energy Procedia*, *63*, 6053–6066. https://doi.org/10.1016/J.EGYPRO.2014.11.638

Nelson, P.H., Batzle, M.L. and Fanchi, J., 2006. Single-phase permeability. *Petroleum engineering handbook: General engineering: Richardson, Texas, Society of Petroleum Engineers*, *1*, pp.687-726.

Nesselroade, J.R. and Cattell, R.B. eds., 2013. *Handbook of multivariate experimental psychology*. Springer Science & Business Media, Plenum Press, New York.

Nielsen, L.C., Bourg, I.C. and Sposito, G., 2012. Predicting CO_2–water interfacial tension under pressure and temperature conditions of geologic CO_2 storage. *Geochimica et Cosmochimica Acta*, *81*, pp.28-38.

Nischal, Rajiv & Kumar, Adesh & Vasudeva, Sudhir. (2012). Unlocking Potential of Offshore Marginal Fields in India: A Success Story. Society of Petroleum Engineers. doi:10.2118/155145-MS

NNPC (Nigeria National Petroleum Corporation), 2010. Development of Nigeria's Oil Industry. [Online] Available from http://www.nnpcgroup.com/NNPCBusiness/BusinessInformation/OilG asinNigeria/DevelopmentoftheIndustry.aspx [6/6/2017]

NPC (National Petroleum Council), 2011. Onshore Conventional Oil Including EOR[online] from < http://www.npc.org/Prudent_Development-Topic_Papers/15_Onshore_Conventional_Oil_Incl_EOR_Paper.pdf > [20/07/2017]

Ocean News 2017. Unlocking Marginal Fields at Subsea Expo 2017. [Online] Available from <https://www.oceannews.com/news/subsea-intervention-survey/unlocking-marginal-fields-at-subsea-expo-2017> [Accessed 6/10/2017]

Ogunlude, P., Abunumah, O. and Gobina, E., 2020. A Study of Gas Diffusion Characteristics on Nano-Structured Ceramic Membranes. *European Journal of Engineering and Formal Sciences*, *4*(1), pp.21-23.

Ogunlude, P., Abunumah, O., Orakwe, I., Shehu, H., Muhammad-Sukki, F. and Gobina, E., 2019. Comparative evaluation of the effect of pore size and temperature on gas transport in nano-structured ceramic membranes for biogas upgrading. *WEENTECH proceedings in energy*, *5*(1).

Ohen, H.A. and Kersey, D.G., 1992. Permeability: Part 5. Laboratory Methods. In Morton-Thompson, D. and Woods, A.M. eds., 1993. *Development geology reference manual: AAPG methods in exploration series, no. 10* (No. 10). AAPG.

Oil and Gas Authority, 2016. Enhanced Oil Recovery Strategy. [Online] Available from https://www.gov.uk/government/uploads/system/uploads/attachment_data/file/540028/OGA_EOR_Strategy.pdf [Accessed 6/7/2017]

Olbricht, W.L., 1996. Pore-scale prototypes of multiphase flow in porous media. *Annual review of fluid mechanics*, *28*(1), pp.187-213.

Olinsky, A., Chen, S. and Harlow, L., 2003. The comparative efficacy of imputation methods for missing data in structural equation modelling. *European Journal of Operational Research*, *151*(1), pp.53-79.

Orakwe, I.R. 2018. Design and testing of an integrated catalytic membrane reactor for deoxygenating water using hydrogen for down-hole injection and process applications. *Robert Gordon University, PhD thesis.* https://rgu-repository.worktribe.com/output/242006

Oruwari H. and Adewale D. 2017. The Critical Success Factors for Marginal Oil Field Development in Nigeria. *Journal of Business and Management Sciences.* Vol. 5 (1) pp 1-10.

Osborne, A.F., 1992. Workovers: Part 9. Production Engineering Methods. In Morton-Thompson, D. and Woods, A.M. eds., 1993. *Development geology reference manual: AAPG methods in exploration series, no. 10* (No. 10). AAPG.

Otto, E., Fissan, H., Park, S. H., and Lee, K. W., 1999. The log-normal size distribution theory of Brownian aerosol coagulation for the entire particle size range: Part II. J Aerosol Sci 30(1):16–34

Panteha G., 2018. Introduction to Reservoir Simulation. Available online from <https://www.spe-aberdeen.org/wp-content/uploads/2018/06/Devex-2018-Introduction-to-Reservoir-Simulation.pdf accessed> 16/02/2021

Paul, O. 2013. Government Challenges Marginal Field and Indigenous Operators TO Unlock Potential Oil and Gas Resources. Quarterly In-House Journal of the Department of Petroleum Resources. Vol. 7 (2) pp.1

Pedersen, K.S. and Lindeloff, N., 2003, January. Simulations of compositional gradients in hydrocarbon reservoirs under the influence of a temperature gradient. In *SPE Annual Technical Conference and Exhibition*. Society of Petroleum Engineers.

Peng, Z., Gai, S., Barma, M., Rahman, M.M., Moghtaderi, B. and Doroodchi, E., 2021. Experimental study of gas-liquid-solid flow characteristics in slurry Taylor flow-based multiphase microreactors. *Chemical Engineering Journal*, *405*, p.126646.

Peramanu, S., Pruden, B.B. and Rahimi, P., 1999. Molecular weight and specific gravity distributions for Athabasca and Cold Lake bitumens and their saturate, aromatic, resin, and asphaltene fractions. *Industrial & engineering chemistry research*, *38*(8), pp.3121-3130.

Pershad, H., Durusut, E., Alan, C., Black, D., Mackay, E.J. and Olden, P., 2012. Economic impacts of CO_2-enhanced oil recovery for Scotland.

Peters, K.E., Curry, D.J. and Kacewicz, M., 2012. An overview of basin and petroleum system modeling: Definitions and concepts, *in* Peters, Kenneth E., Curry, D.J. and Kacewicz, M., eds., Basin modeling: New

horizons in research and applications: *AAPG Hedberg Series no. 4, p. 1-16*.

Petroleum Solutions. 2017. Our Customers. [Online] Available from <http://www.petroleumsolutions.co.uk/ourcustomers.html> [Accessed 6/10/2017]

Philip H. N. 1994. Permeability-porosity relationships in sedimentary rocks. Log Analyst 35(3) pp.38-62.

Philip H. Nelson and Michael L. Batzle, Fanchi, J.R., 2007. Volume I–General Engineering. *Petroleum Engineering Handbook; Lake, LW, Ed.; Society of Petroleum Engineers: Richardson, TX*.

Pilvin, P., 2019. Continuum Mechanics. In *Mechanics-Microstructure-Corrosion Coupling* (pp. 49-63). Elsevier.

Poiseuille, J.L.M., 1940. Experimental investigations upon the flow of liquids in tubes of very small diameter (Vol. 1, No. 1).

Pourhadi, S. and Fath, A.H., 2019. Performance of the injection of different gases for enhanced oil recovery in a compositionally grading oil reservoir. *Journal of Petroleum Exploration and Production Technology*, pp.1-21.

Prada, A. and Civan, F., 1999. Modification of Darcy's law for the threshold pressure gradient. *Journal of Petroleum Science and Engineering*, *22*(4), pp.237-240.

Pruess, K., 1991. TOUGH2: A general-purpose numerical simulator for multiphase fluid and heat transfer. *LBL-29400. Lawrence Berkeley Laboratory, Berkeley, CA*.

PSAC, 2015. Well Cost Study. [Online] Available from http://www.psac.ca/wp-content/uploads/wcs_sample.pdf [20/11/2017]

Putnam, J.M., 2013. Enhanced Oil Recovery Field Case Studies: Chapter 14. Facility Requirements for Implementing a Chemical EOR Project. Elsevier Inc. Chapters.

Qasem, F.H., Malallah, A., Nashawi, I.S. and Mir, M.I., 2016. Inflow performance relationships for layered solution-gas drive reservoir. *International Journal of Petroleum Engineering*, *2*(4), pp.265-288.

Rabbani, H.S., Or, D., Liu, Y., Lai, C.Y., Lu, N.B., Datta, S.S., Stone, H.A. and Shokri, N., 2018. Suppressing viscous fingering in structured porous media. *Proceedings of the National Academy of Sciences*, *115*(19), pp.4833-4838.

Rafik, B. and Kamel, B., 2017. Prediction of permeability and porosity from well log data using the nonparametric regression with multivariate analysis and neural network, Hassi R'Mel Field, Algeria. Egyptian journal of petroleum, 26(3), pp.763-778.

Ramey Jr, H.J., 1973. Correlations of surface and interfacial tensions of reservoir fluids. *Society of Petroleum Engineers*.

Ran, Q., Ren, D., Wang, Y., Tong, M., Sun, Y., Yan, L., Dong, J., Wang, Z., Xu, M., Li, N., Peng, H., Chen, F., Yuan, D., Xu, Q., Wang, S. And Wang, Q., 2019. Chapter 7 - Volcanic Gas Reservoir Development Technologies. In: Q. Ran, D. Ren, Y. Wang, M. Tong, Y. Sun, L. Yan, J. Dong, Z. Wang, M. Xu, N. Li, H. Peng, F. Chen, D. Yuan, Q. Xu, S. Wang and Q. Wang, eds, *Development of Volcanic Gas Reservoirs.* Gulf Professional Publishing, pp. 541-888.

Ranade, V.V. And Bhandari, V.M., 2014. Chapter 1 - Industrial Wastewater Treatment, Recycling, And Reuse: An Overview. In: V.V. Ranade And V.M. Bhandari, Eds. *Industrial Wastewater Treatment, Recycling And Reuse.* Oxford: Butterworth-Heinemann. Pp. 1-80

Reid, G., 2015. Enhanced Oil Recovery for Small Producers? Presented at the RPSEA Forum Small Producer Needs December 15th. Albuquerque, New Mexico

Reid, R. C.; Prausnitz, J. M.; Poling, B. E., 1987. The Properties of Gases and Liquids, 4th ed. McGraw-Hill: New York.

Richard, L., 2007. Chapter 15 – Relative Permeability and Capillary Pressure. In: Volume I–General Engineering. *Petroleum Engineering Handbook; Lake, LW, Ed.; Society of Petroleum Engineers: Richardson, TX*. Pp. 727-765

Rick, J S and Diana, M. 1993. Reserves estimation. In Morton-Thompson, D. and Woods, A M (eds), *Development geology reference manual: AAPG methods in exploration series*, 10 edn. AAPG, Tulsa, Oklahoma

Ridgway, C.J., Gane, P.A. and Schoelkopf, J., 2002. Effect of capillary element aspect ratio on the dynamic imbibition within porous networks. *Journal of colloid and interface science*, *252*(2), pp.373-382.

Risby, M.S. and Hamouda, A.M.S., 2011. Modeling ballistic impact on textile materials. *Computer Technology for Textiles and Apparel*, pp.146-172.

Robert, P.S., 2007. Chapter 6 – Oil System Correlations. In Lake, LW (Ed.) *Petroleum Engineering Handbook; Society of Petroleum Engineers: Richardson, TX*. Pgs. 257-331

Robinson, B.M., 1992. Production Problems: Part 9. Production Engineering Methods. In Morton-Thompson, D. and Woods, A.M. eds., 1993. *Development geology reference manual: AAPG methods in exploration series, no. 10* (No. 10). AAPG.

Robinson, J.P., Tarleton, E.S., Millington, C.R. and Nijmeijer, A., 2004. Solvent flux through dense polymeric nanofiltration membranes. *Journal of membrane science*, *230*(1-2), pp.29-37.

Rochinha, F., 2011. Journal of the Brazilian Society of Mechanical Sciences and Engineering (Online).

Rodríguez, F. and Christopher, C.A., 2004. Overview of Air Injection Potential for PEMEX. In *AAPG International Conference*.

Roefs, P., Moretti, M., Welkenhuysen, K., Piessens, K. and Compernolle, T., 2019. CO_2-enhanced oil recovery and CO_2 capture and storage: An environmental economic trade-off analysis. *Journal of environmental management*, *239*, pp.167-177.

Ronald E. T., 2001. Enhanced Oil Recovery. [Online] Available from http://memberfiles.freewebs.com/50/69/68186950/documents/Enhanced%20Oil%20Recovery_EOR-2.pdf

Rostami, A., Daneshi, A. and Miri, R., 2020. Proposing a rigorous empirical model for estimating the bubble point pressure in heterogeneous carbonate reservoirs. *Advances in Geo-Energy Research*, *4*(2), pp.126-134.

Rostami, A., Hemmati-Sarapardeh, A. and Mohammadi, A.H., 2019. Estimating n-tetradecane/bitumen mixture viscosity in solvent-assisted oil recovery process using GEP and GMDH modeling approaches. *Petroleum Science and Technology*, *37*(14), pp.1640-1647.

Ruikang, B., Jinchuan, Z., Xuan, T., Lu, Y., Shengling, J., Peixian, Z., Huaqiang, G. and Zongyu, W., 2010. Characteristics of energy fields and the hydrocarbon migration-accumulation in deep strata of Tahe Oilfield, Tarim Basin, NW China. *Petroleum Exploration and Development*, *37*(4), pp.416-423.

Sadd, M.H., 2018. *Continuum Mechanics Modeling of Material Behavior*. Academic Press.

Saini, D., 2019. Characterization and Determination of CO 2-Reservoir Oil Miscibility. In *CO₂-Reservoir Oil Miscibility* (pp. 19-36). Springer, Cham.

Sakthikumar, S., Madaoui, K. and Chastang, J., 1995, January. An investigation of the feasibility of air injection into a waterflooded light oil reservoir. In *Middle East Oil Show*. Society of Petroleum Engineers.

Saleh, L.D., Wei, M. and Bai, B., 2014. Data analysis and updated screening criteria for polymer flooding based on oilfield data. SPE Reservoir Evaluation & Engineering, 17(01), pp.15-25.

Sam, S A M 1993, 'Water Flooding' in Morton-Thompson, D. and Woods, A M (eds), *Development geology reference manual: AAPG methods in exploration series*, 10 edn. AAPG, Tulsa, Oklahoma

Sánchez-Minero, F., Sánchez-Reyna, G., Ancheyta, J. and Marroquin, G., 2014. Comparison of correlations based on API gravity for predicting viscosity of crude oils. *Fuel*, *138*, pp.193-199.

Satter, A. and Iqbal, G.M., 2015. Reservoir engineering: the fundamentals, simulation, and management of conventional and unconventional recoveries. Gulf Professional Publishing. Waltham, MA.

Satter, A. and Iqbal, G.M., 2016. Waterflooding and waterflood surveillance. *Reservoir Engineering*, pp. 289–312. doi:10.1016/B978-0-12-800219-3.00016-4.

Schatzinger, R., 1999. Reservoir Characterisation-Recent Advances. *Am. Assoc. Petrol. Geol. Mem*, *71*, p.404.

Schowalter, T.T., 1979. Mechanics of secondary hydrocarbon migration and entrapment. *AAPG bulletin*, *63*(5), pp.723-760.

Scot, M. 2014. Marginal oil fields 'worth £40bn to UK' [Online] Available from http://www.scotsman.com/business/companies/energy/marginal-oil-fields-worth-40bn-to-uk-1-3497431 [Accessed 6/10/2017]

Sebastian, H.M., Lin, H.M. and Chao, K.C., 1981. Correlation of solubility of hydrogen in hydrocarbon solvents. *AIChE Journal*, *27*(1), pp.138-148.

Shanmugam, G., 2018. Slides, Slumps, Debris Flows, Turbidity Currents, and Bottom Currents: Implications. Reference Module in Earth Systems and Environmental Sciences.

Sharipov, F., 2017. Ab initio simulation of gaseous mixture flow through an orifice. *Vacuum*, *143*, pp.106-118.

Shehu, H., 2018. *Innovative hydrocarbons recovery and utilization technology using reactor-separation membranes for off-gases emission during crude oil shuttle tanker transportation and natural gas processing* (Doctoral dissertation).

Shelton, J.L. and Morris, E.E., 1973. Cyclic injection of rich gas into producing wells to increase rates from viscous-oil reservoirs. *Journal of Petroleum Technology*, *25*(08), pp.890-896.

Sheng, G., Zhao, H., Su, Y., Javadpour, F., Wang, C., Zhou, Y., Liu, J. and Wang, H., 2020. An analytical model to couple gas storage and transport capacity in organic matter with noncircular pores. *Fuel*, *268*, p.117288.

Sheng, J.J., 2011. Chapter 4 - Mobility Control Requirement In Eor Processes. In: J.J. Sheng, Ed, Modern Chemical Enhanced Oil Recovery. Boston: Gulf Professional Publishing, Pp. 79-100.

Sheng, J.J., 2011a. Mobility Control Requirement in EOR Processes. *Modern Chemical Enhanced Oil Recovery*, pp. 79–100. doi:10.1016/B978-1-85617-745-0.00004-8.

Sheng, J.J., 2011b. Polymer Flooding. *Modern Chemical Enhanced Oil Recovery*, pp. 101–206. doi:10.1016/B978-1-85617-745-0.00005-X.

Shepherd, M., 2009. *Oil field production geology: AAPG Memoir 91* (Vol. 91). AAPG.

Shuker, M.T., Buriro, M.A. and Hamza, M.M., 2012, December. Enhanced oil recovery: a future for Pakistan. In *SPE/PAPG annual technical conference*. OnePetro.

Siena, M., Guadagnini, A., Della Rossa, E., Lamberti, A., Masserano, F. and Rotondi, M., 2016. A novel enhanced-oil-recovery screening approach based on Bayesian clustering and principal-component analysis. *SPE Reservoir Evaluation & Engineering*, *19*(03), pp.382-390.

Sinanan, B. and Budri, M., 2010, June. Planning, Execution & Surveillance of Enhanced Oil Recovery Projects. In *Trinidad and Tobago Energy Resources Conference*. OnePetro.

Skerlec, G. M., 1999. Treatise of Petroleum Geology/Handbook of Petroleum Geology: Exploring for Oil and Gas Traps. Chapter 10: Evaluating Top and Fault Seal.

Slatt, R.M. and Galloway, W.E., 1992. Geological heterogeneities: Part 6. Geological methods. In Morton-Thompson, D. and Woods, A.M. eds., 1993. *Development geology reference manual: AAPG methods in exploration series, no. 10* (No. 10). AAPG.

Slatt, R.M., 2013a. Basics of Sequence Stratigraphy for Reservoir Characterisation. In *Developments in Petroleum Science* (Vol. 61, pp. 203-228). Elsevier.

Slatt, R.M., 2013b. *Stratigraphic Reservoir Characterisation for Petroleum Geologists, Geophysicists, and Engineers: Chapter 4. Tools and Techniques for Characterising Oil and Gas Reservoirs* (Vol. 61). Elsevier Inc. Chapters.

Slider, H.C., 1983. Worldwide practical petroleum reservoir engineering methods. PennWell Books. Tulsa, Oklahoma.

Smalley, P. C., Ross, A. W., Brown, C., Moulds, T. P., and Smith, M. J. (2009). Reservoir Technical Limits: A Framework for Maximizing Recovery from Oil Fields. Society of Petroleum Engineers. doi:10.2118/109555-PA

Smith, D., Ahmadi, G., Ji, C., Bromhal, G. and Ferer, M.V., 2002, January. Experimental and Numerical Study of Gas-Liquid Displacements in Flow Cells, With Application to Carbon Dioxide Sequestration in Brine Fields. In *Fluids Engineering Division Summer Meeting* (Vol. 36150, pp. 1289-1293).

Smith, W.R. and Missen, R.W., 2005. A note on Dalton's law: Myths, facts, and implementation. *Journal of chemical education*, *82*(8), p.1197.

Soares, E.J., Carvalho, M.S. and Mendes, P.S., 2005. Immiscible liquid-liquid displacement in capillary tubes. *J. Fluids Eng.*, *127*(1), pp.24-31.

Soares, E.J., Carvalho, M.S. and Mendes, P.S., 2006. Gas-displacement of non-Newtonian liquids in capillary tubes. *International journal of heat and fluid flow*, *27*(1), pp.95-104.

Soares, E.J., Mendes, P.R. and Carvalho, M.D.S., 2008. Immiscible liquid-liquid displacement in capillary tubes: viscoelastic effects. *Journal of the Brazilian Society of Mechanical Sciences and Engineering*, *30*(2), pp.160-165.

Song, W., Liu, H., Wang, W., Zhao, J., Sun, H., Wang, D., Li, Y. and Yao, J., 2018b. Gas flow regimes judgement in nanoporous media by digital core analysis. *Open Physics*, *16*(1), pp.448-462.

Song, W., Yao, B., Yao, J., Li, Y., Sun, H., Yang, Y. and Zhang, L., 2018a. Methane surface diffusion capacity in carbon-based capillary with application to organic-rich shale gas reservoir. *Chemical Engineering Journal*, *352*, pp.644-654.

Spinelli, C.M., Demofonti, G., Di Biagio, M. and Lucci, A., 2012, January. CO_2 Full Scale Facilities Challenges for EOR/CCTS Testing on Transportation

Issues. In the Twenty-second International Offshore and Polar Engineering Conference. International Society of Offshore and Polar Engineers.

Standard, A.S.T.M., 2017. D7137/D7137M-17, Standard Test Method for Compressive Residual Strength Properties of Damaged Polymer Matrix Composite Plates. *ASTM International, West Conshohocken, PA*.

Standing, M.B., 1947, January. A pressure-volume-temperature correlation for mixtures of California oils and gases. In *Drilling and Production Practice*. American Petroleum Institute.

Starov, V.M. and Zhdanov, V.G., 2001. Effective viscosity and permeability of porous media. *Colloids and Surfaces A: Physicochemical and Engineering Aspects*, *192*(1-3), pp.363-375.

Stephanie Glen 2014, "Dispersion / Measures of Dispersion: Definition" From StatisticsHowTo.com: Elementary Statistics for the rest of us! https://www.statisticshowto.com/dispersion/

Stephen, R. (2012a) 'Increased Oil Production with Something Old, Something New.' Journal of Petroleum Technology 64 (10) pp.37-50

Suman, J.R., 1934, January. The Well-Spacing Problem-Low Well Density Increases Ultimate Recovery. In Drilling and Production Practice. American Petroleum Institute.

Sun, Z., Li, X., Shi, J., Zhang, T. and Sun, F., 2017. Apparent permeability model for real gas transport through shale gas reservoirs considering water distribution characteristic. *International Journal of Heat and Mass Transfer*, *115*, pp.1008-1019.

Sundén, B. and Fu, J., 2016. *Heat transfer in aerospace applications*. Academic Press.

Surguchev, L. and Li, L., 2000, January. IOR evaluation and applicability screening using artificial neural networks. In *SPE/DOE Improved Oil Recovery Symposium*. Society of Petroleum Engineers.

Surguchev, L.M., 2009. Air Injection to Improve Oil Recovery from Mature Light Oil Field. International Research Institute of Stavanger http://www. ccop. or. th/eppm/projects/16/docs/Surguchev2% 20Air% 20Injectio, (20ENG), p.202009.

Surguchev, L.M., Koundin, A. and Yannimaras, D., 1999, January. Air injection-cost effective IOR method to improve oil recovery from depleted and waterflooded fields. In *SPE Asia Pacific Improved Oil Recovery Conference*. Society of Petroleum Engineers.

Surguchev, L.M., Reich, E.M., Berenblyum, R. and Shchipanov, A., 2010, January. Improved oil recovery methods: applicability screening and potential evaluation. In *SPE Russian Oil and Gas Conference and Exhibition*. Society of Petroleum Engineers.

Sweatman, R.E., Crookshank, S. and Edman, S., 2011, May. Outlook and technologies for offshore CO_2 EOR/CCS projects. In *Offshore Technology Conference*. OnePetro.

Sydansk, R.D., 2007. Polymers, gels, foams, and resins in Holstein, E. D., ed., Volume V–Reservoir Engineering and Petrophysics. *Petroleum Engineering Handbook; Lake, LW, Ed.; Society of Petroleum Engineers: Richardson, TX*. pp.1219-1224.

Taber, J.J., Martin, F.D. and Seright, R.S., 1997. EOR screening criteria revisited—part 2: applications and impact of oil prices. *SPE Reservoir Engineering*, *12*(03), pp.199-206.

Tan, Z., 2014. Basic Properties of Gases. In Air Pollution and Greenhouse Gases (pp. 27-58). Springer, Singapore.

Tat, M.E. and Van Gerpen, J.H., 2000. The specific gravity of biodiesel and its blends with diesel fuel. *Journal of the American Oil Chemists' Society*, *77*(2), pp.115-119.

Taylor, G.I., 1960. Deposition of a viscous fluid on a plane surface. *Journal of Fluid Mechanics*, *9*(2), pp.218-224.

Technovio, 2017. Global Enhanced Oil Recovery Market 2017-2021. Available [online] from: https://www.technavio.com/report/global-enhanced-oil-recovery-market [access 22/09/2017]

Tecs, 2019. Mean free path & collision frequency. Available at: https://www.tec-science.com/thermodynamics/kinetic-theory-of-gases/mean-free-path-collision-frequency/ [Accessed September 8, 2021].

Teigland, R. and Kleppe, J., 2006, January. EOR survey in the North Sea. In *SPE/DOE Symposium on improved Oil Recovery*. Society of Petroleum Engineers.

Thomas, S., Ali, S. M. F., Scoular, J. R., & Verkoczy, B. 2001. Chemical Methods for Heavy Oil Recovery. Petroleum Society of Canada. doi:10.2118/01-03-05

Thornton, B., Hassan, D. and Eubank, J., 1996. Horizontal well cyclic combustion, Wabasca air injection pilot. *Journal of Canadian Petroleum Technology*, *35*(09).

Thorpe, S.A., 2008. '*Fluid Dynamics, Introduction, and Laboratory Experiment*'. In Steele, J.H., Thorpe, S.A. and Turekian, K.K., (eds). Encyclopedia of ocean sciences, 2nd edn, Pages 578-580. Academic Press, Cambridge, MA

Tiab, D. and Donaldson, E.C., 2015. *Petrophysics: theory and practice of measuring reservoir rock and fluid transport properties*. Gulf professional publishing.

Tiab, D. And Donaldson, E.C., 2016. Chapter 10 - Reservoir Characterisation. In: D. Tiab And E.C. Donaldson, Eds, *Petrophysics (Fourth Edition).* Boston: Gulf Professional Publishing, Pp. 583-640.

Tonezzer, M., Izidoro, S.C., Moraes, J. and Dang, L.T.T., 2019. Improved gas selectivity based on carbon modified SnO2 nanowires. *Frontiers in Materials*, *6*, p.277.

Towler, B. F., 2007. PEH: Gas Properties. In Fanchi, J.R., (Ed.) Volume I–General Engineering. Petroleum Engineering Handbook; Lake, LW, Ed.; Society of Petroleum Engineers Pgs. 217-256: Richardson, TX.

Tricot Y. M. (1997) Surfactants: Static and Dynamic Surface Tension. In: Kistler S.F., Schweizer P.M. (eds) Liquid Film Coating. Springer, Dordrecht

Trujillo Portillo, M.L., Mercado Sierra, D.P., Maya, G.A., Castro Garcia, R.H., Soto, C.P., Perez, H.H. and Gomez, V., 2010, January. Selection methodology for screening evaluation of enhanced-oil-recovery methods. In *SPE Latin American and Caribbean Petroleum Engineering Conference*. Society of Petroleum Engineers.

Tungdumrongsub, S. and Muggeridge, A.H., 2010, January. Layering and oil recovery: the impact of permeability contrast, gravity, viscosity and dispersion. In *SPE Europec/EAGE Annual Conference and Exhibition*. Society of Petroleum Engineers.

Tunio, S.Q., Tunio, A.H., Ghirano, N.A. and El Adawy, Z.M., 2011. Comparison of different enhanced oil recovery techniques for better oil productivity. *International Journal of Applied Science and Technology*, *1*(5).

Valougeorgis, D., Vargas, M. and Naris, S., 2016. Analysis of gas separation, conductance and equivalent single gas approach for binary gas mixture flow expansion through tubes of various lengths into vacuum. *Vacuum*, *128*, pp.1-8.

Van der Poel, C. and Killian, J.W., 1957, October. Attic Oil. In *Fall Meeting of the Society of Petroleum Engineers of AIME*.

Van Krevelen, D.W. and Te Nijenhuis, K., 2009. Chapter 8 - Interfacial Energy Properties. In: D.W. Van Krevelen And K. Te Nijenhuis, eds, *Properties of Polymers (Fourth Edition)*. Amsterdam: Elsevier, pp. 229-244.

Vavra, C.L., Kaldi, J.G. and Sneider, R.M., 1992. Geological applications of capillary pressure: a review. *AAPG bulletin*, *76*(6), pp.840-850.

Vega, B. and Kovscek, A.R., 2010. Carbon dioxide (CO_2) sequestration in oil and gas reservoirs and use for enhanced oil recovery (EOR). In *Developments and Innovation in Carbon Dioxide (CO_2) Capture and Storage Technology* (pp. 104-126). Woodhead Publishing.

Velarde, J., Blasingame, T.A. and McCain Jr, W.D., 1997, January. Correlation of black oil properties at pressures below bubble point pressure-A new approach. In *Annual Technical Meeting*. Petroleum Society of Canada.

Wang, D., 2013. *Enhanced Oil Recovery Field Case Studies: Chapter 4. Polymer Flooding Practice in Daqing*. Elsevier Inc. Chapters.

Wang, H., Su, Y., Wang, W., Sheng, G., Li, H. and Zafar, A., 2019b. Enhanced water flow and apparent viscosity model considering wettability and shape effects. *Fuel*, *253*, pp.1351-1360.

Wang, H., Su, Y., Zhao, Z., Wang, W., Sheng, G. and Zhan, S., 2019a. Apparent permeability model for shale oil transport through elliptic nanopores considering wall-oil interaction. *Journal of Petroleum Science and Engineering*, *176*, pp.1041-1052.

Wang, J., Chen, L., Kang, Q. and Rahman, S.S., 2016. Apparent permeability prediction of organic shale with generalized lattice Boltzmann model considering surface diffusion effect. *Fuel*, *181*, pp.478-490.

Wang, J., Wu, S., Li, Q., Zhang, J. and Guo, Q., 2020. Characterization of the pore-throat size of tight oil reservoirs and its control on reservoir

physical properties: A case study of the Triassic tight sandstone of the sediment gravity flow in the Ordos Basin, China. *Journal of Petroleum Science and Engineering*, *186*, p.106701.

Wang, W. and Gupta, A., 1999, January. Transmissibility Scale-up in Reservoir Simulation. In *Annual Technical Meeting*. Petroleum Society of Canada.

Wang, X., Chen, J., Ren, D. and Shi, Z., 2020a. Role of Gas Viscosity for Shale Gas Percolation. *Geofluids*, *2020*.

Warner, H.R., and Holstein, E.D., 2007. Chapter 12 – Immiscible Gas Injection in Oil Reservoirs. In Lake, L.W., Fanchi, J.R., Arnold, K., Clegg, J.D., Holstein, E.D. and Warner, H.R. eds., 2007. *Petroleum engineering handbook: reservoir engineering and petrophysics* (Vol. 5). Society of Petroleum Engineers. Pgs. 1103-1147

Weberg, E.B., Silberberg, M.S. and Weberg, E.B., 2009. *Student Study Guide to Accompany Chemistry: The Molecular Nature of Matter and Change; Martin S. Silberberg*. McGraw Hill.

Wei, N., Feng, Y., Sun, W., Cheng, Y., Dong, M., Song, Y., Wu, C., Liu, G. and Qiu, Y., 2021. Experimental study on the conductance of pure and binary gas mixtures. *Vacuum*, *189*, p.110277.

Weinaug, C.F. and Katz, D.L., 1943. Surface tensions of methane-propane mixtures. *Industrial & Engineering Chemistry*, *35*(2), pp.239-246.

Weisstein, E.W., 1999. Circle. From Mathworld—a wolfram web resource. [online] Available From: *http://mathworld. wolfram. com/Circle. html*. [Accessed 02/02/2020].

Weisstein, E.W., 2003. Circle. [online] Available From: *https://mathworld. wolfram. com/*. [Accessed 02/02/2020].

Welkenhuysen, K., Meyvis, B., Swennen, R. and Piessens, K., 2018. Economic threshold of CO_2-EOR and CO_2 storage in the North Sea: A case study

of the Claymore, Scott and Buzzard oil fields. *International Journal of Greenhouse Gas Control*, *78*, pp.271-285.

Wheaton, R., 2016. *Fundamentals of applied reservoir engineering: appraisal, economics and optimization*. Gulf Professional Publishing.

Whitson, C.H. and Brulé, M.R., 2000. *Phase behavior* (Vol. 20, p. 233). Richardson, TX: Henry L. Doherty Memorial Fund of AIME, Society of Petroleum Engineers.

Whitson, C.H., 1993. Petroleum Reservoir Fluid Properties: Part 10. Reservoir Engineering Methods. In Morton-Thompson, D. and Woods, A.M. eds., *Development geology reference manual, pgs 504-507: AAPG methods in exploration series, no. 10* (No. 10). AAPG.

Widmoser, P., 1983. Seepage and groundwater: Developments in water science, 13. MA Marino and JN Luthin. Elsevier, Amsterdam, 1982. xvi+ 490 pp., Dfl. 250. ISBN 0-444-41975-6. *Agricultural Water Management*, *6*(4), pp.411-412.

Will, B., 2019. 6 Different Ways to Compensate for Missing Values In a Dataset (Data Imputation with examples), Popular strategies to statistically impute missing values in a dataset. Towards Data Science [online] Available From: https://towardsdatascience.com/6-different-ways-to-compensate-for-missing-values-data-imputation-with-examples-6022d9ca0779?gi=cb7ff87846d0 [Accessed 2 August, 2018].

Wilson, A., 2015. Pelican Lake: First Successful Application of Polymer Flooding in a Heavy-Oil Reservoir. *Journal of Petroleum Technology*, *67*(01), pp.78-80.

Winland, H.D., 1976. Evaluation of gas slippage and pore aperture size in carbonate and sandstone reservoirs: Amoco Production Company Report F76-G-5, 25 p. *Tulsa, Oklahoma*.

Worldvest 2015. Marginal Fields. <http://worldvest-ap.com/index.php/marginal-field-investment-opportunities/> [Accessed 6/10/2017]

Wu, K., Chen, Z. and Li, X., 2015. Real gas transport through nanopores of varying cross-section type and shape in shale gas reservoirs. *Chemical Engineering Journal*, *281*, pp.813-825.

Wu, S., Li, Z., Wang, Z., Sarma, H.K., Zhang, C. and Wu, M., 2020. Investigation of CO_2/N_2 injection in tight oil reservoirs with confinement effect. *Energy Science & Engineering*, *8*(4), pp.1194-1208.

Wu, T., 2005. Permeability prediction and drainage capillary pressure simulation in sandstone reservoirs (Doctoral dissertation, Texas A&M University).

Wu, Z. and Liu, H., 2019. Investigation of hot-water flooding after steam injection to improve oil recovery in thin heavy-oil reservoir. *Journal of Petroleum Exploration and Production Technology*, *9*(2), pp.1547-1554.

Yongxiang, C., Xin, W., Kezhen, H. and Mingzhe D. 2014. A data mining approach to finding relationships between reservoir properties and oil production for CHOPS, In Computers & Geosciences, Volume 73 (2014), Pages 37-47, ISSN 0098-3004, https://doi.org/10.1016/j.cageo.2014.08.006.

Yu, J.J., Li, Y.R., Ruan, D.F. and Wu, C.M., 2019. Aspect ratio and capillary ratio dependence of thermal-solutal capillary-buoyancy flow of a binary mixture in an annular pool. *International Journal of Thermal Sciences*, *136*, pp.347-356.

Yu, W. and Sepehrnoori, K., 2018. *Shale gas and tight oil reservoir simulation*. Gulf Professional Publishing.

Yu, X., Ma, Y.Z., Psaila, D., La Pointe, P., Gomez, E. and Li, S., 2011. Reservoir characterisation and modeling: a look back to see the way forward. in Y. Z. Ma and P. R. La Pointe, eds., Uncertainty analysis and reservoir modeling: AAPG Memoir 96, p. 289–309.

Yu-shu, W. and Karsten P., 1996, Flow of Non-Newtonian fluid in porous media. In Corapcioglu, M.Y., 1996. *Advances in porous media* (p87-179). Elsevier Science B.V. Amsterdam.

Zekri, A. and Jerbi, K.K., 2002. Economic evaluation of enhanced oil recovery. *Oil & Gas Science and Technology*, *57*(3), pp.259-267.

Zeng, Z. and Grigg, R., 2006. A criterion for non-Darcy flow in porous media. *Transport in porous media*, *63*(1), pp.57-69.

Zerafat, M.M., Ayatollahi, S., Mehranbod, N. and Barzegari, D., 2011, January. Bayesian network analysis as a tool for efficient EOR screening. In *SPE Enhanced Oil Recovery Conference*. Society of Petroleum Engineers.

Zhang, J. and Yang, R., 2018. A further study on Welge equation. *Energy Exploration & Exploitation*, *36*(5), pp.1103-1113.

Zhang, J.X. and Hoshino, K., 2018. *Molecular Sensors and Nanodevices: Principles, Designs and Applications in Biomedical Engineering*. Academic Press.

Zhang, K., Chen, Y., Zhang, L., Yao, J., Ni, W., Wu, H., Zhao, H. and Lee, J., 2015. Well pattern optimization using NEWUOA algorithm. *Journal of Petroleum Science and Engineering*, *134*, pp.257-272.

Zhang, S., Zhuang, Y., Liu, L., Zhang, L. and Du, J., 2020. Optimization-based approach for CO_2 utilization in carbon capture, utilization and storage supply chain. *Computers & Chemical Engineering*, *139*, p.106885.

Zhang, T., Li, X., Shi, J., Sun, Z., Yin, Y., Wu, K., Li, J. and Feng, D., 2018. An apparent liquid permeability model of dual-wettability nanoporous

media: A case study of shale. *Chemical Engineering Science*, *187*, pp.280-291.

Zhang, T., Wu, R., Zhao, C.Y., Evangelos, T. and Abdolreza, K., 2020. Capillary instability induced gas-liquid displacement in porous media: Experimental observation and pore network model. *Physical Review Fluids*, *5*(10), p.104305.

Zhao, H., Ning, Z., Wang, Q., Zhang, R., Zhao, T., Niu, T. and Zeng, Y., 2015. Petrophysical characterisation of tight oil reservoirs using pressure-controlled porosimetry combined with rate-controlled porosimetry. *Fuel*, *154*, pp.233-242.

Zhuang, H., Han, Y., Sun, H. and Liu, X., 2020. Dynamic well testing in petroleum exploration and development. Elsevier.

Zhuravljov, A. and Lanetc, Z., 2019. Relevance of analytical Buckley–Leverett solution for immiscible oil displacement by various gases. Journal of Petroleum Exploration and Production Technology, 9(1), pp.617-626.

Zou, C., Chang, Y., Wang, G. and Lan, L., 2011. Calculation on a reasonable production/injection well ratio in waterflooding oilfields. *Petroleum Exploration and Development*, *38*(2), pp.211-215.

APPENDIX A

Table A 1 Some modified, derived, proposed equations in the PhD thesis.

S/N	Quantity	Remark	Equation	Equation Number
1	Capillary Pressure	Normalised for thermophysical properties & Parachor.	$P_c = \dfrac{2\left(Pch_o\left[\frac{\rho_o}{MW_o}\right] - Pch_g\left[\frac{\rho_g}{MW_g}\right]\right)^4 cos\theta}{r}$	0-1
2	Capillary Number	Normalised for thermophysical properties & Parachor.	$N_c = \dfrac{v\mu}{\left(Pch_o\left[\frac{\rho_o}{MW_o}\right] - Pch_g\left[\frac{\rho_g}{MW_g}\right]\right)^4}$	0-2
3	Viscosity	Normalised for isothermal radial gas flow	$\mu = -\dfrac{\pi h}{4Q_2 P_2}\left(\dfrac{P_1{}^2 - P_2{}^2}{\left(\frac{1}{r_1} - \frac{1}{r_2}\right)}\right)$	0-3
4	Displacement Factor	Normalised for thin-film capillary number & saturation.	$E_d = 1 - \dfrac{(N_c)^{\frac{1}{2}}}{s_{oi}}$	0-4
5	Sweep Optimisation Parameter	Proposed: Normalised for flowrate and mobility	$SOP\,(P,T) = \dfrac{V_{gas}}{\lambda_{gas}}$	0-5
6	Mobility	Normalised for single- & two-phase velocity.	$M_{i\infty} = \dfrac{M_i V_{i\infty}}{V_i}$	0-6
7	Gas Flow	Normalised for radial gas flow.	$Q_{std} = 858\dfrac{K}{\mu}\dfrac{h}{T}\dfrac{(P_1{}^2 - P_2{}^2)}{\ln\frac{r_1}{r_2}}$	0-7
8	Gas Flow	Normalised for radial flow & heat capacity.	$Q_{std} = 858\dfrac{K}{\mu}\dfrac{hMC_p(P_1{}^2 - P_2{}^2)}{\ln\frac{r_1}{r_2}}$	0-8
9	Gas Flow	Normalised for radial flow, heat capacity & comparative study.	$Q_{std-apparent} = \dfrac{K}{\mu}MC_p(P_1{}^2 - P_2{}^2)$	0-9
10	Mean Mobility	Graphical method: Slope ($\frac{\mu}{K}$).	$\left[\dfrac{Q_{std}}{858hMC_p}\right]_i = \left[\dfrac{K}{\mu}\left(\dfrac{(P_1{}^2 - P_2{}^2)}{\ln\frac{r_1}{r_2}}\right)\right]_i$	0-10
11	Mean Mobility	Graphical method: Slope ($1/\frac{\mu}{K}$).	$\dfrac{\mu}{K}\left(\dfrac{Q_{std}\ln\frac{r_1}{r_2}}{858hMC_p}\right) + P_2{}^2 = P_1{}^2$	0-11
12	Mobility	Normalised for radial flow & heat capacity.	$M_i = \left(\dfrac{K}{\mu}\right)_i = \left(\dfrac{Q_{std}}{858hMC_p}\dfrac{\ln\frac{r_1}{r_2}}{(P_1{}^2 - P_2{}^2)}\right)_i$	0-12

APPENDIX B
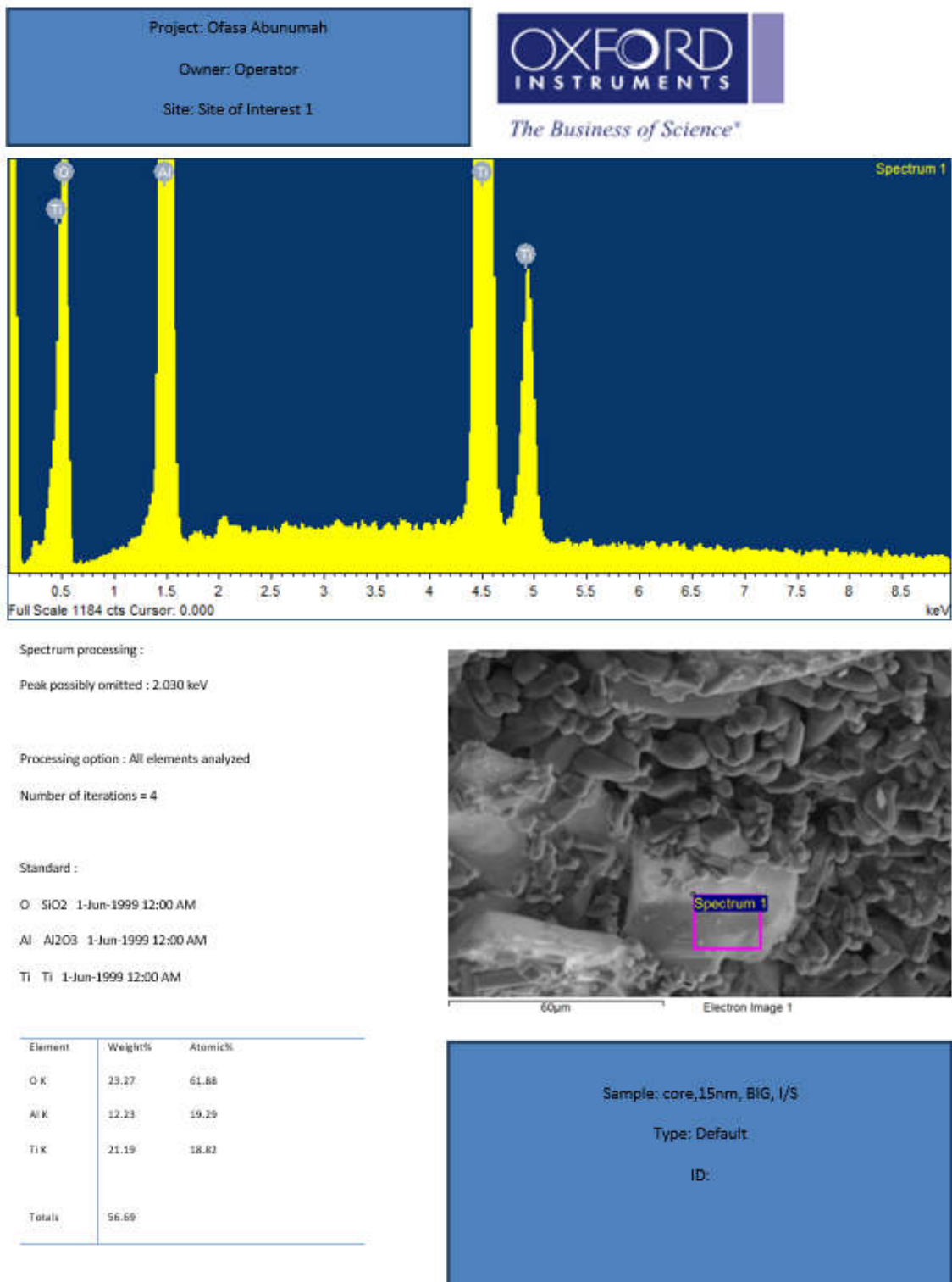
Figure B 1 EDS and morphology analysis for Core-2 sample.
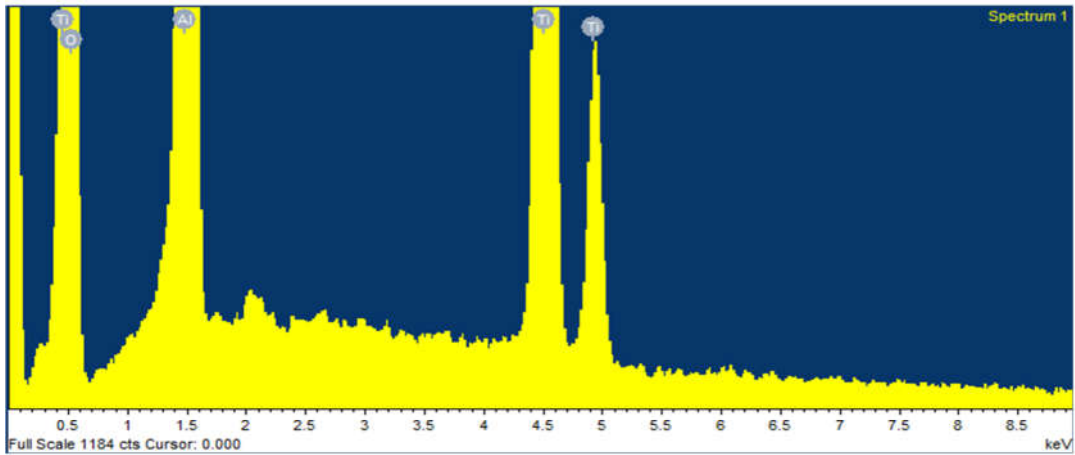
Spectrum processing :

Peak possibly omitted : 2.041 keV

Processing option : All elements analyzed

Number of iterations = 5

Standard :
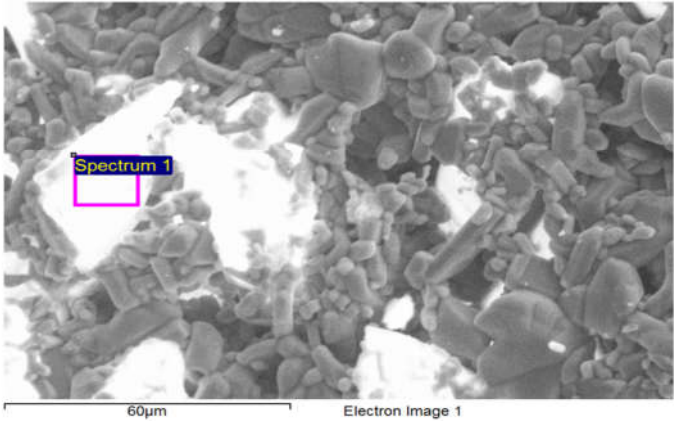
O   SiO2   1-Jun-1999 12:00 AM

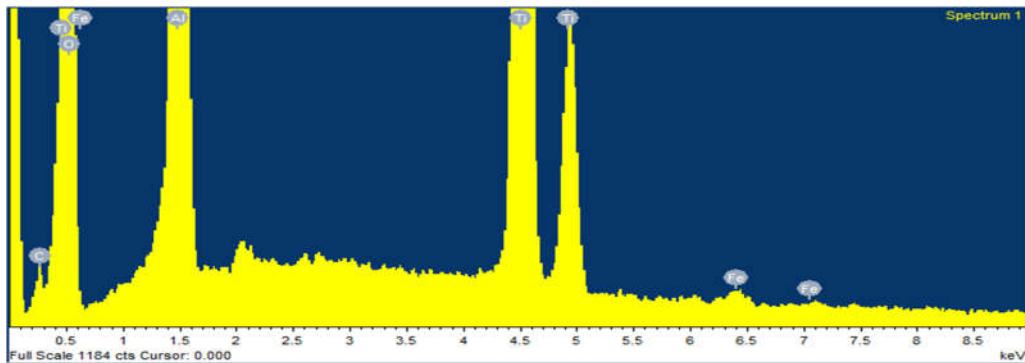Al   Al2O3   1-Jun-1999 12:00 AM

Ti   Ti   1-Jun-1999 12:00 AM

Element	Weight%	Atomic%
O K	67.38	68.40
Al K	36.64	22.06
Ti K	28.14	9.54
Totals	132.16	

Sample: Core-3, 200nm, SMALL, I/S

Type: Default

ID:

Figure B 2 EDS and morphology analysis for Core-3 sample.

Spectrum processing :

Peak possibly omitted : 2.038 keV

Processing option : All elements analyzed

Number of iterations = 5

Standard :

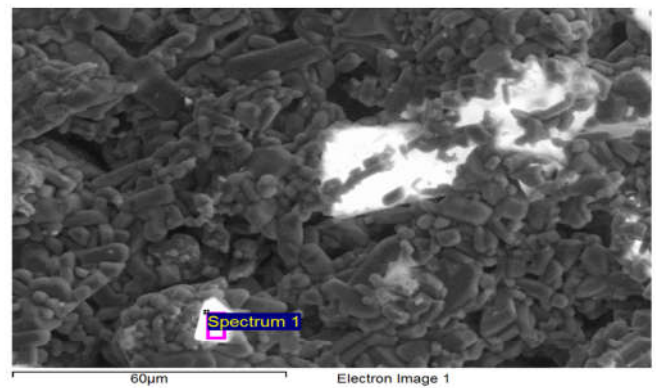C   CaCO3   1-Jun-1999 12:00 AM

O   SiO2   1-Jun-1999 12:00 AM

Al   Al2O3   1-Jun-1999 12:00 AM

Ti   Ti   1-Jun-1999 12:00 AM

Fe   Fe   1-Jun-1999 12:00 AM

Element	Weight%	Atomic%
C K	4.10	5.94
O K	57.29	62.29
Al K	32.34	20.85
Ti K	29.80	10.82
Fe K	0.32	0.10
Totals	123.84	

Sample: Core-4, 6000nm, small, I/S

Type: Default

ID:

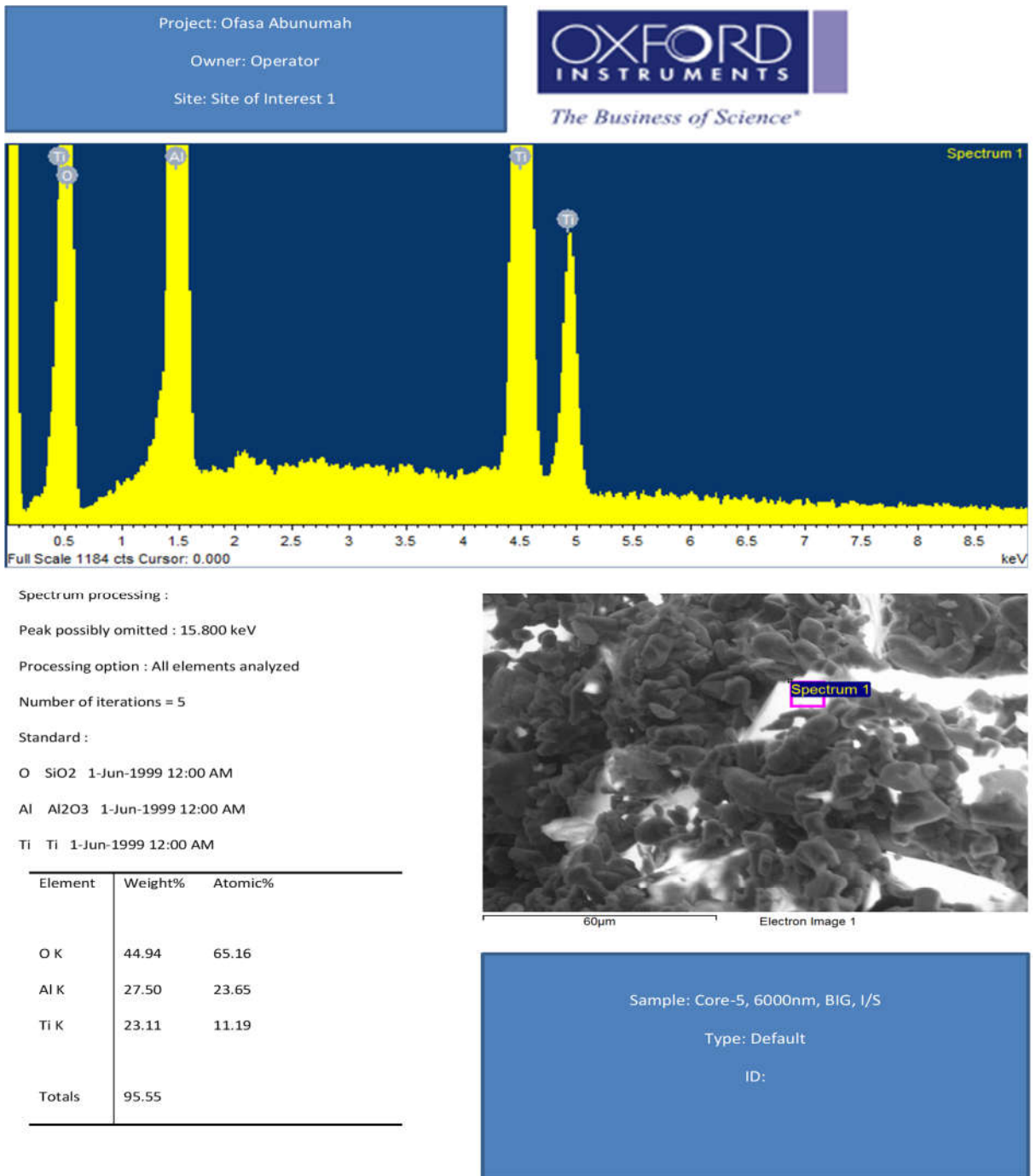*Figure B 3 EDS and morphology analysis for Core-4 sample.*

Figure B 4 EDS and morphology analysis for Core-5 sample.